CONTRIBUTIONS TO THE 6th INTERNATIONAL SYMPOSIUM ON GRANITIC PEGMATITES

EDITORS

WILLIAM B. SIMMONS
KAREN L. WEBBER
ALEXANDER U. FALSTER
ENCARNACIÓN RODA-ROBLES
SARAH L. HANSON
MARÍA FLORENCIA MÁRQUEZ-ZAVALÍA
MIGUEL ÁNGEL Galliski

GUEST EDITORS

ANDREW P. BOUDREAUX
KIMBERLY T. CLARK
MYLES M. FELCH
KAREN L. MARCHAL
LEAH R. GRASSI
JON GUIDRY
SUSANNA T. KREINIK
C. MARK JOHNSON

COVER DESIGN BY RAYMOND A. SPRAGUE
PRINTED BY RUBELLITE PRESS, NEW ORLEANS, LA

PREFACE

Phosphate Theme Session

Dedicated to: François Fontan, André-Mathieu Fransolet and Paul Keller,

It is a pleasure for the organizing committee to introduce the special session on phosphates, as an important part of the program of the 6th International Symposium on Granitic Pegmatites.

The complexity of phosphate associations, commonly occurring as a mixture of several fine-grained phases, make their study difficult. However over the last decades, the number of publications on pegmatite phosphate minerals has increased exponentially as a result of new techniques. The early investigations focused on description, composition and paragenesis. Now that most of the phases have been extensively described and replacement sequences of secondary phosphates are better understood, we are at the beginning of a new frontier of investigations of the petrogenetic role of phosphates during the evolution of the pegmatites and on their relationship to other mineral phases, such as silicates. These kinds of studies are getting more and more abundant, with some interesting examples in this volume.

We take this opportunity to honor François Fontan, Paul Keller and André-Mathieu Fransolet. These three exceptional researchers have contributed enormously to the advancement in the knowledge on phosphates during the last decades. They worked individually and jointly, always in an enthusiastic, effective and tireless way. They passed their knowledge and interest in phosphates onto many younger researchers. Now we would like to thank them sincerely for all their work.

François Fontan was born in Toulouse (France) in 1942, and he passed away six years ago, in July 2007, at the age of 64. François spent his career in research with the CNRS, at the Université Paul-Sabatier in Toulouse (France). He obtained his Doctorat d'Etat in 1971, under the guidance of François Permingeat, a founder of the International Mineralogical Association. He was particularly involved in investigations of the mineralogy and genesis of phosphate minerals in granitic pegmatites. With other specialists, he worked on the characterization of complex assemblages of phosphates in pegmatites in several European and African countries. Among his list of more than one hundred articles are descriptions of eight new mineral species. Fontanite, ($Ca[(UO_2)_3(CO_3)_2O_2]\bullet 6(H_2O)$) was named in recognition of his accomplishments.

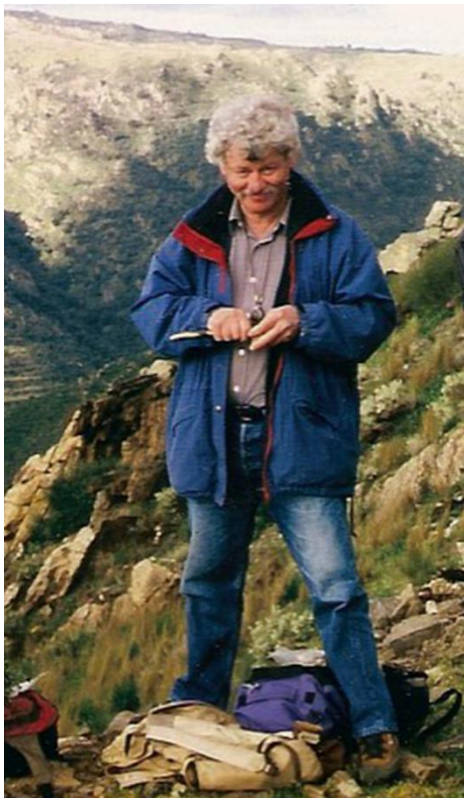

André-Mathieu Fransolet was born in Heusy (Belgium) in May of 1947. He finished his studies in Geology at the Université de Liège in October of 1969. In 1975 he defended his PhD Thesis on Geological and Mineralogical Sciences, at the same university, where he also developed most of his fruitful research, until he retired last year. During that time he published more than one hundred papers, most of them on phosphates associated with pegmatites all over the world and he contributed to the discovery of ten new mineral species. There are two mineral phases named after him: Fransoletite ($H_2Ca_3Be_2(PO_4)_4 \bullet 4(H_2O)$) and parafransoletite ($Ca_3Be_2(PO_4)_2(PO_3,OH)_2 \bullet 4(H_2O)$)

Paul Keller was born in Sarata, Romania in 1940. He finished his studies in Crystal Chemistry of Phosphates and Arsenates at The University of Stuttgart (Germany), in 1973. He worked for many years at the Institut für Mineralogie und Kristallchemie, at the University of Stuttgart (Germany), where he retired in 2006. His research on phosphates was very broad, with the publication of more than one hundred scientific papers, including the discovery of close to a dozen new mineral species. The phosphate paulkellerite ($Bi_2Fe(PO_4)O_2(OH)_2$) was named after him, in recognition of his productive career. (photograph courtesy of Anthony Kampf).

TABLE OF CONTENTS

KEYNOTE SPEAKERS

CONTRIBUTIONS

CRYSTAL CHEMISTRY AND GEOTHERMOMETRIC APPLICATIONS OF PRIMARY PEGMATITE PHOSPHATES

F. Hatert
Université de Liège, Laboratoire de Minéralogie B18, B-4000 Liège, Belgium. fhatert@ulg.ac.be

Introduction

Iron-manganese phosphate minerals are widespread in medium to highly evolved LCT granitic pegmatites, ranging from the beryl-columbite-phosphate subtype to the spodumene subtype. These phosphates play an essential geochemical role in the evolution processes affecting pegmatites, and a good knowledge of their crystal chemistry and of their stability fields is absolutely necessary to better understand the genesis of pegmatites. Among iron-manganese phosphates, several groups are of peculiar interest, since they form primary (magmatic) or high-temperature hydrothermal minerals. These groups are phosphates of the triphylite-lithiophilite [$Li(Fe^{2+},Mn^{2+})PO_4$-$Li(Mn^{2+},Fe^{2+})PO_4$], karenwebberite-natrophilite [$Na(Fe^{2+},Mn^{2+})PO_4$-$Na(Mn^{2+},Fe^{2+})PO_4$], and sarcopside-zavalíaite series [$(Fe^{2+},Mn^{2+})_3(PO_4)_2$-$(Mn^{2+},Fe^{2+})_3(PO_4)_2$], as well as alluaudite- and wyllieite-type phosphates. The crystal-chemical features of these minerals, as well as some experimental data on their stability fields, will be successively presented in this lecture. They demonstrate how a global approach, combining laboratory experiments with petrographic and crystallographic measurements on natural samples, is necessary to decipher all aspects of these complex minerals.

Primary Li- and Na-bearing phosphates of the triphylite group

In pegmatites, primary phosphates of the triphylite-lithiophilite series form masses that can reach several meters in diameter, enclosed in silicates. During the oxidation processes affecting the pegmatites, these olivine-type phosphates progressively transform to ferrisicklerite-sicklerite [$Li_{1-x}(Fe^{3+},Mn^{2+})(PO_4)$-$Li_{1-x}(Mn^{2+},Fe^{3+})(PO_4)$] and to heterosite-purpurite [$(Fe^{3+},Mn^{3+})(PO_4)$-$(Mn^{3+},Fe^{3+})(PO_4)$], according to the substitution mechanism $Li^+ + Fe^{2+} \rightarrow [] + Fe^{3+}$.

The crystal structure of minerals of the triphylite-lithiophilite series (triphylite: a = 4.690, b = 10.286, c = 5.987 Å, *Pbnm*) has been investigated from synthetic samples and natural minerals (Hatert *et al.* 2011a, 2012), and is characterized by two types of octahedral sites: the $M(1)$ octahedra occupied by Li, and the $M(2)$ sites occupied by Fe and Mn. A natural sample from the Altai Mountains, China, was recently investigated by Hatert *et al.* (2012), in order to understand the structural variations occurring during the oxidation of lithiophilite into sicklerite. Five single-crystals, corresponding to intermediate members of the lithiophilite-sicklerite series, were extracted from a thin section and are orthorhombic, space group *Pbnm*, with unit-cell parameters ranging from a = 4.736(1), b = 10.432(2), c = 6.088(1) Å (lithiophilite) to a = 4.765(1), b = 10.338(2), c = 6.060(1) Å (sicklerite). The structures show a topology identical to that of olivine-type phosphates, with Li occurring on the $M(2)$ site and showing occupancy factors from 0.99 Li atoms per formula unit (*p.f.u.*) (lithiophilite) to 0.75 Li *p.f.u.* (sicklerite). These values are in good agreement with the values measured by SIMS (Secondary Ion Mass Spectrometry), which indicate Li values from 0.96 to 0.69 Li *p.f.u.*

Natrophilite, $NaMnPO_4$, is another pegmatite phosphate with the olivine structure, in which the $M(1)$ site is occupied by Na while the $M(2)$ site contains the smaller divalent cations. Recently, the Fe-analogue of natrophilite was found at the Malpensata granitic pegmatite, Colico commune, Lecco province, north Italy (Vignola *et al.* 2011). This phosphate, $Na(Fe^{2+},Mn^{2+})PO_4$, has been named karenwebberite in honour of Dr. Karen Louise Webber, Assistant Professor Research at the Mineralogy, Petrology and Pegmatology Research Group, Department of Earth and Environmental Sciences, University of New Orleans, Louisiana, U.S.A. (IMA 2011-015). It forms late stage magmatic exsolution lamellae up to 100µm thick, hosted in graftonite and associated with Na-bearing ferrisicklerite and with an heterosite-like phase (Fig. 1a). Karenwebberite is orthorhombic, space group P*bnm*, a =4.882(1)Å, b = 10.387(2)Å, c = 6.091(1) Å, V = 308.9(1)Å^3, and Z = 4. The mineral shows the olivine structure, with $M(1)$ occupied by Na and $M(2)$ occupied by Fe and Mn.

Karenwebberite is also a polymorph of marićite, $NaFePO_4$ (a = 6.861(1), b = 8.987(1), c = 5.045(1) Å, *Pmnb*), which shows a crystal structure distinct

from that of olivine. This polymorphic relationship is of particular interest, since the transformation between olivine-type and marićite-type phosphates is temperature–dependant, as shown experimentally by Corlett and Armbruster (1979). These authors confirmed that olivine–type $Na(Fe,Mn)PO_4$ phosphates are low-temperature polymorphs of marićite–type phosphates, and that the transition between the two polymorphs of $NaMnPO_4$ occurs around 325°C (P = 100 bars). Hydrothermal investigations performed on alluaudite–type phosphates at 1 kbar (Hatert *et al.* 2006 and 2011b) also produced several marićite–type phosphates with various Fe/(Fe+Mn) ratios; these results indicate a transition temperature of about 500–550°C between karenwebberite and marićite. Consequently, karenwebberite certainly crystallized below 550°C in the Malpensata dyke.

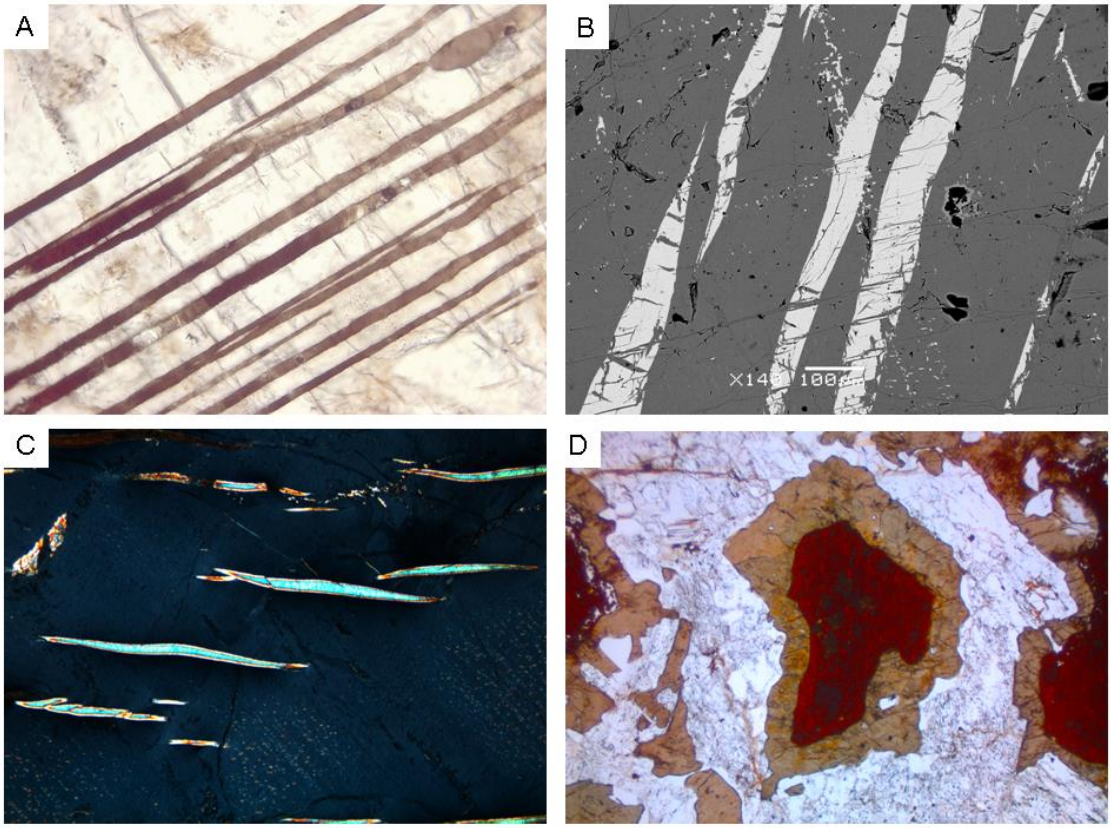

Fig. 1: A) Exsolution lamellae of karenwebberite (light brown), oxidized into Na-bearing ferrisicklerite (dark brown) and included in graftonite. Malpensata pegmatite, Colico, Italy (plane polarized light; the length of the photograph is 1.5 mm). B) Triphylite (dark grey) including lamellae of sarcopside (white), Cañada pegmatite, Spain (sample SS-3, BSE image). C) Lamellae of zavalíaite included in lithiophilite, La Empleada pegmatite, San Luis, Argentina (crossed polars; the length of the photograph is 2.5 mm). D) Rim of qingheiite-(Fe^{2+}) (brown) surrounding frondelite (red) in a quartz-albite matrix. Sebastião Cristino, Minas Gerais, Brazil (plane polarized light, sample SC-34).

Phosphates of the sarcopside group and their exsolution textures

Lamellar triphylite + sarcopside $[(Fe,Mn)_3(PO_4)_2]$ associations are well known in numerous rare-element granitic pegmatites (Fig. 1b). These intergrowths are traditionally interpreted as exsolution textures, and Moore (1972) suggests the existence of a complete $Li(Fe,Mn)(PO_4)$-$(Fe,Mn)_3(PO_4)_2$ solid solution at high temperature. According to this hypothesis, exsolutions of sarcopside into triphylite, or of triphylite into sarcopside, would appear during cooling, depending on the composition of the parent high-temperature unique phase.

Hatert *et al.* (2007) performed hydrothermal experiments between 400 and 700°C (1 kbar), in order to determine the stability field of the triphylite + sarcopside assemblage. These experiments indicate that the triphylite + sarcopside assemblage is a primary assemblage in granitic pegmatites, since

it has been reproduced hydrothermally at 500 and 700°C (1 kbar). The electron-microprobe and SIMS analyses of these synthetic phosphates show that the Li content of triphylites significantly increases with temperature, from 0.72 *a.p.f.u.* at 400°C, to 0.037 *a.p.f.u.* at 700°C, for the $LiFe_{2.5}(PO_4)_2$ starting composition. By comparison with the analytical data collected on natural assemblages, these experimental results provide a relatively accurate determination of the temperature at which the exsolutions crystallized.

Zavalíaite, ideally $(Mn^{2+},Fe^{2+},Mg)_3(PO_4)_2$, is a new phosphate mineral species from the La Empleada granitic pegmatite, San Luis province, Argentina (Hatert *et al.* 2013), which forms exsolution lamellae occurring within lithiophilite (Fig. 1c). Zavalíaite is the Mn^{2+}-rich equivalent of sarcopside and of chopinite $[(Mg,Fe)_3(PO_4)_2]$, and belongs to the sarcopside group of minerals. Its single-crystal unit-cell parameters are a = 6.088(1), b = 4.814(1), c = 10.484(2) Å, β = 89.42(3)°, V = 307.2(1) Å^3, space group $P2_1/c$. The mineral is named in honour of María Florencia de Fátima Márquez Zavalía (or Márquez-Zavalía (1955-)), researcher and Head of the Department of Mineralogy Petrography and Geochemistry, IANIGLA, CCT Mendoza, CONICET, Argentina, for her contribution to the knowledge of Argentinean mineralogy.

The genesis of zavalíaite lamellae is compared to the genetical processes responsible for the formation of sarcopside lamellae observed in triphylite. Exsolutions of zavalíaite appeared during the cooling of primary, Li-poor lithiophilite; consequently, this mineral can be considered as a primary phosphate, which crystallized under pegmatitic conditions similar to those of lithiophilite formation. Starting from the proportions of zavalíaite in the exsolution textures (less than 10% zavalíaite), and using the experimental triphylite-sarcopside geothermometer described by Hatert *et al.* (2007, 2009), a temperature of ca. 300°C can be estimated for the crystallisation of zavalíaite exsolutions. This temperature is in good agreement with those occurring in such lithiophilite-rich evolved pegmatites.

Alluaudite- and wyllieite-type phosphates: the transition between primary minerals and Na-metasomatic phases

The alluaudite group of minerals consists of Na-Mn-Fe-bearing phosphates which are known to occur in Li-rich granitic pegmatites. Due to their flexible crystal structure, which is able to accommodate Fe^{2+} and Fe^{3+} in variable amounts, alluaudites are very stable and crystallize from the first stages of pegmatite evolution to the latest oxidation processes. These minerals exhibit chemical compositions ranging from $Na_2Mn(Fe^{2+}Fe^{3+})(PO_4)_3$ to $NaMnFe^{3+}{}_2(PO_4)_3$, with Mn^{2+} or some Ca^{2+} replacing Na^+, Fe^{2+} replacing Mn^{2+}, and some Mg^{2+} or Mn^{2+} replacing iron. The alluaudite structure was described on a natural sample from the Buranga pegmatite, Rwanda. The mineral is monoclinic, space group $C2/c$, and the structural formula corresponds to $X(2)X(1)M(1)M(2)_2(PO_4)_3$, with four formula units per unit cell. The structure consists of kinked chains of edge-sharing octahedra stacked parallel to {101}. These chains are formed by a succession of $M(2)$ octahedral pairs linked by highly distorted $M(1)$ octahedra. Equivalent chains are connected in the b direction by the $P(1)$ and $P(2)$ phosphate tetrahedra to form sheets oriented perpendicular to [010]. These interconnected sheets produce channels parallel to the c axis, channels which contain the X sites.

Hatert *et al.* (2006) explored the geothermometric potential of the $Na_2(Mn_{1-x}Fe^{2+}{}_x)_2Fe^{3+}(PO_4)_3$ solid-solution series (x = 0 to 1), which represents the compositions of natural weakly oxidized alluaudites; they performed hydrothermal experiments between 400 and 800°C, at 1 kbar. Under an oxygen fugacity controlled by the Ni/NiO buffer, single-phase alluaudites crystallize at 400 and 500°C, whereas the association alluaudite + marićite appears between 500 and 700°C. The limit between these two fields corresponds to the maximum temperature that can be reached by alluaudites in granitic pegmatites, because marićite has never been observed in these geological environments. Because alluaudites are very sensitive to variations of oxygen fugacity, the field of hagendorfite, $Na_2MnFe^{2+}Fe^{3+}(PO_4)_3$, has been positioned in the $f(O_2)$-T diagram, and provides a tool that can be used to estimate the oxygen fugacity conditions which prevailed in granitic pegmatites during the crystallization of this phosphate.

Hydrothermal experiments were also performed by Hatert & Fransolet (2006) in the Na-Fe^{2+}-Fe^{3+} (+PO_4) ternary system, between 400 and 700°C, at 1 kbar. Alluaudite-type phosphates were observed between 400 and 700°C, and occupy the central part of the Na-Fe^{2+}-Fe^{3+} diagram. Electron-microprobe

analyses indicate that the compositional field of alluaudites covers ca. 10 % of the diagram surface at 400°C, but only ca. 2-3 % at 500 and 600°C. The results of these experiments are applicable to Fe-rich alluaudites, as for example ferrohagendorfite from Angarf-sud, Morocco, which exhibits an ideal chemical composition $Na_2Fe^{2+}{}_2Fe^{3+}(PO_4)_3$. Alluaudite-type compounds with similar compositions were obtained between 400 and 700°C in the hydrothermal experiments, thus confirming again the existence of primary alluaudites in granitic pegmatites.

In order to constrain the conditions of temperature and oxygen fugacity which occurred in pegmatites, we also decided to reproduce experimentally several associations of pegmatite phosphates. Primary alluaudite + triphylite assemblages were reported in the Hagendorf-Süd (Germany), Buranga, and Kibingo (Rwanda) pegmatites, and the hydrothermal experiments (P = 1 kbar, T = 400-800°C) lead to the crystallisation of alluaudite + triphylite at 400 and 500°C, and of alluaudite + triphylite + maricite at 600 and 700°C (Hatert *et al.* 2011b). In these experiments, significant amounts of Na were observed in synthetic triphylites; the Na content of triphylites consequently constitutes a geothermometric tool that can be used to constrain the temperature conditions in which the alluaudite + triphylite assemblages crystallized in pegmatites.

Qingheiite-(Fe^{2+}), ideally $Na_2Fe^{2+}MgAl(PO_4)_3$, is a new mineral species recently described in the Sebastião Cristino pegmatite, Minas Gerais, Brazil (Hatert *et al.* 2010). It occurs as rims around frondelite grains, included in a matrix of quartz and albite (Fig. 1d). The mineral exhibits a wyllieite-type structure, topologically identical to that of alluaudite, with single-crystal unit-cell parameters a = 11.910(2), b = 12.383(3), c = 6.372(1) Å, β = 114.43(3)°, V = 855.6(3) Å^3, space group $P2_1/n$. Since frondelite from Sebastião Cristino is an oxidation product of primary triphylite, rims of qingheiite-(Fe^{2+}) can be interpreted as the result of a reaction between this primary Mg-bearing triphylite (source of Fe, Mn, Mg, P) and albite from the matrix (source of Na, Al). This reaction certainly took place at the albitization stage, during which high amounts of Na were available. The oxidation processes affecting the pegmatite subsequently oxidized triphylite in ferrisicklerite and then in frondelite, and provoked an oxidation of qingheiite-(Fe^{2+}) following the substitution mechanism $Na^+ + Fe^{2+} = \square + Fe^{3+}$. This oxidation is responsible for the presence of vacancies and Fe^{3+} in qingheiite-(Fe^{2+}).

References

Corlett, M.I. and Armbruster, T. (1979): Structural relations between maricite and natrophilite in the system NaFePO4-NaMnPO4. GAC-MAC Join annual meeting, 4(44), 1979.

Hatert, F. & Fransolet, A.-M. (2006): The stability of iron-rich alluaudites in granitic pegmatites : an experimental investigation of the Na-Fe(II)-Fe(III) (+PO4) system. Berichte der Deutschen Mineralogischen Gesellschaft, Beihefte zum European Journal of Mineralogy, 18, 53.

Hatert, F., Fransolet, A.-M., and Maresch, W.V. (2006): The stability of primary alluaudites in granitic pegmatites: an experimental investigation of the Na2(Mn1-xFe2+x)2Fe3+(PO4)3 solid solution. Contribution to Mineralogy and Petrology, 152, 399-419.

Hatert, F., Roda-Robles, E., Keller, P., Fontan, F. & Fransolet, A.-M. (2007): Petrogenetic significance of the triphylite + sarcopside intergrowths in granitic pegmatites : an experimental investigation of the Li(Fe,Mn)(PO4)-(Fe,Mn)3(PO4)2 system. Granitic pegmatites: the state of the art, Book of Abstracts, 44.

Hatert, F., Ottolini, L., Keller, P., Fransolet, A.-M. (2009): Crystal chemistry of lithium in pegmatite phosphates: A SIMS investigation of natural and synthetic samples. Estudos Geológicos 19(2), 131-134.

Hatert, F., Baijot, M., Philippo, S. & Wouters, J. (2010): Qingheiite-(Fe2+), Na2Fe2+MgAl(PO4)3, a new phosphate mineral from the Sebastião Cristino pegmatite, Minas Gerais, Brazil. European Journal of Mineralogy, 22, 459-467.

Hatert, F., Ottolini, L., Fontan, F., Keller, P., Roda-Robles, E. & Fransolet, A.-M. (2011a): The crystal chemistry of olivine-type phosphates. 5th International symposium on granitic pegmatites,-PEG2011, Abstract book, 103-105.

Hatert, F., Ottolini, L., and Schmid-Beurmann, P. (2011b): Experimental investigation of the alluaudite + triphylite assemblage, and development of the Na-in-triphylite geothermometer: applications to natural pegmatite phosphates. Contributions to Mineralogy and Petrology, 161, 531-546.

Hatert, F., Ottolini, L., Wouters, J. & Fontan, F. (2012): A structural study of the lithiophilite-sicklerite series. Canadian Mineralogist, 50, 843-854.

Hatert, F., Roda-Robles, E., de Parseval, P. & Wouters, J. (2013): Zavalíaite, (Mn2+,Fe2+,Mg)3(PO4)2, a new member of the sarcopside group from the La Empleada pegmatite, San Luis Province, Argentina. Canadian Mineralogist, 50, 1445-1452.

Moore, P.B. (1972): Sarcopside: its atomic arrangement. American Mineralogist, 57, 24-35.

Vignola, P., Hatert, F., Fransolet, A.-M., Medenbach, O., Diella, V, and Ando', S. (2011): Karenwebberite, IMA 2011-015. CNMNC Newsletter No. 10, October 2011, page 2551; Mineralogical Magazine, 75, 2549-2561.

READING PEGMATITES: WHAT MINERALS SAY

D. London
ConocoPhillips School of Geology & Geophysics, University of Oklahoma, Norman, OK (USA) 73019: dlondon@ou.edu

Each of the families, groups, and species of minerals found in granitic pegmatites contributes some information to the whole understanding of these rocks. The petrologic significance of some abundant and accessory minerals from pegmatites is briefly summarized below.

Feldspars: Sodic plagioclase (Pl) and alkali feldspar (Kfs) constitute ~ 65% of pegmatites by mode or norm. The vast majority of pegmatites contain solvus Pl-Kfs pairs from the start, which constrains pegmatite crystallization to temperatures below the feldspar solvus crest (< ~ 700°-685°C). Accurate feldspar solvus thermometry, however, puts the crystallization temperature of pegmatites at ~ 450°C, and feldspar crystallization is isothermal, following the ingress of the 450°C isotherm into pegmatites (London *et al.* 2012). In conjunction with a conductive cooling model, the primary crystallization of feldspars and the consequent exsolution to perthite in an 80 cm-thick dike at Ramona, California (USA) appears to have occurred over a span of a few of weeks.

The An content of Pl decreases smoothly and continuously from pegmatite margins to center, and the K/Rb and K/Cs ratios of Kfs increase. Both reflect sequential crystallization of pegmatites from margin to center, and both are consistent with normal igneous fractionation trends, uninterrupted by hydrothermal processes. Plagioclase is prevalent in marginal zones, whereas Kfs is more abundant in central zones. This fractionation trend between Pl and Kfs is **NOT** consistent with a thermally-driven diffusion gradient (Jahns and Burnham 1969), in which Kfs precipitates in cooler regions and Pl in hotter zones (Orville 1963). It ***IS***, however, consistent with the patterns of sequential feldspar fractionation that arise from the crystallization of significantly undercooled granitic melts.

Quartz: Quartz is basically unstudied, except for an extensive but private data base in the industrial realm. Pegmatitic quartz tends to contain less Al, Ti, Fe, and alkalis than do quartz phenocrysts from rhyolites, and unlike phenocrystic quartz, pegmatitic quartz lacks appreciable cathodoluminescence (CL) or CL zoning. Thus, although the morphology of quartz in pegmatites is igneous, its composition, fluid inclusion populations, and isotopic composition all suggest that pegmatitic quartz does not preserve its original igneous composition well (i.e., it is extensively recrystallized in the subsolidus).

Micas: Evolutionary trends in the compositions of micas from LCT and NYF pegmatites have been well described for decades, and those trends are consistent with normal igneous fractionation. From the margins inward, the micas are first depleted in Mg, then in Fe as Al replaces octahedral Fe, culminating in a final enrichment in Li, F, and Mn. Beyond that, the micas have provided little else in the way of petrogenetic information.

Lithium Aluminosilicates: The lithium aluminosilicates eucryptite (α-$LiAlSiO_4$), spodumene (α-$LiAlSi_2O_6$), and petalite ($LiAlSi_4O_{10}$) constitute an important petrogenetic grid for LCT pegmatites, because the stability relations among these minerals are functions only of P and T in the quartz-saturated environment of pegmatites (London 1984). Where all three minerals occur (e.g., Tanco, Canada; Bikita, Zimbabwe), their sequential crystallization follows an isobar from ~ 525°-350°C at ~ 280 MPa (London 1986); below ~ 350°C, the cooling path follows a geotherm into the stability field of eucryptite + quartz. The inflection in the cooling curve from isobaric to the geothermal gradient at Tanco (London 1986) and Harding, New Mexico (USA)(Chakoumakos and Lumpkin 1991) denotes the temperature (~ 350°C) of the host rocks upon emplacement of these pegmatites. That temperature at an emplacement depth of ~ 8.8 km corresponds to a geothermal gradient of ~ 35°C/km, which unrealistically higher than the calculated cratonic geotherm of the Canadian shield in the Archean (~ 24°C/km: Chloe *et al.* 2009). A tentative conclusion is that the region of the Superior province that contains the Tanco pegmatite possessed local heat due to the emplacement of nearby plutons. It is an important but heretofore unstudied fact that some cratonic provinces are dominated by spodumene-bearing pegmatites, whereas others are petalite-bearing, with implied differences in temperature or depth of pegmatite emplacement in the various continental settings.

Garnet: Pegmatitic garnet consists mostly of almandine-spessartine solid solutions with minor grossular and negligible pyrope components. Where studied, the spessartine content increases with pegmatite fractionation. Interestingly, the Nernst distribution coefficient for Mn/Fe between garnet/melt is > 1. Therefore, the crystallization of garnet does ***NOT*** control the increasing Mn/Fe ratio of melt from granitic sources to the most differentiated pegmatites (Černý *et al.* 1985). The compositions of pegmatitic garnets, together with the low modal abundance of biotite, render garnet-biotite thermometry meaningless and not applicable to pegmatites.

Tourmaline: Evolutionary trends in the composition of tourmaline in pegmatites mirror those of the micas, and have been known for decades. The stability of tourmaline in pegmatites, however, now has a firm basis for understanding the relationships between tourmaline crystallization, melt composition, and temperature and pressure. The Li-free tourmalines are stable to ~ 750°C and at any pressure above ~ 50 MPa (London 2011). The solubility (saturation) of tourmaline in melt, however, is a function mostly of the activity products of B and Al in the melt, and of temperature. The solubility of Li-free tourmaline in granitic melt, as measured by the B content of melt at saturation, decreases from 2 wt% B_2O_3 in melt at 750°C, 200 MPa to only 0.1 wt% B_2O_3 in melt at 450°C.

Li-rich tourmaline is unstable below 200 MPa at any temperature. Based on existing work (London 2011), the elbaite component increases with increasing pressure; relationships with regard to temperature are more complex and are still being worked out. However, the stability field for elbaite appears to correspond to that of spodumene. Lithium adopts octahedral coordination in both phases, which coordination is favored by increasing pressure and decreasing temperature.

Phosphates: Equilibria among feldspars, LiAl-silicates, garnet, and their corresponding phosphates buffer melt compositions between ~ 0.5-2.5 wt% P_2O_5. This range of phosphorus concentration is also recorded by the alkali feldspars. Even the most P-rich pegmatites contain < 1 wt% P_2O_5 in their bulk compositions, where known.

Beryl: The most beryl-rich pegmatites known contain an average of 205 ppm Be. At that concentration, a weakly peraluminous granitic melt becomes beryl-saturated below 600°C (Evensen *et al.* 1991). Beryl (and columbite) are common accessory minerals of the border zones of pegmatites, consistent with a low temperature of crystallization along the margins.

Pollucite: Pollucite marks the highest degree of chemical saturation in granitic melts. London (2008) calculated that the Tanco pegmatite achieved saturation in pollucite at ~ 385°C, after ~ 50% of the pegmatite-forming melt had crystallized. Based on its Cs content, London (2008) estimated that as much as 18,000 km^3 of rock might have been involved in the partial melting event that led to the formation of the Tanco pegmatite.

References

Černý, P., R. E. Meintzer, A. J. Anderson (1985) Extreme fractionation in rare-element granitic pegmatites: selected examples of data and mechanisms. Canadian Mineralogist, vol. 23, 381-421.

Chakoumakos, B. C., G. R. Lumpkin (1990) Pressure-temperature constraints on the crystallization of the Harding pegmatite, Taos County, New Mexico. Canadian Mineralogist, vol. 28, 287-298.

Chloe, M. A., C. Jaupart, J.-C. Mareschal (2009) Thermal evolution of cratonic roots. Lithos, vol. 109, 47–60.

Evensen J. M., D. London, R. F. Wendlandt (1999) Solubility and stability of beryl in granitic melts. American Mineralogist, vol. 84, 733-745.

Jahns, R. H., C. W. Burnham (1969) Experimental studies of pegmatite genesis: I. A model for the derivation and crystallization of granitic pegmatites. Economic Geology, vol. 64, 843-864.

London, D. (1984) Experimental phase equilibria in the system $LiAlSiO_4$-SiO_2-H_2O: a petrogenetic grid for lithium-rich pegmatites. American Mineralogist, vol. 69, 995-1004.

London, D. (1986) The magmatic-hydrothermal transition in the Tanco rare-element pegmatite: evidence from fluid inclusions and phase equilibrium experiments. American Mineralogist, vol. 71, 376-395.

London, D. (2008) Pegmatites. Canadian Mineralogist Special Publication 10, 368 p.

London, D. (2011) Experimental synthesis and stability of tourmaline: a historical overview. Canadian Mineralogist, vol. 49, 117-136.

London, D., G. B. Morgan VI, K. A. Paul, B. M. Guttery , G.B. (2012) Internal evolution of a miarolitic granitic pegmatite: the Little Three Mine, Ramona, California (USA). Canadian Mineralogist, vol. 50, 1025-1054.

Orville, P.M. (1963) Alkali ion exchange between vapor and feldspar phases. American Journal of Science, vol. 261, 201-237

THE LATE-STAGE MINI-FLOOD OF CA IN GRANITIC PEGMATITES: A WORKING HYPOTHESIS

R. Martin
Earth & Planetary Sciences, McGill University, robert.martin@mcgill.ca

The textural and compositional data amassed in recent years show convincingly that granitic pegmatites are indeed igneous rocks. What many fail to realize, however, is that in general, the mineralogy of these rocks is not igneous. What I intend to show, in this essay, is that a full understanding of the make-up of a granitic pegmatite requires knowledge of subsolidus modifications that are largely "orchestrated" by assemblages beyond the outer contact of the intrusive body.

Phase-equilibrium investigations predict that the fractional crystallization of a high-temperature feldspar or feldspars from a batch of granitic magma, be it of orogenic (LCT) or anorogenic (NYF) affiliation, will lead to a gradual increase in Rb and Cs, and a gradual decrease in the amount of Ca. Thus one can expect the Ca content of the primary feldspars to decrease progressively from the walls inward, as the melt migrates inexorably toward the pseudoternary minimum or eutectic in the calcium-free system Ab–Or–Qtz–H_2O. Although the sodic plagioclase does attain An_0 in most cases, the bulk composition of the pegmatite may still contain a fraction of weight percent of CaO, which accounts for the Ca complexed with part of the fluorine in the melt.

The Ca content of the primary feldspars is not easily erased in going down-temperature, owing to the coupled substitution Ca + Al for Na + Si. It tends to be locked in. On the other hand, the (Al,Si)-disordered state of the early-formed feldspar is partly or completely destroyed. The development of microcline twinned according to the albite and pericline laws is a subsolidus inversion; it does not occur in the presence of a silicate melt. This inversion initially involves the hydrogen ion as a catalyst, and may later involve molecules of H_2O as a solvent participating in solution-and-redeposition steps that coarsen the twin microstructure.

In an LCT pegmatite, fluorapatite is confined to the earliest stage of crystallization, near the outer contact, where it commonly forms acicular crystals oriented perpendicular to the outer contact. It then disappears, not because of a shortage of phosphorus, but rather of calcium. Nodules of a primary phosphate mineral, typically manganoan triphylite, may well accumulate as the core zone is approached, but these nodules are devoid of fluorapatite. At a later stage, coarse euhedral crystals of fluorapatite are found in cavities that are attributed to dissolution by the caustic orthomagmatic fluid. The late appearance of striking crystals of fluorapatite is attributed to an influx of calcium from outside the system. The LCT pegmatites of the Oxford suite, in Maine, provide excellent examples of this association.

In an NYF pegmatite, there may very well be a late development of calcium-bearing accessory phases such as pyrochlore, microlite, fersmite, and fluorite. The elements contributed to the cavity environment from beyond the outer contact may include Mg and B, which account for the striking development of zoned crystals of liddicoatite, fluor-dravite and danburite in the well-studied Anjanabonoina NYF pegmatite, in central Madagascar. In general, these late minerals are atypical of an NYF pegmatite, and account for a "mixed NYF–LCT" signal that confuses petrogenetic interpretations.

A "mini-flood of Ca", as Richard H. Jahns called it, is produced late in the development of the pegmatite. In the context of LCT pegmatites emplaced into the calc-alkaline host-rocks of the Southern California batholith, he considered that these more calcic rocks were surely involved. He also appealed to a leaching of the early-formed oligoclase or andesine produced by the pegmatite-forming magma in the wall zone and border zone. He was correct in identifying plagioclase as a principal reactant in the flood-producing reaction, but did not recognize the mechanism of massive and sudden liberation of Ca.

Everyone who learns about phase diagrams relevant to igneous petrology gets to know the binary system Ab–An at one atmosphere. This was an early chapter in the Ph.D. thesis of Norman Levi Bowen, completed in 1912. The determination of the liquidus and solidus is clearly a solid contribution to an understanding of the differentiation of magmas. However, Bowen and his successors to this day, even those working with H_2O as a component in the system, have been totally incapable of shedding light on the phase diagram Ab–An below the solidus. All valiant attempts fail because of kinetic reasons. There is agreement that there are three solvi, named

Peristerite, Bøggild and Huttenlocher, but no one has been able to map these in T–*X* space. TEM-scale photos show clearly that perthite-like exsolution lamellae do form, and presumably coarsen to a limited extent with annealing on geological time-scales. To state the problem concisely, all plagioclase compositions between $An_{1–2}$ and $An_{95–100}$ are metastably stuck somewhere below the solidus. These bulk compositions have begun to order (Al–Si) and to exsolve, but have not gotten very far because of the coupled substitution quoted earlier.

As Richard Jahns used to say, granitic pegmatites are prone to stew in their own juice. This juice acts as the catalyst in transforming the early-formed disordered K-feldspar to microcline or a mixture of microcline + orthoclase, both showing a twinned microtexture. As it becomes progressively enriched in fluorine, it becomes increasingly aggressive, and can create cavities by dissolution. More importantly in this context, it can leak into the country rock laterally and from the roof of zoned pegmatites; there it meets the metastably stuck plagioclase in any lithology that it encounters. The aggressive fluid, likely somewhat alkaline, promptly dissolves the plagioclase, and deposits in its place pure albite and K-bearing phases, possibly muscovite and microcline. Metamorphic petrologists agree that below 400°C, the phase diagram for the system Ab–An shows a stable coexistence of $An_{0–1}$ and $An_{95–100}$. The dissolution of a calcic plagioclase will shift the pH of the fluid to acidic values owing to the local consumption of Na + K and the massive liberation of Al + Ca. This acidic fluid then re-enters the cooling pegmatite, and there starts a new cycle of solution-and-redeposition steps. It is aggressive toward microcline and orthoclase, and efficiently replaces them by albite + muscovite, likely at a temperature in the range 250–400°C.

The reconstruction described above has major ramifications concerning the economic aspects of granitic pegmatites. The mini-flood of Ca (and Al) is clearly carried by an aqueous fluid that has lost K to the exocontact but has picked up Na (from the net dissolution of plagioclase) to account for the Na-metasomatic reactions that are widespread and indiscriminate within the zoned pegmatite. The fact that minerals of tantalum, lithium and tin are intimately associated with the albite-dominant replacement units shows that mineralization is due to a hydrothermal process, not a magmatic one. The aqueous fluid evidently is able to leach and transport these elements, and deposits tantalite-(Fe), tantalite-(Mn), micas of the lepidolite series and cassiterite as part of the replacement assemblage.

PRODUCTIVE "ZONES" IN GEM-BEARING PEGMATITES OF CENTRAL MADAGASCAR, GEOCHEMICAL EVOLUTION AND GENETIC INFERENCES

F. Pezzotta
Natural History Museum, C.so Venezia 55, 20121 Milano, Italy. fpezzotta@yahoo.com

Most gem-bearing pegmatites are miarolitic, are highly evolved, and belong to the LCT family. Gem crystals of several mineral species (e.g. tourmaline-supergroup minerals, beryl varieties, spodumene varieties, spessartine, topaz, etc.) may be present in pegmatites with two different occurrences: (1) in rare and small primary cavities dispersed in the central portions of pegmatitic bodies, providing very limited amount of crystals, generally of high gemological quality; (2) in a series of more or less large, partially interconnected primary cavities, occurring in core zones and characterizing limited portions or sectors of pegmatitic bodies, providing for large quantities of crystals, of low, to medium to high gem quality. Such pegmatite portions or sectors are called "productive zones" or just "zones by gem miners.

As described above, occurrence (1) is the most common; small-scale gem mines can operate over long periods tunneling in pegmatites and finding occasionally only very small quantities (in the order of tens of grams to a few hundred grams) of gem-quality crystals. In some rare cases, gem mines encounter a "zone" (occurrence 2), in which a series of large gem-pockets is discovered, with the production of large quantities of gem-quality crystals (exceptionally in the order of hundreds of kilos and even tons).

"Zones" physically correspond to the cores of well-structured and large "pegmatite macrostructures" (PM), these last defined in Pezzotta (2009) as the ensemble of rock structures of a pegmatitic body formed under *the same evolutional process*; which means, formed starting from the same *pocket of homogeneous pegmatitic melt or fluid*, from which during crystallization the typical pegmatitic heterogeneites formed. It is important to notice that not all cores of gem-bearing pegmatites contain a "zone", and that PM may or may not (and in gem-pegmatites in general "not") correspond to the entire volume of the pegmatitic body. In many cases a single pegmatitic body contains several PM, of different sizes and,as a consequence, with different structure (zoning), with the largest PM generally being more complex. This phenomenon has been related in Pezzotta (2009) to a "size factor".

Gem bearing pegmatites in Madagascar are distributed mostly in the central and south of the island. Economically, the most important ones are those characterized by the occurrence of red and multicolored tourmaline ("liddicoatite" and "elbaite", Pezzotta & Laurs, 2011). Tourmaline bearing pegmatites occur in pegmatitic fields hosted in many different rock units (paragneiss, quartzites, marbles, and migmatites), belonging to different geologic domains and sub-domains (geologic framework here used for reference from Tucker *et al.*, 2011): the Antananarivo domain, characterized by the fields of Anjoma, Valozoro-Camp Robin, Alaka Misy Itenina; the Itremo sub-domain, characterized by the fields of Sahatany, Manapa, Anjanabonoina, Vohitrakanga, Ambalamahatsara; the Ikalamavony sub-domain, characterized by the fields of Bevoandrano, Ikalamavony, Tsitondroina, Mandrosonoro-Ambatovita. Only one important tourmaline deposit (Anjahamiary, Pezzotta, 2003), and a few minor ones, are known in south Madagascar (Anosyen domain).

Gem bearing pegmatites of central and south Madagascar are associated with a late Neoproterozoic tectono-magmatic event (age between 570 and 540 Ma, Pezzotta, 2005, and references therein) characterized by the intrusion of syenite and granite plutons, emplaced in an extentional tectonic regime.

Rarity of these gem-bearing pegmatites, coupled with scarce and/or incomplete exposure, alteration, and irrational mining, make the documentation and mapping of PM in Madagascar difficult. Nevertheless, several examples have been observed and sampled by the author in the Sahatany, Manapa, Anjanabonoina, Valozoro, Ambatovita, Bevoandrano, and Tsitondroina fields. Gem-tourmaline bearing pegmatites in Madagascar are in general of tabular shape and they are from sub-horizontal through gently to steeply dipping. Sizes range from a few meters in thickness and some tens of meters in length up to some tens of meters in thickness and over 1 km in length. The thickest dikes have a more or less layered structure, with

layers characterized by variations in the grain size (from fine to medium to coarse) and in the content of minerals (sodic and potassic feldspars, quartz, tourmaline, garnet, Nb-Ta oxides, danburite, spodumene). Layers have thicknesses ranging from centimeters to about one meter. Very rare miarolitic cavities of small size (a few decimeters across), with gem-quality crystals mostly of tourmaline, can occur dispersed inside the coarse-grained bands. Thinner dikes (decimeters up to meters in thickness) are generally not layered and have lateral variations in the rock grain size and mineral distribution.

PMs develop in more or less large sectors of dikes, in many cases occupying the entire thickness of the dike but in some thick dikes, only a portion of it. In the large subhorizontal Tsarafara pegmatite in the Sahatany valley, the author observed in one vertical section three well structured, complexly zoned, and distinct PM corresponding to three "productive zones". PM containing "productive zones" occurring in dikes belonging to different fields, have similar features which include: a lower border zone, roughly layered with fine to medium grained aplitic-pegmatitic rock; an intermediate zone of pegmatitic grain size enriched in tourmaline and accessories; a lower portion of the core zone, characterized by abundant cleavelandite and large to enormous crystals of quartz, tourmaline, beryl, spodumene, and abundant blades of purple Li-rich mica; an upper portion of the core zone composed mostly by large to giant crystals of microcline, in some cases partially replaced by cleavelandite and an upper border zone of coarse to medium-fine grained aplitic-pegmatitic rock.

In most of the pegmatite fields, the largest PM are characterized by a complex structure and a core containing a "zone". Nevertheless, in some fields, the most complex and large PM do not contain gem-bearing cavities. In these cases, gem-production is confined to dispersed, small, and rare miarolitic cavities in coarse-grained lenses in the dikes, or in small PM characterized by a more or less simple structure. An example is the Bevoandrano pegmatite field, south of Ikalamavony, in the Fianarantsoa province. In this field, as the thickness of the PM exceeds several meters, a series of rock units develop in the core zone, including masses of granular lepidolite, masses of milky quartz, extensive albitized volumes, more or less associated with amblygonite masses, and large tapering spodumene crystals. In this case, large quantities of more or less opaque, polychrome, tourmaline crystals form, frozen in the rock, and no cavities develop. In the author's experience, not a single "zone" producing gem-quality crystals has been found until now in Bevoandrano.

The Tsitondroina field, located west of Ikalamavony, Fianarantsoa region, represents a different case in which, miarolitic cavities containing gem crystals occur only in the largest PM, which is the most important known deposit, composed of a gigantic PM, over 300 meters long and over 40 meters thick, hosted in a pegmatitic vein which can be traced in the field for over 1.5 km in length.

Highly evolved to extremely evolved geochemical features of "zones", are:

Mineralogy – Exotic mineralogy typically characterizes the most evolved portions of gem-bearing pegmatitic dikes. "Zones" in gem-tourmaline pegmatites in Madagascar are characterized by the occurrence of the famous, multicolored crystals of fluor-liddicoatite (Lussier & Hawthorne, 2011). These are large tourmaline crystals of first generation grown across all stages of formation of the core zones of PM, ranging in composition from primitive "dravite-schorl", , to highly evolved "liddicoatite-elbaite", both with variable Ca, Na, □ in the X site. Zoning patterns evidenced by slicing the crystals across the C-axe, from the base to the termination (represented by the antilogous pole), are the result of variable occurrence and combination of crystal forms (more steep pyramids and dipyramids produce more complex patterns across c-axe) and variations in the ratio between prismatic and pyramidal-pedion growth. Such compositional, structural and morphological variations represent an extraordinary record of the chemical-physical variations during crystal growth, and further studies are in progress about this topic.

Boron isotopes - Pezzotta *et al.* (2010) sampled a series of gem-bearing pegmatitic dikes hosted in paragneiss and marbles of the Itremo domain, In these pegmatites, minerals with B in 3-fold coordination with O (3BC), dumortierite and tourmaline supergroup minerals ("dravite-elbaite-liddicoatite"), and danburite with B in 4-fold coordination (4BC), formed during all stages of crystallization of the pegmatitic veins. "Dravite" and dumortierite are confined to the most primitive rock units; "elbaite-liddicoatite" and danburite formed up

until the latest stages of crystallization (miarolitic zone) of the veins. The central, most evolved zone of numerous pegmatites is characterized by a suite of borates that include the 4BC rhodizite-londonite solid solution, with local strong Rb enrichments, the 4BC behierite-schiavinatoite solid solution (Ta borate and Nb borate, respectively), and, occasionally, the 3BC hambergite.

B isotopic studies were conducted on: (1) "tourmaline", danburite, and hambergite sampled from the border zone to the mica-rich, highly evolved, core zone of the famous and large Anjanabonoina pegmatite (AJB); (2) "tourmaline", danburite, rhodizite-londonite, and behierite-schiavinatoite sampled in the border zone and in the highly evolved core zone (micafree) of two representative pegmatites, in the Tetezantsio area (TTZ). For primitive rock units, the results indicate for AJB: $\delta^{11}B_{dravite}$ 4.70‰ and $\delta^{11}B_{danburite}$ -0.83‰; and for TTZ: $\delta^{11}B_{dravite\text{-}elbaite}$ -2.33‰ and $\delta^{11}B_{danburite}$ -8.45‰. For zoned crystals of "tourmaline" from AJB formed in pegmatitic units of intermediate geochemical evolution, $\delta^{11}B$ is homogeneous with values between 6.21 and 7.38‰. Cogenetic hambergite crystals have similar values ($\delta^{11}B$ 7.02‰). For the most evolved rocks from AJB: $\delta^{11}B_{elbaite\text{-}schorl\ core}$ 6.94‰ and $\delta^{11}B_{liddicoatite\ rim}$ 14.72‰ and $\delta^{11}B_{danburite}$ from -0.26‰ to 8.03‰ $_{(rim)}$; and for TTZ: $\delta^{11}B_{elbaite\text{-}liddicoatite}$ 0.60‰, $\delta^{11}B_{danburite}$ -6.72‰, $\delta^{11}B_{rhodizite}$ -6.93‰, $\delta^{11}B_{behierite}$ -10.70‰.

These data indicate that cogenetic 3BC ("tourmaline", hambergite) and cogenetic 4BC (danburite, rhodizite, behierite) represent two distinct B isotopic populations, characterized by rather similar values, with $\delta^{11}B$ of 4BC systematically shifted to lower values with respect to the cogenetic 3BC. Whatever was the nature of the crystallizing medium, the data reported above indicate that an isotopic fractionation process occurred in response of the type of boron coordination in the two major minerals, "tourmaline" and danburite.

The difference in the original composition of the pegmatite-forming medium, and the differences in the local geological conditions (nature of the host rock, P-T conditions), are fundamental to the mineralogy and zoning of PM and in the "size factor" characteristic of PM belonging to different fields. As evidenced in Pezzotta (2005), in the same field, different pegmatite populations develop in different rock units; moreover, the available data obtained by geologic mapping do not show clear relations between spatial distribution of pegmatite and granitoid intrusions. The author proposes a model for the formation of Malagasy gem-bearing pegmatites to be the result of the crystallization of magmatic liquids of "residual composition" resulting from both magmatic fractionation of "migmatitic granites" or from migmatitic segregations, contaminated at different proportions by high-density metamorphic fluids originated at (or close to) the level of intrusion, during the uplift accompanying the late phases of the last upper-Neoproterozoic teconomagmatic event.

References

Lussier A.J., Hawthorne F.C. (2011) Oscillatory zoned liddicoatite from Anjanabonoina, central Madagascar. II. Compositional variation and mechanism of substitution. Canadian Mineralogist 49: 89-104

Pezzotta F. (2005) A first attempt to the petrogenesis and the classification of granitic pegmatites of the Itremo Region (central Madagascar). Abstracts of the Crystallization Processes in Granitic Pegmatites, International Meeting, May 23-29, 2005, Elba Island, Italy

Pezzotta F. (2009): Definition of "pegmatitic macrostructure" and evidences of a "size factor" controlling evolutional processes in pegmatitic rocks. Etudos Geologicos, Contributions of the 4th International Symposium on Granitic Pegmatites – PEG2009BRAIL, 19 (2), 292-293.

Pezzotta F., Dini A., and Tonarini S. (2010) Three- and four-coordinated boron minerals in pegmatites hosted in dolomitic marble in Central Madagascar; paragenesis and boron isotopes. IMA 2010 Bonds and Bridges, Budapest, in press..

Pezzotta F. and Laurs B.M. (2011) Tourmaline: The Kaleidoscopic Gemstone. Elements, 7, 5, 333-338.

Pezzotta F., and Jobin M. (2003) The Anjahamiary pegmatite, Fort Dauphin area, Madagascar. Web site of Mineralogical Society of America. www.minsocam.org/msa/Pegmatites.html.

Tucker R.D., Roig J.Y., Macey P.H., Delor C., Amelin Y., Armstrong R.A., Rabarimanana M.H., and Ralison A.V. (2011) A new geological framework for south-central Madagascar, and its relevance to the "out-of-Africa" hypothesis. Precambrian Research, 185, 109-130.

PEGMATITIC ROCKS IN A MIGMATITE-GRANITE COMPLEX (NW PORTUGAL)

M. Areias, M. Ribeiro, A. Dória
CGUP/DGAOT-FCUP, Porto, Portugal (maria.areias@gmail.com)

Geometry, structure and mineralogy

In NW Portugal a migmatite massif surrounding a synorogenic granite occurs within the axial zone of the Iberian Variscan Orogen along the western border of the Central Iberian Zone (CIZ). This massif includes metatexites and diatexites, both cut by a set of pegmatitic and granitic bodies and veins. The pegmatitic bodies exhibit variable geometry and dimension, both concordant or discordant with the structure of the host migmatite rocks (N150° to N170º; 90º).

Three types of veins were investigated: (i) aplite-pegmatites (APG) veins; (ii); pegmatoid (PGTD) veins; and (iii) leucocratic patch (LCP) veins.

The APG veins (Fig. 1A) (thickness: cm to m; length: 10 to hundreds meters) have sharp contacts, striking N110º to N140º and internal zonation. The zoning comprises: i) an aplitic central zone, composed by quartz, albite, biotite and aligned trails of tourmaline (schorl) and garnet (Fe+Mn+F bearing); ii) an intermediate coarser-grained zone with perthitic feldspar, albite, quartz, tourmaline and muscovite. The feldspar has irregular borders and abundant fine-grained matrix-mineral inclusions; iii) a medium-grained quartz-feldspathic zone with fine-grained mica, quartz and tourmaline agglomerates; and iv) a quartz-albite fringe adjacent to host rock (comb structures). The albite contains abundant apatite inclusions.

The PGTD veins (Fig.1B) are coarse-grained biotite-rich without internal structure and with irregular geometry parallel to the migmatite structure striking N120º to N150º. These veins, associated with diatexites, have gradually coarsening grain size towards the center of the body and are composed of plagioclase (An_{20}), quartz, orthoclase, biotite, cordierite, sillimanite, garnet, rare andalusite, and pseudomorphic, fine-grained clusters of white mica after biotite. The coarse-grained perthitic K-feldspar contains inclusions of plagioclase, biotite, cordierite and quartz with irregular or rounded morphology. Some aligned bands of biotite-cordierite-sillimanite (schlieren) occur in the quartz-feldspathic zones.

The LCP veins (Fig. 1C) show diverse geometry, with tabular or irregular bodies, parallel or intersecting the migmatitic structure. They are characterized by a leucocratic matrix with feldspar, plagioclase, quartz and medium to coarse-grained muscovite and biotite-chlorite-rutile-muscovite±tourmaline±fibrolite clusters. The abundant coarse-grained and anhedral K-feldspar (microcline) develops intergrowths with plagioclase and contains rounded inclusions of quartz, plagioclase and biotite.

Geochemistry

The pegmatoid bodies, leucosomes, diatexites and associated granites show low concentration of Fe, Mg, Ca, Mn, Th and HSFE regarding the Upper Continental Crust – UCC (Taylor & McLennan, 1985). The contents of LILE are similar to the UCC (Fig. 1D).

The APG are most enriched in Mn, Mg, Ta, Nb, Cs and Be and depleted in K, Ba, Sr, Th and Ti. The chondrite-normalized (Boynton, 1984) REE pattern has low ΣREE, negative Eu anomaly and low HREE fractionation.

The chemical composition of PGTD veins is similar to the associated diatexites. The REE pattern is characterized by moderate ΣREE, absence of a Eu anomaly and variable fractionation trends of HREE.

The LCP veins and leucosomes show similar REE pattern, with positive Eu and Tb anomalies, low ΣREE and variable fractionation of HREE.

The granitic rocks yield moderate ΣREE, a negative Eu anomaly and high REE fractionation ($16 \leq La/Lu \leq 45$).

In all the lithologies, the ΣREE is related to zircon and garnet content. The Eu anomaly shows a positive correlation with K/Na. In the garnet bearing rocks the fractionation of HREE is lower.

Discussion

The APG veins show mineralogical composition and structural zoning similar to typical granitic pegmatites. The PGTD veins show chemical and mineralogical affinity with diatexites and the LCP veins show the same affinity with metatexitic leucosomes. This suggests different time and origin of the studied veins although they all have pegmatitic texture (coarse grain) and granitic composition.

The central aplitic zone of the APG seems to be the earliest with nucleation of Na, Mn and Fe phases without K. The growth of orthoclase and muscovite, indicating a period of K abundance, is confined to

the intermediate zone. Lastly, the comb intergrowth of quartz-albite, with abundant apatite inclusions and rare orthoclase+muscovite indicates high Na, Ca and P content and low K content.

In diatexites the K-feldspar was the last phase, as indicated by the inclusions of all other paragenetic minerals. In the leucosomes the intergrowths of plagioclase and K-feldspar indicate that the first was replaced by the last one. Some of the leucosomes show replacement of biotite by tourmaline.

The sequence of minerals growing in the APG veins seems to be related to the sequential stages of anatexis: i) a first melt without K-feldspar, resulting from the water-undersaturated breakdown of biotite, with anhydrous peritetic minerals (cordierite and garnet) and rich in plagioclase + quartz; the aplitic inner part of the APG is probably related to this stage; ii) in a second stage, the progression of melting promoted the grow of large orthoclase and replacement of plagioclase by K-feldspar in leucosomes and diatexites; these fluids have not reached the entire migmatitic complex since there are diatexites and metatexites without K-feldspar; iii) in a later stage, the APG growth was marked by a quartz-albite comb structure, with abundant apatite inclusions indicating the effect of the K-poor and Na+P - rich fluid. This last phase could coincide with the emplacement and crystallization of P-rich granites and release of B-rich fluids that gives rise to the development of tourmaline-bearing veins.

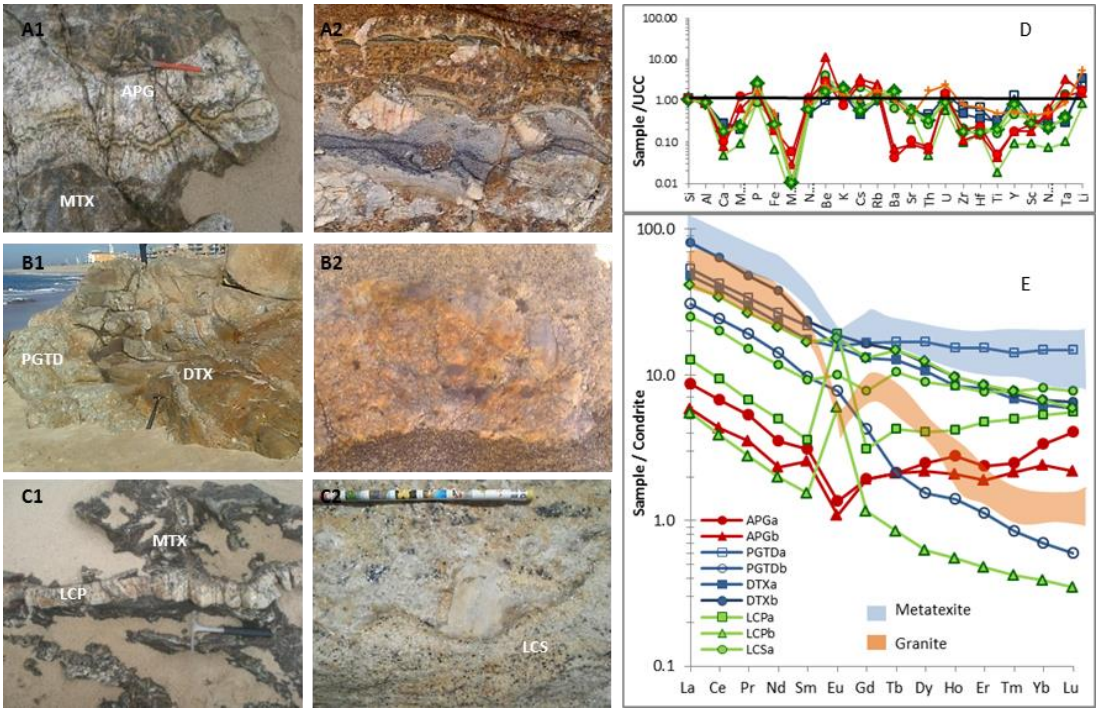

Fig. 1: A1) Transgressive aplitopegmatite vein in metatexite (MTX); A2) APG detail; B1) Pegmatoid veins (PGTD) associated with diatexite (DTX); B2) PGTD detail; C1) Transgressive leucocratic patch (LCP) vein in metatexite (MTX). C2) Leucosome (LCS). D) UCC-normalized multi-element diagram. E) Chondrite-normalized REE pattern diagram including granite and metatexite.

Acknowledgments

Research integrated in the activities of CGUP, with financial EU funds by FEDER/OPHP and FCT (fellowship nº SFRH/BD/65509/2009) and PETROCHRON project (PTDC/CTE-GIX /112561/2009).

References

Taylor, S.R, McLennan S.M (1985): The continental crust. Its composition and evolution. Blackwell Scientific Publication, London, 312.

Boynton W.V. (1984): Geochemisytry of rare earth elements: metrorite studies. In Henderson P. (ed), Rare earth element geochemistry. Elsevier, pp 63-114.

UNRAVELING THE FLUID EVOLUTION OF MINERALIZED PEGMATITES IN NAMIBIA

L. Ashworth[1], J. Kinnaird[1], P. Nex[1,2]
[1] Economic Geology Research Institute, School of Geosciences, University of the Witwatersrand
luisa.ashworth@gmail.com
[2] Umbono Financial Services

Introduction

Namibia is renowned for its abundant mineral resources. A large proportion of these resources is hosted in the metasedimentary lithologies of the Damara Belt, the northeast-trending inland branch of the Neoproterozoic Pan-African Damara Orogen. Deposit types include late- to post-tectonic (~ 523 – 506 Ma) LCT (Li-Be, Sn-, and miarolitic gem-tourmaline-bearing) pegmatites, and uraniferous pegmatitic sheeted leucogranites (SLGs), which have an NYF affinity.

Fluid Inclusion Results

Fluid inclusion studies reveal that although mineralization differs between the different types of pegmatites located at different geographic locations, and by extension, different stratigraphic levels, the fluid inclusion assemblages present in these pegmatites are similar. Thorough fluid inclusion petrography indicated that although fluid inclusions are abundant in the pegmatites, no primary fluid inclusions could be identified, and rather those studied are pseudosecondary and secondary. Fluid inclusions are aqueous-carbonic, carbonic, and aqueous.

Three types of pseudosecondary fluid inclusion were observed. Aqueous-carbonic pseudosecondary inclusions contain halite and an unidentified, acicular opaque phase. In the Li-Be and gem tourmaline-bearing pegmatites, these inclusions contain pure CO_2, however in the Sn-bearing pegmatites trace amounts of CH_4 are present. These inclusions homogenize at temperatures (Th) ranging from 320 – 330 °C, and their density is intermediate (0.7 – 0.8 g/cc). The presence of halite crystals in these inclusions indicates salinity in excess of 23.3 equivalent wt % NaCl (Shepherd, *et al.*, 1985). Qualitative PIXE micro-elemental maps show the presence of Fe, Mn, Cu, and Zn, suggesting that the trapped fluids are far more compositionally complicated than indicated by microthermometry alone. Saline aqueous inclusions containing halite and two opaque phases homogenize at lower temperatures (100 – 120 °C), and their density ranges from 0.9 – 1.0 g/cc. Pure CO_2 pseudosecondary inclusions are observed only in the pegmatitic SLGs. They homogenize at a temperatures ranging from 7 °C to 15 °C, and their density is relatively high (0.8 – 0.9 g/cc).

Multiple secondary fluid inclusion populations are present in the pegmatites. The three populations observed are of similar composition, Th, and density to the pseudosecondary populations, however they are less saline (12 – 15 equivalent wt % NaCl).

Stable Isotopes

Oxygen isotope ratios in quartz show a bimodal distribution (Fig. 1). This suggests an I-type affinity for the samples showing lower $\delta^{18}O$ ratios ($\delta^{18}O$ = 11 – 13 ‰) i.e. the Li-Be pegmatites and pegmatitic SLGs, and an S-type affinity for those with higher ratios ($\delta^{18}O$ = 15 – 16 ‰) i.e. the miarolitic and

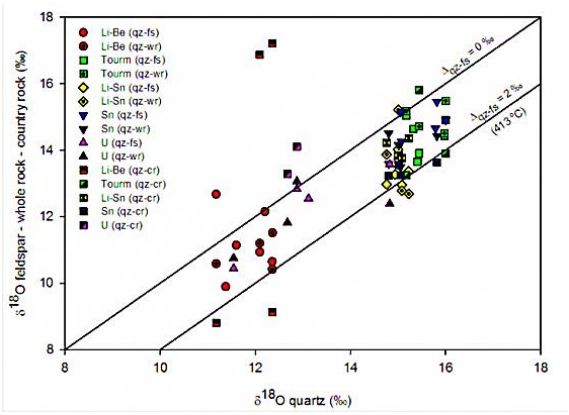

Fig. 1: $\delta^{18}O$ ratios for quartz, feldspar, whole rock samples taken from mineralized pegmatites in Namibia, and their adjacent country rocks.

Sn-bearing pegmatites. This is corroborated by the fact that the metapelitic and carbonate country rocks in the vicinity of the latter exhibit similar $\delta^{18}O$ ratios to those of the pegmatites, while the same is not true of the I-type pegmatites and their country rocks, which are carbonates, metapelites, and granodiorites. The $\delta^{18}O$ ratios of the S-type pegmatites are high, and this is consistent with the derivation of these magmas from a sedimentary source. However, the ratios of I-type pegmatites are elevated above those of typical I-type granites, which typically range from $\delta^{18}O = 7 – 9$ ‰, suggesting either a low-temperature exchange with meteoric fluid, high-temperature hydrothermal exchange with $\delta^{18}O$ country rocks, or the derivation of these pegmatites from a non-pelitic source (Sharp, 2007). δD values range from -40 ‰ to -90 ‰ indicating that the pegmatitic fluids are primary magmatic.

Geochemistry

Trace elements show that both LCT and NYF pegmatites fall within the range of syn- to post-collisional granites (Fig. 2A). Rare earth element concentrations in all of the LCT pegmatites are low. Although there is some scatter in REE abundance, all of the pegmatites show a relative enrichment in LREE in comparison to HREE, and a strong Eu anomaly (Fig. 2B). The NYF pegmatitic SLGs contain higher abundances of REEs, and a depletion in LREE in comparison to HREE (Fig. 2B).

Conclusions

Trace element data indicate that all of the pegmatites studied are syn- to post-collisional. Fluid inclusion studies show that there is no significant compositional variation in fluid inclusions from the different types of (Li-Be, Sn, Li-Sn, miarolitic) coeval LCT pegmatites and NYF uraniferous pegmatitic SLGs, however the compositions of the fluids are far more complicated than can be modeled using microthermometry alone. Therefore, fluids alone cannot be responsible for the differences in mineralization observed in these pegmatites. Oxygen isotope ratios show that there are two populations of pegmatite with different sources, and that the role of the country rock is important particularly in those pegmatites of an S-type affinity.

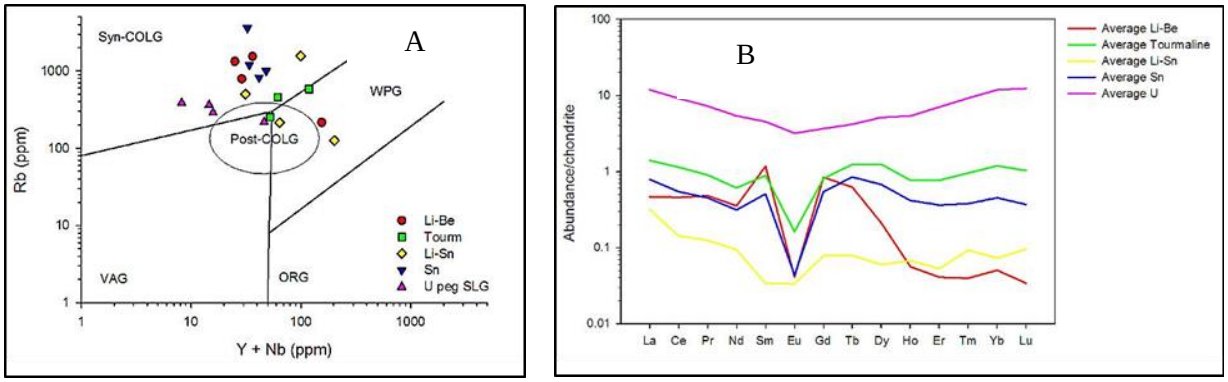

Fig. 2: A) Tectonic discrimination diagram for mineralized pegmatites in Namibia; B) Average normalized REE patterns of mineralized pegmatites in Namibia.

References

Sharp, Z. (2007): Principles of Stable Isotope Geochemistry, Pearson Prentice Hall, Upper Saddle River, pp 344.

Shepherd, T., Rankin, A.H., Alderton, D.H.M. (1985): A Practical Guide to Fluid Inclusion Studies, Blackie, New York, pp 239.

THE PHOSPHATE MINERALS ASSEMBLAGES FROM JOCÃO PEGMATITE, MINAS GERAIS, BRAZIL

M. Baijot[1], F. Hatert[1], S. Philippo[2]
[1] Laboratory of Mineralogy, University of Liège, Belgium, mbaijot@ulg.ac.be
[2] Mineralogy section, Natural History Museum of Luxembourg

In Brazil occurs one of the most important pegmatite provinces in the world , the Eastern Brazilian Pegmatite Province (EBPP). This province is located at the Eastern side of the Saõ Francisco craton, mainly in the state of Minas Gerais.The Conselheiro Pena district forms part of the EBPP where two intrusions crosscut the basement rocks and its cover: the Galiléia and Urucum magmatic suites which correspond to metaluminous and peraluminous magmas, respectively. The Galiléia suite consists in granodiorite and tonalite and the Urucum suite is composed of four different facies of granite. In August 2008 and July 2010, we visited several pegmatites located in the Conselheiro Pena district in order to investigate the petrography of phosphate minerals and their relationships with associated silicates.

Among these pegmatites, the Jocão pegmatite, also called Cigana or Boa Vista Cigana pegmatite, is intruded in the garnet-, biotite-, and sillimanite-bearing schists of the São Tomé Formation (Rio Doce group, Late Proterozoïc). Although the pegmatite was under water when we visited, we were able to collect phosphate minerals and associated silicates from the dumps. According to their macroscopic features, three types of phosphate occurrences may be distinguished. After the magmatic stage during which the primary phosphates crystallized, each type of occurrence was altered by pegmatitic processes, under different physico-chemical conditions, leading to different phosphate mineral assemblages. The petrographic observations, X-ray diffraction measurements, and electron-microprobe analyses that were performed on these minerals allowed us to characterize these three different phosphate minerals assemblages.

The first assemblage (I) consists of dendritic and skeletal textures involving feldspar (generally albite) and triphylite (Figs 1a, 1b). This triphylite may also form complex intergrowths with associated garnet, quartz, and apatite (Fig. 1b). Then triphylite evolved under poor oxidizing conditions. The first hydrothermal stage was a hydroxylation stage during which triphylite was only replaced by hureaulite along its cleavage planes. In some rare cases, hureaulite is associated with barbosalite. The second alteration stage corresponds to meteoric processes, which are responsible for the formation of ludlamite and vivianite replacing triphylite. These two minerals are ferrous iron bearing phosphates with high water content.

The second assemblage (II) occurs as a nodule (15 cm in diameter) covered by oxides. The only primary mineral of this assemblage is triphylite, which evolved under more oxidizing conditions. The first hydrothermal transformation is the progressive oxidation of this triphylite, $Li(Fe^{2+},Mn^{2+})PO_4$, coupled with a simultaneous Li-leaching, yielding to ferrisicklerite, $Li_{<1}(Fe^{3+},Mn^{2+})PO_4$, and heterosite, $(Fe^{3+},Mn^{3+})PO_4$, successively. This oxidation mechanism corresponds to the so-called "Quensel-Mason" sequence. The second hydrothermal stage corresponds to a hydroxylation process; the mineral species which are formed during this stage depend on the species they alter. For example, in Fig. 1c, we see the contact between triphylite and ferrisicklerite in the same optical orientation. Nevertheless, triphylite is altered by barbosalite and hureaulite, while ferrisicklerite is altered by janhsite and/or frondelite *s.l.* All these hydroxylated species occurred in the cleavages planes of the previous unaltered minerals (Fig. 1c). The last alteration stage lead to the formation of meteoric phosphate species, like phosphosiderite, leucophosphite and whitmoreite, and of Fe-Mn bearing oxides, which result in the disappearance of former petrographic texture.

The third assemblage (III) also occurs as an elliptic nodule reaching 70 cm x 50 cm x 50 cm. This nodule presents intergrowths between ferrisicklerite/ heterosite and a reddish massive beusite (Fig. 1d). Garnet may also be present in this assemblage. The textural relationships between the lamellae of ferrisicklerite and heterosite in beusite, $(Mn,Fe,Ca)_3(PO_4)_2$, correspond to exsolutions lamellae, which are formed at the expense of high temperature homogenous Ca-Li bearing graftonite-beusite-like phase: when the temperature decreased, Li migrate into triphylite (which are later altered to ferricklerite and heterosite) and Ca into the larger M1 site of beusite. Intergrowths of triphylite in beusite are less common than exsolution of triphylite in graftonite or lithiophilite in beusite. The bulk composition of the high temperature homogenous

phase and the partition coefficient allow us to better understand these exsolutions lamellae of triphylite in beusite. After this magmatic process come the hydrothermal stages. The first one corresponds to the "Quensel-Mason" sequence; this oxidation stage does not alter beusite. Nevertheless, the second hydroxylation stage more strongly affects beusite than ferrisicklerite and heterosite lamellae. The replacement of beusite by an intimate polygranular mixture of orange pleochroic hureaulite and tavorite progressed from the contact with the exsolutions, leaving the latter almost unaltered. However, heterosite is replaced by OH-rich fluorapatite and staněkite. After this stage, another stage is characterized by an increase of Ca^{2+} and H_2O activities, indicated by the replacement of hureaulite and tavorite by minerals of the mitridatite-robertsite series. In the border of the nodule, beusite and heterosite are completely replaced by intimate polygranular intergrowths mainly constituted by frondelite, robertsite-mitridatite and oxides. Phosphosiderite and leucophosphite are scarcer. In the inner part of this border, lamellae of heterosite are only replaced by (Mn-Fe)-bearing oxides and beusite by the intimate intergowths. However, in the external part of the border, the exsolution texture is completely obscured by other secondary mineral species. In assemblage III a rare silico-phosphate mineral also occurs, harrisonite $Ca(Fe^{2+},Mg)_6(SiO_4)_2(PO_4)_2$, which was previously reported in only one pegmatite from Czech Republic (Skoda *et al.*, 2007). According to the textural relationship with associated minerals, it seems that harrisonite has a hydrothermal origin. This mineral was probably formed after dissolution of garnet by Ca-Fe and P-rich hydrothermal fluids. Apatite, which replaces heterosite, is often associated with harrisonite and may be formed simultaneously or shortly before the formation of this phase because the crystallization of phosphates and silicates is considered as a sequential crystallization.

As we have seen above, the primary phosphate minerals occur in different type of assemblages. In assemblage I, triphylite is dendritic and show intergrowths with silicates (albite Fig.1a, garnet, Fig. 1b); in assemblage II, triphylite occurs as massive nodules; and in assemblage III triphylite forms exsolution lamellae in massive beusite. Moreover, the oxidation affecting the whole nodules of each assemblage increases from the core to the border. In assemblage II a mineral zonation occurs, which is underlined by the different colour of the Quensel-Mason sequence minerals: greenish for triphylite (core), brownish for ferrisicklerite (transition zone), purple for heterosite (external zone) and, finally a dark colour for the oxides (cover). In assemblage III, lamellae of ferrisicklerite only occur in the core of the nodule, while they take the purplish colour of heterosite on the border (Fig 1d). These features will be discussed and the different nodules will be chronologically positioned in the global setting of the pegmatite.

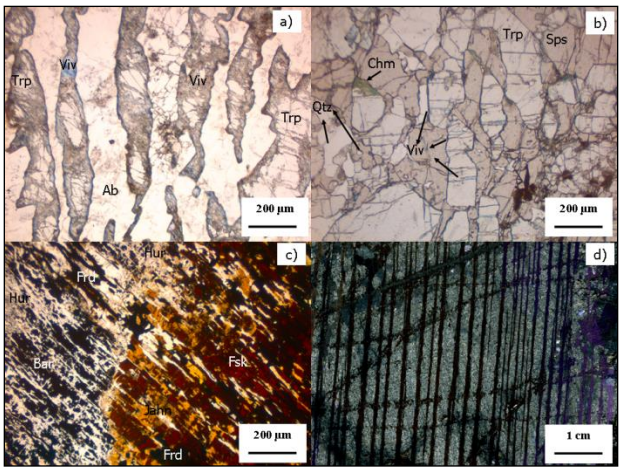

Fig. 1: The three different phosphate assemblages. a, b: assemblage I; c: assemblage II; d assemblage III. Trp: triphylite; Ab: albite; Viv: vivianite; Sps: spessratine; Chm: chamosite; Qtz: quartz; Hur: hureaulite; bar: barbosalite; Frd: frondelite; Fsk: ferrisicklerite.

Reference

Škoda, R., Staněk, J., Čopjaková, R. (2007): Minerální asociace fosfátových nodulí z granitického pegmatitu od cyrilova u velkého meziříčí, moldanubikum; Část I primární a exsoluční fáze. Acta Mus. Moraviae, Sci. geol., vol. 92, 59-74.

PRELIMINARY CRYSTALLOGRAPHY AND SPECTROSCOPY DATA OF EUCLASE FROM NORTHEAST OF BRAZIL

S. Barreto, de B.[1], V. Zebec[2], A Čobić[3], R.Wegner[4], R Brandão[1], P. Guzzo[5], L. Santos[1], V. Begić[3], V. Bermanec[3]
[1] Department of Geology, Federal University of Pernambuco, Recife PE, Brazil email sandrabrito@smart.net.br
[2] Croatian Natural History Museum, Zagreb, Croatia
[3] Institute of Mineralogy and Petrography, Department of Geology,University of Zagreb, Croatia
[4] Department of Geology, Mining School, Federal University of Campina Grande, Brazil
[5] Department of Mining Engineering, Federal University of Pernambuco, Recife PE, Brazil

Gem-quality euclase is not common. Because of this, spectroscopy and crystallography studies are important for its characterization. The investigated euclase samples were collected at the Jacú and Mina do Santino pegmatites, which are complex pegmatites located in the Equador district, state of Rio Grande do Norte-Brazil, and are part of the Borborema Pegmatitic Province (BPP). Samples from both localities are well-formed monoclinic crystals with prismatic forms. The crystals are colorless with patchy colored domains. Crystals from Mina do Santino pegmatite are colorless or with greenish-blue domains (Fig. 1a). The Jacú pegmatite samples are zoned with colorless and grayish-blue domains, and some crystals are bicolored with colorless and blue zones (Fig. 1b).

XRD patterns of natural and samples heated at 1025°C were analyzed using the X'Pert High Score program (Panalytical, 2004). All crystals were confirmed as single-phase euclase with small differences in unit cell parameters. Unit cell parameters were calculated using Unit Cell programme (Holland & Redfern, 1997). For a natural sample from the Jacú pegmatite (sample: 2018) cell parameters are: a = 4.7814(2) Å, b = 14.3355(7) Å, c = 4.6348(2) Å and β = 100.331(5) ° and for a natural sample from Mina do Santino pegmatite (sample: 1474): a = 4.7842(3) Å, b = 14.3391(6) Å, c = 4.6356(2) Å and β = 100.311(5) °. Heating of euclase samples at 1025°C for 3 hours results in a breakdown of the euclase structure to several products: coesite (SiO_2), phenakite (Be_2SiO_4), mullite ($Al_{4+2x}Si_{2-2x}O_{10-x}$) and a beryllium aluminium silicate ($2BeO \cdot 3.67Al_2O_3 \cdot 6SiO_2$), JCPDS card 18-204, previously reported in literature (Graziani & Guidi, 1980).

Crystals of euclase were measured using a two-circle goniometer. They are well developed with the following forms: {100}, {120}, {130}, {140}, {010}, {011}, {021}, {031}, {041}, {111}, {131}, $\{\bar{1}21\}$, $\{\bar{1}02\}$, $\{\bar{2}01\}$, $\{\bar{1}11\}$, $\{\bar{1}31\}$, $\{\bar{2}11\}$ and $\{\bar{2}21\}$ An additional form appears on most of the crystals, but it was not possible to determine the indices precisely. It was identified as an {hkl} that approaches the position of form {263}, with ρ = 43°08'- 53°07' and φ = 40°59' – 56°25'. Identification of forms was done using axial ratio a:b:c=0.3237:1:0.3332 after Goldschmidt (1916).

UV-VIS to near infrared absorption spectra (300-1100 nm) were acquired using a Perkin Elmer Lambda-35 UV-VIS spectrometer (2.0 nm slit,1.0 nm data interval, and 120 nm/min scan speed) at room temperature, unpolarized, in the colorless and blue domains of the samples. In the blue sample from Mina do Santino, in the region of 400 nm-190 nm, absorbance saturation was observed with a large band toward the ultraviolet. In the visible region, a principal band at 670-687 nm was identified and correlated to the Fe^{2+}-Fe^{3+} charge transfer transition, reported by Mattson and Rossman (1987) and mentioned by Guedes *et al.* (2006) in attempting to explain the blue color. A second band at 436 nm could possibly correlate with the 411 nm band of Cr^{3+} (Krambrock *et al.*, 2008) (Fig. 1c). Other bands were identified in the near infrared (904 nm and 981 nm), but the band assignment is still dubious. For the colorless sample of Mina do Santino only the absorption toward the UV region and the band at 981 nm are present without any expression of iron absorption (Fig. 1d). In the Jacú Pegmatite the grayish-blue color may be related to the presence of solid acicular inclusions, possibly tourmaline (Fig. 1e) and these nanoscale inclusions could be responsible for the differences between absorption spectra (Fig. 1f). The absorption spectra for euclase from the Mina do Santino and Jacú pegmatites reveal different causes of the blue color for each location. Chemical analyses, a detailed optical study as well as an additional study about the inclusions present in this gem material will be done later.

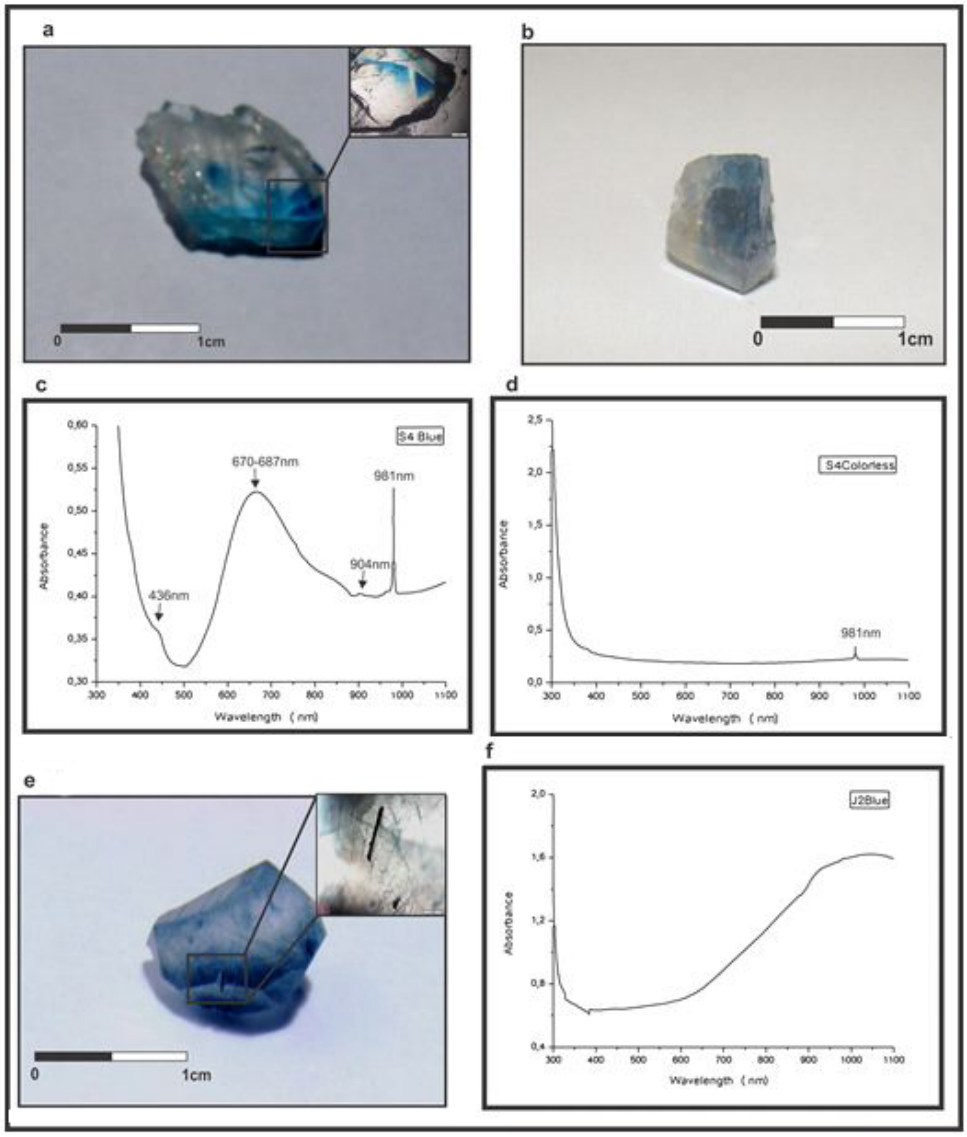

Fig. 1: Images and absorption spectra of euclase from the BPP. a) Image of the Mina do Santino sample (S4) with blue and colorless domains, in detail photomicrograph of blue zones (20X). b) Image of Jacú (J2 sample) with blue domain. c) Unpolarized spectra of blue zone in Mina do Santino (S4). d) Unpolarized spectra of the colorless region (S4) Mina do Santino. e) Image of Jacú sample (J4) and photomicrograph of acicular inclusions (100X), f) Unpolarized spectra of blue zone of Jacú (J2).

References

Goldschmidt, V. (1916): Atlas der Krystallformen Text, Band III. Carl Winters Universitätsbuchhandlung, Heidelberg.

Graziani, G. & Guidi, G. (1980): Euclase from Santa do Encoberto, Minas Gerais, Brazil. The American Mineralogist, vol. 65, 183-187.

Guedes, K.J.; Krambrok, K. ; Pinheiro, M.V.R. and Menezes Filho, L.A.D. (2006): Natural iron-containing blue and colorless euclase studied by electron paramagnetic resonance. Physics and Chemistry of Minerals, vol. 33, 553-557.

Kambrock, K., K.J. Guedes, & M.V.B. Pinheiro, (2008): Chromium and vanadium impurities in natural green euclase and their relation to the color. Physics Chemistry of Minerals, vol. 35, 409-415.

Holland, T.J.B. & Redfern, S.A.T. (1997): Unit cell refinement from powder diffraction data: the use of regression diagnostics, Mineralogical Magazine, vol.61, 65-77.

Mattson, S.M. and Rossman, G.R. (1987): Identifying characteristics of charge transfer transitions in minerals.Physics and Chemistry of Minerals, vol.14, 94-99.

Panalytical (2004): X'Pert High Score Plus, version 2.1, Panalytical, Almelo, The Netherlands.

TWO GENERATIONS OF MICROCLINE FROM MOUNT MALOSA PEGMATITE, ZOMBA DISTRICT, MALAWI

V. Bermanec[1], M. Horvat[2], Ž. Žigovečki Gobac[1], V. Zebec[3]
[1] Institute of Mineralogy and Petrography, Department of Geology, Faculty of Science, University of Zagreb, Horvatovac 95, 10000 Zagreb, Croatia, vberman@public.carnet.hr
[2] Croatian Geological Survey, Sachsova 2, 10000 Zagreb, Croatia
[3] Croatian Natural History Museum, Demetrova 1, 10000 Zagreb, Croatia

Introduction

The Zomba-Malosa pluton is composed of syenite and quartz-syenite, with an inner ring of quartz-microsyenite, and an outer ring of peralkaline granite (Bloomfield, 1965) associated with miarolitic, granitic and alkaline pegmatites (Guastoni *et al.*, 2003). Structural ordering in twinned and untwinned microcline crystals from Mount Malosa pegmatites was investigated.

Materials and methods

The microcline examined is a 10 cm white crystal that exhibits a Baveno twin (Fig. 1 - a) with the surface of some crystal faces covered with late-stage, transparent colorless feldspar crystals (Fig. 1 - b). A black aegirine crystal, a common mineral in the alkali pegmatites of Mount Malosa, is also present (Fig. 1 - c). Thin sections that contained both observable feldspar phases were cut from the sample and analyzed with polarizing microscope.

Both the early-white and late-colorless phases were analyzed with Philips X'pert Pro powder diffractometer (CuKα radiation filtered with a graphite monocrystal monochromator, running at 40 kV and 40 mA). XRPD data were collected from 4 to 65 °2θ, and identified and indexed using the X'Pert program Highscore Plus v. 2.1 software (PANalytical, 2004) and ICDD Powder Diffraction File 2 database (2004). Unit cell parameters were calculated using the program "UnitCell" (Holland & Redfern, 1997). Triclinicity (Δ) was calculated using the formula $\Delta = 12.5*[d(131)-d(\bar{1}31)]$ of Goldschmidt & Laves (1954) and the ordering index and the ΣAl at the T_1 sites, according to Neves & Godinho (1995).

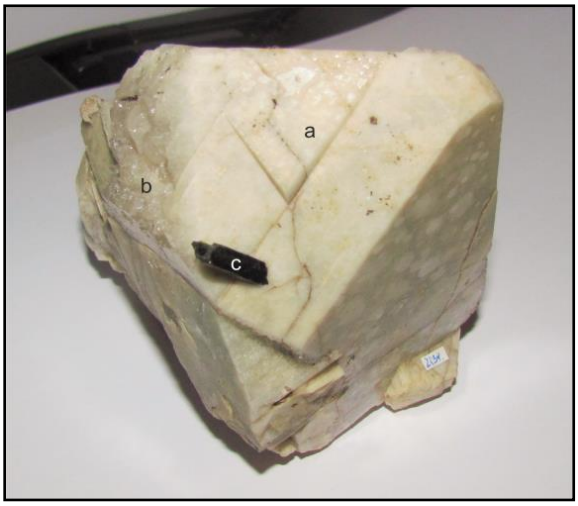

Fig. 1: Microcline crystal with Baveno twin from Mount Malosa pegmatite (10 cm in size). a - large twinned crystal (white); b - late crystals (transparent, colorless); c - aegirine crystal (black).

Results

Polarizing microscope observations confirm two generations of microcline growth, the early phase exhibits a characteristic microscopic tartan twin pattern where the later crystals occur single crystals do not (Fig. 2). XRPD analyses show that in addition to microcline, minor quartz is also present. Both the early-white and late-colorless microcline show split {131} potassium feldspar reflections reflecting their triclinic symmetry. Calculated values of triclinicity (Δ = 0.981 (late / transparent / colorless) and Δ = 0.968 (basic crystal body/white) and lattice parameters (a = 8.583(1) Å, b = 12.974(2) Å and c = 7.224(1) Å, with α = 90.62(2)°, β = 115.93(1)°, γ = 87.67(1)° and a = 8.581(1) Å, b = 12.969(2) Å and c = 7.225(1) Å, with α = 90.67(2)°, β = 115.94(1)°, γ = 87.60(1)° respectively, are characteristic for low microcline. The ordering index

and the ΣAl at the T_1 sites, calculated according to Neves & Godinho (1995), for both investigated zones is 100% confirming maximal ordering, i.e. low microcline (Kroll & Ribbe 1987). The degree of ordering in the transition zone was not determined .

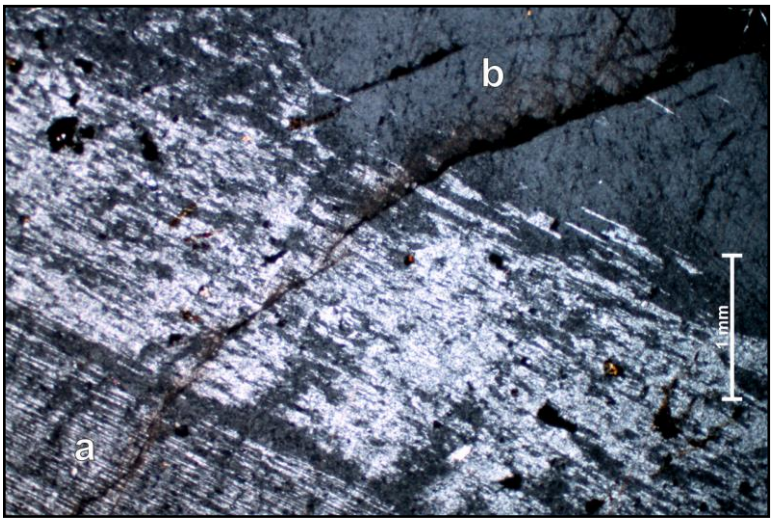

Fig. 2: Microphotograph of the investigated sample. a - microcline with a characteristic single set of thin lamellae (early phase); b - homogeneous single crystal of microcline (late phase). A transition zone is recognized between these two parts (a and b) of the crystal.

Conclusion

The investigated microcline sample from the Mount Malosa pegmatite contains two generations of low microcline: an early twinned crystal that is coated on some faces with late-stage crystals. Microcline crystals of both generations revealed maximum triclinicity and a high ordering state for potassium feldspars. The transition zone was not investigated due to an inability to separate it. The inner part of the crystal (early phase) likely crystallized as monoclinic feldspar and subsequently inverted to triclinic symmetry. The second generation of microcline (late phase) crystallized directly as maximally triclinic microcline. Further research of transition zone and its interface to both investigated microcline generations is necessary.

References

Bloomfield, K. (1965): The geology of the Zomba area. Bulletin Geological Survey Malawi, 16, 1-193.

Holland, T. J. B. &. Redfern, S. A. T. (1997): Unit cell refinement from powder diffraction data: the use of regression diagnostics. Mineralogical Magazine, 61, 65-77.

Goldschmidt, J. R. & Laves, F. (1954): The microcline-sanidine stability relations. Geochimica Cosmochimica Acta, 5, 1-19.

Guastoni, A., Pezzotta, F. & Demartin, F. (2003): Le pegmatite di Zomba-Malosa. Rivista Mineralogica Italiana, 27, 66-77.

Kroll, H. & Ribbe, P. H. (1987): Determining (Al-Si) distribution and strain in alkali feldspars using lattice parametres and diffraction-peak positions: a review. American Mineralogist, 72, 491-506.

Neves, L. J. P. F. & Godinho, M. M. (1995): Estimação expedita do ordenamento Al-Si do feldspato potássico-uma reapreciação. Memórias e Notícias, Publ. Dep. Ciências da Terra e do Mus. Lab. Mineral. Geol. Univ. Coimbra, 120, 15-24.

PANalytical (2004): X'Pert Highscore Plus v. 2.1, PANalytical B. V., Almelo.

Powder Diffraction File 2 (2004): Database Sets 1-54. International Centre for Diffraction Data (ICDD), Newton Square.

CHRYSOBERYL IN ASSOCIATION WITH SILLIMANITE AT RONCADEIRA IN THE BORBOREMA PEGMATITE PROVINCE, NORTHEASTERN BRAZIL: PETROGENETIC AND GEMOLOGICAL IMPLICATIONS.

H. Beurlen[1*], D. Rhede[2], R. Thomas[2], D. Soares[3], M. Da Silva[1].
[1] Departamento de Geologia, Universidade Federal de Pernambuco (UFPE), beurlen@ufpe.br
[2] Helmholtz-Zentrum Potsdam, GFZ, German Research Centre for Geosciences, Germany
[3] Instituto Federal de Educação, Ciência e Tecnologia da Paraíba (IFPB),Campina Grande – Paraíba, Brazil

The occurrence of chrysoberyl (Cbl) in the Roncadeira pegmatite (4 km WNW of the Nova Palmeira township), in the Borborema Pegmatite Province (BPP), in Paraiba, northeast Brazil was first reported by Beurlen *et al.* (2008), without any mineralogical details. The "Roncadeira pegmatite" was described by Roy *et al.* (1964) as a string of usually less than two meter thick, cassiterite-, columbite- and beryl-bearing pegmatite lenses enclosed in the sillimanite-garnet-cordierite-biotite schists and gneisses of the Neoproterozoic Seridó Formation, in the Seridó Foldbelt, in the Northern Domain of the Borborema Tectonic Province. Peak metamorphism of the host rocks reached high amphibolite grade (600°C, 3.5 to 5 kbar) at about 590 Ma. The rare-element class (REL) Be-Li-Ta-Sn mineralized pegmatites of the BPP were emplaced at 500-520 Ma under retrograde regional greenschist facies conditions along reactivated older strike-slip shear zones (NNE) and related tension (NE) or extension fractures (EW) (Araújo *et al.* 2005 and references therein). The group of pegmatite lenses at Roncadeira strikes NNE, parallel or sub-parallel to the foliation of the enclosing biotite-schists, and has a subvertical dip toward the SSE that crosscuts the more gentle dipping foliation of the host-rocks (biotite-schists). Beurlen *et al.* (2008) identified ferrowodginite, tapiolite-(Fe), "tantalian rutile", titanian ixiolite, garnet, zircon, Cbl and gahnite in addition to the other dominant accessory minerals (cassiterite, beryl and columbite-tantalite group minerals) already reported by Roy *et al.* (1964).

The Roncadeira pegmatite lenses are nearly homogeneous or weakly zoned. Usually they display an up to decimeter thick muscovite enriched border zone that was distinguished as "greisen" by Roy *et al.* (1964), followed inward by the wall zone composed of a medium grained aggregate of quartz + K-feldspar + muscovite ± albite. The main ore minerals cassiterite and ferrowodginite occur as millimeter- up to centimeter-sized disseminated grains which are enriched in the border zone and less commonly in the wall zone. In addition to muscovite, quartz and feldspar, sillimanite is observed as a widespread accessory mineral in the border and wall zones. These zones are clearly related to small shear zones, mostly replacing muscovite or bordering augen of K-feldspar and albite grains or forming nodular fibro-radial bunches in association with quartz. In the center of the pegmatite. Very locally it is possible to observe a distinct discontinuous intermediate zone composed predominantly of blocky K-feldspar and an intermittent quartz core. Still less abundant are small lenticular subconcordant pockets of banded saccharoidal, albite-dominated aplite. The albite rich portions of this "banded sodic aplite" contain, in addition to the accessory minerals listed above, a few up to 0.3 mm sized grains of the *"zinconigerite-6N6S"* variety of the nigerite group.

Chrysoberyl (Cbl) was found only in a few decimeter-sized boulders of banded albite-dominated saccharoidal aplite (+quartz + muscovite) in the dumps of one lens at Roncadeira. In most samples, chrysoberyl crystals were found clearly related and restricted to lenticular quartz+sillimanite aggregates in shear zones crosscutting the banded albitic aplites (Fig. 1). Cbl occurs as up to 15 mm long and 4 mm thick tabular very pale yellowish-green transparent crystals, sometimes distinguished by the typical pseudo-hexagonal cyclic penetration twinning. In thin section, the crystals are colorless, without visible pleochroism and have no visible "alexandrite effect". Weak pleochroism is shown only in more than 0.2 mm "thick sections" prepared for fluid inclusion studies and electron-microprobe analyses (EMPA). A porphyro-poikiloblastic origin of the Cbl is indicated by the presence of small inclusions of rounded quartz grains and radial micro aggregates of sillimanite along the crystal borders. A metamorphic-metasomatic origin of the chrysoberyl by the reaction:

$$\textbf{beryl+albite+muscovite+}H^+ \textbf{ = chrysoberyl + quartz+sillimannite + Na + K + }H_2O\textbf{,}$$

seems to be the most plausible of several reactions proposed by Franz and Morteani (1984) for the metamorphic formation of Cbl and best explains the observed textural relations.

The macroscopic identification of the Cbl based on the typical twinning, was confirmed by the optical properties in thin section, with X-ray diffractometry, and RAMAN-spectrometry.

Electron-microprobe analyses of the Cbl were performed in the wave-dispersive mode of the JEOL JXA-8500F (Hyperprobe) at the Helmholtz Centre Potsdam, German Research Centre for Geosciences, GFZ-Potsdam, Germany. The EMPA analyses revealed the presence of only small amounts of iron, between 1.1 to 1.6 wt. % FeO_{total} , and low contents of SiO_2 (< 0.05 wt%). The potential chromophore trace elements are insignificant, (V below the 0.01% level, Cr and Ti below detection limits). This is consistent with the very light yellowish-green color, transparency, and absence of dichromatism ("alexandrite effect") of the Cbl crystals when observed with hand lens or naked eye. A slightly oscillating composition with crystal-growth zones is observed in BSE image due to the small variations of the iron content. The chemical formula based on 13 EMPA analyses is $Be_{1.000}\,Fe_{0.024}\,Si_{0.001}\,Al_{1.975}O_4$.

The assumed tectono-metamorphic origin of sillimanite + chrysoberyl + quartz at high-grade metamorphic conditions suggest either the existence of a new generation of syn-metamorphic REL-pegmatites in the BPP or a late-tectonic recurrent increase of regional metamorphic P-T conditions in the area of the Roncadeira occurrences. Another less probable alternative is a metastable formation of chrysoberyl and sillimanite at lower, retrometamorphic P-T conditions.

The recognition of the presence of chrysoberyl in the BPP is important because, in addition to the implications on the local pegmatite genesis, it opens up the possibility for finding the gem-variety *alexandrite* in the BPP by exploration of similar pegmatites at the intersection with orthoamphibolite intercalations known to occur in the Seridó Formation, NNE-ward from Roncadeira.

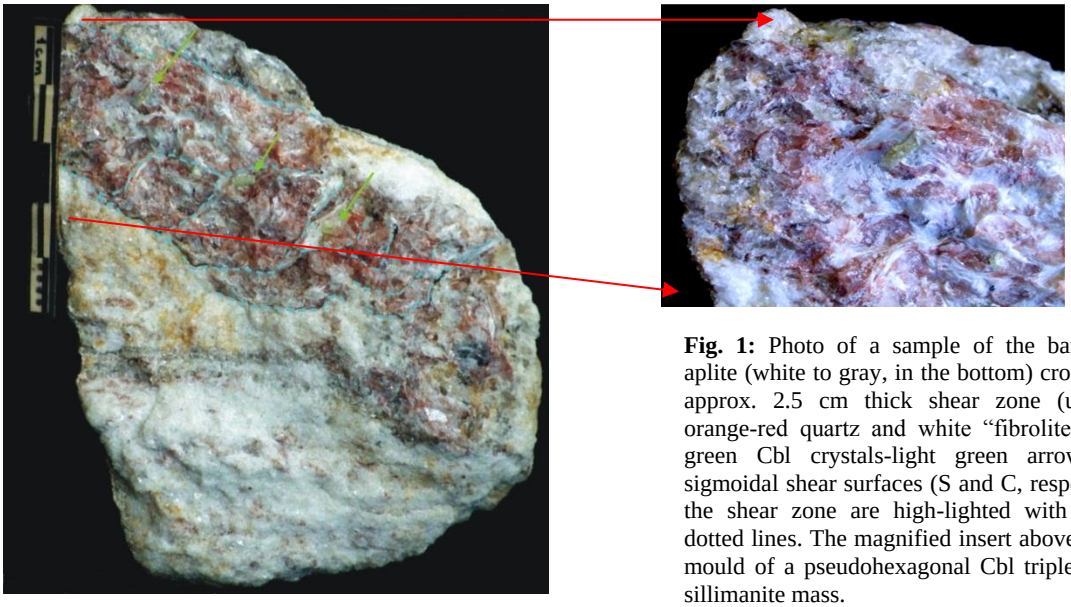

Fig. 1: Photo of a sample of the banded sodic aplite (white to gray, in the bottom) crosscut by an approx. 2.5 cm thick shear zone (upper part: orange-red quartz and white "fibrolite" and pale green Cbl crystals-light green arrows). Some sigmoidal shear surfaces (S and C, respectively) in the shear zone are high-lighted with light blue dotted lines. The magnified insert above shows the mould of a pseudohexagonal Cbl triple twin on a sillimanite mass.

Acknowledgements

Review by W. Skip Simmons and M.A. Galliski is gratefully acknowledged.

References

Araújo M.N.C., Vasconcelos P.M., Silva F.C.A., Jardim de Sá E.F., J.M. Sá (2005): 40Ar/39Ar geochronology of gold mineralization in Brasiliano strike-slip shear zones in the Borborema province, NE Brazil. J South Amer Earth Sci, vol. 19: 445-460

Beurlen H., Da Silva M.R., Thomas R., Soares D.R., P. Olivier (2008): Nb–Ta–(Ti–Sn)–oxide mineral chemistry as tracers of rare-element granitic pegmatite fractionation in the Borborema Province, northeastern Brazil. Mineral Deposita, vol. 43, 207-228

Franz, G., G. Morteani (1984): The formation of chrysoberyl in metamorphosed pegmatites. J Petrol, vol. 25, 27-52.

Roy, P.L., Dottin O., H.L. Madon (1964): Estudo dos pegmatitos do Rio Grande do Norte e da Paraíba. Superintendência de Desenvolvimento do Nordeste (SUDENE), Série Geol. Econ. 1: pp. 1-124.

CARTOGRAPHY TO CHEMISTRY: ESTIMATING THE BULK COMPOSITION OF THE MT MICA PEGMATITE VIA MAP ANALYSIS, MAINE, USA

A. Boudreaux[1], L. Grassi[1], W. Simmons[1], A. Falster[1], K. Webber[1], G. Freeman[2]
[1] Dept. of Earth & Env. Sci., University of New Orleans, New Orleans, LA 70149, apboudr1@uno.edu
[2] Coromoto Minerals, 48 Lovejoy Road, Paris, ME 04271

The purpose of this study was to increase the general understanding of the bulk chemical composition of the Mt Mica pegmatite, located in Oxford County, Maine. Mt Mica, and other members of the Oxford Pegmatite Field, are classified as LCT-type (Lithium, Cesium, Tantalum) pegmatites and are genetically related to the late-Paleozoic Alleghenian Orogeny. The very heterogeneous nature of Mt Mica leads to difficulties in discerning bulk chemical composition via fusion ICP analysis of whole-rock samples. This study attempts to amend existing Mt Mica ICP bulk geochemical data (Table 1a) by using map analysis as a means of integrating the chemical composition of the large lepidolite and K-feldspar masses (intentionally excluded from whole rock core samples) and estimating weight percent H_2O contained in miarolitic cavities, all of which were accurately mapped during mining.

A detailed geologic map (Fig.1), provided by mine owner Gary Freeman, shows the spatial distribution and aerial extent of pockets, massive lepidolite, microcline, and xenoliths superimposed on a shaded layer that represents the mined area. The map was analyzed via "ImageJ", a freeware image-analysis software, by color-thresholding to specific lepidolite mass and K-feldspar polygons. After setting the appropriate map scale, the program then provided area calculations for the targeted map elements. The software was also used to measure linear distances of pocket axes.

Area calculations of lepidolite were converted to volume based on thickness information provided by Gary Freeman. Thin sections of Mt Mica lepidolite masses were point-counted to determine modal percentage of actual mica within the lepidolite masses. The appropriate percentage of lepidolite mica was then milled, added to a second aliquot of powder from the original 45 whole-rock cores, and reanalyzed. This provided a new whole-rock bulk chemistry dataset that accounts for the measured lepidolite masses.

Volumes of open spaces were calculated by best-fit ellipsoid, given two perpendicular, horizontal axes from the map and an estimated vertical dimension from the cross-section. Pocket fill estimates from Gary Freeman and porosity analysis of Mt Mica pocket fill material helped to refine the volume of open space in each pocket and the percentage of open space in the whole pegmatite. Assuming that the open space was filled with water, water density (calculated at 3 kbar and 625°C based on phase equilibria) was used to convert volume percent pocket H_2O to weight percent. Structurally bound water was determined by LOI above 500°C, and is shown in Table 1b.

In addition, fluorine was quantified by fusing the whole-rock powders (post addition of lepidolite) into glass beads and analyzing them via electron microprobe for major and common minor elements. Fluorine values were averaged and incorporated into the new dataset.

Finally, the resulting whole-rock composition (Table 1b) was run through a custom-made spreadsheet which estimates the normative mineralogy of Mt Mica via iterative calculation. In this process, using the actual analyzed compositions of each Mt. Mica mineral, all boron was used to make tourmaline (composition 99% schorl 1% elbaite), 25% of remaining fluorine was used to make lepidolite, and 90% of K remaining after these two phases was used to make muscovite. The weight percent quantities for all remaining oxides were then inserted into a standard CIPW normative calculation. The resulting bulk mineralogy is given in Table 2. These results show that Mt Mica is a plagioclase ($An_{1.8}$) dominant pegmatite with virtually no K-feldspar in the outer zones of the pegmatite. Thus, Mt Mica can be classified as an albite-dominant granitic pegmatite.

MM-45A			
oxide	**wt. %**	**element**	**ppm**
SiO_2	71.82	Sr	44
TiO_2	0.067	Ba	34
Al_2O_3	16.74	Nb	18.8
FeOt	1.11	Ta	3.61
MnO	0.022	Zr	24
MgO	0.15	Hf	1.5
CaO	0.49	Sn	59
Na_2O	5.45	Cs	47
K_2O	1.86	Rb	326
P_2O_5	0.21	B*	240
Li_2O*	0.08		
TOTAL		**98.00 wt. %**	

MM-45B			
oxide	**wt. %**	**element**	**ppm**
SiO_2	72.08	Sr	44
TiO_2	0.067	Ba	35
Al_2O_3	17.33	Nb	23.5
FeOt	1.21	Ta	6.3
MnO	0.039	Zr	17
MgO	0.15	Hf	1
CaO	0.48	Sn	84
Na_2O	5.35	Cs	99.9
K_2O	2.08	Rb	636
P_2O_5	0.20	B*	287
Li_2O*	0.24		
H_2O (pocket)	0.22		
LOI	0.94		
F $^{\alpha}$	0.25		
subtotal		100.64 wt.%	
- O Ξ F		0.11 wt.%	
TOTAL		**100.53 wt.%**	

Table 1: a) Bulk geochemistry of Mt Mica based on ICP analyses of 45 whole-rock cores, excluding lepidolite masses: MM-45A, and b) including lepidolite, calculated pocket water, structurally-bound water, and fluorine: MM-45B. (analyzed via *Direct-Coupled Plasma Spectrometry, $^{\alpha}$ EMPA).

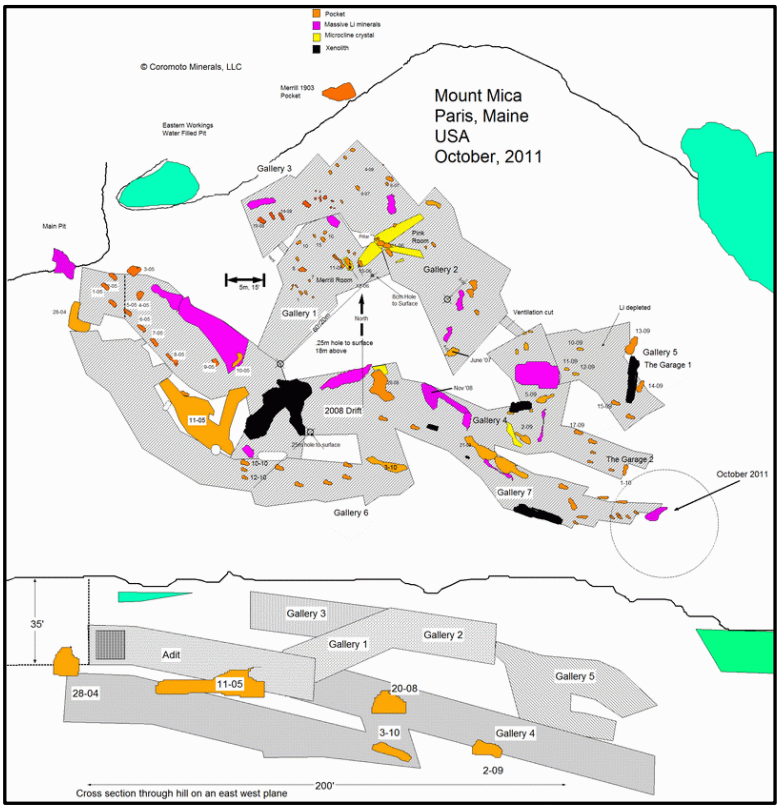

Fig. 1: Geologic map and cross-section of Mt Mica, provided by mine owner Gary Freeman.

normative mineral	**wt.%**
plagioclase (An 1.8)	45.29
quartz	30.35
muscovite*	17.82
hypersthene	1.80
lepidolite*	1.30
orthoclase	1.12
tourmaline*	0.89
corundum	0.83
apatite	0.48
ilmenite	0.11
magnetite	0.07
fluorite	0.05
TOTAL	**100.11**

Table 2. Estimated bulk mineralogy of Mt Mica via CIPW normative calculation. [* calculated independently of CIPW norm]

ACCESSORY MINERALOGY OF AN EVOLVED PEGMATITE, DICKINSON COUNTY, MICHIGAN

T. Buchholz, A. Falster [2], W. Simmons[2],
1140 12th Street North, Wisconsin Rapids, Wisconsin 54494 (buchholz@wctc.net)
[2] Department of Earth and Environmental Sciences, University of New Orleans, New Orleans, Louisiana 70148

Central Dickinson County in the Upper Peninsula of Michigan is home to approximately ninety known pegmatite occurrences (James *et al.*, 1961), few of which have been studied. Recently, material from a small beryl-rich pegmatite was examined in order to characterize its mineralogy and fractionation. It is spatially associated with Lower Proterozoic metamorphic rocks of the Peavy Node which were deformed and metamorphosed during the Penokean Orogen (Atoh and Klasner, 1989), and shows some indications of minor deformation. Hence, the pegmatite is probably late- to post-Penokean in age, though, no radiometric dating has been done. Local control for pegmatite emplacement appears to be related to the Felch Trough (a prominent E/W syncline) since the majority of pegmatites in Dickinson County are located just to the north of, or within, this syncline.

The unnamed pegmatite is located in the SW ¼ SE ¼ section 30, T42N, R29W (Robinson and Carlson, in prep.). Yellow-green beryl crystals are common in the inner intermediate zones adjacent to a massive quartz core. Miaroles are present but are small and do not exceed several cubic centimeters. Examination of samples and heavy mineral separates from this pegmatite revealed a relatively highly fractionated mineralogy. To date, Mn-rich almandine, gahnite, schorl, columbite-(Fe), tantalite-(Fe), tapiolite-(Fe), U-rich pyrochlore, microlite and U-rich microlite, sparse uraninite as inclusions in U-rich microlite, hafnian (and HREE-rich) zircon, beryl, bertrandite, apatite(CaF), HREE-rich xenotime-(Y), sparse grayite, calcite, pyrite, a smectite-group mineral replacing beryl, and hematite have been identified. Notably, bertrandite forms tiny blocky crystals in thin, late fractures, and also clear bladed crystals, sometimes embedded in a smectite-group mineral, in small vugs in the intermediate zones near the core margin; the necessary Be was likely derived from altering beryl. Identity of the clear bladed crystals as bertrandite was confirmed via powder XRD; the pattern was in excellent agreement with bertrandite.

Columbite-group minerals from this dike are often distinctly zoned, ranging in composition from columbite-(Fe) with up to about 62 wt% Nb_2O_5, through compositions corresponding to tantalite-(Fe), to outer zones of tapiolite-(Fe) that range up to about 78.5 wt% Ta_2O_5. (Fig. 1) Columbite-group crystals are often overgrown by, or otherwise closely associated with pyrochlore-group phases such as U-rich pyrochlore, and microlite to U-rich microlite.

Muscovite from this pegmatite generally exhibits "kinking". This together with thin fractures cutting quartz and feldspars and lined with small crystals of quartz, feldspar and (in some cases) bertrandite and minor bastnäsite-group minerals suggests some degree of deformation during or subsequent to emplacement.

Attoh and Klasner (1989) found shallow negative gravity anomalies in the Peavy metamorphic node and interpreted them as products of partial melting during Penokean metamorphism, and further determined that pressure and temperature conditions during metamorphism of the Peavy Node would have been conducive to partial melting of granitic and pelitic rocks at shallow depths. If so, these intrusions may have been the source for the numerous granitic and pegmatitic dikes mapped in this area by James *et al.* (1961).

References

Attoh, K., Klasner, J.S. 1989: Tectonic implications of metamorphism and gravity field in the Penokean orogeny of northern Michigan. *Tectonics*, V. 8, no. 4, p. 911-933.

James, H.L., L.D. Clark, C.A. Lamey, F.J. Pettijohn. 1961: *Geology of Central Dickinson County, Michigan*, USGS Professional Paper 310, Washington, DC. 176 pages.

Robinson, G. W. 2004: *Mineralogy of Michigan by E.W. Heinrich*, Houghton, MI: A. E. Seaman Mineral Museum, Michigan Technological University.

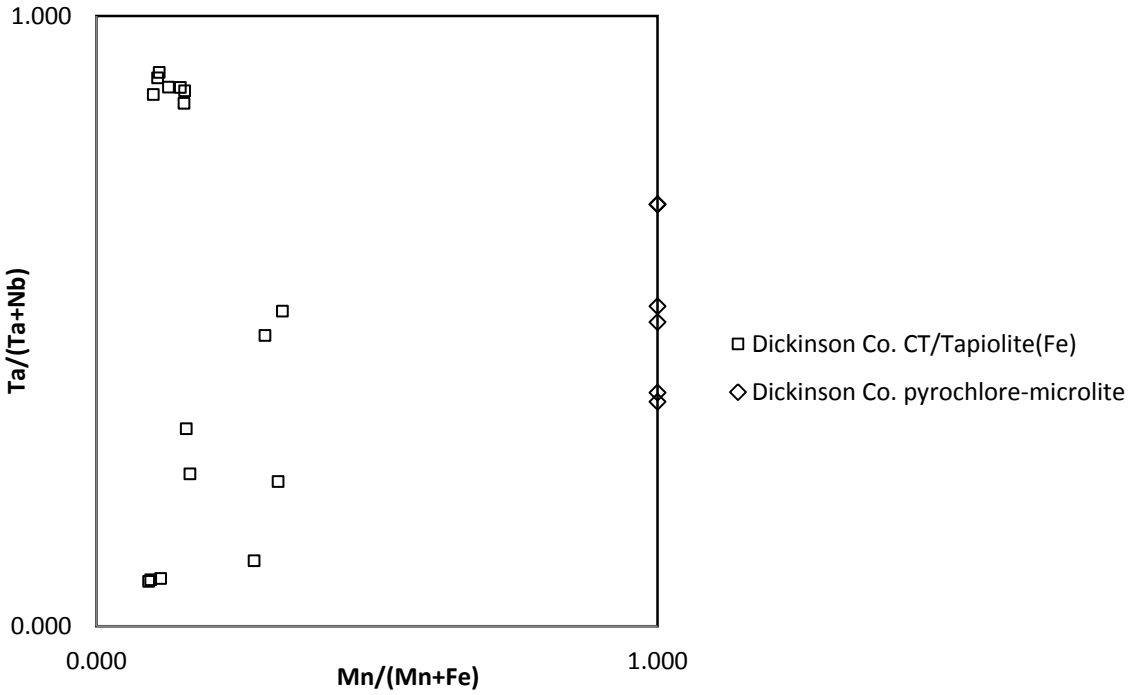

Fig. 1: Columbite-group quadrilateral of columbite-group and microlite-pyrochlore species from the pegmatite in Dickinson Co., Michigan.

THE PONTE SEGADE DEPOSIT (GALICIA, NW SPAIN): A RECENTLY DISCOVERED OCCURRENCE OF RARE-ELEMENT PEGMATITES

F. Canosa, M. Fuertes-Fuente, A. Martin-Izard
Geology Department (University of Oviedo) Spain, canosa@geol.uniovi.es, mercedf@geol.uniovi.es
amizard@geol.uniovi.es

Introduction

In the Ponte Segade area (Galicia, NW Spain) rare-metal mineralization associated with cassiterite-rich quartz veins, albite-rich leucogranites and pegmatites have recently been discovered (Canosa *et al.*, 2012). This work focuses on the Ponte Segade pegmatites and the aim is to describe the geological features and mineralogy of these bodies.

Geological setting

The Ponte Segade Deposit is located in the NW of the Iberian Peninsula (northern Galicia). Geologically, this area is in the Iberian Massif, which presents the westernmost exposures of the European Variscides in the southwestern limb of the arc described by this chain in Western Europe. The belt has been divided into several zones (Julivert *et al.*, 1972), the inner one being the "Central Iberian Zone" (CIZ) where Ponte Segade deposit is located (Figure 1). In the CIZ, two main units are distinguished: the Esquisto-Grauváquico Complex and the Ollo de Sapo Antiform Unit (OSAU). This Unit, lower Ordovician in age, comprises augen-gneisses, porphyroblastic schists, quartzites and slates. These rocks are the core of an antiform developed during the D3 phase of the Variscan Orogeny (Matte, 1968). Variscan synkinematic S type granitoids intrude the OSAU, and Ponte Segade Deposit is related to these intrusions.

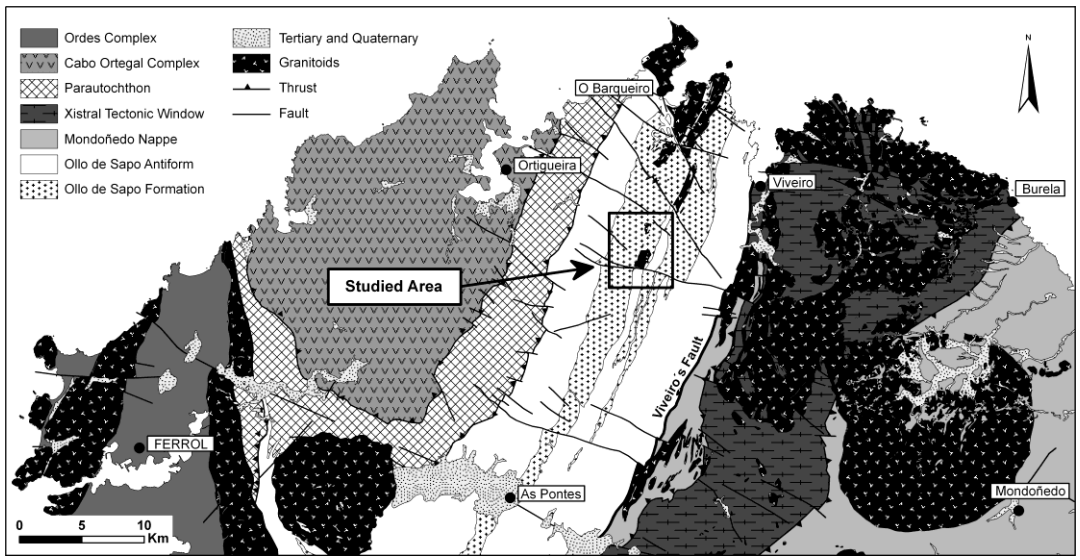

Fig. 1: Regional geological map showing where the studied area is located in the OSAU. Modified from SITGA & IGME (2005).

Ponte Segade pegmatites: geological features and mineralogy

In the Ponte Segade area the pegmatites are mainly intragranitic bodies hosted by albite-rich leucogranites. However, a few bodies are hosted by the augen-gneisses of the Ollo de Sapo Antiform Unit (OSAU). They form tabular and lenticular bodies with thickness ranging from 1 cm up to 5 m. According to their internal structure, mineralogy and petrology two groups are distinguished: (i) zoned pegmatites and (ii) layered aplite-pegmatites.

The *zoned pegmatites* are more abundant and show a poorly-developed internal structure, with a border zone mainly made up of comb-textured crystals of muscovite and quartz. The accessory minerals are K-feldspar, beryl, Ta-rich cassiterite, arsenopyrite, Ta-Nb bearing oxides, fluorapatite and molybdenite. The core zone is formed by massive quartz together with K-feldspar and muscovite. The

main accessory minerals are beryl, Ta-rich cassiterite, arsenopyrite, Ta-Nb bearing oxides, fluorapatite and tourmaline (schorl).

The Ta-Nb-bearing oxides appear as microinclusions in Ta-rich cassiterite or as small idiomorphic crystals in quartz veinlets that cut this cassiterite. The oxides are members of the columbite-tantalite and wodginite series, and microlite (Canosa *et al.* 2011).

The *layered aplite-pegmatites* are scarcer and have a banded structure in which aplitic and pegmatitic bands with thickness between 1 and 20 cm alternate, the aplitic bands being the thickest. The aplitic bands are made up of albite, quartz, muscovite and K-feldspar along with tourmaline, beryl, phosphates**,** cassiterite and arsenopyrite as main accessory minerals. The pegmatitic bands are formed by K-feldspar, muscovite and quartz, with accessory tourmaline and phosphates minerals.

From EMPA, beryl from the layered aplite-pegmatite bodies shows Cs–Na-enriched compositions of up to 7.8 wt% Cs_2O, with an average of around 5 wt% Cs_2O, and a mean value of 1.8 wt% Na_2O. According to EMP data, the phosphates are montebrasite, eosphorite, goyazite and fluorapatite. Montebrasite and eosphorite appear as patches replacing albite and K-feldspar. Eosphorite also occurs filling cavities together with beryl, fluorapatite and aggregates of goyazite and fluorapatite. In addition, goyazite as core in the fluorapatite crystals is relatively abundant. Tourmaline forms massive deep blue aggregates or, more rarely, deep blue prismatic crystals. The tourmaline chemical compositions allow us to classify it intermediate in composition between elbaite and schorl, according to Henry *et al.* (2011) classification.

Conclusions

Considering the mineralogy and geological features, the newly discovered pegmatites outcropping in the Ponte Segade area could be classified as belonging to the LCT family and rare-element class according to Černý and Ercit (2005) classification.

References

Canosa, F., Fuertes-Fuente, M., Martin-Izard, A. (2011): Mineralization of Sn-Ta-Nb oxides in Ponte Segade Deposit (North of Galicia, NW Spain). In: Let´s talk ore deposits. Ediciones Universidad Católica del Norte, Antofagasta, Chile, 163-165.

Canosa, F., Martin-Izard, A., Fuertes-Fuente, M. (2012): Evolved granitic systems as a source of rare-element deposits: The Ponte Segade case (Galicia, NW Spain). Lithos, vol. 153, 165-176.

Černý, P., Ercit, S. (2005): The classification of granitic pegmatites revisited. Canadian Mineralogist, vol. 43, 2005-2026.

Henry, D., Novak, M.,Hawthorne, F.C., Ertl, A., Dutrow, B., Uher, P., Pezzotta, F.(2011). Nomenclature of the tourmaline supergroup-minerals. Am. Mineralogist, vol. 96, 895–913.

Julivert, M., Fontbote, J.M., Ribeiro, A., Nabais Conde, L. (1972): Mapa Tectónico de la Península Ibérica y Baleares a escala 1:1.000.000. Memoria explicativa: 1-113 (1974). Instituto Geológico y Minero de España (IGME).

Matte, Ph (1968) La structure de la virgation hercynienne de Galice (Espagne). Revue de Geologie Alpine 44:1-128

SITGA & IGME (2005) Mapa xeolóxico de Galicia (Magna).

CONTACT ZONE MINERALOGY AND GEOCHEMISTRY OF MOUNT MICA PEGMATITE, OXFORD CO., MAINE, USA

K. Clark[1], W. Simmons[1], K. Webber[1], A. Falster[1], E. Roda-Robles[2], G. Freeman[3]
[1] Dept. of Earth & Environ. Sciences, University of New Orleans, New Orleans, LA, USA, ktclark1@uno.edu
[2] Dept. de Mineralogía y Petrología, Univ. del País Vasco UPV/EHU, P.O. Box. 644, E-48080 Bilbao, Spain
[3] Coromoto Minerals, LLC, Mount Mica, Oxford County, ME

To document the nature of the pegmatite-country rock interface, a mineralogical and geochemical study of the interaction between the Mt. Mica pegmatite in Oxford Co. Maine with the surrounding migmatitic host rock was conducted. The pegmatite-country rock contact at Mt. Mica is sharp and visually distinct in areas where pegmatite cuts the melanosome component of the migmatite. The contact is gradational with no chill margin or obvious reaction or comb structure where the pegmatite cuts the leucosomes of the migmatite. This study focuses on the minerals biotite, garnet and tourmaline to determine interactions and the extent of elemental exchange between the pegmatite and its surrounding country rock.

Samples were collected from the country rock and pegmatite across the contact zone and analyzed by fusion ICP, electron microprobe (EMP), direct-coupled plasma spectroscopy (DCP), and scanning electron microscopy (SEM). Samples were collected from various locations at the pegmatite-country rock contact zone, inside and outside of the mine. Studied intervals are: pegmatite (*P2*) > 15cm from contact, contact pegmatite (*P1*) < 15cm of contact, country rock contact (*CR1*) < 15 cm of contact, country rock between 15cm and 8m of contact (*CR2*) and country rock > 8m of contact (*CR3*). These last samples are considered to be unaffected by the pegmatitic intrusion and representative of normal country rock biotite, garnet and tourmaline. Several samples of intermingled felsic and mafic composition were collected from areas inferred to be the result of extensive interaction, where the contact is indiscernible. These are referenced as Hybrid (*H*) samples. Leucosome samples collected at a distance > 8m are referenced as (*L*).

Tourmaline

EMP analysis of hand-picked tourmaline revealed schorl composition (Hawthorne *et al.*, 1999). Pegmatite samples (*P*) show an increased dravite component approaching, but not crossing into the dravite field. All samples plot within the schorl field on the Na/(Na+Vac) (X-site) vs. Al/(Al+Fe) (Y-site) diagram. All tourmaline samples analyzed have low to negligible Al_y.

Biotite

Chemical analysis of biotite was obtained by EMP. All samples had SiO_2 values > 34 wt.% which allowed for lithium oxide wt. % calculations using the equation $(0.289*SiO_2)$ - 9.658, for samples where MgO < 6 wt.%, and the equation [2.7/(0.35+MgO)]- 0.13, where MgO > 6 wt.% (Tischendorf, 1997). Close to the contact (*CR2*), the $[Fe_{(tot)+}Mn+Ti-Al_{(vi)}]$ values are > 0.5 and the [Mg-Li] values are < 0.6. These samples plot within the siderophyllite field (Fig. 1). Biotite at the contact (*CR1*) and biotite at distances > 8m (*CR3*), plot within the Fe-biotite field (Fig 1) (Tischendorf, 1997). Hybrid samples plot in both fields. Calculation of biotite Fe^{3+}/Fe^{2+} ratios were determined by redox titration from meticulously handpicked grains. Ratios were near zero for all country-rock biotite. Biotite from within the pegmatite (*P*) contained only a minor component of Fe^{3+}, 0.03 *apfu*. Fe/(Fe+Mg) ratios from all locations ranged from 0.585 to 0.904 indicating the biotite is Fe-rich. The highest Fe/(Fe+Mg) ratios occur in (*CR2*), between 15cm to 8m from the contact and average 0.875 with the lowest ratio closest to the contact indicating higher Mg incorporation but not amounts great enough to cross from Fe-rich biotites to Mg-rich biotites. The occurrence of biotite decreases significantly crossing from country rock to pegmatite with no biotite occurring in the pegmatite < 15cm from the contact.

Garnet

Garnets were typically pink in color ranging from 0.5 to 2 mm in size. EMP analysis was conducted on hand-picked garnets and yielded an overall average garnet composition of: Alm 71.1%, Sps 17.1%, Prp 10.2%, Grs 1.6%. The abundance of garnet in the country rock decreases towards the contact with no garnet found in the country rock from the contact to 3cm nor within the pegmatite samples (*P1*). Garnet is rare within the pegmatite at distances > 15cm except in the garnet line where it

is relatively abundant. Analysis of these garnets show higher Mn compared to garnets from the country rock, ranging between: Alm 39.9%, Sps 59.3%, Prp 0.0%, Grs 0.7% and Alm 62.0%, Sps 36.6%, Prp 0.7%, Grs 0.7%.

Mg/(Mg+Fe) ratios are relatively consistent across the pegmatite-country rock contact ranging from 0 to 0.171 in samples from the garnet line (*P2*), 0.126 to 0.177 in samples (*CR1*) and 0.151 to 0.171 in samples (*CR3*). Garnet from *H* and *L* samples have the lowest non-pegmatitic ratios, averaging 0.081and 0.098 respectively.

Thermometry

Biotite-garnet thermometry was evaluated for country rock samples containing the mineral pairs. Temperature estimates using the non-ideal mixing parameters of Bhattacharya *et al.* (1992) yielded a temperature range of 650-690°C, with an average country-rock temperature of approximately 670°C.

Discussion and Conclusions

Measured biotite Fe^{3+}/Fe^{2+} ratios were used to calculate oxygen fugacity, based on biotite-garnet thermometry and P-T estimates from mineral assemblages and phase equilibria (650°C and 3 Kb) (Guidry, this issue). Using the diagram of temperature vs. oxygen fugacity contoured with the $Fe^{2+}/(Fe^{2+} + Fe^{3+})$ ratio of Wones *et al.* (1965), f_{O2} is estimated to be -17. This indicates that the country rock and the pegmatite formed under oxidizing conditions near the QFM buffer. Evidence for elemental exchange between the country rock and pegmatite was not substantial, except for minor leakage of B to form tourmaline at the contact. It is possible that the Mount Mica pegmatite formed from anatexis, but based on analytical and textural evidence it is concluded that it most likely did not form *in situ*, but migrated into the country rock under regional metamorphic conditions.

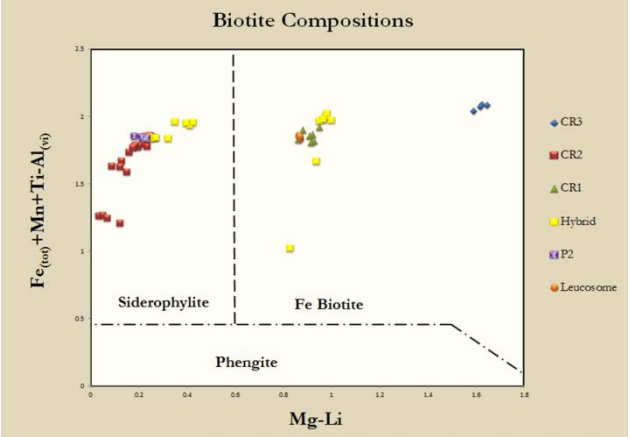

Fig. 1: Biotite compositions adapted from Tischendorf (1997).

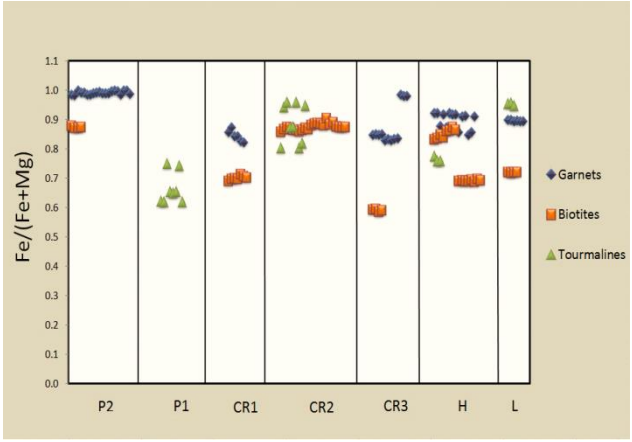

Fig. 2: Fe/(Fe+Mg) ratios versus distance from contact of biotite, garnet and tourmaline.

References

Bhattacharya, A., L. Mohanty, A. Maji, S. Sen, M. Raith (1992): Non-ideal mixing in the phlogopite-annite binary: constraints from experimental data on Mg-Fe portioning and a reformulation of the biotite-garnet geothermometer, Contributions to Mineralogy and Petrology, 111, 87-93.

Hawthorne, F.C., D. Henry (1999): Classification of the minerals of the tourmaline group. European Journal of Mineralogy, 11, 201–215.

Tischendorf, G., B. Gottesman, H. Forster, R. Trumbull (1997): On Li-bearing micas: estimating Li from electron microprobe analysis and an improved diagram for graphical representation, Mineralogical Magazine, 61, 809-834

Wones, D., H. Eugster (1965): Stability of Biotite: Experiment, Theory, and Application, The American Mineralogist, 50, 1228-1272.

PRELIMINARY ^{57}FE MÖSSBAUER SPECTROSCOPY STUDY OF METAMICT ALLANITE-(CE) FROM GRANITIC PEGMATITE, FONE, AUST-AGDER, NORWAY

A.Čobić[1], C.McCammon[2], N.Tomašić[1], V.Bermanec[1]

[1] Institute of Mineralogy and Petrology, Dept. of Geology, Faculty of Science, Horvatovac 95, Zagreb ancobic@geol.pmf.hr

[2] Bayerisches Geoinstitut, Universität Bayreuth, D-95440 Bayreuth

Allanite-(Ce) is classified as a member of the epidote group, allanite subgroup, which is derived from clinozoisite by homovalent substitutions and one coupled heterovalent substitution: $^{A2}(REE)^{3+} + {}^{M3}Fe^{2+} \rightarrow {}^{A2}Ca^{2+} + {}^{M3}Fe^{3+}$ (Armbruster *et al.*, 2006). There are eight structurally different cation sites (A1-A2, M1-M3, T1-T3) along with 10 anion sites (O1-O10) (Dollase, 1971). A1 and A2 are large, 10- and 11- coordinated sites, respectively, where large ions are located. The A1 site usually accommodates Ca, while A2 accommodates REE+actinides; M1-M3 are octahedrally coordinated, more or less distorted sites which accommodate smaller cations (Al, Fe^{3+}, Mn^{3+}, Cr^{3+}, V^{3+}, Fe^{2+}, Mg^{2+}, Mn^{2+}) (Dollase, 1971; Armbruster *et al.*, 2006). M1 and M2 are moderately distorted sites. M2 accommodates exclusively Al, while M1 accommodates divalent and trivalent cations (Dollase, 1971; Armbruster *et al.*, 2006). The M3 site is the most distorted and accommodates larger cations, e.g. Fe^{2+}, (Kartashov *et al.*, 2002; Armbruster *et al.*, 2006). T site is tetrahedrally coordinated and usually accommodates Si^{4+} (Dollase, 1971; Armbruster *et al.*, 2006).

In this study, Mössbauer spectra were collected on one treated sample: natural (ALF), annealed for 24 h at 650°C in air (ALF_650), and hydrothermally treated for 2 h at 150°C (ALF_AK) in order to possibly determine site occupancy, iron valence and coordination number, and to observe processes connected with possible changes in the valence of iron due to treatment.

Mössbauer spectra of allanite-(Ce) sample are complex and consist of several doublets (fig. 1), i.e. more than one position and/or oxidation state is present in the crystal structure. Unshaded doublets (fig. 1) represent Fe^{3+} cations in different positions; light grey shaded doublets represent Fe^{2+} cations in different positions. The hyperfine parameters for samples ALF and ALF_AK are: CS = 0.323(2) - 1.03(5) mm/s; QS = 0.89(6) - 2.6(1) mm/s and CS = 0.33(1) - 1.01(3) mm/s; QS = 0.86(4) - 2.45(9) mm/s, respectively. The data are very similar for both samples (fig. 1) which indicates that no significant change, i.e. oxidation or diffusion of iron, occurred during the hydrothermal treatment of the sample. Fe^{3+}/Fe_{total} ratios are virtually the same in both samples, 0.75, which confirms that no oxidation occurred during the treatment.

As for the sample annealed at 650°C in air (ALF_650), all iron was oxidized to Fe^{3+} (fig. 1, fig. 2) which is consistent with the literature (Dollase, 1973).

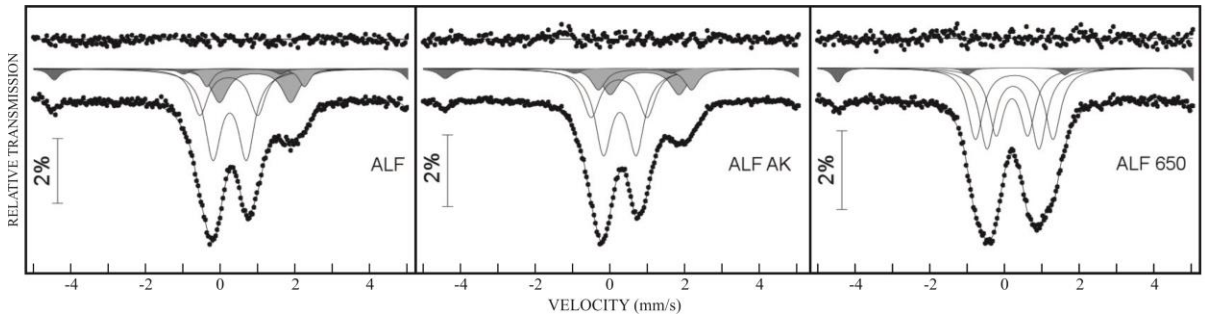

Fig. 1: Mössbauer spectra of allanite-(Ce) sample: natural (ALF), hydrothermally treated (ALF_AK), annealed at 650°C in air (ALF_650) (Fe^{2+}- light grey shaded doublet; Fe^{3+}- unshaded doublet; Fe_2O_3 – dark grey shaded doublet)

The hyperfine parameters for ALF and ALF_AK are roughly consistent with data from literature (Kartashov *et al.*, 2002; Malczewski & Grabias, 2008; Nagashima & Akasaka, 2010; Škoda *et al.*, 2012; fig. 2), hence it could be possible to attribute different doublets to specific crystallographic sites. Thus, in this investigation, both Fe^{3+} and Fe^{2+} could be assigned to both M1 and M3 positions (fig. 2). Nevertheless, it is not possible to unambiguously assign different doublets to specific crystallographic

sites without additional data, e.g. microprobe or crystal structure refinement data. It can be seen that, while data from several sources analyzing epidote (Nagashima & Akasaka, 2010), allanite-(Ce) (Malczewski & Grabias, 2008) and allanite-(Nd) (Škoda *et al.*, 2012) are extremely close and the doublet assignments are the same, the situation is a little bit different for ferriallanite-(Ce) (Kartashov *et al.*, 2002) (fig. 2). Thus, additional investigations are necessary in order to unambiguously assign the doublets to different crystallographic positions.

.

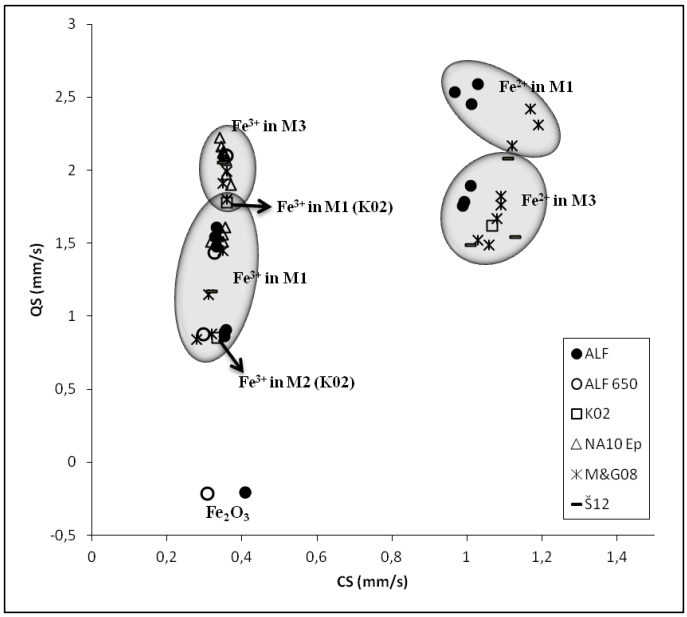

Fig. 2: Hyperfine parameters (CS-centre shift and QS – quadrupole splitting) for sample ALF and ALF_AK plotted against data from the literature. K02 - Kartashov *et al.* (2002); NA10Ep - Nagashima & Akasaka (2010); M&G08 - Malczewski & Grabias (2008); Š12 - Škoda *et al.* (2012). Data for site occupancy from Kartashov *et al.* (2002 which differ from other literatue data are marked with an arrow. Fe_2O_3 – hematite in sample ALF and ALF_650.

Dark grey doublets (fig. 1) represent Fe_2O_3, which is an impurity in allanite and could be easily distinguished from paramagnetic Fe^{3+} and Fe^{2+} in Mössbauer spectra due to the marked differences in hyperfine parameters (CS = 0.41(2) mm/s and QS = -0.21(5) mm/s; fig. 2).

These are minor impurities since this phase was not observed in the XRPD pattern (Čobić *et al.*, 2010, sample N1) possibly due to nanometer grain size as a result of metamictization induced alterations. Also, this phase remains stable under both annealing in air and hydrothermal treatment.

References

Armbruster, T., Bonazzi, P., Akasaka, M., Bermanec, V., Chopin, C., Giere, R., Heuss-Assbichler, S., Liebscher, A., Menchetti, S., Pan, Y. & Pasero, M. (2006): Recommended nomenclature of epidote-group minerals. European Journal of Mineralogy, vol. 18, 551-567.

Čobić, A., Bermanec, V., Tomašić, N. & Škoda, R. (2010): The hydrothemal recrystallization of metamict allanite-(Ce). The Canadian Mineralogist, vol. 48, 513-521.

Dollase, W. A. (1971): Refinement of the crystal structures of epidote, allanite and hancockite. American Mineralogist, vol. 56, 447-464.

Dollase, W. A. (1973): Mössbauer spectra and iron distribution in the epidote-group minerals. Zeitschrift fur Kristallographie, vol. 138, 41-63.

Kartashov, P. M., Ferraris, G., Ivaldi, G., Sokolova, E. & McCammon, C. A. (2002): Ferriallanite-(Ce), CaCeFe3+AlFe2+(SiO4)(Si2O7)O(OH), a new member of the epidote group: description, X-ray and Mössbauer study. Can Mineral, vol. 40, 1641-1648.

Malczewski, D. & Grabias, A. (2008): 57Fe Mössbauer spectroscopy of radiation damaged allanites. Acta Physica Polonica A, vol. 114, 1683-1690.

Nagashima, M. & Akasaka, M. (2010): X-ray Rietveld and 57Fe Mössbauer studies of epidote and piemontite on the join Ca2Al2Fe3+Si3O12(OH)-Ca2Al2Mn3+Si3O12(OH) formed by hydrothermal synthesis. American Mineralogist, vol. 95, 1237-1246.

Škoda, R., Cempírek, J., Filip, J., Novák, M., Veselovský, F. & Čtvrtlík, R. (2012): Allanite-(Nd), CaNdAl2Fe2+(SiO4)(Si2O7)O(OH), a new mineral from Åskagen, Sweden. American Mineralogist, vol. 97, 983-988.

CRYSTAL CHEMISTRY OF $M^{2+}Be_2P_2O_8$ (M^{2+} = CA, SR, PB, BA) BERYLLOPHOSPHATES: A COMPARISON WITH FELDSPAR ANALOGUES

F. Dal Bo[1*], F. Hatert[1], C. Rao[2]
[1] Laboratory of Mineralogy B.18, University of Liège, B-4000 Liège, Belgium. (*fdalbo@ulg.ac.be)
[2] Department of Earth Sciences, Zhejiang University, Hangzhou 310027, China.

Only 19 natural beryllophosphates are reported in the litterature, occuring mainly in granitic pegmatites and resulting from the reaction of beryl with P-bearing hydrothermal solutions (Kampf, 1992; Cerný, 2002). The formation of these minerals is highly dependent upon the pH, the temperature, the availability of specific alkali cations, and the Be/P ratio of the solution (Kampf *et al.*, 1992). Despite their low abundance, beryllophosphates crystallize in many structure types, characterized by different polymerization degrees of the BeO_4-PO_4 tetrahedra: these compounds form chain structures (fransoletite $[Ca_3Be_2(PO_4)_2(PO_3OH)_2.4H_2O]$, väyrynenite $[MnBe(PO_4)(OH)]$), sheet structures (herderite $[CaBe(PO_4)(F,OH)]$, uralolite $[Ca_2Be_4(PO_4)_3(OH)_3.5H_2O]$), framework structures (hurlbutite $[CaBe_2P_2O_8]$, babefphite $[BaBe(PO_4)F]$, beryllonite $[NaBe(PO_4)]$), and structures containing clusters of tetrahedra (gainesite $[Na_2Zr_2[Be(PO_4)_4].1.5H_2O]$) (Hawthorne & Huminicki, 2002). Furthermore, Harvey & Meier (1989) have synthesized five beryllophosphates with zeolite-type structures. Recently twe new mineral strontiohurlbutite $[SrBe_2P_2O_8]$ was discovered in the Nanping No. 31 pegmatite, Fujian Province, China (Rao *et al.*, 2012).

The low number of natural and synthetic beryllophosphates reported in the literature prompted us to investigate the M^{2+}-Be-PO_4 system (M^{2+} = Ca, Sr, Pb, Ba, Zn, Cd), by using hydrothermal synthesis techniques at low temperature (200°C) and low pressure (autogenous pressure), and high temperature (400°C and 600°C) and high pressure (1 kbar). The experiments at low temperature and pressure were performed in Parr autoclaves, using BeO, H_3PO_4, $CaHPO_4$, $Sr(NO_3)_2$, $Pb(NO_3)_2$, $Ba(OH)_2.8H_2O$, $Zn(OH)_2$ or $Cd(OH)_2$ as starting materials. In the case of experiments at high temperature and pressure, crystals synthesized at low temperure-pressure were crushed and used as starting material.

During these syntheses different beryllophosphates were obtained: $CaBe_2P_2O_8$, $SrBe_2P_2O_8$, $PbBe_2P_2O_8$ and $BaBe_2P_2O_8$. These compounds have large stability fields and are observed in all the hydrothermal synthesis performed whatever the temperature and pressure conditions applied. The crystallographic parameters of these compounds are listed in the Table 1. $CaBe_2P_2O_8$, $SrBe_2P_2O_8$ and $PbBe_2P_2O_8$ crystallized in the same space group and are isostructural. Their structure consists of corner-sharing BeO_4 and PO_4 tetrahedra assembled in 4- and 8-membered rings; these rings are perpendicular to the *a* axis. The 4-membered rings consist of a pair of tetrahedra pointing upwards (U) and pair of tetrahedra pointing downwards (D), and therefore UUDD type rings are observed. The 8-membered rings are formed by linking four 4-membered rings, and show only one pattern: DDUDUUDU (Fig. 1a). BeO_4 and PO_4 tetrahedra are also connected by corner-sharing to form a double crankshaft chain running along the *a* axis. The bivalent cations are located in the 8-membered rings and occur in 7+3-coordinated polyhedron, characterized by 7 short bonds and 3 long bonds. By considering only the 7 shortest bonds, this polyhedron can be described as a combination of a square pyramid and of a trigonal prism, with one square face in common.

Stuctural crystallography of beryllophosphates with formula M^{2+}-Be-PO_4 (M^{2+} = Ca, Sr, Pb) is fascinating, since their structures can be compared to those of aluminosilicates belonging to the feldspar family (anorthite $[Ca(Al_2Si_2O_8)]$, slawsonite $[Sr(Al_2Si_2O_8)]$, and paracelsian $[Ba(Al_2Si_2O_8)]$), to those of borosilicates as danburite $[CaB_2Si_2O_8]$ and pekovite $[SrB_2Si_2O_8]$, and to those of the synthetic compounds $SrGa_2Si_2O_8$ and $SrGa_2Ge_2O_8$.

$BaBe_2P_2O_8$ showed a structure completely different from the other beryllophosphates investigated in this study. The structure of $BaBe_2P_2O_8$ is based on a double layer of tetrahedra containing both berylium and phosphorus in a 1/1 ratio. These tetrahedra are assembled in 6-membered rings forming channels parallel to the *c* axis. Parallel to the *a*-*b* plane, a ring is connected to 6 other rings to form an infinite layer. In the *c* direction, the tetrahedra are also linked by their apical oxygens, thus forming a double layer with all tetrahedra of the same layer pointing in one direction (Fig. 1b). These layers are connected by the Ba atoms, located in a twelve-coordinated polyhedra.

The Ba polyhedra has a very regular hexagonal shape and showed 12 identical bonds of 2.976(2) Å length. This barium beryllium phosphate is isostructural with dmisteinbergite, a hexagonal polymorph of $CaAl_2Si_2O_8$ (Takéuchi & Donnay, 1959).

Table 1: Unit-cell parameters for synthetic beryllophosphates with the general formula $M^{2+}Be_2P_2O_8$

	$CaBe_2P_2O_8$	$SrBe_2P_2O_8$	$PbBe_2P_2O_8$	$BaBe_2P_2O_8$
Space Group	$P2_1/c$	$P2_1/c$	$P2_1/c$	$P6/mmm$
a (Å)	7.809(1)	8.000(1)	8.088(1)	5.028(1)
b (Å)	8.799(1)	8.986(1)	9.019(1)	5.028(1)
c (Å)	8.309(1)	8.418(1)	8.391(1)	7.466(1)
β (°)	90.51(1)	90.22(1)	90.12(1)	-
V (Å³)	570.98(2)	605.10(6)	612.22(1)	163.51(1)
Z	4	4	4	1
Natural analogue	Hurlbutite[1]	Strontiohurlbutite[2]	-	-

[1] Lindbloom *et al.*, 1974
[2] Rao *et al.*, 2012

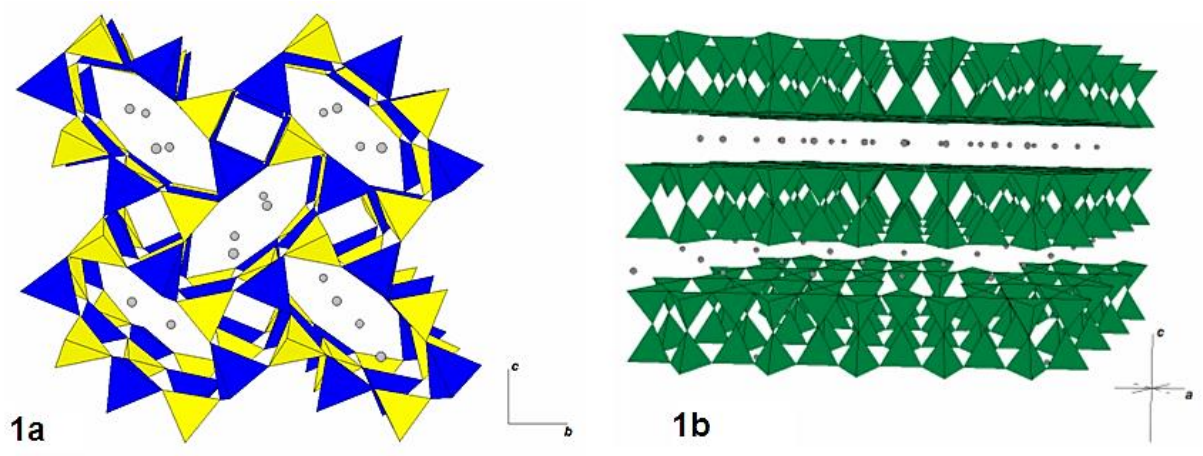

Fig. 1a. Structure of $CaBe_2P_2O_8$: $SrBe_2P_2O_8$ and $PbBe_2P_2O_8$; PO_4 are yellow, BeO_4 are blue and spheres represent M^{2+} cations. **1b**. Structure of $BaBe_2P_2O_8$: $(Be,P)O_4$ are green and spheres represent Ba atoms.

References

Cerný, P. (2002): Mineralogy of Beryllium in Granitic Pegmatites. Reviews in Mineralogy & Geochemistry. 50, 405-444.

Harvey, G. & Meier, W.M. (1989): The Synthesis of Beryllophosphate Zeolites. Zeolites: Facts, Figures, Future. 49, 237-254.

Hawthorne, F.C. & Huminicki, D.M.C. (2002): The Crystal Chemistry of Beryllium. Reviews in Mineralogy & Geochemistry. 50, 333-403.

Kampf, A.R. (1992): Beryllophosphate chains in the structures of fransoletite, parafransoletite and erleite and some general comments on beryllophosphate linkages. American Mineralogist. 77, 848-856.

Kampf, A.R., Dunn, P.J., Foord, E.E. (1992): Parafransoletite, a new dimorph of fransoletite from the Tip Top Pegmatite, Custer, South Dakota. American Mineralogist. 77, 843-847.

Lindbloom, J. T., Gibbs, G. V. and Ribbe, P. H. (1974): The crystal structure of hurlbutite: a comparison with danburite and anorthite. American Mineralogist 59, 1267-1271.

Rao, C., Wang, R., Gu, X., Hu, H. and Dong, C. (2012): Strontiohurlbutite, IMA 2012-032. CNMNC Newsletter No. 14, October 2012, page 1285; Mineralogical Magazine, 76, 1281-1288.

Takéuchi, Y. & Donnay, G. (1959): The crystal structure of hexagonal $CaAl_2Si_2O_8$, Acta Crystallographica 12, 465-470.

SPATIAL STATISTICAL ANALYSIS APPLIED TO RARE-ELEMENTS LCT-TYPE PEGMATITE FIELDS: AN ORIGINAL APPROACH TO CONSTRAIN FAULTS-PEGMATITES-GRANITES RELATIONSHIPS

S. Deveaud[1,2,3], C. Gumiaux [1 ,2,3], E. Gloaguen [1,2,3], Y. Branquet[1,2,3]
BRGM, ISTO, UMR 7327, BP 36009, 45060 Orléans, France; S.Deveaud@brgm.fr
[2] CNRS/ISTO, UMR 7327, 45060 Orléans, France
[3] Université d'Orléans, ISTO, UMR 7327, 45071 Orléans

The emplacement of LCT (Lithium-Cesium-Tantalum) - type pegmatite fields and their relationships with hosting rocks are commonly studied with petrographic, geochemical and isotopic analyses. Although these methods are efficient to understand the process of differentiation and/or enrichment in rare-elements during the crystallization of pegmatites, they are not appropriate to understand at field scale the LCT pegmatites' emplacement. Here we apply a spatial statistical analysis to the LCT-pegmatites field of Monts d'Ambazac, in the Saint Sylvestre Granitic Complex (Massif Central, France, Cheilletz *et al.* 1992, Raimbault 1998), in order to constrain and discuss spatial relationships between pegmatites, granites and faults. Various numeric variables (distance to the nearest neighbor, Ripley's L'-function, Euclidean distance, spatial density distribution, cluster analysis) have been computed to quantify both i) the spatial distribution layout of the pegmatite occurrences, including their grouping/scattering and aligning features, and ii) the overlap or proximity of the pegmatites with given rock types or structures. We show that a spatial relationship can be quantified between LCT-type pegmatites and a ~N to NNE trending faults family; with 50% of the pegmatite occurrences located at less than 500 m away from one of these faults. This result is confirmed by the spatial relationships between the pegmatites set distribution and the highest spatial density of this trend fault class. Moreover we statistically demonstrate the high clustering rate of the pegmatites set. These clusters are preferentially oriented in the same N015° direction than the trend of the A class-faults, themselves, which is parallel to a large sheared corridor described in the central part of the study area. In contrast to analyses on relationships between faults and pegmatites, our results point out a lack of spatial link between each pegmatite subtypes and several potential granitic sources. We thus suggest that pegmatites are emplaced along A-faults trend. The development of these faults could be favored by and focused in the central part of the granitic complex beforehand affected by a large shear-zone. These results reveal the efficiency and the interest of such statistical approach to better constrain the LCT type pegmatites – faults – granites model. We think that such approach should be more systematically applied to LCT pegmatite fields' exploration, particularly to poorly exposed domains.

References

Cheilletz, A., Archibald. D. A., Cuney, M., and Charoy, B. (1992): Ages $^{40}Ar/^{39}Ar$ du leucogranite à topaze-lépidolite de Beauvoir et des pegmatites sodolithiques de Chèdeville (Nord du Massif Central, France). Signification pétrologique et géodynamique. C.R. Acad. Sci. Paris, 315, 326-336.

Raimbault, L. (1998): Composition of complex-lepidolite type granitic pegmatites and of constituent of columbite-tantalite, Chèdeville, Massif Central, France. The Canadian Mineralogist, vol. 36, 563-583.

BE AND ZN BEHAVIOR DURING ANATETIC FORMATION OF EARLY PEGMATOID MELTS IN VARISCAN TERRAINS – AN EXAMPLE FROM THE ARGA PEGMATITE FIELD, NORTHERN PORTUGAL

P. Dias[1], C. Leal Gomes[2]
[1]CIG-R, University of Minho, Braga, Portugal patriciasdias@gmail.com
[2]DCT, University of Minho, Braga, Portugal

In the region of Serra de Arga, Dias (2012) and Dias & Gomes (this volume) identified a set of peraluminous pegmatoid veins that are anatectic in origin. Silurian host rocks enriched in fluxing constituents underwent partial melting to produce these veins. From the genetic viewpoint, they exhibit compositional and textural similarities to muscovite and abyssal class pegmatites. Equilibrium metamorphic assemblages suggest that melting occurred at temperatures of 650-710 ° C and pressures 2.9-4.2 kbar (andalusite and sillimanite isograds). These veins exhibit several structures and mineral associations that resulted from primary evolution of melts and derived fluids. The presence of schlieren suggests that these melts were mobile, with selective separation via filter-pressing and seismic-pumping. These processes may be responsible for the formation of cumulate cordierite textures. Some segregated veins exhibit internal zonation that resulted from *in situ* fractional crystallization. The final stages are marked by subsolvus and subsolidus evolution of the primary mineral assemblage, often associated with ductile-brittle deformation that facilitated percolation of the fluids responsible for the alteration.

Pegmatoids with this petrogenetic framework show marked beryllium enrichment which is attributed to the transference of highly anomalous Be contents from pre-metamorphic volcanic protoliths that underwent alkaline metasomatism. Nearby tourmalinites, amphibolites, metavolcanic rocks (leptite-like rocks with abundant oligoclase), and heterogeneous tourmaline and apatite rich phyllites have Be contents between 4 and 10 ppm. These highly differentiated values are strongly above the average values of the crust and mantle. The results of batch-melting modeling of the enclosing tourmalinites are consistent with this origin.

In addition to the high Be content in the protoliths, Be incorporation in segregation melts is also related to the incompatible nature of Be as it is easily incorporated into the melt. The absence of cordierite and sillimanite, which easily incorporate Be, allow Be to enter the melt phase. The following mineralogic assemblages reflect the different generations of vein deposits present: 1. chrysoberyl and beryl in veins associated with the typomorphic peraluminous minerals cordierite and andalusite; 2. chrysoberyl in quartz-muscovite facies with prismatic sillimanite and lazulite-scorzalite; 3. chrysoberyl and beryl in quartz-muscovite veins; 4. beryl in peraluminous sodic-potassic veins with montebrasite comb-structure growths; 5. beryl in cordierite pseudomorphs in the type 1 veins; 6. metasomatic emerald in melanosomes peripheral to type 3 veins; 7. chrysoberyl, quartz and sillimanite intergrowths in reaction coronas between beryl and albite in sodic-potassic peraluminous veins with typomorphic lazulite-scorzalite. Assemblages 1 and 2 imply chrysoberyl equilibrium or late crystallization of Cord + And + Mu and Sil + Qz + Mu + Ab ± Fk. Chrysoberyl is present only in mineral assemblages where andalusite and cordierite are abundant and in quartz impoverished facies. In veins with lazulite-scorzalite, chrysoberyl is associated with muscovite and gahnite. Both chrysoberyl and gahnite may be included in the Al phosphate. In type 3 occurrences, beryl occurs as oversized comb-structured crystals consistent with rapid crystallization. Chrysoberyl occurs predominantly along the main concentrations of muscovite within the veins. Assemblages 5 and 6 result from alteration by late fluids, processes which tend to occur at low T. Emerald occurs in biotite and tourmaline melanosomes. Type 7 assemblages with chrysoberyl formed at the expense of beryl (BASH system compatible reactions), possibly in connection with a thermal anomaly resulting from emplacement of Variscan granites. This temperature anomaly was high enough to metamorphose pegmatoids to transition beryl => chrysoberyl (Gomes, 1997).

The subsolidus reequilibration of cordierite would produce quartz + beryl intergrowths and muscovite/chlorite replacement masses. Geometric patterns of Be release from the cordierite lattice produce the following textures: 1 – beryl-quartz intergrowths in the core of pseudomorphs enveloped by chlorite + muscovite; 2 - texturally disseminated beryl in the micaceous and chloritic mass, forming low granulometry crystals with oscillatory concentric zoning; 3 - various coronitic aspects of

beryl within the pseudomorphs suggests the deposition in inter-granular spaces after sub-graining of precursor cordierite. This occurred during cycles of deformation and late-stage alteration of cordierite. In the first scenario, for a relatively consistent beryl modal proportion of 25%, a concentration of 3.25 wt% of Be in the primary cordierite is inferred. The average beryl modal proportions in the assemblage with chrysoberyl is 1.5% (in scenario 2). Beryl related to the subsolidus alteration of cordierite retains a relatively high Fe and Mg content (Fe>Mg) with Cs_2O ranging from 0.13 to 0.24 wt. %.

Typological analysis of evolutionary trends interpreted from the variability of beryl composition, suggest the existence of a convergence domain in a Al- (Na + K + Cs) - (Fe + Mg + Ti + Cr + V + Mn) *apfu* ternary diagram. In this diagram it is possible to isolate the following convergence composition Al_{93} $(Na + K + Cs)_4$ $(Fe + Cr + Ti + V + Mg + Mn)_3$.

Textural and mineralogic analysis suggest that gahnite, with an average composition of $(Zn_{0.6},Fe_{0.34},Mn_{0.01})Al_2O_4$, accompanies all primary beryl growth. Gahnite crystals are euhedral to subhedral and exhibit ordered intergrowths with quartz. Particularly interesting are the star-like intergrowths of gahnite and quartz that often occur as inclusions in beryl. They may represent early intergrowths that crystallized prior to beryl, thus are true inclusions, or are the result of symplectitic intergrowths. The Zn required to form gahnite was also derived from the volcanic host rocks and may have been released from zincian biotite or by desulfurization of sphalerite in the protolith during metamorphism (e.g. Spry & Scott, 1986). Gahnite also occurs in albitic veins associated with abundant tourmaline, hambergite, rhodizite-londonite, pollucite and OH-herderite, possibly formed under late-stage, low temperature conditions.

The observed Be enrichment correlates with the degree of partial melting, suggesting that it is behaving as a compatible rather than an incompatible element in these Mg and Fe enriched peraluminous melts. This may lead, in appropriate metamorphic conditions, to early Be extraction in ferromagnesian phases and Al oxides which crystallize under desilication conditions. However, Be concentration increases in the remaining liquid phase during fractionation and becomes abundant in the late-stage hydrothermal fluids, suggesting that this behaviour transitions to incompatible.

Acknowledgements

This work received support from Fundação para a Ciência e a Tecnologia (FCT) through a PhD fellow. The chemical analytical work was possible with the contribution and support of LNEG - S. Mamede de Infesta to which we are duly acknowledged. The authors also thank the conference reviewers and editors whose suggestions and comments substantially improved the abstract.

CIG-R is supported by the pluriannual program of the Fundação para a Ciência e a Tecnologia, funded by the European Union (FEDER program) and the national budget of the Portuguese Republic (PEst-OE/CTE/UI0697/2011).

References

Dias, P. A. (2012): Análise estrutural e paragenética de produtos litológicos e mineralizações de segregação metamórfica – Estudo de veios hiperaluminosos e protólitos poligénicos Silúricos da região da Serra de Arga (Minho). PhD thesis, University of Minho, Portugal, 464p.

Gomes, C. L. (1997): Evolução em subsolidus de paragéneses pegmatíticas – Sistema granítico residual da Serra de Arga (Minho – N de Portugal). Actas X Semana de Geoquímica/IV Congresso de Geoquímica dos Países de Língua Portuguesa, Braga, Portugal, 195-198.

Spry, P.G.& Scott, S.D. (1986): The stability of zincian spinels in sulfide systems and their potential as exploration guides for metamor- phosed massive sulfide deposits. Econ. Geol., 81, pp. 1446–1463.

STRUCTURAL AND PARAGENETIC ANALYSIS OF SWARMS OF BUBBLE LIKE PEGMATITES IN A MIAROLITIC GRANITE FROM ASSUNÇÃO SOUTH – VISEU – CENTRAL PORTUGAL

P. A. Dias[1], P. Araújo[2], M. Pereira[2], B. Pereira[1], J. Azevedo[1], J. Oliveira[1], J. Carvalho[3], C. Leal Gomes[2]
[1] Sinergeo Lda., Edíficio IEMINHO - Vila Verde - Portugal, patriciasdias@gmail.com
[2] DCT, Campus de Gualtar - University of Minho – Braga – Portugal
[3] GGC Lda., Rua Cunha Jr., 41 - B - s 1.6 – Porto - Portugal

Shallowly emplaced hydrated granitic magmas may produce miarolitic cavities, some of which are lined with minerals. Essential to the formation of miarolitic cavities is exsolution of a fluid phase that results from fluid immiscibility when $P_{fl} > P_{lit}$. Whether volatiles escape or are entrapped within the melt is a function of both temperature and pressure. Entrapment is more likely if heat is rapidly dissipated from a rapidly cooling melt, thus miaroles are more common in fine-grained rocks. The less dense volatiles rise into the apical zones of a magma chamber when the degree of crystallization of the melt is low (e.g. Candela, 1997).

The Ferreira de Aves pluton (Viseu) is a two-mica syn-to late tectonic granite associated with the 3rd phase of Variscan deformation (300-330 Ma). This deformation led to conditions during magma emplacement that were conducive to exsolution of a vapor phase. The miarolitic rock is a fine-grained granite that abruptly transitions to porphyritic, medium-grained granite. Large miarolitic pegmatites emplaced at higher levels in the magma chamber are zoned irregular bodies with a quartz core, beryl and Li-phosphates. This suggests the miarolitic granite represents a region in the magma chamber where bubbles coalesce to form large pegmatites (Leal Gomes and Nunes, 2003). The structural control of these granites is well defined as they strike N35°E, parallel to regional shear structures and sub-parallel to the orientation of the plutonite cupola.

The mineralogical assemblage in the miaroles is similar to that of the parental granite, essentially quartz, feldspar and muscovite. Individual and small (between 5 cm^3 and 1 dm^3) miaroles may be clustered into swarms. The average bubble volume is 86 cm^3 for a population of 130 measured miaroles. Most miaroles are lenticular with significant deformation from spherical shapes. This may be due to magmatic flow with low viscosity of the liquid. The three axes of the ellipsoids are a) – stretching, parallel to the flow lineation; b) – flattening; c) - orthogonal to b. The dominant flow lineation direction is N45°E, subparallel to the major transcurrent surrounding structures.

The mineral assemblages in the miaroles are variable and can be subdivided as follows: 1)- *quartz + chlorite ± muscovite ± alkali-feldspar intergrowths,* 2)- *void with inward crystallizing quartz + muscovite ± microcline;* 3a)- *quartz + muscovite ± K-feldspar ± F-apatite, non-graphic quartz + schorl or chlorite + quartz as late-stage phases;* 3b)- *microcline ± quartz ± muscovite coating the cavity and late green lepidolite or chlorite/chamosite ± muscovite ± goethite ± kaolinite;* 4)- *dominant microcline inward crystallization; 5)- late graphic schorl/quartz; 6)- quartz ± muscovite lining the cavities and late green lepidolite or chlorite/chamosite ± pyrrothite.* The most important distinction in these assemblages is the variability of potassium feldspar, tourmaline and the late mineral assemblages. Type 1 bubbles represent the early stages of morphological and mineralogical development. The size and intergrown minerals suggest they resulted from small amounts of exsolved fluids. In morphologically evolved miaroles, cavities are small and localized with inward growth of quartz, muscovite and feldspar (Fig. 1-A). Type 3b miaroles host larger amounts of alkali-feldspar, which lines cavities filled with quartz and muscovite or other phylossilicates (Fig. 1-B). The bubbles richer in alkali feldspar may indicate higher rates of inward fractionation, and the establishment of liquid-liquid interfaces relative to the granite. In other cases, K-feldspar occurs in the form of one or two included megacrysts (Fig. 1-C). In type 6 occurrences, feldspar is particularly scarce, occurring in units with tourmaline, lepidolite or chlorite / chamosite and eventually late-stage pyrrhotite that fills in the interstitices (Fig. 1-D). As a result of the enrichment in boron, tourmaline is relatively abundant. Some unusual bubbles contain only graphic intergrowths of tourmaline and quartz (Fig. 1-E).

Along the periphery of most bubbles, centimeter scale halos are rich in albite and depleted in quartz and ferromagnesian minerals. It is in type 5 and 6 occurrences, with scarce or absent feldspar and graphic tourmaline, that the albitic surrounding volume is greater.

Additionally, bubbles often show radial fractures resulting from hydraulic stress release.

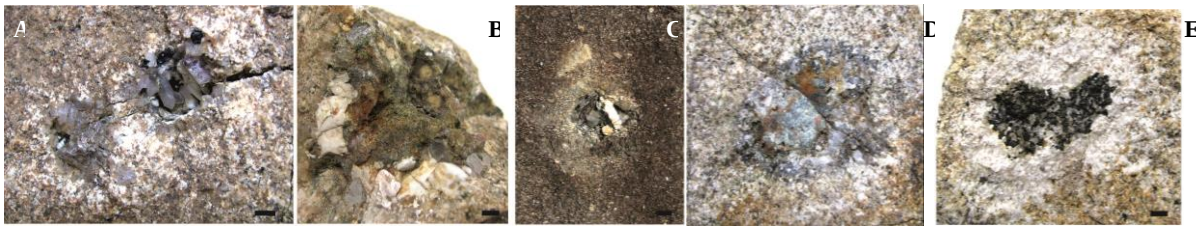

Fig. 1: –Examples of miarolitic pegmatites with contrasting forms and mineral assemblages. Scale bar is 0.5 cm.

Through the above observations it was possible to identify a consistent structural pattern of distribution of bubbles within the granitic host and a mineralogic typology determined by the abundance and textural arrangements of some typomorphic phases. From this, it is deduced:

Transcurrent kinematics promotes decompression and enhances fluid immiscibility, with decisive influence on the amount of bubbles along structural corridors.

i. Mobility in apical fronts generating growth is marked internally by inward crystallization and uprising late assemblages; the higher boron enrichment promotes low viscosity magmatic flow.

ii. Petrographic arguments suggest granite / pegmatite transitions characterized by liquid-liquid interfaces and fractionation conditions generating internal zoning.

iii. The domain of immiscibility occurs at low degree of crystallization of the host with rare phenocrysts in the surrounding granitic matrix.

iv. Evolutionary trends are the result of the following events: *fractional crystallization*, *early equilibrium crystallization* or *late metasomatism - immiscibility*.

Acknowledgements

This contribution results from work undertaken within the project PROSPEG (ref. 11480), co-supported by the "ON.2 – O Novo Norte" and QREN, through the European Regional Development Fund (ERDF). The authors acknowledge the conference reviewers and editors whose suggestions and comments substantially improved the abstract.

References

Candela, P. A. (1997): A review of shallow, ore-related granites: textures, volatiles, and ore metals. Journal of Petrology, 38(12), 1619-1633.

Leal Gomes, C., Nunes, J. E. L. (2003): Análise paragenética e classificação dos pegmatitos graníticos da Cintura Hercínica Centro-Ibérica. A Geologia de Engenharia e os Recursos Geológicos, Coimbra – Imprensa da Universidade, II, 85-109.

PETROGENESIS OF PERALUMINOUS ANATECTIC PEGMATOIDS

P. A. Dias[1], C. Leal Gomes[2]
[1] CIG-R, University of Minho, Braga, Portugal; patriciasdias@gmail.com
[2] DCT, University of Minho, Braga, Portugal

In the region of Serra de Arga (Minho, Portugal) peraluminous veins were evaluated in an effort to characterize these deposits and determine the processes involved in their genesis. Although these veins exhibit textures similar to those typical of pegmatites that formed from fractional crystallization of a granitic melt, they are mineralogically distinct from pegmatites that outcrop nearby (syn-tectonic relatively to late Variscan deformation, 330 Ma). Thus, this project focuses on the parental enclosing rocks as a potential source for these veins, through partial melting and metamorphic segregation processes. Nevertheless, because metamorphic conditions did not reach sufficiently high pressures and temperatures to induce melting, as evidenced by the absence of extensive migmatitization in the nearby terrains, it is likely that constituents such as B, F, P and Li present in pre-metamorphic protoliths resulted in a depression of the *liquidus* temperature and facilitated partial melting and subsequent segregation.

The adjacent outcrop area is a meta-volcanosedimentary terrain that lies between the Orbacém thrust and the Vigo-Régua shear zone. In this area, metamorphosed pelitic formations are interbedded with calc-silicate rocks including amphibolites, black schists, quartz phyllites, tourmalinites and felsic metavolcanics. These sedimentary and volcanogenic rocks underwent medium-high grade metamorphism. Deformation associated with the D2 Variscan phase (340 Ma) is well represented in this sector and have allowed for P-T increments and peaks needed for melting, mainly at host sites, corresponding to low pressure domains, where *liquidus* depressor constituents were mobilized producing peraluminous melts.

In addition to these fluxing elements, the potential protoliths were enriched in incompatible elements that were remobilized into the segregated products. Be, Li, Nb, Ta and Sn contents of potential protolithic facies were normalized to average values of the crust and mantle and equivalent rocks. These elements are enriched by several orders of magnitude in the protoliths. The remobilization of these incompatible elements is reflected in the presence of Ti-Nb-Ta-Sn oxides, Be minerals (beryl and chrysoberyl) and Li minerals (montebrasite) in the vein deposits. Deformation and metamorphism of ilmenite may have released Nb and Ta that led to the formation of struverite, Fe-columbite and tapiolite.

The diversity of texture and mineral assemblages within these veins allowed for a classification based on the proportions of essential minerals (andalusite, sillimanite, cordierite, feldspars) and the presence of some typical accessory phases (corundum, beryl, chrysoberyl, lazulite-scorzalite) (Dias, 2012). The proposed model for melt generation and mobilization begins with dehydration and fluid release; fluxes can be mobilized at this stage or during the anatexis of volatile enriched rocks where partial melting forms discrete units that are not continuous or migmatitic. These partial melts formed under hydrous conditions where the collection of newly-formed leucosomes was accommodated by dilation that arose during Variscan deformation. This syn-kinematic melt generation formed vein-like structures via "filter-pressing" and "seismic-pumping" mechanisms. Subsequent modification of the melt through fractional crystallization is evidenced by the mineral zonation within the veins. The method of melt generation can be inferred from textural and mineralogical analysis of veins at micro and mesoscopic scales. In one location at Serro, on the northern flank of Serra de Arga, incipient leucosome mobilizations and veins that typically host cordierite are enclosed in tourmalinites. The mineralogy and texture of these units appear to be related to the production and evolution of melt material as the leucosomes occur as small stringers where garnet may form as the result of incongruent melting of tourmaline. These stringers can evolve into larger volume domains that are segregated into zones containing predominantly cumulate cordierite associated with zones containing andalusite + cordierite + muscovite + garnet + apatite that host tourmalinite schlieren indicative of magmatic flow. Because these veins have a marked mafic character, they may represent segregations from a more leucocratic melt. Proximal to these mafic veins are thicker leucocratic veins. They are composed of cordierite and chrysoberyl along the margins with

andalusite further inward marking the transition to a quartz-muscovite core. Garnet restite stringers are also present. These veins may have formed by mobilization of a more fractionated and hydrated anatectic magma. The coexistence of these transitions, suggests that the veins formed by partial melting of the host tourmalinite in which subsequent separation of a leucocratic and fractional crystallization produced more leucocratic melts.

The P-T regime for partial melting was determined using a garnet-biotite geothermometer (Hodges & Spear, 1982) and the presence of the garnet-quartz-plagioclase-sillimanite assemblage (Hodges & Crowley, 1985). This yielded pressures between 2.9-4.2 kbar and temperatures between 650-710 º C. Additionally, the presence of iron-rich cordierites is consistent with low pressure conditions for melts generation. Thus, is likely that an intermediate path of decreasing pressure under isothermal conditions produced melts that were mobilized into the cordierite stability field which could be possible at the transition and regression gap between second and third Variscan folding phases.

These data suggest that the segregated veins represent an initial stage of melt mobilization in the vicinity of productive lithologies and may also be considered predecessors of widespread anatexis that was capable of producing granitic rocks such as St. Ovídeo granite. Normative compositions of the veins and St. Ovídeo granite, in the Qz-Ab-Or diagram, support the idea that, to some extent, these pegmatoids tend to S type granitic compositions.

The partial melting origin for the pegmatoids was evaluated using a batch melting model for Rb, Ba, and Sr for several of the potential parent lithologies. Batch melting of tourmalinites could be produced with mobilization of 30% to 90% melt. A more elaborate attempt to simulate tourmalinite melting to produce rocks with the assemblage andalusite + cordierite + quartz ± muscovite ± apatite ± chrysoberyl ± struverite ± tapiolite using Ba, Rb, Sr, Be, and REE showed that 10% melting could produce compositions similar to the veins if an early separation of a mineral fraction composed of 62% plagioclase + cordierite was coupled with additional melting of apatite and garnet.

Acknowledgements

This work received support from Fundação para a Ciência e a Tecnologia (FCT) through a PhD fellow. The chemical analytical work was possible with the contribution and support of LNEG - S. Mamede de Infesta to which we are duly acknowledged. The authors also thank the conference reviewers and editors whose suggestions and comments substantially improved the abstract.

CIG-R is supported by the Pluriannual program of the Fundação para a Ciência e a Tecnologia, funded by the European Union (FEDER program) and the national budget of the Portuguese Republic (PEst-OE/CTE/UI0697/2011).

References

Dias, P. A. (2012): Análise estrutural e paragenética de produtos litológicos e mineralizações de segregação metamórfica – Estudo de veios hiperaluminosos e protólitos poligénicos Silúricos da região da Serra de Arga (Minho). PhD thesis, University of Minho, Portugal, 464p.

Hodges, K. V. & Spear, F. S. (1982): Geothermometry, geobarometry and the Al_2SiO_5, triple point at Mt. Moosilauke, New Hampshire. Am. Mineral., 67, pp. 1118-1134.

Hodges, K.V. & Crowley, P.D. (1985): Error estimation and empirical geothermobarometry for pelitic systems. Am. Mineral., 70, pp. 702-709.

BERYL AND BE-MINERALIZATION IN PEGMATITES OF THE OXFORD PEGMATITE FIELD, MAINE, USA

A. Falster[1], J. Nizamoff [2], W. Simmons[1], R. Sprague[3]
[1]Dept. of Earth & Environmental Sciences, University of New Orleans, New Orleans, LA 70148;afalster@uno.edu
[2] Omya Inc., 39 Main Street, Proctor, VT 05765
[3]10 Yates Street, Mechanic Falls, ME 04256

Pegmatites in the Oxford pegmatite field in SW Maine are host to a large number of Be-bearing mineral species (Grew 2002). The most common Be mineral is beryl, which is wide-spread in these pegmatites. In general, the less evolved pegmatites have common blue to blue-green beryl and sometimes a small amount of hydroxylherderite and/or bertrandite as the dominant Be-minerals. More evolved pegmatites carry morganite and other Be-minerals such as beryllonite and roscherite group species along with hydroxylherderite and bertrandite. Beryl occurs in the massive pegmatite as greenish, bluish to yellow crystals that are generally opaque to translucent, which in some cases in the form of truly elephantine crystals, in excess of 5.5 m (Bumpus pegmatite). In miarolitic cavities, gem varieties such as aquamarine, heliodor, morganite and cesian beryl occur in a few pegmatites. Some of the finest and largest gem-quality beryl, notably aquamarine and heliodor were recovered at the Orchard pegmatite. Some beryl from Oxford pegmatites is enriched in Cs (Fig. 1). The Emmons pegmatite contains cesian beryl and morganite from Mount Mica and the Bennett pegmatite are also enriched in Cs. Even though the Orchard pegmatite appears to be relatively simple, there is moderate Cs-enrichment present in these beryls as well (Fig. 1).

In most Oxford County pegmatites, Be-mineralization typically begins and ends with beryl and no secondary Be-species occur. In the rarer, more evolved pegmatites, early beryl is in many cases replaced by bertrandite or by hydroxylherderite (if phosphate ions were available in the fluids). Beryllonite, roscherite group species and in one location, väyrynenite have also been documented but are quite rare.

At the Emmons pegmatite, some beryl crystals show evidence of dissolution and replacement during the later stages of pegmatite formation. The resulting voids commonly host a variety of secondary Be-minerals, such as beryllonite, hydroxylherderite and bertrandite associated with superb purple, blue, or teal fluorapatite. The molds of former beryl crystals are partially filled with up to about 25% with an assemblage of secondary fluorapatite and hydroxlherderite or with beryllonite and minor amounts of hydroxylherderite and fluorapatite. As primary beryl was dissolved, a significant influx of P and Ca entered into the voids as excess Be, Al and Si were removed.

Hydroxylherderite, $CaBePO_4(OH)$, is the second most abundant Be-mineral following beryl in pegmatites in the Oxford pegmatite field of Maine (Emmons, DumperDew, Bennett, Havey, and Mount Mica pegmatites). All are OH dominant but those from the Emmons and Havey pegmatites are the most F-rich (Fig. 2).

Hydroxylherderite, and herderite, are typical miarolitic cavity minerals which require high fluorine activity. Typical associations include fluorapatite, muscovite, and tourmaline. It is possible that the formation of hydroxylherderite vs. herderite is related to competition for F among these species and as it forms late, most of the F may have already been consumed by the other F-bearing mineral species.

Beryllonite is much rarer and restricted to the highly evolved pegmatites, notably the Emmons pegmatite where it occurs in beryl molds.

Phenakite is relatively common only at the Orchard pegmatite where it forms prismatic crystals in miarolitic cavities. Phenakite is an uncommon Be mineral in the Oxford pegmatite field. Phenakite is commonly found in the alkali granite to silica poor syenite environment where higher activity of K+ and Na+ destabilize beryl in favor of phenakite and feldspars (Černý 2002). It does not appear to be an alteration product in the Oxford County pegmatites and likely formed as a primary phase in miarolitic cavities, possibly linked with localized increased alkali ion activity.

Moraesite occurs in small cavities and spaces between pocket crystals in a number of pegmatites in the area but it is sensitive to weathering and mechanical disturbances. The roscherite group minerals greifensteinite, zanazziite and roscherite have also been identified at Newry and the Estes pegmatites.

The following Be-bearing mineral species occur very rarely in the Oxford Co., pegmatites: Euclase, gainesite, glucine, hurlbutite (in a single specimen

which was poorly documented), mccrillisite, uralolite and väyrynenite.

The Oxford pegmatite field is one of the more Be-species-rich pegmatite districts in the world and fine specimens of these minerals are still currently being produced in the active mines.

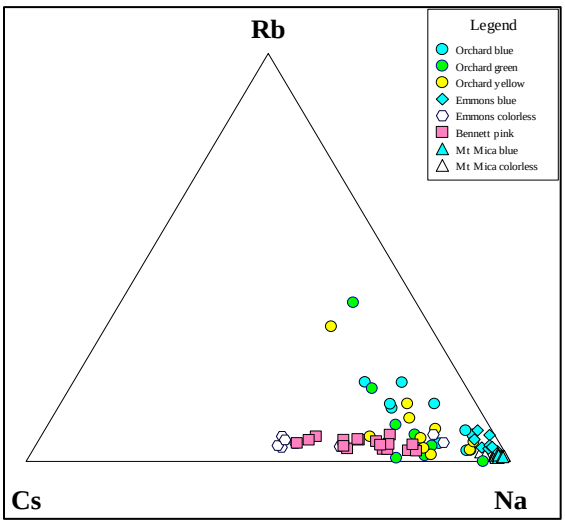

Fig. 1: Ternary plot of Cs, Rb, and Na (*apfu*) in in beryl of the Orchard pegmatite field

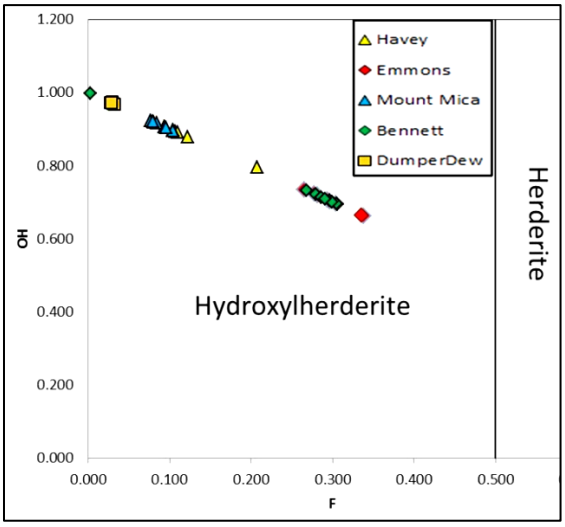

Fig. 2: Plot of F vs. OH (*apfu*) in hydroxyl-herderite from pegmatites in the Oxford pegmatite field beryl of the Orchard pegmatite field.

References

Černý, P. (2002). Mineralogy of beryllium in granitic pegmatites. In: Beryllium, mineralogy, petrology, and geochemistry. Reviews in mineralogy and geochemistry, volume 50. 405-444.

Grew, E.S. (2002). Mineralogy, petrology and geochemistry of beryllium: an introduction and list of beryllium minerals. In: Beryllium, mineralogy, petrology, and geochemistry. Reviews in mineralogy and geochemistry, volume 50. 1-76.

COMPOSITIONAL AND TEXTURAL EVOLUTION OF AMPHIBOLE AND TOURMALINE IN ANATECTIC PEGMATITE CUTTING PYROXENE GNEISS NEAR MIROŠOV, MOLDANUBIAN ZONE, CZECH REPUBLIC

P. Gadas[1], M. Novák[1], J. Filip[2], M. Galiová Vašinová[3]
[1] Department of Geological Sciences, Masaryk University, Brno, Czech Republic, pgadas@centrum.cz
[2] Regional Centre of Advanced Technologies and Materials, Palacký University, Olomouc, Czech Republic
[3] Department of Chemistry, Masaryk University, Brno, Czech Republic

The mineral assemblage tourmaline+amphibole only exceptionally occurs in magmatic/metamorphic rocks including granitic pegmatites. Textural relations indicate high disequilibrium; amphibole is typically replaced by tourmaline during B-metasomatism (e.g. Morgan & London 1987) or both minerals occur in different pegmatite units (Novák *et al.* 2013). In granitic pegmatites, amphiboles (tremolite-actinolite, edenite, hastingsite) are several orders less abundant then tourmaline-group minerals, and they are present almost exclusively in strongly contaminated pegmatites (Žáček 2007, Novák *et al.* 2013). At Mirošov, a common pegmatite (Pl+Kfs+Qz+Amp+Tur+Aln) cuts a small lens of pyroxene gneiss (Di+Grs/Adr+Qz+Pl+Amp). The field observations show that the melt was produced by anatexis of surrounding amphibolite (Amp+Pl+Qz±Kfs±Bt) and then it intruded into more brittle pyroxene gneiss (fig. 1a). A pegmatite dike, up to 20 cm thick, shows simple symmetric zoning and mineral assemblages from (i) a narrow contact unit (Pl+Prh+Ttn), through (ii) a granitic unit with amphibole (AM3) + tourmaline (TU1) locally mutually intergrown, to (iii) a coarse-grained unit with amphibole (AM4), and (iv) a central part with graphic intergrowths of tourmaline (TU2) + quartz, up to 5 cm wide (fig. 1b). Accessory allanite-epidote, titanite, apatite, zircon, pyrite and rare stibarsen, arsenopyrite, sphalerite, magnetite and native Bi and As are present in almost all units. Pegmatitic metatects from amphibolite (with metamorphic amphibole AM1) contain common grains of amphibole (AM2; Fig. 2a, b).

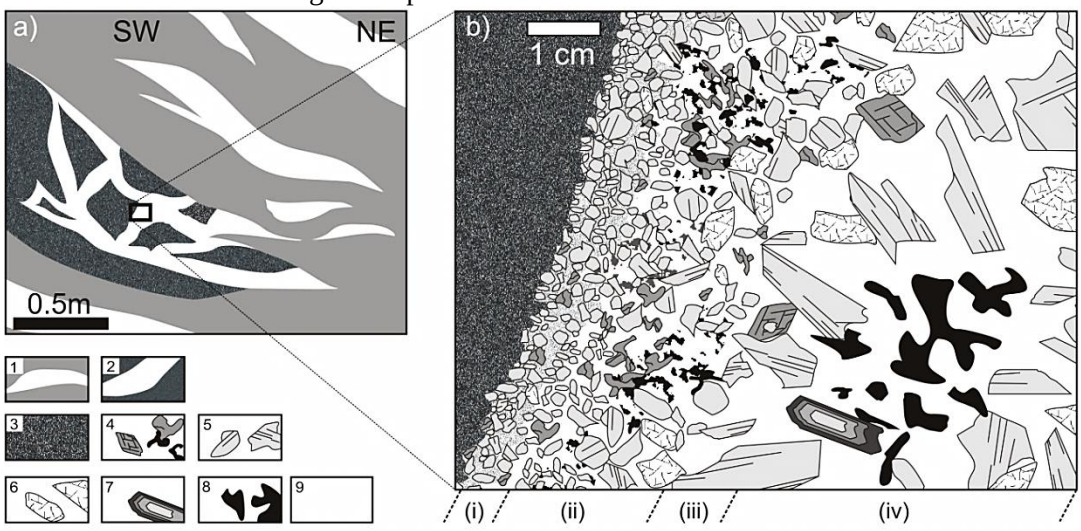

Fig. 1: Schematic relations of pyroxene gneiss, pegmatite and migmatized amphibolite (a); section through half of pegmatite from pyroxene gneiss (b). 1 – migmatized amphibolite with leucosome; 2 – pyroxene gneiss with pegmatites; 3 – pyroxene gneiss; 4 – amphibole AM3 (grey anhedral) and AM4 (grey euhedral) with tourmaline TU1 (black); 5 – plagioclase; 6 – K-feldspar; 7 – allanite-epidote; 8 – tourmaline TU2 (black); 9 – quartz; (i)-(iv) – individual pegmatite units.

The compositional evolution of amphiboles show: magnesio-hornblende (AM1) in amphibolite → edenite to pargasite (AM2) in pegmatitic leucosome → ferro-edenite (AM3) → ferro-pargasite (AM4) the latter two from pegmatite cutting pyroxene gneiss (fig. 2a). Increases of Na, K, Ti (fig. 2b), Mn and Cl (fig. 2c) in the same way are typical. Both tourmaline-group minerals TU1 and TU2 are sector- to patchy-zoned and contain rare thin veinlets of tourmaline TU3. They show compositional evolution: Ca-rich schorl to Na-rich feruvite (TU1) → schorl/feruvite with Fe^{2+}/Fe_{tot}^{+} = 0.63 (TU2) → Ca-rich dravite/schorl (TU3) (fig. 2d,e,f).

Compositional evolution of amphibole along with the field observations indicate anatectic origin of pegmatitic melt from migmatized amphibolite. The gradual decrease of Mg/Fe and increased contents of K, Na and Mn in amphiboles are most likely related to fractionation of the pegmatite

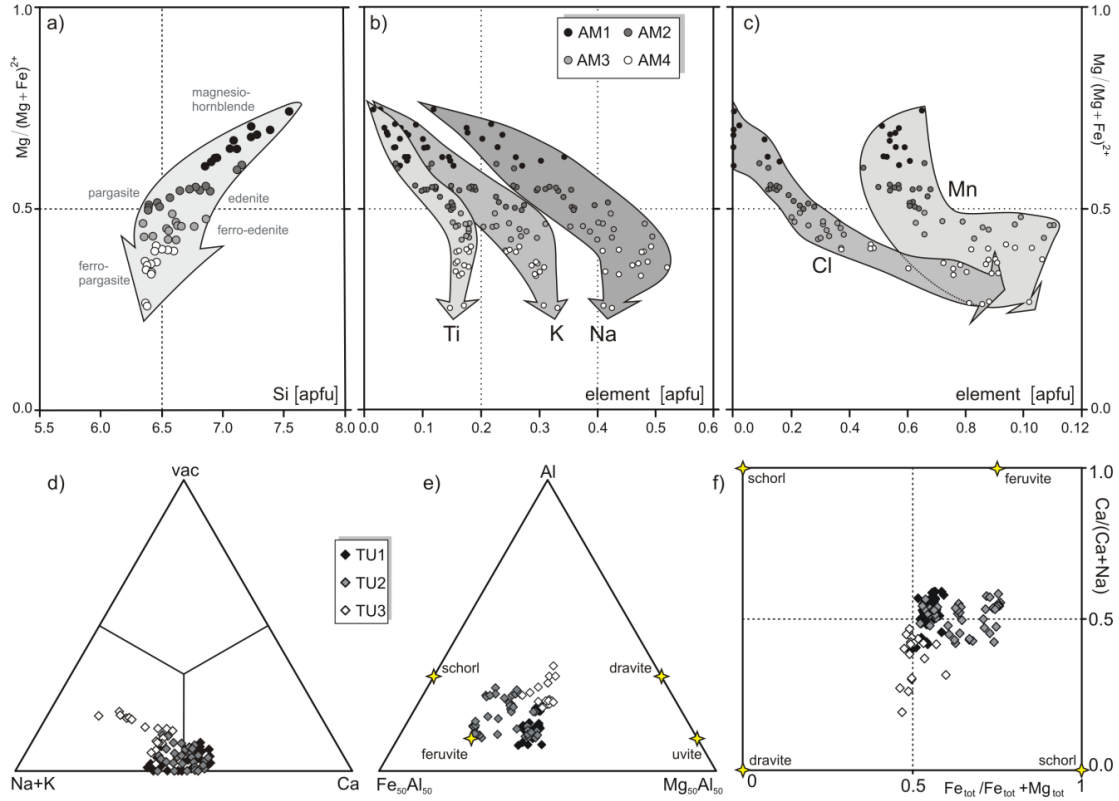

Fig. 2: Amphibole (a,b,c) and tourmaline-group minerals (d,e,f) plots. The evolution of contents of Si (a), Ti, K, Na (b) and Cl, Mn (c) from AM1 to AM4 as ratios of X_{Mg}/element (*apfu*); the evolution of chemical composition of tourmaline-group minerals in X-site (d), as ratio of Fe-Al-Mg (e), and the ratio of X_{Ca}/X_{Fe} (f). End-members of related tourmaline-group minerals are shown as yellow stars (e,

melt, whereas apparent Ca-enrichment of tourmaline-group minerals indicates contamination from the host pyroxene gneiss. Elevated contents of Cl in amphibole (≤ 0.09 *apfu* , ≤0.34 wt.% Cl in AM4) are in contrast with Cl-poor and K-rich amphiboles from contaminated pegmatites in Vlastějovice (Žáček 2007, Novák *et al.* 2013). In the granitic unit, the assemblage of TU1+AM3 may achieve equilibrium in high activities of Ca, B and Al whereas in the central parts increasing activity of Fe and namely B produced the assemblage TU2+Qz. Re-opening of the pegmatite system in subsolidus is documented by late veinlets of Mg-enriched tourmaline TU3.

The amphibole±tourmaline-bearing pegmatites from Mirošov represent a specific example of an anatectic pegmatite where the protolith is a strongly migmatized amphibolite with numerous, small concordant anatectic pegmatite bodies (Pl+Qz+Amf+Kfs). Part of the more evolved metatectic melt intruded the adjacent pyroxene gneiss and the melt was subsequently contaminated mainly during subsolidus (TU3).

This work was supported by the research project GAP210/10/0743 to PG, MN and JF

References

Morgan, G.B., VI, D. London (1987): Alteration of amphibolitic wallrocks around the Tanco rare-element pegmatite, Bernic Lake, Manitoba. American Mineralogist, vol. 72, 1097-1121.

Novák, M., T. Kadlec, P. Gadas (2013): Geological position, mineral assemblages and contamination of granitic pegmatites in the Moldanubian Zone, Czech Republic; examples from the Vlastějovice region. Journal of Geosciences, vol. 58 (in print).

Žáček, V. (2007): Potassian hastingsite and potassichastingsite from garnet - hedenbergite skarn at Vlastějovice, Czech Republic. Neues Jahrbuch für Mineralogie Abh., vol. 184, 161–168

REGIONAL ZONING IN A LCT (LI, CS, TA) GRANITE-PEGMATITE SYSTEM IN THE EASTERN PAMPEAN RANGES OF SAN LUIS, ARGENTINA

M. Galliski[1]
IANIGLA-CCT MENDOZA-CONICET, galliski@mendoza-conicet.gov.ar

Introduction

The regional zoning of granitic pegmatite types is well established and there is a general scheme of spatial variation in relation with the parental granites (Heinrich 1953, Černý 1992). However, in some cases, there occur local variations that deviate from the ordinary. Oyarzábal *et al.* (2009) described the regional zoning of the Totoral Pegmatite Field (TPD) in the southern part of the Eastern Pampean ranges of San Luis and demonstrated the parental relationships between leucogranites and pegmatites. This contribution explores the possible interpretation of the anomalies in the regional distribution of the pegmatites, and their links with granites and tungsten-bearing aplites.

Geological Setting of the Totoral Pegmatite Field

The TPF is located in a block of basement formed by the Pringles Metamorphic Complex (PMC), intruded by the Pampa del Tamboreo tonalite (PT), and the Cerro La Torre (LT), and Paso del Rey (PR) leucogranites. In a distance of ~18 km, the metamorphism of the thick and strongly folded, mostly psammopelitic sequence of PMC grades from granulite facies in the contact with a belt of small mafic-ultramafic intrusives in the west, to amphibolite and greenschist facies eastward. The main lithologies comprise migmatites, gneisses, micaschists, phyllites and slates arranged in NNE-SSW trending belts that include bands of mylonites preferably present in the high grade rocks.The migmatites, showing evidence of *in situ* melting, occur in the west side of the PMC, while the granites and pegmatites are emplaced in the micaschistbelt. The protolith of the PMC is a clastic sequence deposited in the western border of Gondwana during the Lower Paleozoic, and the age of the metamorphism varies between 484±7 Ma and 460 Ma (*Cf.* Sims *et al.* 1998, Steenken *et al.* 2011 and references therein). The PT is an elliptic, small I-type intrusive of tonalitic composition that is located to the south of the granites and was dated at 470± 5 Ma (Sims *et al.* 1998). The TPD is composed of two small stocks and a swarm of granitic sills, dykes, pegmatites, and aplites developed asymmetrically in the eastern flank of the leucogranites. The granite and pegmatite swarms show evidence of having crystallized under a protracted compressive tectonic regime during the collisional Famatinian orogeny (500-440 Ma).

The Parent Leucogranites

The LT leucogranite is a small intrusive, built up by a few hundreds of lenses and sills that include inliers of metamorphics and have a few different petrographic variations.The LT intrusion produced a partial metamorphic overprint in the micaschist, which develops nodules of cordierite or muscovite -locally fibrolite- and widespread tourmalinization. The two common petrographic types are a fine-grained and a pegmatitic-grained rock; both are composed of Qtz+Kfs+Pl+Ms±Gr±Tur±Ap but the former is dominantly monzogranitic while the latter is more potassic. They are high silica granites (~75% SiO_2), strongly peraluminous (ASI = 1.11-1.23), K/Rb (WRA) 431-181, Zr/Hf 23-30, that give low zircon saturation temperatures (641-726º C). The PR is the southernmost, larger stock, of general ovoidal geometry with the main axis oriented N-S, and formed by irregular outcrops composed by three different facies. The main rock is a medium-grained monzogranite composed of Qtz+Kfs+Pl+Ms-Bt±Tur±Gr±Ap±Zr±(Sill),that southward grades to more Kfs-rich variations with irregular pegmatitic segregations. Eastward of these facies and separated by a metamorphic septa, outcrop thick lenses of pegmatitic leucogranites with decimetric Kfs crystals in a matrix of granitic composition. The main facies shows high silica content (73-75 wt.%), is strongly peraluminous (ASI =1.16-1.30), and more evolved than LT, with K/Rb mostly in the range 194-166, Zr/Hf 25-35. The zircon saturation temperatures give values comprised between 667 and 714º C. In between the LT and the PR granites there is a brachyanticline, elongated NE-SW and known as Loma Alta (LA), that show increment in the metamorphic grade, outcrops of sills and lenses of granite, and an associated group of pegmatites.

The pegmatites

Oyarzábal *et al.* (2009) showed that the bodies grouped in the eastern side of LT leucogranite develop a regional zoning with beryl-columbite-phosphate subtype pegmatites with beusite-lithiophilite assemblages near the granite that passes to the east to albite-type pegmatites very near to the transition from

micaschists to phyllites. In a similar way, to the southeast of the LA brachyanticlinal the pegmatites pass from barren dykes close to or included in lenses of leucogranite, to beryl-columbite-phosphate subtypes with predominance of graftonite-triphylite.The pegmatites associated with the PR leucogranite are of albite-spodumene type and spodumene subtype and outcrop at distances of 200-300 m from the lenses of pegmatitic granites. The age of these pegmatites is the same of the granite. They are along a strip subparalell to the granite that have discontinuous outcrops of long and thin folded dykes; eastward of this belt, there are a few albite-rich pegmatites, some with Ta-mineralization, abundant muscovite units and scarce beryl. Farther away, eastward of the three groups, occur 0.15 to 2 m wide and hundreds of meters long, sheared aplite dykes with scheelite mineralization. A few of these dykes show albite-quartz with pegmatitic textures that sharply pass to very fine grained rocks with textural evidences of pressure-quenching. The distance from the granites to the outer mineralization is approximately 2000 m.

Discussion

The regional zoning of the LT and LA groups is normal compared with other worldwide LCT pegmatite groups, except that the different types of Li-bearing pegmatites are absent, though this fact could be due to erosion. The zoning around the PR leucogranite only shows the more evolved Li-bearing pegmatites and albite-rich pegmatites transitional to aplitic dykes. The most primitive pegmatite types are missing without evidences of structural discontinuities.

One possible explanation arises from the subtle geochemical differences between the LT and PR leucogranites. Although the zircon thermometry suggests that both intrusives are of low temperature, the contents of Ba and Pb, recently proposed as a discrimination tool between low-T and higher-T, S-types granites (Finger and Schiller 2012), show that the PR leucogranite is a higher-T intrusive meanwhile LT is a low-T one. This difference suggests that the LT granite was formed by a low degree of fluid-absent muscovite melting of the pelitic protolith. On the contrary, the PR granite would be originated from a larger partial melting of similar protoliths since the melts plot in the field of high-T, S-type granites and this characteristic could have some implications in the Li-bearing parental swarm of pegmatites. It is suggested that the tungsten-bearing mineralization is related to Na-rich, volatile enriched residual pegmatitic melts, genetically linked with the leucogranites that crystallized in brittle host-rocks under periodical opening of the system.

Acknowledgements The author is grateful to W. Simmons and A. Falster for their comments.

References

Černý, P. (1992): Regional zoning of pegmatite populations and its interpretation. Mitt.Österr. Min. Ges. 137, 99-107.

Finger, F. and Schiller, D. (2012): Lead contents of S-type granites and their petrogenetic significance. Contrib. Mineral. Petrol. 164: 747-755.

Heinrich, E. Wm. (1953): Zoning in pegmatite districts. Am. Mineral. 38, 68-87.

Oyarzábal, J. C., Galliski, M. A. and Perino, E. (2009): Geochemistry of K-feldspar and muscovite in rare-element pegmatites and granites from the Totoral pegmatite field, San Luis, Argentina. Resource Geology, 59 (4): 315-329.

Sims, J.P., Skinner, R.G., Stuart-Smith, P.G. and Lyons, P. (1997): Geology and metallogeny of the Sierras de San Luis y Comechingones 1:250.000 mapa sheet. Provinces of San Luis and Córdoba. Anales XVIII, Instituto de Geología y Recursos minerales, SEGEMAR, Buenos Aires.

Steenken, A., López de Luchi, M., MartínezDopico, C.,Drobe, M., Wemmer, K. and Siegesmund, S. (2011): The Neoproterozoic-early Paleozoic metamorphic and magmatic evolution of the Eastern Sierras Pampeanas: an overview. Int. J. Earth Sci 100: 465-488.

THE COMPLEX NB-TA-TI-SN OXIDE MINERAL INTERGROWTHS IN THE LA CALANDRIA PEGMATITE, CAÑADA DEL PUERTO, CÓRDOBA, ARGENTINA

M. Galliski[1], M. F. Márquez-Zavalía[1], P. Černý[2], R. Lira[3], K. Ferreira[2]
[1]IANIGLA, CCT-Mendoza CONICET, Av. Ruiz Leal s/n, Parque Gral. San Martín; C.C.330 (5.500) Mendoza, Argentina
galliski@mendoza-conicet.gov.ar
[2]Department of Geological Sciences, University of Manitoba,Winnipeg, Manitoba R3T 2N2, Canada
[3]CICTERRA-CONICET, Museo de Mineralogía y Geología "Dr. A. Stelzner", F.C.E.F y N. Universidad Nacional de Córdoba.

Introduction

The origin of accessory minerals in granitic pegmatites, especially those that concentrate high-field-strength elements (W, Zr, Nb, Ta, Ti, Sn, Hf, Th, U), is occasionally multi-episodic under variable physico-chemical conditions. In this paper we describe an assemblage of "*ixiolite*", tantalian rutile, wodginite-group and columbite-group minerals, cassiterite and pyrochlore-supergroup minerals that occurs in a rare-element granitic pegmatite of the beryl-columbite-phosphate subtype in the Eastern Pampean Ranges, Argentina.

Geological Setting of the Parent PegmatiteS

The studied paragenesis is found in the La Calandria pegmatites, located on the western slope of the Sierra Grande de Córdoba at Cañada del Puerto, central Argentina. The pegmatite dikes are mostly emplaced in biotite-muscovite mylonitic gneisses ("augen gneiss"), and subordinate metaquartzites and calc-silicate layers. Locally, these dikes also crosscut lens-shaped bodies of gabbro. These dikes outcrop intermittently over a distance of ~ 250 m. Thicknesses vary in each pegmatite and along strike from 0.2 to 1.5 m. Pegmatites are well zoned and symmetrical. The contact with the countryrock is sharp and easily traced, followed by a border zone 1-2 cm thick, mostly composed of albite with subordinate quartz grains (~1 cm). The border zone grades into another coarser-grained zone (2-2.5 cm) made of quartz, K-feldspar, albite and some muscovite which extends about 3 cm inwards. Zonation continues with coarser grain sizes, including 1 to 3cm-sized topaz crystals (frequently andpartially replaced by 2*M*1 yellowish green muscovite) grading into a zone rich in K-feldspar and quartz where cm-sized nodules of triplite, some rounded grains of pyrochlore-supergroup minerals, and 1-2 cm aggregates of dark Nb-Ta oxides are found. In some sectors, a quartzcore is developed.The largest mining pit (~5 m deep, up to 4m wide) was excavated at the southernmost outcrop on a 1 m thick pegmatite dike. This part of the pegmatite is intruded into a dark bluish-gray, medium-sized gabbro body. The pegmatite zoning starts with a border zone ~1 cm thick composed of Qtz-Pl-Ms, followed inwards by Qtz-Pl-Kfs. Other mineral species found in this pit are rare biotite, topaz, triplite, Nb-Ta-Ti oxide minerals (up to 1cm sized crystals, partially altered), and pyrochlore-supergroup minerals.

Mineralogy of the Oxide Mineral Intergrowths

The oxide mineral intergrowths are composed of a very intricate and complex association of more than one generation of "*ixiolite*", wodginite-group minerals, tantalian rutile, columbite-group minerals, cassiterite, and pyrochlore-supergroup minerals.

Ixiolite-wodginite-group minerals: These minerals occur in three principal forms: (i) as mm-sized irregular grains with abundant exsolutions of tantalian rutile and secondary fluorcalciomicrolite, (ii) as fine exsolutions regularly dispersed in grains of tantalian rutile, and (iii) as very thin rims that form the interphase between major grains of tantalian rutile and ixiolite-wodginite of another generation.

The chemical composition of these phases is variable, but in most of the grains there is a slight predominance of Nb over Ta and a clearly defined predominance of Fe over Mn; the composition in terms of Mn#-Ta# is outside the ixiolite field of Černý & Ercit (1989) and in a gap in the titanianixiolite – titanian columbite from selected worldwide occurrences (Černý *et al.* 1998). Titanium is abundant with maximum and [average] contents of 13.67 [6.02] TiO_2 wt.%, tungsten values are 3.66 [1.84] wt.% WO_3, whereas SnO_2shows 7.82 [2.79] wt%, and ZrO_2 1.59 [0.46] wt.%. The contents of Ti and Sn in the most enriched samples are in excess of those from other worldwide occurrences of titanianixiolite studied by Černý *et al.* (1998), but in the same range that some of the compositions given by Beurlen *et al.* (2007) for ixiolites from the Borborema pegmatite province. The sum of these elements, when the data are plotted in the $Mn + Fe_t - Nb + Ta - Ti + Sn + Zr$

diagram, shows a field that encompasses the fields of columbite-, wodginite-group minerals and, to a degree, of ixiolite, mostly along the line 2:1, but outside from the domains of ixiolite from the Borborema pegmatite province (Beurlen *et al.* 2007).

Tantalian rutile: It is present as mm-sized grains irregularly associated with ixiolite-wodginite-group minerals or as anhedral inclusions in these minerals. The largest grains locally contain irregular exsolutions of ixiolite or infrequent exsolutions of cassiterite or wodginite. This last phase usually shows frequent patchy zoning in the largest grains and also in the exsolutions, which occasionally show very thin rims of titanowodginite or ixiolite. Less frequently, especially when some crystals grow on the border of the ore mineral aggregates in contact with quartz, oscillatory compositional zoning is present. Titanium contents are high with a maximum of 61.67 wt.% TiO_2. Ta_2O_5 is also high at 44.97 [36.45] wt.%, whereas Nb_2O_5 is lower at 22.17 [10.25] wt.%. Iron, dominantly as Fe_2O_3, is also a major oxide at 11.61 [7.09] wt.% Fe_2O_3 and 7.55 [4.65] wt.% FeO. Tin is also a main element, peaking at 8.84 [2.16%] wt% SnO_2. Tungsten contents are invariably low, up to 0.56 wt.% WO_3[0.26%].

Columbite-group minerals: Columbite-(Mn) is present in a single grain sampled in the inner part of the pegmatite, with chemical compositions very depleted in Fe and with low contents of W, Ti and Sn. However, in the periphery of the grain, these elements gradually increase and plot in the domain of ixiolite or titanowodginite.

*Cassiterite:*This mineral was only detected as ≤ 100 μm irregular exsolutions in tantalian rutile, close to the contact with a grain of a possible wodginite-group mineral.The cassiterite exsolutions have variable compositions with SnO_2 up to >90 wt.% and 5 wt.% Fe_2O_3. Other exsolutions, with compositions of titanowodginite and ferrotitanowodginite, coexist with the cassiterite exsolutions in tantalian rutile.

Conclusions

The minerals present in the examined assemblage are not in equilibrium and comprise magmatic and subsolidus phases distinguished texturally and chemically. The primary, magmatic stage of mineralization possibly crystallized ixiolite I + tantalian rutile I in the outer zones of the pegmatite and, less frequently, local columbite-Mn in the inner part. Subsolidus unmixing of ixiolite I produced wodginite-group minerals I + tantalian rutile II. Contemporaneously, tantalian rutile I locally exsolved wodginite-group mineral II + cassiterite. Localized Ca- F-rich hydrothermal overprint transformed tantalian rutile I to tantalian rutile III + ixiolite II + fluorcalciomicrolite. Besides, the hydrothermal overprint produced peripheral transformation of columbite-(Mn) to ixiolite III and widespread distribution of fluorcalciomicrolite throughout the polygranular assemblage.

Acknowledgements: The authors are grateful to A. Falster for the comments.

References

Beurlen, H., Barreto, S. B., Silva, D., Wirth R. & Olivier P. (2007): Titanianixiolite - niobian rutile intergrowths from the Borborema Pegmatite Province, Northeastern Brazil. Can. Mineral. 45, 1367–1387.

Černý, P., &Ercit, T.S. (1989): Mineralogy of niobium and tantalum: crystal chemical relationships, paragenetic aspects and their economic implications. *In* Lanthanides, Tantalum and Niobium (P. Möller, P. Černý, & F. Saupé,eds.). *Springer-Verlag*, Berlin, 27-79.

Černý, P., Ercit, T. S., Wise, M. A., Chapman, R. & Buck, H. M.(1998): Compositional, structural and phase relationships in titanianixiolite and titanian columbite-tantalite. Can. Mineral. 36, 547–561.

GRANITIC PEGMATITES IN THE YUKON, NORTHWEST TERRITORIES AND BRITISH COLUMBIA, CANADA

L. Groat, J. Cempirek, A. Dixon
Department of Earth, Ocean and Atmospheric Sciences, University of British Columbia, Vancouver, BC V6T 1Z4, Canada, groat@mail.ubc.ca

Until recently not much has been known about pegmatites in Canada's northern territories and the more isolated parts of mountainous British Columbia. However improved access over the last two decades has led to a number of discoveries and an increasing amount of scientific research.

The Little Nahanni Pegmatite Group (LNPG) was discovered in 1960 along the border between the Yukon and Northwest Territories, has been the most studied (Groat *et al.* 1994, 2003; Mauthner 1996). The Group consists of a swarm of subvertically dipping, cm- to meter scale LCT- type pegmatites extending over a 15 km strike length. The dikes intrude siliciclastic and calcareous units of the Precambrian to Lower Cambrian Yusezyu and Narchilla formations. Varying degrees of albitization and phyllic alteration of the dikes are associated with ore-grade Ta-Nb and Sn-W mineralization. Most recently Barnes *et al.* (2012) studied the lithium isotope signature of the pegmatites, and Burns *et al.* (2013) presented preliminary results on a fluid inclusion study.

Gordey and Anderson (1993) were the first to described pegmatites within the hornblende-bearing, composite O'Grady batholith, approximately 100 km north of Tungsten in the western Northwest Territories. Since 2006 the pegmatites have produced small amounts of gem tourmaline. Ercit *et al.* (2003) showed that the pegmatites belong to the elbaite subtype of rare-element granitic pegmatite. In 2008 a new pegmatite field was discovered south of the batholith; these have not yet been mapped or sampled.

The Rau pegmatite field was discovered *ca.* 2006 approximately 100 km northeast of Mayo in the Yukon Territory. The pegmatites are hosted by carbonate rocks of the Devonian Bouvette Formation and are close to the 63 Ma Rackla pluton, which is primarily a coarse-grained biotite-muscovite granite with aplitic phases near the margins. The pegmatite field lies between the Rackla pluton and the carbonate-hosted disseminated Au-Ag Rau (Tiger) deposit approximately 1.7 km west of the pluton. Both the pegmatites and the Rau deposit are probably related to the pluton.

The majority of pegmatites occur in two groups. The first group is approximately 0.5 km northwest of the closest exposure of the Rackla pluton and consists of two subparallel and subhorizontal dikes. Dike 1 is approximately 10 m long and 0.1-0.5 m wide. Strike is 133º and dip is shallow (approximately 15º) to the west. Dike 2, approximately 6 m southwest of Dike 1, can be traced for about 14 m and is 0.1-0.5 m wide. The strike is 140º and the dip is approximately 15º to the west. Both appear concordant to bedding.

The second group, located approximately 0.7 km west of the closest exposure of the Rackla pluton and 0.3 km southwest of the first group, consists of at least seven dikes 0.15-1 m wide that can be traced for up to 60 m. Strikes range from 80-168º and dips from subvertical to 48º to the west. Most appear concordant to bedding.

Dike 1 of the first group appears to be the most evolved pegmatite dike in the field. It is hosted in dolomite-rich limestone and its exocontact contains common F-rich tremolite, fluoborite, norbergite, Rb-bearing fluorphlogopite, F-rich talc, pyrite, chalcopyrite, arsenopyrite, calcite, and rare dolomite. The pegmatite border zone contains common uvitic tourmaline, F-rich tremolite, F,Rb-rich phologopite and fluorite. The wall and intermediate zones are characterized by common F-rich schorl, muscovite, apatite, and rare beryl. The center part of the dike contains common amazonite, albite, pink and blue tourmaline, muscovite, siderite and fluorite. Primary accessory minerals enclosed in the albite include common U,Th-rich zircon (Zr/Hf ~ 15-18, locally up to 1.7), thorite, monazite and columbite-group minerals. Secondary Ta,Nb-oxide minerals, scheelite and uraninite are common, and rare calcioancylite-(Ce) after monazite was found.

Columbite-group minerals (CGM) show a primary compositional trend from manganocolumbite to manganotantalite with Mn/(Fe+Mn) ~ 0.95, Ta/(Nb+Ta) between 0.05 and 0.5, and minor (FeTa) → (ScTi) substitution. Secondary CGM show dissolution-reprecipitation textures and significant iron enrichment resulting in Mn/(Fe+Mn) ~ 0.2; Ta/(Nb+Ta) ratios and Sc,Ti contents are similar to the primary CGM.

Secondary CGM are accompanied by F-dominant microlite, scheelite, and by rare Ta,Nb-rich cassiterite, wodginite and Sc,W,Ti-rich ixiolite/wodginite.

Tourmaline-group minerals exhibit extreme variability from Ca-rich dravite and uvite in the border zone to schorl-foitite in the wall and intermediate zones to zoned crystals with fluor-schorl and fluor-elbaite composition rimmed by fluor-dravite and dravite in the pegmatite core.

The Rau I pegmatite is an example of *in situ* pegmatite contamination. Formation of a B,F-rich exocontact skarn zone and high contents of Ca, Mg, carbonates and sulfides result from the interchange of mass and fluids between the cooling pegmatite body and the dolomite host rock.

The pegmatites at Mt. Begbie, approximately 12 km south Revelstoke in British Columbia, have been known since the late 1880s but are only now being studied. At least 55 pegmatite dikes and bodies occur over an area of 0.5 km^2 within metapelites. The orientation of the dikes appears to be controlled by faulting. The pegmatites commonly contain black tourmaline, garnet, biotite, muscovite, rose quartz; some of the pegmatites contain blue-green beryl, multi-colored tourmaline, Fe-Mn phosphates, columbite, chrysoberyl, secondary Be-minerals, cordierite-sekaninaite, andalusite, secondary U-minerals, and two contain lepidolite. The more highly evolved pegmatites are often only meters away from dikes with more primitive mineralogy, and a general fractionation trend has not yet been defined.

References

Barnes, E.M., Weis, D., Groat, L.A. (2012): Significant Li isotope fractionation in geochemically evolved rare element-bearing pegmatites from the Little Nahanni Pegmatite Group, NWT, Canada. Lithos, vol. 132-133, 21-36.

Burns, M.G.G., Kontak, D.J., McDonald, A., Groat, L.A., Kyser,T.K. (2013): Implications of stable isotopes ($\delta^{18}O$, δD, $\delta^{13}C$) for magma and fluid sources in an LCT pegmatite swarm in the NWT, Canada: Evidence for involvement of multiple fluid reservoirs. Geological Association of Canada/Mineralogical Association of Canada Program with Abstracts.

Ercit, T.S., Groat, L.A., Gault, R.A. (2003): Granitic pegmatites of the O'Grady batholith, N.W.T., Canada: A case study of the evolution of the elbaite subtype of rare-element granitic pegmatite. Canadian Mineralogist, vol. 41, 117-137.

Gordey, S.P., Anderson, R.G. (1993): Evolution of the northern Cordilleran miogeocline, Nahanni map area (105I), Yukon and Northwest Territories. Indian and Northern Affairs Canada, NWT geological Mapping Division, Open File EGS 1995-10.

Groat, L.A., Ercit, T.S., Raudsepp, M., Mauthner, M.H.F. (1994): Geology and mineralogy of the Little Nahanni Pegmatite Group, part of NTS area 105 I/02. Economic Geology Survey Open File 1994-14. DIAND, NWT.

Groat, L.A., Mulja, T., Mauthner, M.H.F., Ercit, T.S., Raudsepp, M., Gault, R.A., Rollo, H.A. (2003): Geology and mineralogy of the Little Nahanni rare-element granitic pegmatites, Northwest Territories. Canadian Mineralogist vol. 41, 139-160.

Mauthner, M.H.F., 1996. Mineralogy, geochemistry and geochronology of the LittleNahanni Pegmatite Group, Logan Mountains, southwestern Northwest Territories. M.Sc. thesis, University of British Columbia, Vancouver, British Columbia.

LCT AND NYF PEGMATITES IN THE CENTRAL ALPS. EXHUMATION HISTORY OF THE ALPINE NAPPE STACK IN THE LEPONTINE DOME

A. Guastoni[1], G. Pennacchioni[2],
[1]Museum of Mineralogy, University of Padova, Via Matteotti 30, I-35100, Padova, Italy
alessandro.guastoni@unipd.it
[2] Department of Geosciences, University of Padova, Via Gradenigo 6, I-35131 Padova, Italy

Summary

A major (a few km wide and more than 90 km long) pegmatitic field occurs in the Alpine nappe pile of the central-western Alps just north of the Insubric Line. It hosts widespread dikes of leucocratic dikes, ranging from pegmatite to aplite, with only a minor part (less than 5%) of pegmatites showing a more complex texture, and geochemical enrichments in LILE, HFSE or REE. These pegmatites intrude or cross-cut the Alpine Lepontine nappe boundaries along the Southern Steep Belt (SSB), near the contact with the Insubric Line, as well as the tonalities and granodiorites of the Oligocence Masino-Bregaglia and the slightly younger two mica granite of the San Fedelino stock (fig. 1).

A series of 11 pegmatites were selected for mineralogical, geochemical, and textural analysis. Crystal-chemistry studies were performed on accessory minerals including Nb-Ta-Y-REE oxides, tourmaline and phosphates. Major and trace elements geochemistry of pegmatite bulk rock, rock-forming and accessory minerals (on the basis of several proxies as Al/Ga; K/Rb; K/Ba; K/Cs; Nb/Ta; Ba/Rb; Rb/Sr; Y/Ce; LREE/HREE; Zr/Hf) allowed the distinction of different pegmatite populations ranging from NYF (niobium yttrium, fluorine), to LCT (lithium, cesium, tantalum) pegmatites or mixed LCT-NYF signatures. Actually, LCT pegmatites of the Central Alps do not reach a high degree of geochemical evolution. The most evolved pegmatites of the Codera valley and are characterized by a mineralogy consisting of elbaite, Mn-phosphates, pink-beryl and Cs-rich feldspars. In the Vigezzo valley, NYF and LCT populations are hosted within leucocratic orthogneiss belonging to Pioda di Crana and Camughera-Moncucco units and to ultramafic rocks of Antrona-Zermatt Sass units. In this latter case the pegmatites show incipient albitization. In the Mesolcina valley, LCT and mixed LCT-NYF miarolitic pegmatites cross cut amphibolites and migmatitic gneiss. In the Codera valley LCT and NYF pegmatites are respectively hosted in tonalites and granodiorites.

Macrostructural and microstructural characters indicate notable differences between syngenetic dikes hosted within the Masino-Bregaglia intrusion and the epigenetic pegmatites hosted in the Southern Steep Belt. In the former case, the pegmatites intruded the host rock during relatively high ambient temperatures (> 450 °C), and have been involved in crystal-plastic deformation with pervasive recrystallization of quartz. These pegmatites have lobate, anastomized margins, and develop minor aplite apophyses which depart from the main pegmatite body. Epigenetic pegmatites within SSB intruded into a cooler host rock. These pegmatites have straight margins, crosscut the metamorphic foliation and do not show any overprinting ductile deformation. Albitized pegmatites of Pizzo Marcio-Alpe Rosso underwent changes triggered by metamorphic reactions with ultramafic enclosing rocks by intensive circulation of supercritical fluids and successive K-Na metasomatic replacements (Guastoni *et al.*, 2008). The Emerald Pizzo Marcio dike has pinch and swell structures but the core of the pegmatite is unaffected by albitization and still shows graphic quartz-feldspar textures. The Colonnello pegmatite (Pizzo Paglia) has straight contacts against the host migmatitic rocks; it includes large miarolitic pockets.

Structural data of syngenetic aplites and pegmatites intruded into the Masino Bregaglia pluton and San Fedelino stock indicate these dikes intruded at least 32 to 25 Ma (Hansmann, 1996; Liati *et al.*, 2000; Oberli *et al.*, 2004). Age determinations of epigenetic aplites, pegmatites and porphyritic dikes of the Central Alps have defined an interval range of age for emplacement and crystallization of pegmatites from 32 to 24.1 m.y (Romer *et al.* 1996; Gebauer 1999; Guastoni and Mazzoli 2007).

Are NYF and LCT epigenetic pegmatites related to magmatic sources?

LCT pegmatites studied contain beryl and Be-bearing minerals, whereas NYF pegmatites have enrichments of niobium- tantalum- yttrium- rare-

earths-uranium oxides, phosphates and silicate minerals. The lack of granitoid bodies or dikes outcropping close to the pegmatites and the relative distance of LCT-NYF pegmatites from the Masino-Bregaglia or the San Fedelino intrusive suites suggest the presence of buried satellite granitic bodies similar to the San Fedelino granitic dikes, which intrude the Gruf Complex near the Masino-Bregaglia and the Chiavenna ophiolites in the Chiavenna valley (Ciancaleoni and Marquer, 2006).

How far liquid melts can travel through the crust depends on several factors such as rheology of the crust, temperatures of the host rocks and the physical-chemical characters of pegmatite melts. The transfer of heat in the continental crust, however, is largely by the slow processes of conduction, so the deep parts of the crust are slow to heat up and slow to cool down. Consequently, metamorphic temperatures can remain above solidus (650°C) for long times, like the Lepontine dome which reached its peak temperatures (at 650°C near Bellinzona area) in the SSB at about 32 Ma (Gebauer, 1999).

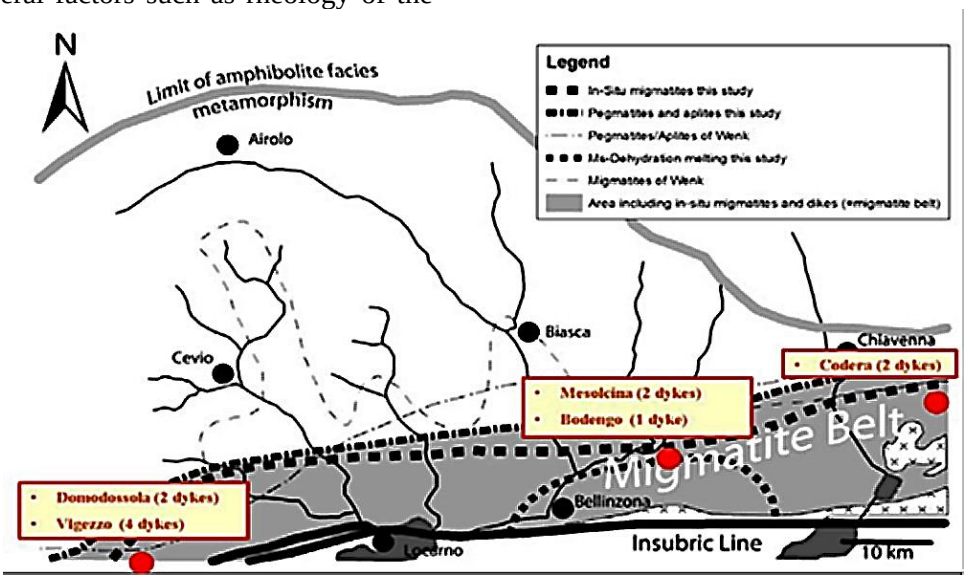

Fig.1: Location of the pegmatite dikes within the migmatite belt and the Masino-Bregaglia intrusion.

References

Ciancaleoni, L. Marquer, D. (2006): Syn-extension leucogranite deformation during convergence in the Eastern Central Alps: example of the Novate intrusion. Terra Nova, vol. 18, 170-180.

Gebauer, D. (1999): Alpine geochronology of the central and Western Alps: new constraints for a complex geodynamic evolution. Schweizerische Mineralogische und Petrographische Mitteilungen, vol. 79, 191-208.

Guastoni, A. (2012): LCT (lithium, cesium, tantalum) and NYF (niobium, yttrium, fluorine) pegmatites in the Central Alps, Proxies of exhumation history of the Alpine nappe stack in the Lepontine dome. Ph.D. thesis, XXIV cycle, Department of Geoscience, University of Padova, 162 pp.

Guastoni, A., Diella, V. Pezzotta, F. (2008): Vigezzite and associated oxides of Nb–Ta from emerald-bearing pegmatites of the Vigezzo valley, Western Alps, Italy. Canadian Mineralogist, vol. 46, 619-633.

Guastoni, A. Mazzoli, C. (2007): Age determination by µ-PIXE analysis of cheralite-(Ce) from emerald-bearing pegmatites of Vigezzo Valley (Western Alps, Italy). Mitteilungen der Österreichischen Mineralogischen Gesellschaft, vol. 153, 297-282.

Hansmann, W. (1996): Age determination on the Tertiary Masino-Bregaglia (Bergell) intrusives (Italy, Switzerland): a review. Schweizerische Mineralogische und Petrographische Mitteilungen, vol. 76, 421-451.

Liati, A., Gebauer, D. Fanning, M. (2000): U–Pb SHRIMP dating of zircon from the Novate granite (Bergell, Central Alps): evidence for Oligocene–Miocene magmatism, Jurassic/Cretaceous continental rifting and opening of the Valais trough. Schweizerische Mineralogische und Petrographische Mitteilungen, vol. 80, 305-316.

Oberli, F., Meier, M., Berger, A., Rosenberg, C.L. Gieré, R. (2004): U-Th-Pb and $^{230}Th/^{238}U$ disequilibrium isotope systematics: Precise accessory mineral chronology and melt evolution tracing in the Alpine Bergell intrusion. Geochimica et Cosmochimica Acta, vol. 68, 2543-2560.

Romer, R. L., Schärer, U. Steck, A. (1996): Alpine and pre-Alpin magmatism in the root-zone of the western Central Alps. Contribution to Mineralogy and Petrology, vol. 123, 138-158

MINERAL-CHEMISTRY OF NB-TA-Y-REE-U OXIDES IN THE PEGMATITES OF CENTRAL ALPS

A. Guastoni
[1]Museum of Mineralogy, University of Padova, Via Matteotti 30, I-35100, Padova, Italy
alessandro.guastoni@unipd.it

Introduction

A series of pegmatites of Alpine age that show geochemical enrichments in LILE, HFSE and REE outcrops from the Centovalli Line in the west, to the Oligocene Masino-Bregaglia intrusive massif to the east. Its geochemical signature ranges from NYF-rare elements-rare earths (REL-REE), to LCT- rare elements lithium (REL-Li) and -miarolitic lithium (Mi-Li), and to the family of mixed LCT-NYF (Guastoni 2012), according to the classification scheme of pegmatites proposed by Černý and Ercit (2005).

These pegmatites contain a number of Nb-Ta-Y-REE-U oxide minerals, including tantalite-columbite and tapiolite series, aeschynite, euxenite and wodginite group minerals. The distribution of these minerals is related with the geochemical population of syngenetic and epigenetic pegmatites distributed along in the granodioritic-tonalitic Masino-Bregaglia intrusion, and within the Alpine Lepontine nappe boundaries in the Southern Steep Belt (SSB), along the contact with the Insubric Line (Guastoni 2012; Guastoni and Pennacchioni 2013).

Mineral-chemistry of Nb-Ta-Y-REE-U oxides

At Grignaschi and Rio Graia dikes chemical analysis give Ta/(Ta+Nb) ratios in the tantalite-columbite series in the range of 42 to 57. At Rio Graia the core portion of the crystal is composed of columbite-(Fe) and the Ta/(Ta+Nb) ratio decreases to 0.42 whilst the rim is composed of tantalite-(Fe) and the Ta/(Ta+Nb) ratio increases to 0.57. Both have Mn/(Mn+Fe) ratio quite homogeneous, within the range of 0.21-0.24. Columbite-tantalites do not incorporate other elements except for SnO_2 up to 0.23 wt.% and UO_2 up to 0.10 wt.% in tantalites from Rio Graia. Tapiolite-(Fe) is invariably conspicuously enriched in Ta and Fe in comparison to tantalite. At both localities the chemical composition of tapiolite-(Fe) is almost identical with Ta/(Ta+Nb) and Mn/(Mn+Fe) values of 0.80 and 0.04 respectively.

At the Arvogno Albertini dike, aeschynite-(Y) versus polycrase-(Y) has strong HREE enrichment with Y+REE in the range of 0.70 to 0.84. Dysprosium oxide has the highest content in the range of 2.64 to 3.35 wt.%. U+Th is quite variable, ranging from 0.07 to 0.22. These minerals suffer the effects of metamictization due to the presence of significant amounts of uranium and thorium.

At Pizzo Marcio-Alpe Rosso the fersmites of the albitized pegmatites are rather homogeneous with Ta/(Ta+Nb) in the range of 0.15 to 0.19. Tantalum-rich fersmite is also present with Ta_2O_5 up to 43.04 wt% with Ta/(Ta+Nb) up to 0.38. This latter value possibly represents the highest Ta_2O_5 content of fersmite published in the literature. Fersmite does not incorporate other elements except for Ce with a content of Ce_2O_3 up to 0.32 wt%. The composition of vigezzite reveals chemical differences with respect to the chemical data from the holotype vigezzite reported by Graeser *et al.* (1979). In addition to high values of Ce_2O_3, significant contents of Nd_2O_3, Sm_2O_3 and Gd_2O_3 were also measured. High TiO_2 and Ce_2O_3 values indicate that vigezzite forms a partial solid-solution with nioboaeschynite-(Ce). The increase in Ta content also indicates a shift toward a partial solid-solution with rynersonite. Moreover, the composition of vigezzite from the Pizzo Marcio-Alpe Rosso dikes shifts at the core toward thorian vigezzite, even if the content is not enough to form a Th-dominant end-member of this group (0.13 *apfu* Th). Chemical analyses of tapiolite-(Fe) show Ta_2O_5 contents up to 86.53 wt.% and FeO up to 8.91 wt.%. Ferrowodginite contains up to 76.58 wt.% Ta_2O_5 and variable Fe/Mn values, with Fe slightly predominant over Mn.

Wodginite of the Colonnello Pizzo Paglia dike has Ta/(Ta+Nb) ratio in the range of 0.92-0.94 and Mn/(Mn+Fe) between 0.68-0.70. It does incorporate other elements with WO_3 up to 0.95 wt.%, UO_2 up to 0.11 wt.%, Gd_2O_3 up to 0.07 wt.% and Yb_2O_3 up to 0.08 wt.%. Wodginite has overgrowths composed of cassiterite.

Columbite-(Fe) at Codera dike is rather homogeneous in composition. The core of the crystal has up to 69.83 wt.% Nb_2O_5 and the rim up to 66.52 wt.%. Columbite-(Fe) incorporates other elements with WO_3 up to 1.20 wt.%, SnO_2 up to 0.28 wt.%, UO_2 up to 0.81 wt.%. Low REE values were also measured and include Y_2O_3 (0.05-0.10 wt.%), Nd_2O_3 (0.05-0.08 wt %), Gd_2O_3 (0.05-0.10 wt.%). Another analyzed sample of columbite-(Fe)

shows at the core of the crystal up to 67.99 wt.% Nb_2O_5 and at the rim 66.08 wt.%. The columbite-(Fe) of this sample also incorporates other elements with WO_3 up to 1.20 wt.%, SnO_2 up to 0.34 wt.%, with UO_2 up to 0.30 wt.%.

At Codera dike euxenite-(Y) is rather heterogeneous in composition. The core has Nb_2O_5 up to 37.3 wt.%, UO_2 up to 20.82 wt.% and Y_2O_3 up to 6.74 wt.%. The border zone of the crystal displays Nb_2O_5 up to 34.97 wt.%, UO_2 up to 15.87 wt.% and Y_2O_3 up to 8.58 wt.%. It is also sensibly enriched in LREE (2.1 wt.%) and HREE (3.2 wt.%) and displays minor amounts of SnO_2 (up to 1.34 wt.%) and WO_3 (up to 1.80 wt.%). Samarskite-(Y) at the core of the crystal has Nb_2O_5 up to 37.45 wt.%, UO_2 up to 11.65 wt.% and Y_2O_3 up to 9.97 wt.%. The border of the crystal has Nb_2O_5 up to 34.94 wt.%, UO_2 up to 10.82 wt.%, Y_2O_3 up to 10.12 wt.%. The sample is also enriched in LREE (1.9 wt.%) and HREE (2.5 wt.%) and has minor SnO_2 (up to 1.99 wt.%) and WO_3 (up to 1.85 wt.%). The highly metamictic state of the crystals does not permit to obtain sufficient diffraction peaks to get reliable cell data.

pegmatites	signatures	mineral	formula	symmetry	space group
Grignaschi, Rio Graia	(LCT, REL-Li)	tantalite-(Fe)	$(Fe,Mn)(Ta,Nb,Ti)_2O_6$	orthorhombic	*Pcan*
Pizzo Marcio-Alpe Rosso	(LCT, REL-Li)	tantalite-(Mn)	$(Mn,Fe)(Ta,Nb,Ti)_2O_6$	orthorhombic	*Pcan*
Pizzo Marcio-Alpe Rosso	(LCT, REL-Li)	columbite-(Mn)	$(Mn,Fe)(Nb,Ta,Ti)_2O_6$	orthorhombic	*Pcan*
Grignaschi, Rio Graia	(LCT, REL-Li)	columbite-(Fe)	$(Mn,Fe)(Nb,Ta,Ti)_2O_6$	orthorhombic	*Pcan*
Grignaschi, Rio Graia	(LCT, REL-Li)	tapiolite-(Fe)	$(Fe,Mn)(Ta,Nb,Ti)_2O_6$	tetragonal	$P4_2/mnm$
Pizzo Marcio-Alpe Rosso	(LCT, REL-Li)	tapiolite-(Fe)			
Pizzo Marcio-Alpe Rosso	(LCT, REL-Li)	fersmite	$(Ca,Ce,REE)(Nb,Ta,Ti)_2(O,OH)_6$	orthorhombic	*Pcan*
Pizzo Marcio-Alpe Rosso	(LCT, REL-Li)	vigezzite	$(Ca,Ce)(Nb,Ta,Ti)_2O_6$	orthorhombic	*Pbnm*
Pizzo Marcio-Alpe Rosso	(LCT, REL-Li)	ferrowodginite	$FeSnTa_2O_8$	monoclinic	*C*2/*c*
Colonnello Pizzo Paglia	(LCT, Mi-Li)	wodginite	$MnSnTa_2O_8$	monoclinic	*C*2/*c*
Garnet Codera	(mixed LCT-NYF, REL)	columbite-(Fe)	$(Fe,Mn)(Nb,Ta,Ti)_2O_6$	orthorhombic	*Pcan*
Garnet Codera	(mixed LCT-NYF, REL)	euxenite-(Y)	$(Y,U,Ca,REE)(Nb,Ti,Ta)_2(O,OH)_6$	orthorhombic	*Pcan*
Garnet Codera	(mixed LCT-NYF, REL)	samarskite-(Y)	$(Y,Fe,U,REE)(Nb,Ta,Ti)(O)_4$	orthorombic	*Pbcn*?
Arvogno Albertini	(NYF, REL)	aeschynite-(Y)	$(Y,Ca,REE)(Ti,Nb,Ta)_2(O,OH)_6$	orthorhombic	*Pbnm*
Arvogno Albertini	(NYF, REL)	polycrase-(Y)	$(Y,U,Ca,REE)(Ti,Nb,Ta)_2(O,OH)_6$	orthorhombic	*Pcan*

Table 1 - Distribution of Nb-Ta-Y-REE-U oxides in the pegmatites of Central Alps

References

Černý, P. Ercit, T.S. (2005) The classification of granitic pegmatites revisited. Canadian Mineralogist, vol. 43, 2005-2026.

Graeser, S. Schwander, H., Hänni, H. Mattioli, V. (1979): Vigezzite, $(Ca,Ce)(Nb,Ta,Ti)_2O_6$, a new aeschynite-type mineral from the Alps. Mineralogical Magazine, vol. 43, 459-462.

Guastoni, A. (2012): LCT (lithium, cesium, tantalum) and NYF (niobium, yttrium, fluorine) pegmatites in the Central Alps, Proxies of exhumation history of the Alpine nappe stack in the Lepontine dome. Ph.D. thesis, XXIV cycle, Department of Geoscience, University of Padova, 162 pp.

Guastoni, A. Pennacchioni G. (2013): LCT and NYF pegmatites in the Central Alps. Exhumation history of the Alpine nappe stack in the Lepontine dome. PEG 2013, 6th International Symposium on Granitic Pegmatites, Abstract This Volume.

MINERALOGY AND GEOCHEMISTRY OF PELITIC COUNTRY ROCK WITHIN THE SEBAGO MIGMATITE DOMAIN, OXFORD CO., MAINE

Jon D. Guidry, Alexander Falster, William Simmons, Karen Webber
Dept. of Earth & Environmental Sciences, University of New Orleans, New Orleans, LA, USA, jdguidry@uno.edu

Pelitic country rock and their rock-forming minerals of the Sebago Migmatite Domain (SMD) were analyzed to evaluate their relationship to pegmatites found in the Oxford pegmatite field in the SMD. The SMD country rock is amphibolite-grade metapelite within the Central Maine Belt and is associated with the Acadian Orogeny (Solar and Brown, 2001).

Thirteen samples of SMB metapelites trending along a northwest trajectory within Androscoggin, Cumberland, and Oxford Counties, ME were analyzed by FUS-ICP and FUS-MS, and mineral phases were analyzed by EMPA. Whole-rock analyses were split into leucosome, melanosome, and average compositions. CIPW norm calculations of these compositions yield Q values of 29%, 15% & 29%; Ab values of 18%, 19% & 19%; and Or values of 22%, 20% & 21%, respectively (Fig. 1).

The Shand index indicates that leucosomes and melanosomes range between peraluminous and metaluminous compositions, specifically between 1.2 and 3.6 mol. prop Al/(K + Na) plotted against 0.1 to 1.4 mol. prop Al/(K + Na + Ca) and plot within the metasedimentary fields defined by Solar and Brown (2001). K/Rb vs. Cs and K/Rb vs. Rb show Rb enrichment (K/Rb =51.76-377.39) similar to that of the evolved granites studied by Wise and Brown (2001). Figure 2 shows the correspondence of SiO_2 and A) Al_2O_3, B) K_2O, C) (Na_2O + CaO), D) (FeO_{tot} + MgO + TiO_2) to the SMD pelitic metasedimentary rocks of Wise and Brown (2001). Plots of whole-rock chondrite normalized REE content demonstrate the LREE enrichment in all samples. Moreover, LREE enrichment is more pronounced within melanosomes versus that of leucosomes. The melanosomes show a small negative Eu anomaly. The leucosomes show no negative Eu anomaly or a slight positive anomaly (Fig 3).

Biotite samples contain SiO_2 wt. % > 34.0. Li content was determined using the method of Tischendorf (1997). For biotites containing MgO > 6 wt.%, the equation $Li_2O = 155*MgO^{-3.1}$ was employed. For biotites containing MgO < 6 wt.%, the equation $Li_2O = (0.289*SiO_2)-9.568$ was utilized. Calculated (Mg-Li) ranges between 0.352 and 1.407 and (Fe_{tot}+Mn+Ti-Al_{VI}) has a range of 1.526 to 2.927, placing six biotite samples within the Fe biotite field and one in the siderophyllite field. Ratios of Fe/(Fe+Mg) range from 0.541 to 0.837, indicating Fe-rich biotites.

Garnets from two metapelites analyzed by EMP yield average wt.% of 37.1 SiO_2, 22.4 Al_2O_3, 30.1 FeO, 3.1 MgO, 5.0 MnO, and 2.0 CaO. Results indicate almanditic composition with FeO/(FeO+MgO+MnO+CaO) = 0.747.

Feldspars were analyzed using the EMP from leucosomes and melanosomes. The ratio of Na/(Na+Ca+K) yield nearly identical values of 0.79 for feldspars in both leucosomes and melanosomes. Results show that dominantly Na-rich plagioclase feldspars are present within the metapelites of the SMD.

Two whole rock samples were found to contain zircons. Ratios of Zr/Hf for the two samples were 124.2 and 101.8.

Thermometry for whole rock samples was determined from almanditic garnet and Fe biotite compositions, using the garnet-biotite thermometer of Bhattacharya *et al.* (1992), yielding an average temperature of 612ºC. Sillimanite, identified by thin section and XRD, was present in three of the whole rock samples. Mineral assemblages including K-spar, sillimanite, almandine, quartz, and biotite plot at 3.0 kbar and 650°C on the P-T diagram of Spear and Cheney (1989) (Fig.4).

Petrological, mineralogical and geochemical results coupled with phase equilibria suggest that the SMD in the vicinity of the pegmatites formed at about 650°C and 3 kbar. The compositions of the SMD leucosomes closely resembles the bulk compositions of some of the pegmatites in the Oxford pegmatite field suggesting that the pegmatites could be coalesced masses of leucosome derived from the partial melting of the SMD.

References

Bhattacharya, A., L. Mohanty, A. Maji, S. Sen, M. Raith (1992): Non-ideal mixing in the phlogopite-annite binary: constraints from experimental data on Mg-Fe portioning and a reformulation of the biotite-garnet geothermometer, Contributions to Mineralogy and Petrology, 111, 87-93.

Solar, G., M. Brown (2001): Petrogenesis of Migmatites in Maine, USA: Possible Source of Peraluminous Leucogranite in Plutons?. Journal of Petrology, 12, 789-823.

Tischendorf, G., B. Gottesman, H. Forster, R. Trumbull (1997): On Li-bearing micas: estimating Li from electron microprobe analysis and an improved diagram for graphical representation, Mineralogical Magazine, 61, 809-834

Wise, M., C. Brown (2010): Mineral chemistry, petrology and geochemistry of the Senago granite-pegmatite system, southern Maine, USA. Journal of Geosciences.

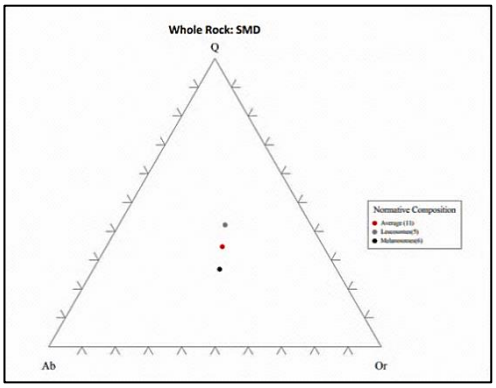

Fig. 1: Normalized composition of SMD whole rock

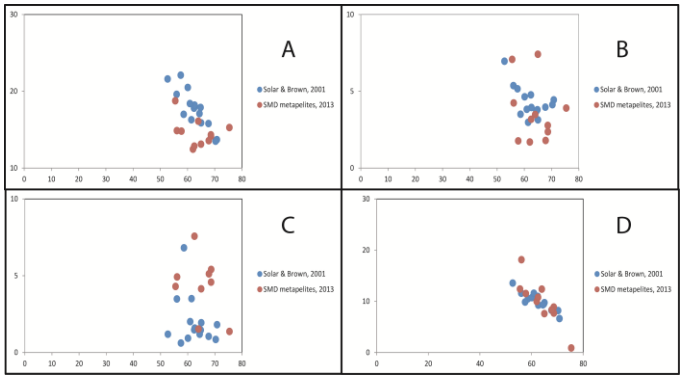

Fig. 2: Metasedimentary rocks, Solar and Brown, 2001 (blue) and Guidry, 2013 (red). SiO_2 vs. A) Al_2O_3, B) K_2O, C) (Na_2O + CaO), D) FeO_{tot} + MgO + TiO_2

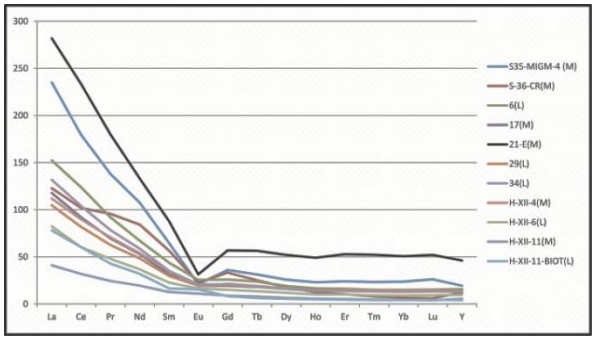

Fig. 3: REE plot of SMD samples

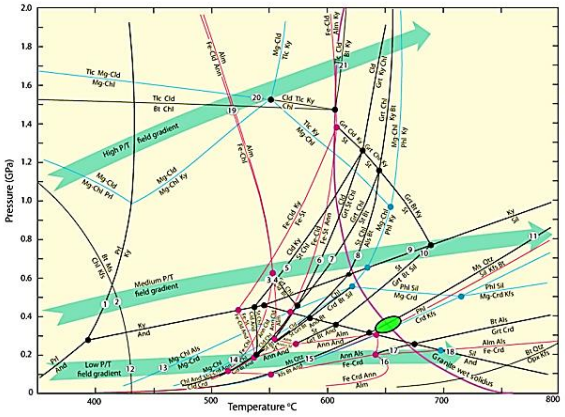

Fig. 4: P-T diagram adapted from Spear and Cheney (1989) with SMD metapelites field in green oval.

WODGINITE GROUP SPECIES FROM THE EMMONS PEGMATITE, GREENWOOD, OXFORD COUNTY, MAINE, USA

S. Hanson[1], A. Falster[2], W. Simmons[2], R. Sprague[3]
[1]Adrian College, Geology Dept. 110 S. Madison St., Adrian, MI, 49221, USA, slhanson@adrian.edu
[2]Department of Earth and Environmental; Sciences, University of New Orleans, New Orleans, LA, 70148, U.S.A
[3]10 Yates Street, Mechanic Falls, ME, 04256, USA

Wodginite was first introduced by Nickel *et al* (1963) and defined by Ferguson *et al.* (1976). It has the general formula ABC_2O_8 where, ideally, A=Mn, B=Sn and C=Ta. However, wodginite exhibits considerable substitution at all of the sites as many of these minerals deviate from the ideal composition at the individual cation by more than 50% (Ercit, 1992a). These authors proposed that these minerals be given group status and classified on the basis of the dominant cation at each of the individual sites. As a result, four wodginite mineral species have so far been defined. They include: wodginite ($MnSnTa_2O_8$), ferrowodginite ($Fe^{2+}SnTa_2O_8$), titanowodginite ($MnTiTa_2O_8$) and lithiowodginite ($LiTaTa_2O_8$). Ercit *et al.* (1992b) also reported 'tantalowodginite' but have since retracted that proposal as the minute quantity of the sample precluded any measurement of Li or the X-ray properties of the sample. Tantalowodginite has Ta dominant over Sn at the B-site. Tantalowodginite", the Ta-rich member of the wodginite group, has been identified from the Emmons pegmatite in Oxford County, Maine where it is associated with wodginite and columbite-tantalite group minerals.

The Emmons pegmatite is a large, peraluminous, LCT-type pegmatite exposed on Uncle Tom Mountain, Greenwood, Oxford County, ME. This gently dipping, 300 Ma dike intrudes Paleozoic schistose and metacarbonate rocks. These carbonate rocks have been altered to a skarn immediately adjacent to the contact. The pegmatite is complexly zoned with a wall zone comprised of K-feldspar, quartz, almandine and tourmaline, var. schorl, that locally exhibits a comb structure. Small pockets containing goyazite occur sporadically in the wall zone near the country rock contact. The intermediate zones are comprised of K-feldspar, quartz, muscovite, and spodumene. A quartz core is poorly defined. Replacement units along the core – intermediate zone boundary have undergone almost total alteration and replacement such that the only primary mineral remaining is muscovite. Secondary minerals include vuggy albite and clevelandite, and a dense and fibrous grayish-green muscovite, which occurs as a fracture filling and as a secondary mineral replacing schorl and garnet. Additionally, pollucite pods several meters in size, large phosphate nodules (30 cm), löllingite with minor arsenopyrite, and nearly gem quality beryl (goshenite) up to 0.3 m in size are present. Wodginite group and columbite group species occur commonly in the core margin, both in the massive pegmatite and in miarolitic cavities. Overgrowths of these minerals are common. In some cases, zoned crystals may have a tantalite-(Mn) core, a "tantalowodginite" mid zone and a wodginite rim. Others exhibit a "tantalowodginite" core with a wodginite rim. These crystals are generally elongated, blunted dipyramidal forms, but rounded and wedge habits are found (Fig. 1). The largest specimen to date measures 11 x 4 cm and sits on a matrix of ball muscovite mica and cleavelandite.

Samples of both core and rim wodginite were analyzed using an electron microprobe. Chemical formula and Fe^{2+}/Fe^{3+} ratios were calculated using the FORTRAN program "Wodginite" (Ercit, 1992a). In all cases, the core compositions have Ta > Sn at the B-site, thus are "tantalowodginite" whereas the rim compositions all have Sn > Ta at the B-site and are wodginite (Fig. 2). Additionally, a significant portion of the A-site is occupied by vacancies in "tantalowodginite' whereas the wodginite sites are fully occupied.

Ercit (1992a) has shown that as the ordering in the wodginite structure increases, from 0 to nearly 100%, there is a corresponding increase in the β angle from approximately 90.9° – 91.4°. The β angle from Emmons wodginite was determined using X-ray diffraction analysis (for "tantalowodginite") and calculated based on chemical composition (both varieties). The "tantalowodginite" cores exhibit near complete ordering with remarkably little variation. In contrast, the wodginite rims exhibit considerable variation in the degrees of ordering, ranging from nearly 0 to nearly 100% with an average of approximately 65% ordering.

The significant, and abrupt, variation in the core to rim compositions of these oxide minerals suggest that several phases of crystallization occurred in the

core of the pegmatite. Cassiterite was the early crystallizing Sn phase. As fractionation continued and the activity of Ta increased, ordered 'tantalowodginite' became the predominant Sn crystallizing phase. During the later stages of core formation, overgrowths of more disordered wodginite crystallized on tantalowodginite outside of the pockets, whereas overgrowths of columbite-tantalite grew around those within the pockets. The relative timing of the crystallization of these two overgrowth types cannot be determined. Finally, as Sn became depleted, columbite tantalite-became the predominant crystallizing phase.

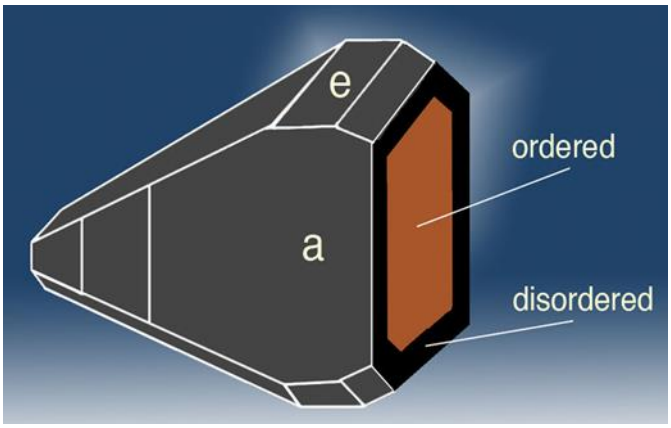

Fig.1: Idealized drawing of a wodginite/ 'tantalowodginite' crystal from the Emmons pegmatite, showing the ordered core of "tantalowodginite" and the overgrowth of ordered wodginite (drawing by Ray Sprague)

References

Ercit, T.S., P. Cerny, F.C. Hawthorne and C.A. McCammon (1992a): The wodginite group. II. Crystal chemistry. Canadian Mineralogist, vol 30, 613-631.

Ercit, T.S., P. Cerny, P. and F.C. Hawthorne (1992b): The wodginite group. III. Classification and new species. Canadian Mineralogist, vol. 30, 633-638.

Ferguson, R.B., F.C Hawthorne, and J.D. Grice (1976): The crystal structures of tantalite, ixiolite and wodginite from Bernic Lake, Manitoba. II. Wodginite. Canadian Mineralogist, vol. 14, 550-560.

Nickel, E.H., J.F. Rowland, and R.C Mcadam (1963): Wodginite B a new tinBmanganese tantalate from Wodgina, Australia and Bernic Lake, Manitoba. Canadian Mineralogist, vol 7, 390-402.

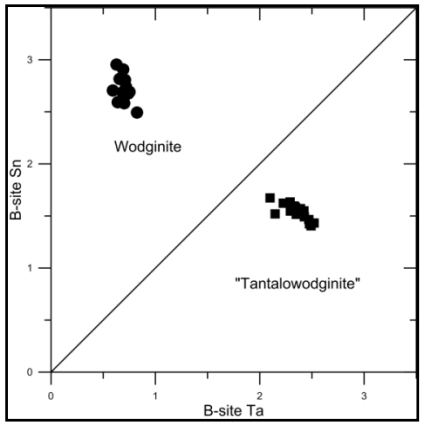

Fig. 2: B-site occupancy showing Sn versus Ta for wodginite group species in the Emmons pegmatite.

MINERALOGY, PETROLOGY AND ORIGIN OF THE KINGMAN PEGMATITE, NORTHWESTERN ARIZONA, USA

S. Hanson[1], W. Simmons[2], A. Falster[2]
[1] Adrian College, Geology Dept. 110 S. Madison St., Adrian, MI, 49221, USA, slhanson@adrian.edu
[2] University of New Orleans, Department of Earth and Environmental Sciences, New Orleans, LA, 70148, USA

The Mojave Pegmatite District, located in northwestern Arizona, is host to several pegmatites. The Kingman pegmatite is unique in that it is the sole pegmatite exposed in the Cerbat Range (~1 ½ km northeast of Kingman, AZ) and is the only pegmatite that is not associated with a genetically related host pluton. The pegmatite is intrusive into the Paleoproterozoic (1.740 – 1.720) orogenic Diana Granite. Electron-microprobe-derived ages on monazite from a satellite quarry located ~1.5 km to the southwest of the main quarry along strike from the Kingman quarry are younger than the Diana Granite, with an average age of 1.561±37 Ga (Simmons *et al.* 2012). The absence of Mesoproterozoic large scale extensional features in northwestern Arizona suggests that in the Mojave Pegmatite District this extension was localized, perhaps due to back arc rifting (Simmons *et al.* 2012).

The Kingman pegmatite is exposed in a roughly 500 m long quarry revealing a dike that trends N50-65°E, dips 60-75°NW and ranges in thickness from 20 to 60 m with a general widening to the northeast (Heinrich 1960). Roughly along strike with the Kingman pegmatite is a small prospect pit that exposes pegmatitic rocks that are inferred to be a continuation of the Kingman pegmatite. Contacts between the Kingman pegmatite and the older host granitic are well defined and, in some locations, exhibit ~0.3 m wide reaction boundaries.

The pegmatite is zoned with a 0.1-0.5 meter thick, discontinuous border zone that is composed almost entirely of microcline and fine-grained quartz. The wall zone averages approximately 4 m in thickness and is comprised predominantly of quartz and white microcline with lesser biotite and accessory allanite group species, magnetite, zircon, titanite, bastnäsite group species, uraninite, apatite, hematite, ilmenite and rutile. In the northern portion of the pegmatite, small amounts of muscovite and rare millimeter sized crystals of garnet are also present. The composite quartz-microcline core ranges in thickness from 10-60 m with microcline masses averaging 3-4 m across and less abundant gray quartz pods that reach approximately 2 x 2 x 5 m (Heinrich 1960).

The Kingman pegmatite exhibits an unusual REE mineral assemblage as HREE-bearing minerals are conspicuously absent; only one small (~1 cm) mass of aeschynite-(Y) was recovered from the satellite quarry (Hanson *et al.* 2012). The only LREE phase abundant in the Kingman quarry is allanite group species which occurs as unusually large, extensively fractured, up to 30 cm pods that are composed of crude metamict black crystals that reach ~25 cm in size. Heinrich (1960) reported that during one excavation in1944, approximately 20 tons of allanite were sent to an unknown buyer. Within the small satellite prospect pit, two large pods (up to 30 cm) of monazite-(Ce) are exposed on the western wall of the cut (Hanson *et al.* 2012). Fluorine-bearing minerals are notably absent from the pegmatite. Thus, the pegmatites are strongly enriched in LREE and extremely depleted in Nb, HREE, and F. These chemical characteristics are atypical for classic Niobium-Yttrium-Fluorine (NYF) pegmatites as described by Černý and Ercit (2005).

Kingman allanite is predominantly Nd-rich allanite-(Ce) (Fig. 1), although some of the samples exhibit Nd-dominant domains near the rims and along fractures, thus are allanite-(Nd). This variability in

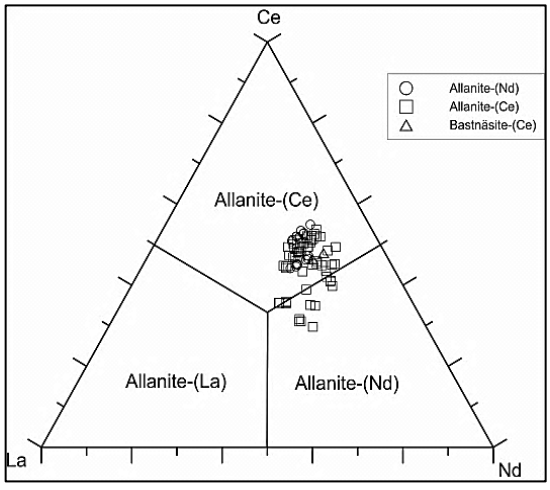

Fig. 1: Allanite-(Ce) from Kingman, AZ

the dominant A-site cation arises from subtle differences in the relative abundance of Ce and Nd with Nd/Ce ratios ranging from 0.57 – 1.51. Additionally, these Nd-rich domains can be correlated to areas where allanite alteration resulted in the formation of bastnäsite-(Ce). Like allanite-(Nd), the bastnäsite-(Ce) has nearly equal Ce and Nd *apfu*.

The absence of HREE-bearing minerals as well as the presence of abundant allanite reflects an extreme LREE enrichment. The near absence of P and F is evidenced by the near absence of monazite and bastnäsite. Although the allanite rims are altered, the enrichment in Nd relative to Ce cannot be attributed to alteration by late-stage oxidizing fluids. The less mobile Ce^{+4} would preferentially remain, leaving the crystals enriched in Ce relative to the other REE. Thus, we suggest that late-stage alteration of allanite-(Ce) to bastnäsite-(Ce) may be the controlling factor. An influx of carbonate-bearing late-stage fluids could have altered biotite, releasing the small amount of F necessary to form bastnäsite-(Ce) with slightly lower Nd/Ce ratios. The redistribution of Ce preferentially into bastnäsite-(Ce) would then lead to greater Nd/Ce ratios in recrystallized allanite fractures and the recrystallized rims.

The Kingman pegmatite exhibits an unusual and extreme LREE enrichment and HREE depletion relative to typical NYF pegmatites. Although partial melting of within-plate granites, followed by partitioning of HREE into a late-stage fluid via fluorine complexing, can lead to LREE enriched granitic rocks, the absence of fluorine, as well as the near absence of HREE-enriched minerals in either the quarry or the dump material, precludes this mechanism of enrichment. Thus, we suggest that this pegmatite is not likely the result of fractionation from a granitic melt but instead has an anatectic origin. Recently, several authors have shown that unusual "parentless" pegmatites may be anatectic origin rather than the result of extreme fractionate of a granitic melt (Martin & De Vito 2005; Ercit, 2006). An anatectic origin from a very small percentage of partial melt could account for the absence of a parent granite as well as the extreme enrichment in LREE and depletion in F, Nb, Ta, and HREE if the protolith were a garnet-biotite±hornblende metamorphic rock. A small degree of partial melting at low temperatures would melt only the felsic component leaving the HREE and F in the residual mafic minerals. This process could conceivably produce a melt with the composition of the Kingman pegmatite.

References

Černý, P. and Ercit, T. (2005): The Classification of Granitic Pegmatites Revisited. Canadian Mineralogist, vol. 43, 2005-2026.

Ercit, T. S. (2006) Ta-Nb geochemical constraints on the petrogenesis of granitic pegmatites in the southwestern Grenville Province, Ontario. GAC-MAC Abstracts, vol. 31, 46.

Gramaccioli and Pezzotta, F. (2000): Geochemistry of yttrium with respect to the rare-earth elements in pegmatites. Memorie della Italiana di Scienze e del Museo Civico di Storia Naturale di Milano, vol. XXX, 111-115.

Hanson, S.L., Falster, A.U., Simmons, W.B. and Brown, T.A. (2012): Allanite-(Nd) from the Kingman Feldspar Mine, Mojave Pegmatite District, northwestern Arizona, USA. Canadian Mineralogist, vol. 50, 815-824.

Heinrich, E. William (1960): Some Rare-Earth Mineral Deposits in Mojave County, Arizona. Arizona Bureau of Mines Bulletin, vol. 167.

Martin, R.F. & DeVito (2005): The patterns of enrichment in felsic pegmatites ultimately depend on tectonic setting. Canadian Mineralogist, vol. 43, 2027-2048.

Simmons, W., Hanson, S.L., Falster, A.U., and Webber, K.,. (2012): A comparison of the mineralogical and geochemical character and geological setting of Proterozoic REE-rich granitic pegmatites in the north-central and southwestern US. Canadian Mineralogist vol. 50, 1695-1712.

RARE EARTH MINERALS OF THE MUKINBUDIN PEGMATITE FIELD, MUKINBUDIN, WESTERN AUSTRALIA

M. Jacobson
markivanjacobson@gmail.com

The area around Mukinbudin, Western Australia has been described as a sea of granite with white caps of pegmatites. These quartz- and feldspar-rich pegmatites are found within an Archaean-aged post-tectonic biotite adamellite or adamellite, having formed outside of the greenstone belts. The adamellites are part of the Murchison terranes, in the Yilgarn Craton. These rare-element pegmatites are classified as members of the allanite-monazite NYF (Niobium-Yttrium-Fluorine) class (Černý, 1991). The three best exposed pegmatites from the nine known localites in the field (Figure 1), Calcaling, Karloning and Mukinbudin Feldspar, all have a quartz core, a discontinuous albitic core-margin unit, a microcline intermediate zone, a graphic granite (quartz-microcline-biotite) wall zone and sometimes a border (medium-grained microcline-plagioclase-quartz-biotite) zone.

Pegmatites within the field were first prospected and mined for snow white quartz circa 1969 with utilization of microcline feldspar and mixed quartz-feldspar starting in the 1975. Detailed summaries of all the pegmatites that were identified in 2007 can be found in Jacobson, Calderwood and Grguric (2007).

By December 2002, the minerals that had been identified from this field were albite, allanite-(Ce), allanite-(Y)?, beryl, biotite (to 1 metre diameter plates), chalcopyrite, euxenite-(Y), fergusonite-(Y), fluorite (green), ilmenite, niobian rutile, hematite, magnetite, microcline (pink, tan, white, light green), molybdenite, monazite, muscovite, quartz (clear, smoky crystals to 60 cms), topaz (white), xenotime-(Y) and zircon (variety cyrtolite).

The Calcaling pegmatite has had the greatest number of identified species due to the active work of Bob Jones (Rural Propecting Pty. Ltd.). From an albitic core-margin unit, euxenite has been found associated with ilmenite and niobian rutile. Niobian rutile forms black metallic to bluish-black metallic equant crystals to 6-10 cm diameter with densities of 4.65-4.54 gm/cc. Standardless energy dispersive spectroscopy indicates 15% Nb_2O_5 and 11% Ta_2O_5.

Flat, bladed ilmenite crystals 0.4-0.8 cm in thickness and up to 15 cm long and wide are also common in albite masses. Standardless energy dispersive spectroscopy indicates only titanium and iron. Crystallizing perpendicular to these blades can be found metamict euhedral euxenite-(Y) crystals intergrown with the equant ilmenorutile crystals.

The euxenite-(Y) crystals are clearly subordinate to the niobian rutile. The largest euxenite crystal is 15 mm long from a wide termination tapering to a narrower crystal base in contact with an ilmenite plate. At its largest, near the termination, the crystal is 8 mm wide and 5 mm thick. These crystals often form a row of "sprouting," intergrown crystals of variable size, all standing on an ilmenite plate. The crystal faces are dull gray to dull black with black, lustrous, glassy interiors. These metamict masses had densities of 5.23-5.29 gm/cc. Standardless energy dispersive spectroscopy indicates 36% Nb_2O_5 with 15% TiO_2, 12% Y_2O_3 and approximately 5% thorium and uranium oxides.

Only one monazite crystal was found in the microcline of the wall zone; it was at least 15 cm long and 5 cm wide with a density of 5.16 gm/cc. The crystal was of typical red-brown color, prominent cleavage and woody type texture with red-stained microcline surrounding the crystal. Beryl, fluorite and molybdenite have also been recovered from this pegmatite.

The Karloning pegmatite is zoned similar to the Calcaling pegmatite with a large albitic core-margin unit containing allanite-(Y), fergusonite-(Y) and xenotime-(Y)?. Allanite-(Y) forms typical black, anhedral metamict masses with an average density of 3.62 gm/cc. Fergusonite-(Y) occurs as radiating, elongated crystals with square cross sections that form partial fan-like aggregrates and as a single elongated crystal emerging from the center of a multiple intergrown crystal nodule of xenotime. Standardless energy dispersive spectroscopy indicates a high percentage of niobium and yttrium with no calcium, and less than 3% each of TiO_2 and SnO_2. Thorium and uranium oxides totaled 9% in the sample. Density measurements on two fragments yielded 5.5 and 5.1 gm/cc respectively. Xenotime-(Y) was found as isolated grayish red crystals with curved crystal faces, to 0.5 cm and as clusters of (2 by 5 cm) of red to tan xenotime in albite. Standardless energy dispersive spectroscopy indicates a high percentage of yttrium oxide and phosphorous. The thorium oxide content was 2%. Zircon at the micron level is intermixed with the xenotime. One small fragment had a measured density of 4.13 gm/cc.

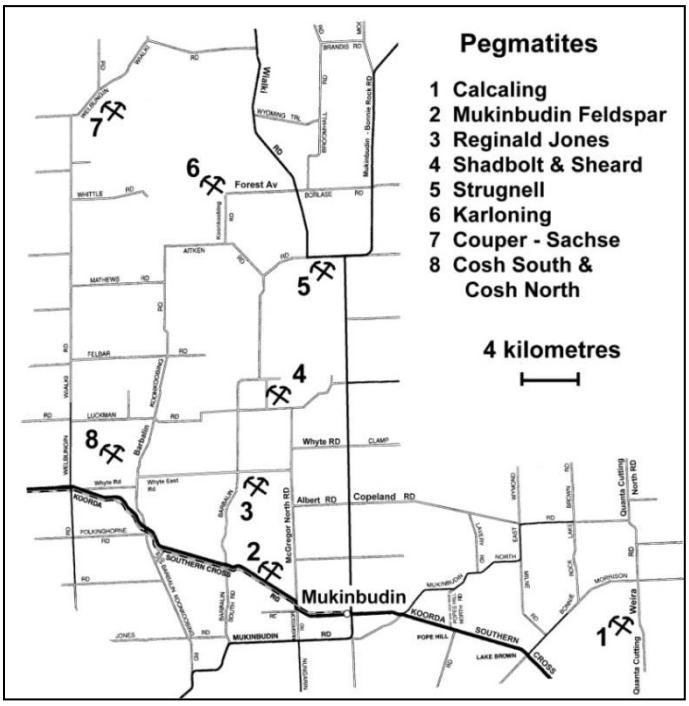

Fig. 1: Central part of the Mukinbudin pegmatite Field, Western Australia

The Mukinbudin Feldspar Mine has been excavated into at least three different pegmatites as exposed in three open pits. These pegmatites are also zoned similarily to both the Calcaling and Karloning pegmatites. The rare-earth minerals from these pegmatites are fergusonite-(Y) associated with zircon variety cytrolite and allanite-(Ce). Fergusonite-(Y) formed intergrown crystals with square cross sections associated with zircon in albite. These masses reached up to 12 cm in diameter, with an average density of 4.90 gm/cc. Groups of brown, lustrous metamict elongated fergusonite-(Y) crystals were also found in albite and microcline, oriented perpendicular to giant biotite crystals, with one end rooted in the biotite. These crystals reached up to 5 mm in length. Standardless energy dispersive spectroscopy indicated minor to no titanium or calcium (<2%), niobium greatly predominant over tantalum, and the weight percent of yttrium about one half of the niobium percentage. Uranium and thorium are also present. The zircon variety cyrtolite is metamict with measured densities of 3.4-3.48 gm/cc. The typical curved, intergrown, multiple crystal faces can be seen where the feldspar has weathered away. Energy dispersive spectroscopy indicated the presence of 2% uranium and 3% thorium. Allanite-(Ce) in masses exceeding several kilograms, have red-brown coatings and specific gravities of 3.39-3.45 gm/cc. The large masses are all rounded with no crystal faces. Energy dispersive spectroscopy indicated Ce is greater than La.

The discovery of abundant fergusonite-(Y), euxenite-(Y), xenotime-(Y)?, zircon, monazite-(Ce)?, niobian rutile, allanite-(?), and topaz in what, prior to 1990, was considered to be a simple pegmatite district is significant. Continued mining in existing quarries and new mining in the numerous virgin pegmatites will probably result in additional mineral species to be identified.

References

Černý, P. (1991): Rare element granitic pegmatites, Part I. Anatomy and internal evolution of pegmatite deposits. Geoscience Canada, vol 18:2, 49-67.

Jacobson, M. I., M. A. Calderwood, B. A. Grguric (2007): Guidebook to the Pegmatites of Western Australia. Hesperian Press, Victoria Park, Western Australia. 356 p.

A STUDY OF HEAVY MINERALS IN A UNIQUE CARBONATE ASSEMBLAGE FROM THE MT. MICA PEGMATITE, OXFORD COUNTY, MAINE

M. Johnson[1], W. Simmons[1], A. Falster[1], G. Freeman[2]
[1] Dept. of Earth & Env. Sci., University of New Orleans, New Orleans, LA 70148, cmjohns6@uno.edu
[2]Coromoto Minerals, 48 Lovejoy Road, Paris, ME 04271

Introduction

In the core margin of the Mt. Mica pegmatite, unusual carbonate-apatite-tourmaline units (Figs. 1 and 2) exist near larger primary miarolitic cavities, masses of lepidolite, and pollucite masses. These units are rich in mineral species, some of which are very rare (such as kosnarite, mccrillisite, and glucine). This study investigates the heavy minerals (>3.0 g/cm^3) near the carbonate-rich units and attempts to gain insight into their formation. The heavy minerals found include pollucite, chalcopyrite, tantalite-columbite, arsenopyrite, lithiophilite, montebrasite, cassiterite, pyrite, uraninite, eosphorite-childrenite, zircon, albite, apatite, tourmaline, siderite, rhodochrosite, and members from the monazite group. In the light fraction glucine, clays and zeolites were found.

Fig. 1: Close-up of carbonate unit surrounded by albite. FOV10 cm

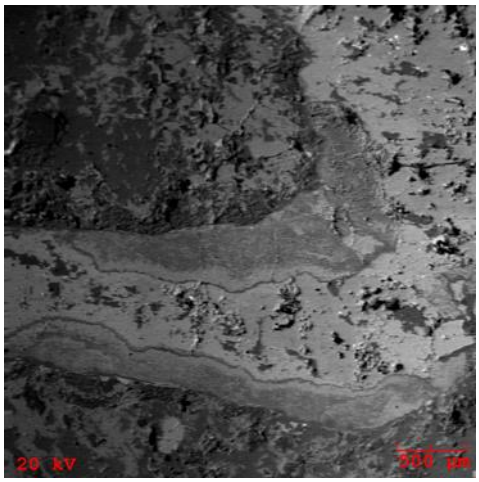

Fig. 2: Backscattered electron image of skeletal intergrowth

Results

Samples were crushed and screened, then separated using a heavy liquid (lithium metatungstate) and investigated in an AMRAY 1820 scanning electron microscope. The carbonate minerals nearly pure siderite and rhodochrosite, which are relatively rare in pegmatites, host a number of heavy mineral phases. The heavy minerals identified include: abundant tourmaline and apatite, and rare zircon, eosphorite, uraninite, pyrite, arsenopyrite, chalcopyrite, cassiterite, montebrasite, columbite-(Mn). In addition, very rare lithiophilite, goyazite, monazite, and pollucite were also identified. An examination of lighter density separates yielded glucine, the rare Be phosphate mineral, found only in two worldwide locations. Mount Mica is the type location for glucine. Mccrillisite and kosnarite, the very rare zirconium phosphates, have been previously reported for Mt. Mica in a similar carbonate assemblage, but were not found during this study. To attempt to quantify the bulk composition of the carbonate assemblage, an EDS wide-area quantification was performed based on eight 4x4 mm areas of a polished sample of one of these carbonate unit (Figs. 3 and 4).

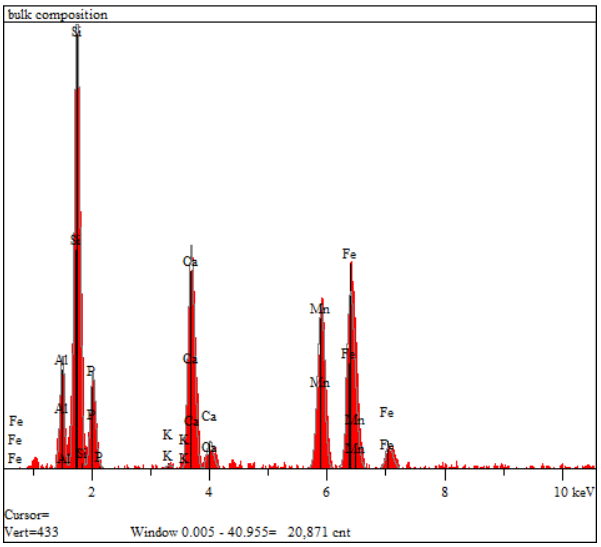

Fig. 3: Bulk Composition Spectrum

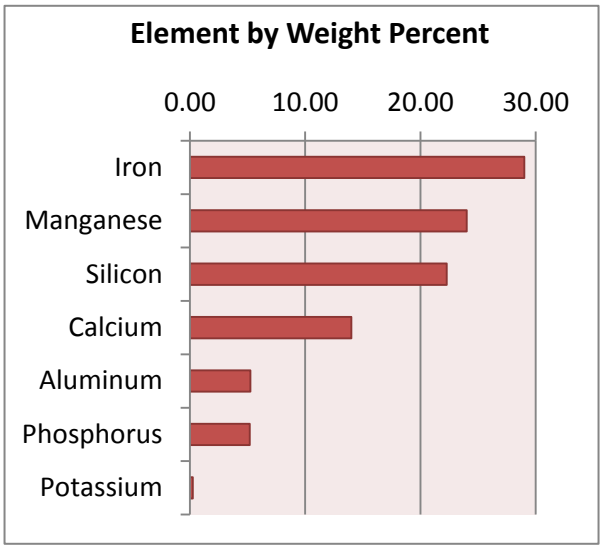

Fig. 4: EDS quantification of spectrum

Conclusions

Carbonate assemblages within pegmatites are rare even though CO_2-rich fluids are present in many pegmatites. Either a reaction of a fluid with elevated levels of CO_2 occurs with pre-existing iron and/or manganese bearing minerals or a primary reaction of the fluid with iron and manganese ions to produce siderite and rhodochrosite. Both iron and manganese constitute the bulk weight percentage in the semi-quantitative analysis. The presence of sulfides, which occur in minor quantities in pegmatites along with the carbonates siderite/rhodochrosite suggests a reaction with a CO_2-rich fluid occurred at temperatures at or below 450ºC. The conditions of formation of other minerals identified within the carbonate unit can be applied to the possible conditions under which the carbonate assemblage formed. Pollucite occurs only in highly evolved LCT-type pegmatites and is typically associated with elbaitic tourmaline and albite. The presence of montebrasite, lithiophilite, lepidolite, tourmaline, and apatite suggests that the carbonate unit developed from a highly fractionated flux-rich melt, during later stages of crystallization. Lepidolite, tourmaline, and montebrasite are intimately associated with the carbonate assemblage. The crystallization of these phases consume flux components resulting in a strongly undercooled melt leading to rapid crystallization and lowered melt solubility that caused the exsolution of H_2O and the CO_2-rich fluid. The CO_2-rich fluid is inferred to then react with late-stage Fe and Mn ions released from altering earlier formed Fe-Mn-bearing minerals (such as schorl and Fe-Mn phosphates) or from interaction with Fe-Mn-bearing fluids infiltrating in from the country rock.

In order to further understand the nature of the unique conditions under which these rare carbonate units form, the entire mineral assemblage should be studied. In addition, assemblages from other pegmatites should be studied for comparison.

STRUCTURAL INSIGHTS GLEANED FROM PALERMO'S TWO NEWEST MINERALS, FALSTERITE AND NIZAMOFFITE

A. Kampf
Natural History Museum of Los Angeles County, akampf@nhm.org

The Palermo No. 1 pegmatite in North Groton, New Hampshire, is one of the foremost localities in the world for pegmatite phosphates. It has thus far yielded 10 new phosphate species. After a hiatus of more than three decades, the last two of these, falsterite and nizamoffite, were discovered in a secondary Zn- and Pb-rich phosphate–carbonate assemblage, also containing minor amounts of sulfide minerals (pyrite, sphalerite, galena, and chalcopyrite), along the margin of a triphylite crystal (Nizamoff *et al.*, 2007). A knowledge of the atomic arrangement of a mineral is crucial to an understanding its properties and conditions of formation. This is very much the case for falsterite and nizamoffite.

Falsterite, $Ca_2MgMn^{2+}{}_2(Fe^{2+}{}_{0.5}Fe^{3+}{}_{0.5})_4Zn_4(PO_4)_8(OH)_4(H_2O)_{14}$, and nizamoffite, $Mn^{2+}Zn_2(PO_4)_2(H_2O)_4$, both contain essential Zn. Schoonerite, $Mn^{2+}Fe^{2+}{}_2Fe^{3+}Zn(PO_4)_3(OH)_2(H_2O)_7\cdot 2H_2O$, is the only other mineral with essential Zn that was first described from this deposit, and it has also been found in association with these phases. The structures of falsterite (Kampf *et al.*, 2012) and schoonerite (Kampf, 1977) are topologically quite different, but they share similar components and structural features. Both structures contain thick slabs composed of linkages of Fe^{2+}, Fe^{3+}, and Mn^{2+} octahedra, Zn polyhedra (ZnO_4 tetrahedra in falsterite and ZnO_5 trigonal bipyramids in schoonerite), and PO_4 tetrahedra. A prominent feature in each slab is an edge-sharing chain of FeO_6 octahedra and the slabs in each are linked by weak bonds – in schoonerite only by hydrogen bonds and in falsterite by both hydrogen bonds and linkages through half-occupied MgO_6 octahedra. This accounts for both minerals having very similar thin bladed habits. However, these minerals differ markedly in color. Schoonerite is orange and weakly pleochroic, while falsterite is greenish-blue and strongly pleochroic. This difference is readily explained by differences in the edge-sharing chains of FeO_6 octahedra. In schoonerite, the chain contains only Fe^{2+}, while in falsterite it contains both Fe^{2+} and Fe^{3+}. (In schoonerite, additional $Fe^{3+}O_6$ octahedra link the chains to one another by corner sharing.) The strong greenish-blue pleochroic color of falsterite is in the direction of the chain and is clearly related to the strong absorption typical of Fe^{2+}–Fe^{3+} charge transfer.

Nizamoffite (Kampf *et al.*, pending) is isostructural with hopeite. The structure contains corner-sharing zigzag chains of ZnO_4 tetrahedra. The chains are connected by corner sharing with PO_4 tetrahedra to form sheets. The sheets are linked to one another through octahedra that contain Zn in hopeite and Mn in nizamoffite. Synthetic hopeites, including those substituted with cations such as Mn^{2+}, Ni^{2+}, and Mg, have been studied extensively because of their technological applications, particularly with respect to corrosion resistant coatings on galvanized steel. In nature, there are two polymorphs of $Zn_3(PO_4)_2\cdot 4H_2O$, hopeite (orthorhombic) and parahopeite (triclinic). In laboratory studies, two orthorhombic polymorphs with somewhat different properties have been reported and have been designated α-hopeite and β-hopeite. α-hopeite is considered more stable and β-hopeite forms at lower temperature (20°C), but the structures of the two polymorphs are apparently identical except for the orientation of the H atoms of one of the H_2O groups (Herschke *et al.* 2004). The locations of the H atoms and the configuration of the hydrogen bonds in nizamoffite most closely correspond with those in α-hopeite.

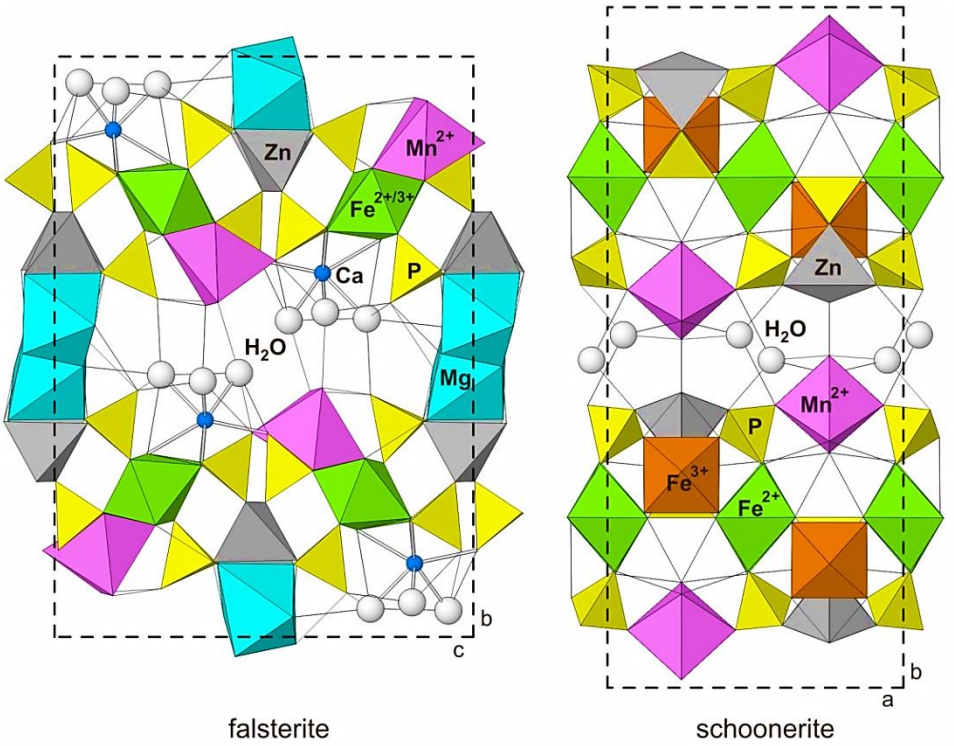

Fig. 1: The crystal structures of falsterite and schoonerite. Hydrogen bonds are shown as thin black lines. Note that edge-sharing chains of FeO_6 octahedra extend into the page.

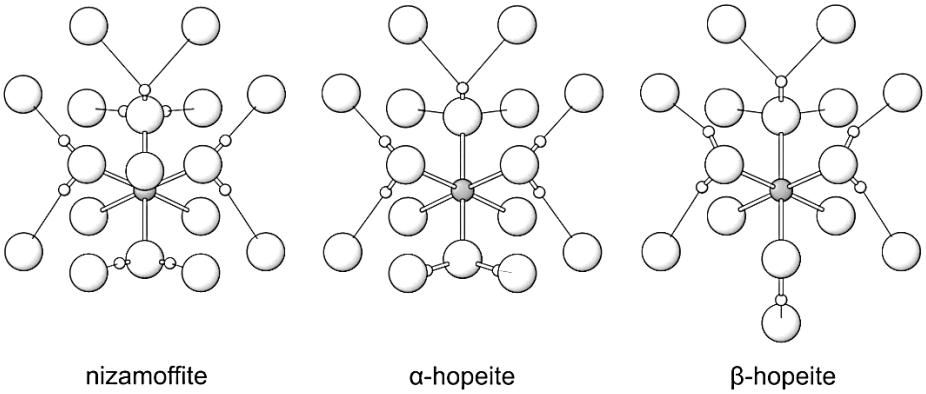

Fig. 2: Hydrogen bonding in nizamoffite, hopeite-α, and hopeite-β. Hydrogen bonds are shown as thin black lines. The gray spheres are the octahedrally coordinated cations (Mn in nizamoffite; Zn in hopeite) and the bonds to the O atoms surrounding them are shown as sticks.

References

Herschke, L., Enkelmann, V., Lieberwirth, I., and Wegner, G. (2004): The role of hydrogen bonding in the crystal structures of zinc phosphate hydrates. Chemistry - A European Journal, vol. 10, 2795-2803.

Kampf, A.R. (1977) Schoonerite: its atomic arrangement. American Mineralogist, vol. 62, 250–255.

Kampf, A.R., Falster, A.U., Simmons, W.B., and Whitmore, R.W. (pending): Nizamoffite, $Mn^{2+}Zn_2(PO_4)_2(H_2O)_4$, the Mn analogue of hopeite from the Palermo No. 1 pegmatite, North Groton, Grafton Co., New Hampshire. (submitted for publication).

Kampf, A.R., Mills, S.J., Simmons, W.B., Nizamoff, J.W. and Whitmore, R.W. (2012): Falsterite, $Ca_2MgMn^{2+}{}_2Fe^{2+}{}_2Fe^{3+}{}_2Zn_4(PO_4)_8(OH)_4(H_2O)_{14}$, a new secondary phosphate mineral from the Palermo No. 1 pegmatite, North Groton, New Hampshire. American Mineralogist, vol. 97, 496-502.

Nizamoff, J.W., Whitmore, R.W., Falster, A.U., and Simmons, W.B. (2007): Parascholzite, keckite, gormanite and other previously unreported secondary species and new data on kulanite and phosphophyllite from the Palermo #1 mine, North Groton, New Hampshire. Rocks and Minerals, vol. 82, 145.

PAN-AFRICAN PEGMATITES – POSSIBLY THE BEST PEGMATITES IN THE WORLD?

J. Kinnaird[1], P. Nex.[1, 2]
[1]University of the Witwatersrand, Judith.kinnaird@wits.ac.za
[2] Umbono Financial Services

Throughout Africa, individual pegmatites and their products have been known since the 1920's although studies on pegmatite districts were limited until the late 1960's-1970's. Clifford (1966) noted that certain elements such as Be, W and Sn were generally restricted to the younger orogenic zones. Following significant mineralogical studies on many pegmatites, von Knorring (1970) distinguished between pegmatites in 1100+/-200 Ma orogenic belts and those occurring in belts of 550+/-100 Ma. Regional zoning of pegmatites was noted in Namaqualand (Gevers, 1936: Gevers *et al.*,1937), and for West and Central Africa and Madagascar (Varlamoff 1972a,b). Further mineralogical, geochemical and geochronological studies have shown that African pegmatites span ages from Archaean (Bikita) to the Cambrian and occur in West Africa, particularly Nigeria, NE Africa (Somaliland, Sudan, Ethiopia, and Egypt), in eastern Africa (Rwanda, SW Uganda, Kenya, Tanzania, eastern DR Congo) and in southern Africa (Zimbabwe, Mozambique, Madagascar, Namibia and South Africa). Information is at times difficult to obtain on the mineralogy and local setting of these pegmatites, but there have been few attempts at continent or orogen-wide regional syntheses since the work of Clifford (1966); von Knorring (1970); and von Knorring and Condliffe (1987).

In examining the distribution of these pegmatites, it is clear that from the Mesoproterozoic to the Phanerozoic there is a link between tectonism, magmatism and late-stage pegmatite emplacement. For example, in the Namaqua Belt (southwestern Africa) a number of tectono-stratigraphic terranes, each with their own sedimentary-magmatic-tectonic histories, accreted onto the western margin of the Archaean Kaapvaal craton accompanied by intense deformation and metamorphism and voluminous syn- and post- tectonic granitoids between 1200 Ma to 1000 Ma (Cornell *et al.,* 2006). Post-orogenic pegmatites occur throughout this region and show LCT affinities in the west and east with possible NFY or mixed NYF-LCT pegmatites in the central part of the belt. These pegmatites have produced industrial quantities of feldspar and mica and some producing noted watermelon tourmalines. Hugo (1969) reported minor extraction of gadolinite, rose-quartz, cassiterite, and columbite-tantalite from the pegmatites. These are essentially the same age as pegmatites in Uganda, Rwanda and eastern DRC and related to the formation of Rodinia.

However, it is the late-Neoproterozoic creation of Gondwana, the Pan-African orogeny, that has produced many of the well-known pegmatites that are responsible for much of the gemstone production of Africa and locally have been important producers of mica, feldspar, cassiterite, columbite-tantalite, and beryl. The term Pan-African of Kennedy (1964) refers to orogenic areas surrounding cratons dating from "Late Precambrian to Lower Palaeozoic times (+/-500 Ma)".

In the Damaran of Nambia, swarms of pegmatites occur in the Karibib-Usakos area, where amphibolite facies metamorphism and granite magmatism occurred in response to the closing of the Khomas Ocean as the Kalahari craton subducted beneath the Congo craton. Continental collison occurred at about 530 Ma, with the peak of mineralization and pegmatite formation c.500 Ma as collision led to crustal relaxation and orogenic collapse. Zoned pegmatites (Rubicon, Helicon), Sn-pegmatites (Uis), U-pegmatites (Rossing and Goanikontes) are contemporaneous and have similar structural emplacement controls.

In the Mozambique belt (East African Orogen), collision between East and West Gondwana took place at c.600-550 Ma with late-tectonic extension and plutonism occurring in NE Mozambique at c. 520-515 Ma (Ueda *et al.,* 2012). The Alto Ligonha pegmatite field in the Nampula Block, is known for production of columbite-tantalite, euxenite, monazite, tourmaline, aquamarine, topaz, as well as quartz, mica, beryl and feldspar. The notable Muiane zoned pegmatite would appear to have LCT affinities given the presence of a lepidolite zone containing spodumene. Further north in the Mozambique belt, Ta-Nb mineralization occurs within the Kenticha LCT pegmatite field of Ethiopia, also associated with post-orogenic granites. The Kenticha pegmatite itself has been dated at ~530 Ma (Kuster *et al.,* 2009). In Somaliland, swarms of post-orogenic pegmatites, some of which are zoned, cross-cut an east-west oriented Proterozoic basement. Pegmatites variably

host beryl, tourmaline, columbo-tantalite, monazite and reportedly samarskite and cassiterite locally. It is also possible to extend the pegmatite-post-collisional granite association within the MozambiqueBelt, further north into the Arabian-Nubian Shield where rare-metal peralkaline granites (Nb-Zr-REE-Ta mineralization) and peraluminous granites and pegmatites (Ta-Li-Cs mineralisation) occur (Kuster, 2009).

When the whole of Africa is considered, the character of particular Pan-African pegmatite fields varies across the continent. Von Knorring (1970) noted that the pegmatites of the Damaran Belt of Namibia and the Kibaran Belt of central Africa are characterized by tin-enrichment while in pegmatites of the Mozambique Belt tin-enrichment is notably absent. He considered that pegmatites of the Mozambique Belt, including Madagascar, were relatively enriched in rare-earths compared to the Damaran and Kibaran Belts. West African Pan-African pegmatites, notably those in Nigeria, would appear to show similarites with the Damaran pegmatites of Namibia with both LCT pegmatites and a Sn-W association.

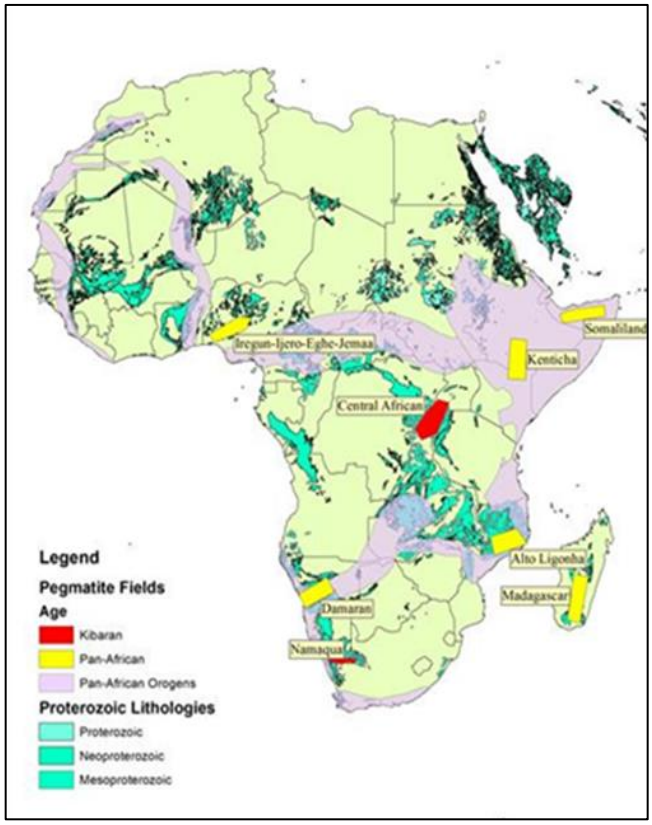

Fig. 1: Simplified map of Africa showing the location of significant pegmatite fields together with the Pan-African structural architecture and distribution of Proterozoic lithologies

References

Clifford, T.N., (1966) Tectono-metallogenic units and metallogenic provinces of Africa. *Earth and Planetary Science Letters* vol. 1, 421-434.

Cornell, D.H., Thomas, R.J., Moen, H.F.G., Reid, D.L., Moore, J.M., Gibson, R.L. (2006) The Namaqua-Natal Province. In: Johnson, M.R., Anhaeusser, C.R., and Thomas, R.J. (Eds.) *The Geology of South Africa.* Geological Society of South Africa, Johannesburg / Council for Geoscience, Pretoria, 325-379.

Gevers, T.W. (1936) Phases of mineralization in Namaqualand pegmatites. *Transactions of the Geological Society of South Africa* vol. 39, 331-377.

Gevers, T.W., Partridge, F.C., Joubert, G.K. (1937) *The pegmatite area south of the orange River in Namaqualand*. Geological Survey of South Africa Memoir 31 pp180.

Hugo, P.J. (1970) *The pegmatites of the Kenhardt and Gordonia Districts, Cape Province*. Geological Survey of South Africa Memoir 58 pp94.

Kennedy, W.Q. (1964) The structural differentiation of Africa in the Pan-African (+/- 500 m.y.) tectonic episode. *Research Institute of African Geology*, University of Leeds, 8th Annual Report, 48-49.

Kuster, D. (2009) Granitoid-hosted Ta mineralization in the Arabian-Nubian Shield: ore deposit types, tectono-metallogenetic setting and petrogenetic framework. *Ore Geology Reviews* **35**, 68-86.

Kuster, D., Romer, R.L., Tolessa, D., Zerihun, D., Bheemalingeswara, K., Melcher, F., Oberthur, T. (2009) The Kenticha rare-element pegmatite, Ethiopia. *Mineralium Deposita* vol. 44, 723-750.

Ueda, K., Jacobs, J., Thomas, R.J., Kosler, J., Jourdan, F., and Matola R. (2012) Delamination-induced late-tectonic deformation and high-grade metamorphism of the Proterozoic Nampula Complex, Mozambique. *Precambrian Research* vols. 196-197, 275-294.

Varlamoff, N. 1972a Central and West African rare-metal granitic pegmatites, related aplites, quartz veins and mineral deposits. *Mineralium Deposita vol.* 7, 202-216.

Varlamoff, N. 1972b *Materiaux pour l'etablissement des types et de la zoneographie des pegmatites granitiques a metaux rares de Madagascar*. Academie royale des Sciences d'Outre-Mer Memoir 18-6 pp71.

von Knorring, O. 1970 Mineralogical and geochemical aspects of pegmatites from orogenic belts of equatorial and southern Africa. In: Clifford, T.N., and Gass, I.G. (Eds.) *African Magmatism and Tectonics*, Oliver & Boyd, Edinburgh, 157-184.

von Knorring, O., and Condliffe, E. 1987 Mineralized pegmatites in Africa. *Geological Journal* vol. 22, 253-270.

SR-AND MN-ENRICHMENT IN FLUORAPATITE FROM GRANITIC PEGMATITES OF OXFORD COUNTY, MAINE

S. Kreinik[1], M. Felch[1], W. Simmons[1], A. Falster[1], R. Sprague[2]
[1] Dept. of Earth & Environmental Sciences, University of New Orleans, New Orleans, LA 70148;skreinik@my.uno.edu
[2]10 Yates Street, Mechanic Falls, ME 04256

Recent finds of beautiful blue and purple fluorapatite, $Ca_5(PO_4)_3(F, Cl, OH)$, from the Emmons, Pulsifer and Harvard pegmatites are among some of the best examples of royal purple and blue apatite recovered from Maine pegmatites in the last couple of decades. The crystals occur principally in vugs in altered beryl crystals and are associated with a replacement assemblage of bertrandite, cookeite, and Fe/Mn oxide pseudomorphs after siderite/rhodochrosite. Olive-green, blue, teal, lilac, white, and colorless fluorapatite occur within molds of replaced beryl crystals, as well as on cleavelandite. Notably, no pink or yellow colors have been found. A correlation between crystal morphology and color exists. Olive-green crystals tend to form simple elongate or stubby prisms with pinacoids. Blue crystals have similar morphology, but shorter aspect ratios. Colorless crystals tend to be more tabular with modifications by dipyramids and other forms. Purple and lilac fluorapatite tends to occur as complex nearly equidimensional crystals with short prismatic or thick tabular morphology.

Fluorapatite samples were taken from the intermediate and core margin zones of five gem-bearing LCT-type pegmatites in Oxford County, Maine: Mt. Mica, Pulsifer, Harvard, Mt. Marie and Emmons. Electron microprobe analyses reveal that most apatite crystals are close to end-member fluorapatite. Some crystals exhibit significant Sr and Mn substitution for Ca. The SrO content ranges from undetectable up to 21.9 wt. %, MnO content similarly ranges from near zero to 5.6 wt. % and FeO content ranges up to 0.151 wt. %. However, the samples exhibit no systematic variation in the abundance of Sr, Mn, or Fe in core to rim traverses of crystals and show no major compositional differences between pegmatites.

Results show that Sr, Mn and Fe substitute for Ca and range significantly between individual sample transects and between crystals. Samples from the Emmons pegmatite show a range of substitution of Mn and Sr with only minor amounts of Fe (Fig. 1). Strontium content is highest along the rim; a similar trend is seen in some samples from the Harvard quarry. The Pulsifer and Mt. Marie fluorapatites have higher contents of Mn with respect to Sr, with minimal Fe enrichment. There appears to be no systematic difference of OH and F proportions within apatite crystals from the Emmons, Pulsifer, and Mt. Marie. Overall, the OH/F ratios range from 0.14 to 1.00 with values predominantly between 0.17 and 0.6. Data from the Harvard quarry show a progressive increase in OH to F ratios from core to rim (Fig. 2). The OH/F ratios in these cores range from 0.23 to 0.39. In the rims, ratios range from 0.14 to 1.00. This highest value occurs in one rim and is the only apatite that has F equal to OH.

These Oxford County pegmatites are not the only localities exhibiting elevated Sr. Similar Sr enrichment has been documented at Lovozero and Murun in Russia, as well as at Lac De Gras, NWT, Canada (see Chakhmouradian, A. R. *et al.* 2002) and in pegmatites in Grafton Co., New Hampshire, notably the Palermo pegmatite group (Hanson *et al.*, 1990), and raises interesting questions about source material.

No consistent relationship between color, hue and minor element content of the chromophoric ions Mn and Fe was found. Other factors, such as structural defects, are inferred to be responsible for the striking colors of these fluorapatites. The elevated strontium content (up to 21.9 wt % SrO) in many of these samples is of particular significance, suggesting significant enrichment of Sr in the parental pegmatitic melts.

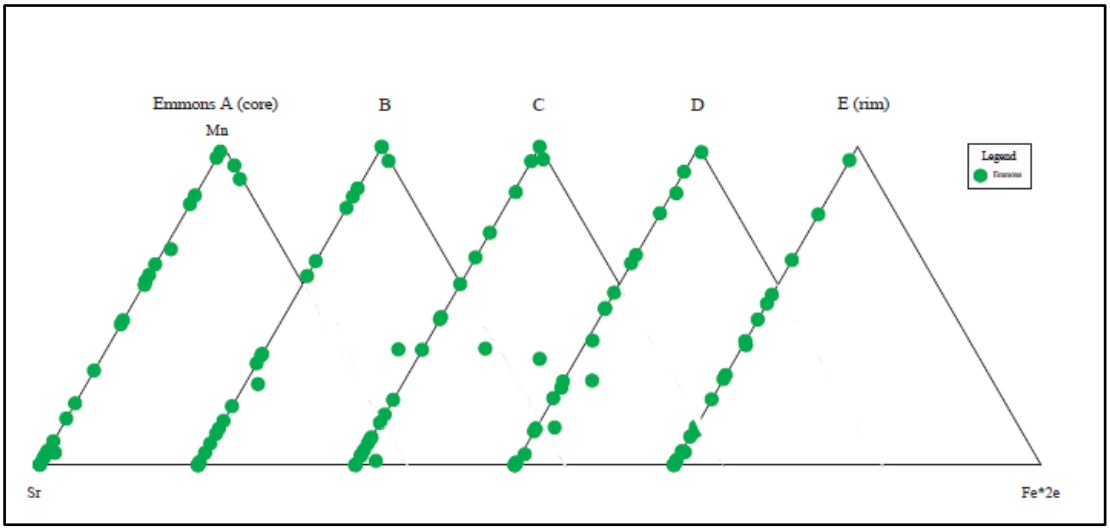

Fig. 1: Emmons Core to rim transect analysis Fe-Mn-Sr

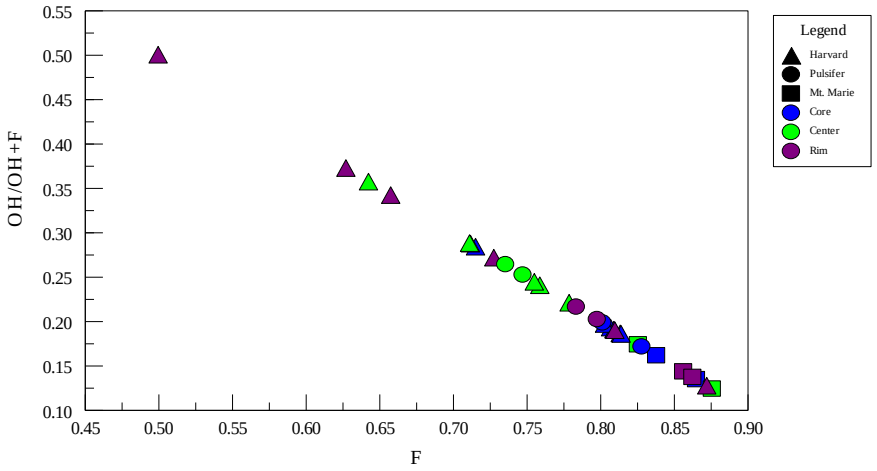

Fig. 2: Harvard, Pulsifer, Mt. Marie Core to Rim OH/(OH+F) analysis

References

Chakhmouradian A.R., Reguir E.P. & Mitchell R.H. (2002) Strontium-apatite: New occurrences, and the extent of Sr-for-Ca substitution in apatite-group minerals. *Can. Mineral.*, 40, 121-136

Hanson, Sarah L., Whitmore, Robert, Dallaire, Donald A., Falster, Alexander U., Simmons, Wm. B. (1990) Late-stage Pocket Apatite from the Palermo No. 1 Mine, North Groton, New Hampshire. Rochester Mineralogical Symposium Abstracts, p. 9-10.

KYSTARYSSKY GRANITE COMPLEX: TECTONIC SETTING, GEOCHEMICAL PECULIARITIES AND RELATIONS WITH RARE-ELEMENT PEGMATITES OF THE SOUTH SANGILEN BELT (RUSSIA, TYVA REPUBLIC)

L. Kuznetsova
Vinogradov Institute of Geochemistry SB RAS, Irkutsk, Russia, lkuzn@igc.irk.ru

Some plutons of Kystaryssky granite complex (KGC): Dzos-Husuingol, Uchug-Lyg, and Tumen-Chulu are spatially associated with rare-element pegmatites of the South-Sangilen pegmatite belt (SSB). The latter is clearly controlled by a sublatitudinal suture zone and includes several pegmatite fields with more than twenty rare-element pegmatite occurrences, all hosted by the Neoproterozoic limestone. The Husuingol field, which incorporates among others - the large Tastyg lithium deposit, is situated in the eastern part of the belt in the vicinity of the Dzos-Husuingol granitic pluton. Lithium pegmatites of the Burcha and Tserigin-Gol fields are located in the middle part of the belt near the Uchug-Lyg granitic pluton. The Kachik field, which includes two big series of lithium pegmatite veins – Sutlug and Harty, is situated in the western part of the belt in the vicinity of the Tumen-Chulu granitic pluton. All pegmatites of the SSB belong to lithium type, spodumene subtype, but have some mineralogical and geochemical similarities with REE-type pegmatites.

New SHRIMP U-Pb dating of zircons from plutons of KGC and from selected lithium-rich pegmatites of SSB have refined their age and tectonic setting. These data show spodumene pegmatite ages from the Tastyg and Sutlug deposits of the SSB as 483 ± 13 and 494 Ma, correspondingly; it is close to the age of Dzos-Husuingol and Tumen-Chulu granite plutons – 489 and 488 Ma, correspondingly (Kuznetsova *et al.*, 2011). Our results suggest that KGC granite and SSB pegmatite ages coincide with the Early Paleozoic collision event during the Sangilen tectono-metamorphic evolution, and may mark the transition from compression (before 490 Ma) to extension (490-430Ma), which was accompanied by formation of strike-slip suture zones (Vladimirov *et al.*, 2005). One of these zones controlled the alignment of sublatitudinal SSB spodumene pegmatites.

Three studied plutons of KGC consist dominantly of biotite porphyritic granite with abundant microcline megacrysts. Minor granodiorite occurs in the outer zones of the main plutons and biotite-muscovite and muscovite leucogranites form small stocks and veins in their vicinity. The latter are accompanied by numerous barren granitic pegmatites. Rare-element spodumene pegmatites are intruded into Neoproterozoic limestone and form a series of different size veins which are generally structurally controlled by linear shear zones. Despite the spatial proximity and similarity in age, of the KGC granite and the pegmatites, there is no geological evidence of a genetic relationship.

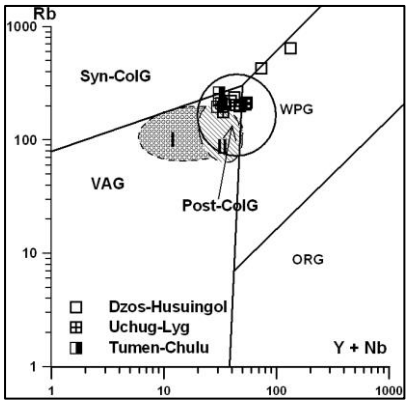

Fig. 1: Geochemical discrimination diagram for KGC granites plotted in Rb vs. (Nb+Y) after (Pearce, 1996)

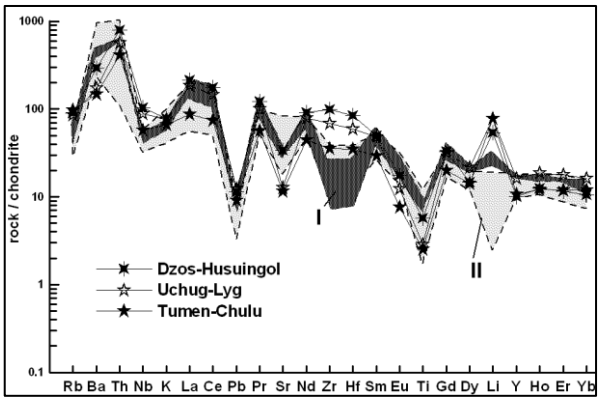

Fig. 2: Chondrite-normalized rare element content in KGC granites vs. Sangilen granites ($Є_3$-O_1)

WPG – within plate, syn-ColG – syn-collisional, post-ColG – post-collisional, ORG – ocean ridge, VAG – volcanic arc, granites. Dashed areas in Fig. 1-2: composition fields of $Є_3$-O_1 granites from Western Sangilen identified as: I – syn- and post-collisional; II - within plate (Kozakov *et al.*, 2003). Chondrite values are from (Taylor and McLennan, 1985).

Geochemically, KGC granitic rocks are classified within the group of ferroan, alkali-calcic, and high-potash granite of A-type affinity. Biotite granites are mildly peraluminous (A/CNK = 1-1.1). Thus, they cannot be definitively defined as I-type or S-type granites. Only in leucogranites does the A/CNK index rise to 1.3. The compositions of KGC biotite granites on the tectonic discrimination diagram (Pearce, 1996) fall in "within plate" (WPG) or in "post collision" (Post ColG) fields (Fig. 1). Their rare-element content, when compared with granites of the same age but different tectonic settings (syn-collisional, post-collisional, within plate) that are exposed in the western part of the Sangilen Highland (Kozakov *et al.*, 2003), shows they have higher Zr, Hf, Nb, Li, Rb contents (Fig. 2). These are not typical of granitic systems evolving towards rare-element granites or pegmatites. On thediagrams K/Rb vs Rb and Zr/Hf vs SiO_2 (Fig. 3) the KGC granites plot along a fractionation pathway that differs from the classical trends characteristic of granites, producing lithophile rare-element deposits (Černý, 1991; Zaraysky *et al.*, 2009).

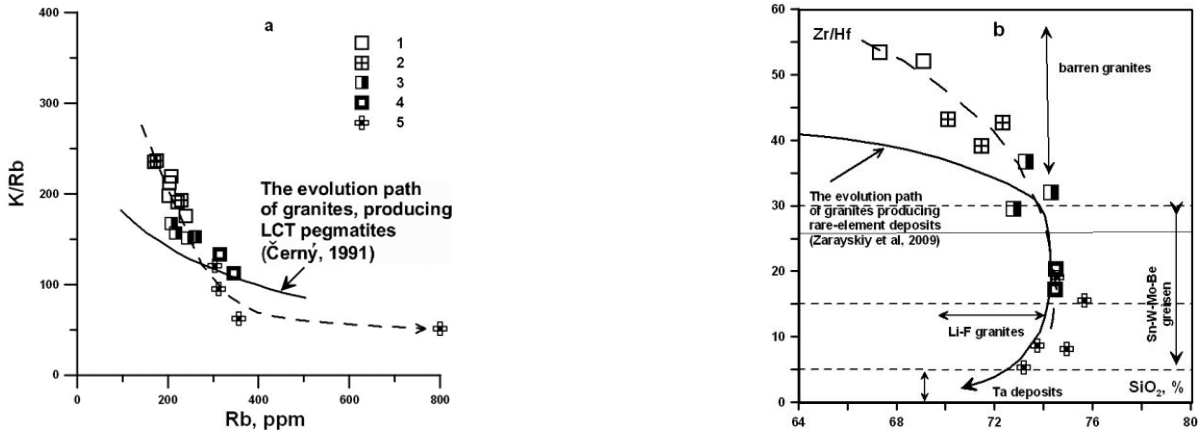

Fig. 3: The evolution paths of the KGC granites plotted in a) K/Rb vs Rb; and b) Zr/Hf vs SiO_2, compared with the characteristic trends of granites, producing lithophile rare-element deposits according to Černý, 1991; Zaraysky *et al.*, 2009.The KGC granites: 1-3 biotite porphyritic granite forming plutons (1- Dzos-Husuingol, 2 – Uchug-Lyg, 3 – Tumen-Chulu); 4 – biotite leucogranite from small stocks, 5 – muscovite pegmatitic leucogranite from veins

The results of our geochemical investigations suggest that KGC granites share some chemical similarities with spodumene pegmatites of this region. Like the KGC granites, the pegmatites are characteristically enriched in two groups of elements (but in differing proportions): Li, Rb, Nb (+Ta, Sn, Be); and Zr, Hf, U (+ Y, REE, Th, Pb). However, significant differences in most of other geochemical parameters between the spodumene pegmatites and the most evolved leucogranites of the KGC suggest they are not cogenetic. It is assumed that both granite systems show mixed tectonic signatures that appear to be the result of (i) post-collisional melting of mixed sources or (ii) significant mantle fluid imprint. To clarify this problem the study of these granitic systems should be continued.

Acknowledgments: this work was supported by the RFBR, project 09-05-01181-a

References

Černý, P. (1991): Rare-element granitic pegmatites. Part II: Regional to global environments and petrogenesis. Geoscience Canada, vol. 18, 68-81.

Kozakov, I.K., V.P. Kovach, V.V. Yarmolyuk *et al.*, (2003): Crust-forming processes in the geological development of the Tyva-Mongolian massif: Sm-Nd isotopic and geochemical data on granitoids. Petrologia, vol. 11 (5), 491-511.

Kuznetsova, L.G., S.P. Shokalsky, S.A. Sergeev (2011): Rare-element pegmatites and pegmatite-bearing granites in the Sangilen mountain area: age, petrogenesis, and tectonic setting. Large igneous provinces of Asia: International Symposium abstract volume, (Russia, Irkutsk, Institute of the Earth Crust SB RAS, August, 20-23 2011), 138-141.

Pearce, J.A. (1996): A user's guide to basalt discrimination diagrams. Wyman D.A. (ed.) Trace elements geochemistry of volcanic rocks: applications for massive sulphide exploration. Geological Association of Canada, Short Course Notes, vol. 12, 79-113.

Vladimirov, V.G., A.G. Vladimirov, A.S. Gibsher *et al.* (2005): Model of tectonic-metamorphic evolution for the Sangilen block (Southeastern Tyva, Central Asia) as a reflection of the Early Caledonian accretion-collision tectogenesis. Earth Sciences Papers, vol. 405 (8), 1159-1165.

Zaraysky, G.P., A.M. Aksyuk, V.N. Devyatova *et al.* (2009): Zirconium-hafnium indicator of rare-element granite fractionation. Petrologia, vol. 17 (1), 28-50.

Taylor S.R., McLennan S.M. (1985) The continental crust: Its evolution and composition. London: Blackwell, 312 p.

THE INFLUENCE OF C-O-H-N FLUIDS ON THE PETROGENESIS OF LOW-F LI-RICH SPODUMENE PEGMATITES, SANGILEN HIGHLAND, TYVA REPUBLIC

L. Kuznetsova[1], V. Prokof'ev[2]
[1]Vinogradov Institute of Geochemistry SB RAS, Irkutsk, Russia, lkuzn@igc.irk.ru
[2]Inst. Of Geology of Ore Deposits, Petrography, Mineralogy and Geochemistry RAS, Moscow, Russia

Fluid inclusions in quartz were studied in spodumene pegmatites from some pegmatite occurrences in the Sangilen mountain area aiming at understanding the influence of C-O-H-N fluids on formation of low-F Li-rich granitoids. These occurrences are hosted by limestone with dispersed carboniferous material of organic origin. SHRIMP U-Pb dating of zircons from lithium-rich pegmatites showed that there were two rare-element pegmatite forming events in this region: first at 494-483 Ma, and second at 290-272 Ma (Kuznetsova et al, 2011). The Husuingol pegmatite field, incorporating the Tastyg lithium deposit, was formed during the first event, and the Sol'belder field originated during the second event. In both fields rare-element pegmatites form series of veins of differening sizes. Most of them belong to spodumene subtype and have weekly zoned internal structure. Fine- to medium-grained quartz-spodumene-two-feldspar mineral assemblage occupies up to 70-80 % of the total volume. This assemblage represents a rather wide evolutionary sequence of compositions (from quartz-spodumene-two-feldspar to almost bimineralic quartz-spodumene), tending towards the enrichment of rocks in spodumene instead of feldspars. Quartz in spodumene pegmatites contains primary magmatic fluid inclusions and lacks secondary inclusions. The goal of this study is to characterize and to compare magmatic inclusion fluid in rare-element pegmatites of the same type, which were formed in the same host rocks, but at different tectonic settings, in order to understand their influence on pegmatite petrogenesis.

Physical-chemical properties of inclusion fluids in quartz were studied by microthermometry; their chemical composition was sampled by a crush and leach extraction of fluid inclusion content from quartz samples (weight 1 g.) and their analysis by gas-chromatography, ion-chromatography and ICP-MS methods. Microthermometric study revealed that primary inclusions are filled with a mixture of dense CO_2±CH_4, N2 gases with a low-salinity water solution. According to ion-chromatography and ICP-MS data the cations in this fluid are dominated by Na, Li, K, Ca; other characteristic cations analyzed are Sr, Ge, W, Rb, Cs, Tl, U, Pb, As, Sb, Zn, Cu, Sn, Fe. The dominant anion is HCO_3^-, levels of B, F, Cl, Br are low.

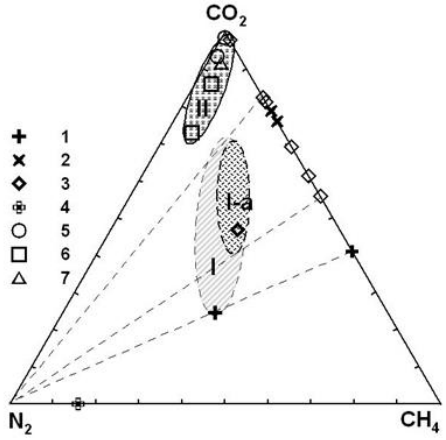

Fig. 1: $XCO_2/XCH_4/XN_2$ molar ratios in gaseous fluids from `quartz of spodumene pegmatites
Dashed areas: Husuingol field - I (including Tastyg deposit - I-a); Sol'belder field - II. Fluid composition from spodumene pegmatites of Husuingol vein series: 1- Sailyg, 2 - Hara-Sug and Pichi-Tastyg, 3-4 – Tastyg; spodumene pegmatites of Sol'belder vein series: 5 - Shuk-Byul, 6 - Kara-Adyr, 7 – Nadejda

Gaseous fluids, extracted from quartz, in each pegmatite field exhibit a large range in $(CO_2+CH_4)/(CO_2+CH_4+H_2O)$ molar ratio, but show relatively constant $CO_2/CH_4/N_2$ and $CH_4/(CO_2+CH_4)$ molar ratios (**Fig. 1, 2-a**). The two latter likely reflect peculiarities of the primary magmatic fluids that exsolved early from the melts in P-T-X conditions specific for each pegmatite field. It is not surprising that these ratios differ strongly between fluids from the spodumene pegmatites of the Husuingol and Sol'belder pegmatite fields as they were formed in different tectonic settings. The variable proportions of carbonic gases and H_2O in the fluids controlled the activity of the main salt components: not only bulk salinity, but molar ratios of the anions (HCO_3^-, B, F Cl) and the cations (Li, Na, K), which show linear correlation trends with carbonic gas ratios -

(CO_2+CH_4) / (CO_2+CH_4+H_2O), and CH_4/(CO_2+CH_4) (**Fig. 2-b-c**). Carbonic gas and water solution
compositional variations during the magmatic stage are thought to reflect changes of both
lithostatic pressure (a tectonic factor) and oxidation-reduction conditions. The influence of progressive melt crystallization on fluid composition was less than expected in Tastyg vein series which is the most differentiated with respect to Li (**Fig. 2-b**). This confirms the supposition (Kuznetsova, 2007; Kuznetsova and Prokof'ev, 2009) that in this case progressive melt crystallization did not play a key role in Li enrichment, but instead the extreme enrichment in Li may occur due to a process of superliquidus delamination of the melt in the magma chamber in a stable reduced fluid regime.

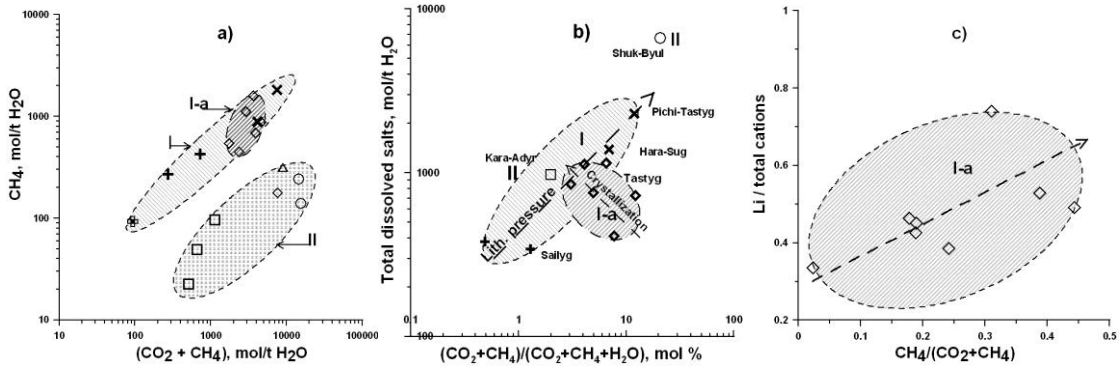

Fig. 2-a-b-c Variations in absolute molar concentrations and molar ratios of inclusion fluid dominant components (based on the reconstructed crush-leach analysis):

a) X_{CH4} vs (X_{CO2} +X_{CH4}); b) total dissolved salts vs (X_{CO2} +X_{CH4}) / (X_{CO2} +X_{CH4}+ X_{H2O}); c) X_{Li} / ΣXcations vs X_{CH4} / (X_{CO2} +X_{CH4}). The arrows (Fig. 2-b) indicate: **Lith. pressure** – the possible direction of increasing lithostatic pressure within pegmatite fields; **Crystallization** – the possible direction of progressive melt crystallization in the Tastyg vein series.

During the formation of spodumene pegmatites in the Husuingol field, incorporating the largest Tastyg lithium deposit, the initial pressure reached 4.2 kb at 600° C and fluids were strongly reduced (Kuznetsova and Prokof'ev, 2008, 2009). Enrichment of spodumene pegmatites in the Husuingol field, not only in Li and other characteristic rare elements (Ta, Nb, Sn, Be), but also in some atypical elements (REE, Y, Zr, Hf, U, Th, Pb), supports the supposition regarding mantle reduced C-O-H-N fluids imprint on their parental granitic melts. The spodumene pegmatites in the Sol'belder river basin crystallized in the presence of more oxidized fluids (composed of dense CO_2 with minor amounts of CH_4 and N_2) and under the higher initial pressure (up to 6 kb at 600° C). It is assumed that increased fluid pressure intensified CO_2 activity which promotes contamination and more intensive crystallization differentiation of the pegmatite melts. This fluid regime is responsible for a great diversity of pegmatite mineralization in the Sol'belder field. It caused the rare-element character of the pegmatites to change from Li dominant, with elevated Ca, Sr, and CO_2, to Li-Cs-Ta character with elevated F & B and the lowest content of REE, Y, Zr, Hf, U, Th, & Pb.

Acknowledgments: this work was supported by the RFBR, project 09-05-01181-a

References

Kuznetsova L.G. (2007): Geochemistry of Li-rich aplite-pegmatites enclosed in bituminous limestones (Sangilen area, south Siberia). Granitic pegmatites – the state of the art. Mem. Un. Porto, (8), 52-53.

Kuznetsova, L.G., V.Yu. Prokofiev (2008): The role of fluids in the formation of limestones-hosted Li-rich aplites and pegmatites. Proceedings of XIII Intern. Conf. on Thermobarogeochemistry and IVth APIFIS Symposium. (Russia, Moscow, IGEM RAN, Sept., 22-25 2008), vol. 1, 102-105.

Kuznetsova, L.G., V.Yu. Prokof'ev (2009): Petrogenesis of anomalous Li-rich spodumene aplites of the Tastyg deposit (Sangilen area, Tuva Republic, Russia). Dokl. Earth Sci., vol. 429 (8), 1262-1266.

Kuznetsova L.G., S.P. Shokalsky, S.A. Sergeev (2011): Rare-element pegmatites and pegmatite-bearing granites in the Sangilen mountain area: age, petrogenesis, and tectonic setting. Large igneous provinces of Asia: International Symposium abstract volume. (Russia, Irkutsk, Institute of the Earth Crust SB RAS, August, 20-23 2011), 138-141.

SEIXOSO-VIEIROS RARE ELEMENT PEGMATITE FIELD: DATING THE MINERALIZING EVENTS

A. Lima[1,2], L. Mendes[1,2], J. Melleton[3,4], E. Gloaguen[3,4], D. Frei[5]
[1] DGAOT, FCUP, R. Campo Alegre, 687, 4169-007 Porto, Portugal (allima@fc.up.pt)
[2] Geology Centre of Porto, R. Campo Alegre, 687, 4169-007 Porto, PortugalPortugal
[3] BRGM, Direction des Géoressources, ISTO, UMR7327, B.P. 36009, 45060 Orléans, France
4 Université d'Orléans, ISTO, UMR 7327, 45071 Orléans, France
[5] Stellenbosch University, Department of Earth Sciences, Private Bag X1, Matieland, 7602, South Africa

The Seixoso-Vieiros Rare Element Pegmatite Field is included in "Galicia Trás os Montes geotectonic zone" in northern Portugal defined by Farias et al (1987). The Seixoso-Vieiros pegmatite field is known for containing numerous granitic pegmatite-aplite veins (Seixoso and Vieiros pegmatites). The area is bounded at the north by the Variscan Celorico de Basto granite massif. On the SE it is bounded by the syn- tectonic Felgueiras granodiorite. Several pegmatites outcrop within cordierite-andalusite isograde Silurian schists. The field is also known for mining of cassiterite and columbite-tantalite in the last century (Maijer, 1965).

In the Seixoso area, an unusual heterogeneous granitic intrusion outcrops as two main apices in Seixoso and Outeiro as granites cupolas (Lima *et al.*, 2009). These rocks show a typical granitic mineral assemblage and exhibit a textural variation from biotite-bearing, at depth, to two mica, or muscovite tourmaline, near the apex roof (Helal *et al.*, 1993).

The Seixoso granite is described as a fine to medium-grain leucogranite, with biotite and muscovite, strongly altered with albitization and greisenization close to the contact zones. The Outeiro granite is layered and shows pegmatitic segregations. In the latter, Li-bearing minerals, such as petalite and spodumene, have been observed. In addition, minerals from the amblygonite-montebrasite series have also been noted within the granitic mineral assemblage (Lima *et al.*, 2009). Other notable accessory minerals include: beryl, chrysoberyl, tourmaline and sekaninaite, and others.

In the Vieiros area, the granitic aplite-pegmatite veins mainly cross-cut schists of Silurian age within the andalusite isograde. A dozen N-S to NE-SW-trending Sn-bearing granitic aplite-pegmatite veins outcrop in the area. They present a rich mineralogy: quartz, K-feldspar, albite, muscovite, petalite, spodumene, amblygonite-montebrasite, cassiterite, columbite-tantalite, tourmaline, and many different sulfides. An albite type pegmatite is exposed in the Vieiros mine and measures 300 meters in length, an average 5 meters in width, and is subvertical, striking E-W, and dips N25°.

During this study (Melleton *et al.*, submitted), columbite and tantalite grains were dated by the U-Pb method, using the LA-SF-ICP-MS technique, from the Outeiro mine granite and the Vieiros mine albite type pegmatite. Results of dating (figure 1) from the Vieiros pegmatite yield an age of emplacement of 301 ± 4 Ma (12 analyses). Ages obtained from the Outeiro granite yield 301 ± 5 Ma (9 analyses) and 316 ± 9 Ma (from two analyses located in cores of two different single grains, and with significantly low concentrations of U). This latter age is interpreted as age of crystallization of the Outeiro granite, and the younger age corresponds to post-emplacement disturbance related to the Vieiros-Seixoso pegmatite emplacement, located in the surrounding area.

Located hundred meters from the Outeiro mine granite, the Seixoso pegmatite shows similar structural and mineralogical features as the Vieiros pegmatite. Therefore, emplacement of these pegmatites and associated fluids could have been the cause of the Outeiro Mine columbite-tantalite rim age. The Celorico de Basto late-D3 granite in the north and the Felgueiras syn-D3 granodiorite in the south had not been directly dated. However, Dias *et al.* (1998) dated equivalent granitoids and obtained ages around 305-308 Ma for the late D3 granite and early ages ranging between 310 and 320 Ma for the syn-D3 granites. Thus, there is not a temporal link between the Vieiros pegmatite emplacement and the surrounding granites of this field.

New samples are being collected in order to understand the different mineralizing events and relationships between other pegmatites and surrounding granitic cupolas of the studied area.

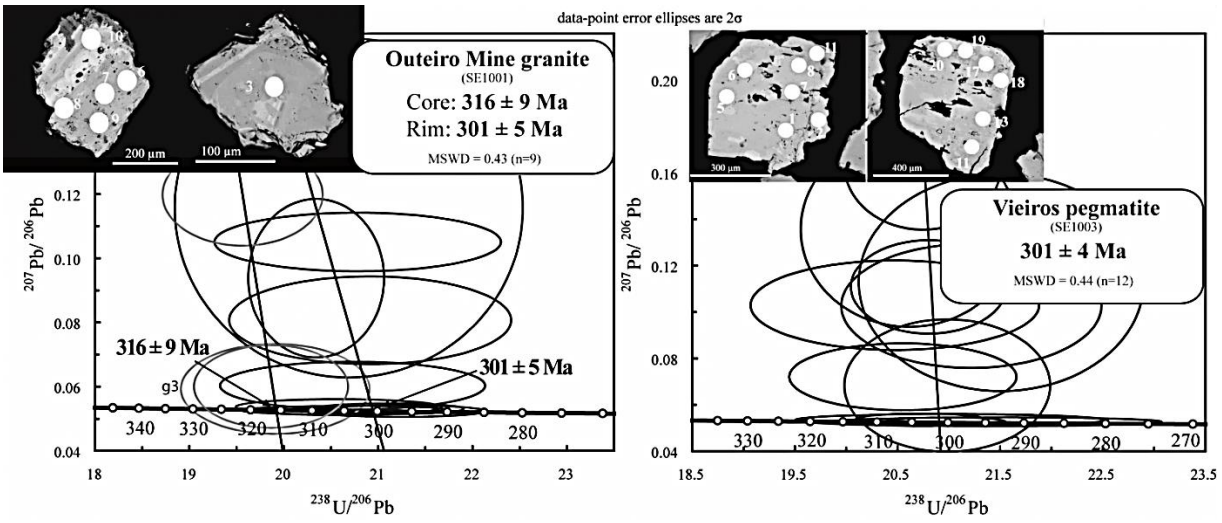

Fig. 1: Results of U-Pb dating on tantalite from the Outeiro Mine granite and the Vieiros pegmatite

References

Dias, G., Leterrier, J., Mendes, A., Simões, P.P., Bertrand, J.M. (1998) U-Pb zircon and monazite geochronology of post-collisional Hercynian granitoids from the Central Iberian Zone (Northern Portugal). Lithos, 45, 349-369.

Farias, P., Gallasteui, G., Lodeiro, F. G.Marquinez, J., Parra, L. M. M., Catalán, J. R. M., Macia, G. P., Fernandez L. R. R. (1987) Appontaciones al Conocimiento de la Litoestratigrafia y Estructura de Galicia central. IX Reunião de Geologia do Oeste Peninsular. Publicação do Museu e Laboratório Mineralógico e Geológico da Faculdade de Ciências, Universidade do Porto, 1, pp. 411- 431. In Spanish.

Helal B., Bilal E., Pereira E. (1993) "Nigerite in rare-element pegmatites and associated granites of Seixoso área (Northern Portugal)". Current Research in Geology Applied to Ore Deposits. Fenoll Hach-Ali, Torres-Ruiz & Gervilla (eds). p.253-257.

Lima A., Rodrigues R., Guedes A., Novák M. (2009) The Rare Elements-Rich Granite Of Seixoso Area (Outeiro Mine). Preliminary results. Estudos Geológicos v. 19 (2), p. 182-187

Maijer, C. (1965) "Geological investigations in the Amarante Region(Northern Portugal) with special reference to the mineralogy of the cassiterite-bearing albite pegmatites". PhD Thesis. Grafi sch Centrum Deltro, Rotherdam, Netherlands, 153 p.

Melleton, J., Gloaguen, E., Frei, D., Lima, A., Roda-Robles, E., Vieira, R., Martins, T. (submitted). Polyphased rare-element magmatism during late orogenic evolution: geochronological constraints from the NW Variscan Iberia. Submitted to Journal of GEOsciences.

CHARACTERIZATION AND ORIGIN OF "COMMON PEGMATITES": THE CASE OF INTRAGRANITIC DIKES FROM THE PAVIA PLUTON (WESTERN OSSA-MORENA ZONE, PORTUGAL)

S.M. Lima[1], A. Neiva[1], J. Ramos[2]
[1] Department of Earth Sciences and Geosciences Centre, University of Coimbra (Portugal), selmalima252@gmail.com
[2] LNEG, S. Mamede de Infesta (Portugal)

Common pegmatites are important ore bodies providing feldspars and quartz for the glass, ceramics and electronics industries (London 2008). Nevertheless, this type of pegmatite is usually ignored or just referenced in most recent literature. Only a few studies exist concerning their characterization and genesis (e.g. Ackerman *et al.* 2007).

Several aplite-pegmatite and pegmatite dikes, mainly oriented NW-SE and NE-SW, were found cutting the different rocks that compose the Pavia pluton and the amphibolitic facies country rocks. The Pavia pluton is a multiphasic intrusive body constructed over ca. 11 m.y. (Lima *et al.* 2012). It is located in western Ossa-Morena Zone (Portugal) and is composed of rocks ranging from biotite>amphibole tonalite to two-mica granite. It intruded the Neoproterozoic Gneiss-Migmatite Complex, metamorphosed in the Early Carboniferous, and the Middle/Upper Cambrian-Ordovician schist, metabasite and metapelite (Moura Schists and Carvalhal Formations). The pegmatites are centimetric to metric tabular dikes characterized by high length/width ratios and sharp, although locally lobated, contacts with the hosts.

The dikes are composed of ordinary igneous minerals that compose the different classes of igneous rocks (quartz + oligoclase to albite + microcline + orthoclase + muscovite + apatite ± biotite ± garnet ± oxides (mainly magnetite) ± epidote ± titanite). None of the 24 sampled dikes are particularly enriched in the minor key elements used to distinguish pegmatite families: LCT type (lithium-cesium-tantalum) and NYF type (niobium-yttrium-fluorine). Maximum contents of these elements are: 39 ppm (Li), 8.2 ppm (Cs), 1.5 ppm (Ta), 9.9 ppm (Nb), 22.5 ppm (Y) and 0.04% (F). The simple mineralogy and lack of conspicuous enrichment in the aforementioned elements allow classification of them as "common pegmatites" (London 2008). Common pegmatites may be included in the abyssal or muscovite classes. The absence of even minor mineralization (barren) and the occurrence of muscovite as a major mineral phase in all the dikes indicate that they belong to the muscovite class of Černý and Ercit (2005).

Age constraining of seven dikes by ID-TIMS U-Pb dating (using zircon and monazite) revealed the existence of, at least, 3 different generations. The first generation (328 Ma) is contemporaneous with the emplacement of the central domain of the pluton (domain I: tonalite, granodiorite and trondhjemite), the second (ca. 324 Ma) is coeval with the emplacement of the flanking rocks (domain II: granodiorites and granite) and the third (319-317 Ma) is related to a late magmatic episode only recorded in microgranite and pegmatite dikes (Lima *et al.* 2012). Overall, they are chemically, isotopically and mineralogically identical. All dikes present microscopic evidences of intense ductile and fragile deformation (e.g. intense dynamic recrystallization of quartz, deformation twins on orthoclase, microkinking and deformation of the twinning/cleavage planes of plagioclase and micas, abundant myrmekites). The host rocks also exhibit this type of deformation which was probably caused by the third Variscan deformation phase affecting the area [D3 at ca. 306 Ma (Moita *et al.* 2005)].

Whole rock variation diagrams suggest that, of the studied granites (*s.l.*), the biotite>muscovite granodiorite (G2G; for dikes emplaced at 328 Ma) and the two-mica granite (G6; for dikes emplaced at ca. 324 Ma) are the most probable parental rocks. The similarity in the whole rock Sr-Nd isotopic data and $\delta^{18}O$ variations of less than 1‰ in addition with the observed positive correlation between $\delta^{18}O$ and SiO_2 (wt. %) from granites (*s.l.*) to dikes confirms that G2G and G6 can, indeed, represent the magmas from which the pegmatites fractionated. However, the increase in K/Rb and Mg/Li with decreasing total FeO, the crosscutting REE patterns and distinctive Eu behavior in contemporaneous dikes, the higher An content of plagioclase from one pegmatite dike compared to plagioclase from G6, the lack of linear trends between micas from G2G and G6 and micas from the two generations of pegmatites and the lower to similar F content of apatite from dikes and apatite from G2G, question the existence of a genetic relation between the granites (*s.l.*) and the dikes by simple continuous fractionation.

The restricted assemblage of accessory minerals (indicating that the Pavia pegmatites are depleted in a number of rare elements, volatile and fluxing components), absence of Sn, Ta and Nb minerals and low sum of these elements in whole rock analyses (3.6 to 12 ppm) is suggestive of a primitive source (cf. Černý 1989). This is in good agreement with the slightly negative εNd_t values (-1.3 to -3.7), low $(^{87}Sr/^{86}Sr)_i$ values (0.70434 to 0.70581) and zircon $\delta^{18}O$ (6.4‰ in the three generations). These values are indicative of mantle-derived melts and indicate that the three generations have a similar and pretty homogeneous source.

The Pavia pluton main granitic phases were interpreted as resulting from fractional crystallization of a mantle-derived melt with very limited crustal contribution (Lima *et al.* 2013) and the geochronological data suggests that it was emplaced by the episodic intrusion of several batches of magma. The episodic character is related to changes in the tectonic regime (compression = emplacement and extension = recharge of the magma chamber) (Lima *et al.* 2012). A relation with coeval but non-outcropping rocks or with neighboring plutons cannot be excluded but, under such complex scenario, it is probable that the genetic relationship between the Pavia granites (*s.l.*) and pegmatites is masked by an intricate mechanism involving small degree differentiation of mantle-derived batch(es) of magma, interaction with new batches of magma and minor interaction with anatectic crustal melts. Interaction with crustal melts is supported by the slightly higher and variable values of whole rock $\delta^{18}O$ (6.6-8.3‰ in the hosts and 8.2-9.6‰ in the pegmatites), slightly negative εNd_t and the small variations in REE contents and in the accessory minerals assemblage. The lack of chemical evolution (via fractionation) between generations spanning over ca. 11m.y. is due to episodic refills of the magma chamber with new isotopically similar and chemically more primitive batches of magma. This mechanism allows to justify the genesis of the three generations of pegmatites that, representing the differentiation products of distinct batches of a similar and fairly primitive and homogeneous source (injected episodically as the result of changes in the tectonic regime), share an identical major and trace geochemical and isotopic compositions. Therefore, the Pavia pegmatites do not represent the final stages of the pluton differentiation but only slightly evolved melts of independent batches of magma. Even though a genetic relation or evolution cannot be traced from the outcropping granites (*s.l.*) to pegmatites, they share the same history and evolution and may, indeed, be genetically related.

Mechanisms like this can bring some light to the frequent difficulty to relate pegmatites and outcropping granites in some pegmatitic fields.

References

Ackerman, L. Zachariáš, J. Pudilová, M. (2007). P-T and fluid evolution of barren and lithium pegmatites from Vlastějovice, Bohemian Massif, Czech Republic. International Journal of Earth Sciences 96, 632-638.

Černý, P. (1989). Contrasting geochemistry of two pegmatite fields in Manitoba: products of juvenile Aphebian crust and polycyclic Archean evolution. Precambrian Research vol. 45 (1-3), 215-234.

Černý, P. Ercit, T.S. (2005). The classification of granitic pegmatites revisited. Canadian Mineralogist vol. 45, 2005-2026.

Lima, S.M. Corfu, F. Neiva, A.M.R. Ramos, J.M.F. (2012). Dissecting complex magmatic processes: an in-depth U-Pb study of the Pavia pluton, Ossa-Morena Zone, Portugal. Journal of Petrology, vol. 53 (9), 1887-1911.

Lima, S.M. Neiva, A.M.R. Ramos, J.M.F. (2013). Adakitic-like magmatism in western Ossa-Morena Zone (Portugal): geochemical and isotopic constraints of the Pavia pluton. Lithos 160-161, 98-116.

London, D. (2008): Pegmatites. The Canadian Mineralogist Special Publication 10, 347 p. (ISBN: 978-0-921294-47-4).

Moita, P. Munhá, J. Fonseca, P.E. Tassinari, C.C.G. Araújo, A. Palácios, T. (2005). Dating orogenic events in the Ossa-Morena Zone. XIV Semana de Geoquímica/VIII Congresso de Geoquímica dos Países de Língua Portuguesa, Aveiro, Portugal, 459-461.

CHAMBER PEGMATITES OF VOLODARSK, UKRAINE, THE KARELIA BERYL MINE, FINLAND AND SHALLOW DEPTH VEIN PEGMATITES OF THE HINDUKUSH- KARAKORUM MOUNTAIN RANGES. SOME OBSERVATIONS ON FORMATION, INNER STRUCTURES, RARE AND GEM CRYSTALS IN THESE OLDEST AND YOUNGEST POCKET CARRYING GEM PEGMATITES ON EARTH

P. Lyckberg[1], V. Chournousenko[2], A. Hmyz[2]
[1] European Commission, lyckberg@pt.lu, [2] Volhyn Quartz Samotsvety

Mining for piezo quartz in Soviet times at Volodarsk-Volhyn in the western endo contact of the 1.7 Ga Korosten Pluton in Ukraine exposed some1500 chamber pegmatites. The pegmatites are cogenetic with the enclosing granite and the most developed single chamber pegmatites are in general spheroidal having formed under uniform conditions with horizontal and vertical stresses equal.

Studies of many of these pegmatites in 6 shafts within the 22 km long field during the past 25 years reveal some new observations. Gem beryl occurs in only 2% of all pockets but locally in significant quantities and of exceptional quality. Some gem beryls studied show original growth of now dissolved lamellar matrix believed to be originally crystallized on ceavelandite at the bottom of the pockets. Careful excavation of several beryl bearing pockets showed beryls to be localized to such a layer of former cleavelandite which ones formed the bottom of the pocket.

Late stage hydrothermal solutions leached quartz from the graphic zone below the pocket. This quartz appears to have been re-deposited as giant crystals on the ceiling. Strong albitization occurred in this leached zone below the pockets. In most pockets the great majority of quartz crystals fell from the roof, some of them breaking and re-crystallizing. The original cleavelandite matrix pocket bottom was broken up and dissolved and thus no beryls have been found growing standing on cleavelandite. In some pockets, a second more extensive layer with slightly to strongly etched beryl was found below the original pocket in the leached zone.

Topaz occurred in around 10% of pockets. In a great majority of pockets topaz was found as loose crystals and only a few samples of heavily damaged crystals on cleavelandite matrix were recovered from the dumps by shaft 2. The authors discovered and excavated several pockets where large champagne/salmon to bi-colored topaz crystals were found.

One extraordinary pocket, named Peter's pocket by the mine geologists, showed rich mineralization in primary orientation. Here, light champagne-colored complex topaz crystals grew from the pocket ceiling, whereas bi-colored crystals of various habits occurred on albite, and zinnwaldite/lepidolite crystals to 10cm in situ on walls and on the floor. One giant crystal found with sharp wedge-shaped termination measured 76 cm in diameter and is the largest known from the deposit. This crystal was found growing in almost vertical position with its termination upwards a meter above the floor of the pocket. It is the first time such rich mineralization was found and studied at this deposit. In the same section of the pocket the authors discovered a pile of some 15 blue topaz cleavages of one former 12*12*20 cm blue topaz crystal. The cleavage pieceshad separated slightly and were leaning against the wall. Different pockets show various late-stage minerals crystallizing between the fractured layered ceiling of the pockets. These include ball like aggregates of 2-6 cm mats and balls of "goethite", and 0.5 to 5 cm siderite rhombs. In some pockets siderite crystals were golden brown and of gem quality. Purple to almost black fluorite of various morphology occurred in several pockets. Kerite was found in as black cotton like wad in topaz pockets. Molybdenite was encountered both in the granite as well as in crystals to 4 cm in one pegmatite. One large pocket yielded blue/purple and green fluorite cubes to 25 cm, octahedra and rare dodecahedra to 15 cm together with calcite.

Work at the Karelia Beryl pegmatite (1.64 Ga) at Kännätsalo, Luumäki, Karlia, Finland during 1984-2004 suggest a spectrum of gem beryl formation in one and the same pegmatite (Lyckberg 2006). Here the finest flawless green gem beryl discovered in the European Union was mined with gemmy crystals to 22 cm length and 1.6 kg weight. Semi gemmy crystals weighed up to 9kg. In the same pocket some rare light pink topaz was found as fragments and yielding cut stones to a few carats.

The Hindukush pegmatites were mined at Dara-i-Nur 1950-60 for beryl with a production of 130t, while gem tourmaline was discovered at Kala village in 1959. In 1969 the first gem tourmaline was found by Jabir (Lyckberg 2011) at the Paprok main pegmatite, Lohi Maden (big Mine) at 4560-4780 m altitude a good 8 hours and 16 km walk to

the WNW of Paprok Village, Nuristan, Afghanistan. Soviet and Afghan geologists studied the very extensive and rich pegmatite fields of NE Afghanistan in the 1960-70's, drilled, mined and recovered gem kunzite, tourmaline, and rare element minerals. Here pegmatites are exposed that formed over 2000m vertically apart. At Noor Ahmed madan large Morganites were found. The Paprok pegmatites have been mined extensively with tunnels reaching 200 m. According to miners, the outer section of the pegmatite was the richest. Pockets have produced not only beautiful multicolored tourmaline specimens in combinations with quartz, feldspars, lepidolite, microlite but also very fine large crystals of gemmy pollucite, hambergite, beryllonite sometimes in combination with gem elbaite crystals and the world´s finest viitaniemiite crystal, 17 cm long on lepidolite. (Lyckberg, 2011). Pegmatites in the Pech Valley are producing very fine morganite crystals to 25cm as well as first and second generation elbaite tourmalines of which the second may be as exceptionally fine gem crystals of green to blue colors reaching 20 cm in length. The most productive pegmatites are at Kala, Ghosallak, Voradesh, Gamata, Kantiwa. Pezzottaite, pollucite, viitaniemiite, fluornatromicrolite and other rare species also occur here. At Mawi in the Konar province a giant pegmatite has been producing morganite, elbaite and extraordinary quantities of huge kunzite crystals to very large size. One pocket yielded 2tons, and several other pockets yielded up to 500 kg. Nilaw and Korgal produce gem tourmaline.To the south, the Pashagar Mine produced 70 smoky quartz specimens with rubellite elbaites. In 2010 an exceptional pocket with perhaps the world's finest Kunzite crystals was found at Waygal. The sharp twinned crystal measures 55 cm long, around 8 cm in square, is flawless and of deep violet color with blue termination.The Paroon pegmatites have produced exceptional indigolite, rose quartz crystals and childrenite. Hydrothermal veins at Chumar Bakhoor where fissures and pockets lined with muscovite crystals upon which blue aquamarine crystals, pink fluor apatite, pink and green fluorite and feldspars occur. Fluorite occurs in several forms typically and pink octahedrons, cube-octahedra, spinel law twins to 20 cm and rare dodecahedra.

The young (5-20Ma) gem pegmatites of the Haramosh Mountains of Pakistan produced tourmaline, topaz, morganite at Stak Nala in 2012. The Dusso Haramosh pegmatites are located on a vertical cliff at high altitude (4200-4500m). Only the local miners are granted access. The first visitor to these pegmatites was the senior author who visited in 2004. Here the very finest of aquamarine and topaz specimens in Pakistan were found in the past, with crystals perched upon snow white albite, associated with schorl, light smoky quartz, green to purple fluorite and green hydroxyl herderite. Pegmatites at Shengus and Bulachi has produced exceptionally blue gem aquamarine crystals to 15cm (2010-2011), goshenite, morganite, väyrynenite, topaz, cassiterite,beryllonite crystals to 35 cm (2012) as well as pollucite to 30cm (2010). Mines in the Shigar Valley continue to produce aquamarine and topaz specimens and the past few years has seen heavy development of 80 aquamarine mines at low altitude at Bensapi bridge (2500m) and the high altitude topaz mines above where in 2012 a large pocket with over 85 exceptional doubly terminated champagne-colored topaz crystals 3-5 cm in size and larger crystals on matrix including a large plate with14 topaz crystals, was discovered. Other pegmatites of this region have recently produced exceptional almost emerald-colored large gem beryl to over 1 kg, and very fine large aquamarines to 15 cm on and off matrix in the past few years.

References

Lyckberg, P. (2004): Ein Neufund phantastischer grüner Edelberylle aus Luumäki, Karelien, Finnland. Mineralien Welt 15 (6), 38-45.

Lyckberg, P. (2006): Miarolitic pegmatites of the Viborg rapakivi granite massif, SE Finland with special attention to the green gem beryl producing Karelia Beryl Mine pegmatite at Luumäki, Karelia. Norsk Bergverksmuseum Skrift. 33, 87-107 Mineral Symposium Kongsberg, Norway.

Lyckberg, P., Chournousenko V.A., Wilson, W.E (2009): Volodarsk-Volhynsk, Zhitomirskaja Oblast, Ukraine: Mineralogical Record 40, 473-506.

Lyckberg, P., (2011): Paprok: Mineralien Welt, vol. 22(3), pp 46-57.

Lyckberg, P (2011): Chumar Bakhoor: Mineralien Welt, 22 (4) pp 67-77.

Lyckberg, P. (2011) Locating Gem Pockets in Pegmatites – A Worldwide Study and Comparison. GIA Conference May 2011, Carlsbad, California. Gems & Gemology 47,111-112.

Lyckberg, P., (2001): Gem pegmatites of Ukraine, Kazachstan and Tajikistan (abstract), Mineralogical Record, 32 (1), 45.

Lyckberg, P. 2004: Recent gem beryl production in Finland. *G&G* **40**: 256-258.

Lyckberg, P. (2005): Gem beryl from Russia and Ukraine. Beryl and its Color Varieties. Lapis Intl., L.L.C., East Hampton, CT, USA, 49-56.

Lyckberg, P., (2005): Finland´s famous find. In Extra Lapis English no 7. Lapis International LLC, 63.

Lyckberg, P., (2011): Upcoming deposits of the world and the russian emerald deposits. From Mines to Market Conference, Jaipur, India. http://m2m.gjepc.org/speakers.html

Lyckberg, P., (2010), April 6th). Lecture Pegmatites on Day of the Geologists at the St Petersburg State University

Lyckberg, P., (2012, November 9th). Lecture Gem Pegmatites: Mindat Conference,Midelt, Morocco.

Lyckberg, P., (2012, November 30th). Lecture Recent Finds around the world: Fersman Museum, Moscow.

Simmons, W.B. (2007): Gem-bearing pegmatites. Geology of Gem Deposits. MAC Short Course Series, 37, 169-206.

Simmons, W.B et al (2012): Granitic Pegmatites as Sources of Colored Gemstones, Elements vol. 8, pp. 281-287

COMPOSITIONAL EVOLUTION OF PRIMARY TO LATE TOURMALINES FROM CONTAMINATED GRANITIC PEGMATITES; A TREND TOWARDS LOW-T FIBROUS TOURMALINES

I. Macek[1], M. Novák[2], R. Škoda[2], J. Sejkora[1]
[1] Department of Mineralogy and Petrology, National Museum, Prague, Czech Republic, ivo_macek@nm.cz
[2] Department of Geological Sciences, Masaryk University, Brno, Czech Republic

The tourmaline-group minerals are useful geochemical indicators (van Hinsberg *et al.* 2011) due to their refractory behavior, crystal structure, which can incorporate a wide spectrum of elements, and a very wide stability field. In order to reveal compositional trends from early to late fibrous tourmalines, we studied chemical compositions of late fibrous tourmalines which overgrow early tourmalines from three externally contaminated LCT granitic pegmatites: (i) simple desilicated pegmatite situated on the contact of serpentinite and migmatic gneiss from Dolní Bory, western Moravia, Czech Republic; (ii) two elbaite-subtype pegmatites Bližná I, Southern Bohemia, Czech Republic (Novák *et al.* 1999, 2012), and (iii) Tamponilapa, Sahatany Valley, Madagascar, the latter two enclosed in silicates-rich dolomite-calcite marbles (Fig. 1).

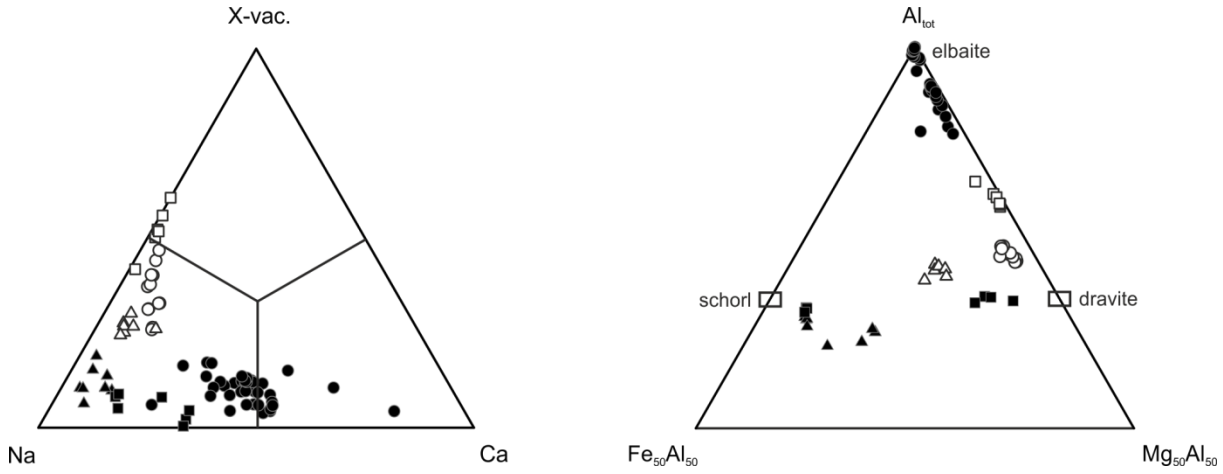

Fig. 1: Chemical compositions of early (solid symbols) and late (empty symbols) tourmalines from the individual localities: triangle – Dolní Bory, circle – Bližná I, square – Tamponilapa.

Additional compositional characteristics of tourmalines at the individual localities are given below. (i) Early black schorl with Ca 0.04–0.12 *apfu*, Mn 0.02–0.14 *apfu*, Al_{tot} 5.07–5.98 *apfu*, Ti 0.07–0.26 *apfu* is overgrown by late fibrous greyish dravite (enclosed in opal-CT) with Ca 0.06–0.14 *apfu*, Mn ≤ 0.01 *apfu*, Al_{tot} 6.07–6.37 *apfu* Ti ≤ 0.05 *apfu*. (ii) Fibrous pale blue dravite with Ca 0.04–0.13 *apfu*, Mn ≤ 0.02 *apfu*, Al_{tot} 6.15–6.36 *apfu* with no significant Ti content grows on an olive green to brown aggregate of liddicoatite-elbaite-uvite with Ca 0.23–0.79 *apfu* , Mn 0.03–0.88 *apfu* , Al_{tot} 6.67–7.66 *apfu* , Ti 0.03–0.21. (iii) Early black schorl Ca 0.13–0.15 *apfu* , Mn 0.06–0.08 *apfu*, Al_{tot} 5.97–6.01 *apfu* , Ti 0.11–0.13 *apfu* and early black dravite with Ca 0.24–0.33 *apfu* , Mn 0.04–0.06 *apfu* , Al_{tot} 5.94–6.01 *apfu* , Ti 0.02–0.05 *apfu* are overgrown by colorless fibrous magnesio-foitite with Ca ≤ 0.02 *apfu* , Mn 0.03–0.06 *apfu* , Al_{tot} 6.92–7.15 *apfu* and Ti content below detection limit.

Textural relations, mineral assemblages, and chemical compositions of the individual tourmalines indicate substantial changes in crystallization conditions such as (i) evident decrease in temperature, (ii) transition of parental medium from pegmatite melt to hydrothermal fluids, and (iii) opening of the system to host rocks in subsolidus. Magnesium in late tourmalines is probably sourced from Mg-rich host rocks (serpentinite, marble). In contrast, disregarding high Ca content in host dolomite-calcite marbles and common diopside, danburite and high Ca in primary tourmalines, late tourmalines are almost Ca-free.

The compositional trends in the individual localities (Fig. 1) are very distinct in highly variable early tourmalines (schorl, dravite, elbaite-

liddicoatite-uvite) but the latter type of tourmaline is dravite or schorl-dravite and the latest fibrous tourmalines are characterized by high Mg contents, low to negligible Ca, Mn, Ti and Fe concentrations and high vacancy in X-site tending to magnesio-foitite. Such compositional characteristics – chiefly high X-site vacancy – are typical for authigenic tourmalines (e.g. van Den Bleekn 2007) and point out that at low-T conditions tourmalines tend to similar compositions (X-site vacant magnesio-foitite or foitite species) disregarding their host rocks.

This work was supported by the research project GAP210/10/0743 to MN and RŠ and by internal grant of the National Museum, Prague 2011/05/IG-PM to IM.

References

Novák, M., J. B. Selway, P. Černý, F. C. Hawthorne (1999): Tourmaline of the elbaite-dravite series from an elbaite-subtype pegmatite at Bližná, southern Bohemia, Czech Republic. European Journal of Mineralogy, vol. 11, 557-568.

Novák, M., R. Škoda, P. Gadas, L. Krmíček, P. Černý (2012): Contrasting origins of the mixed signature in granitic pegmatites; examples from the Moldanubian Zone, Czech Republic. The Canadian Mineralogist - Petr Černý Issue, vol. 50, 1077-1094.

Van Den Bleekn, G., C. Corteel, P. Van Den Haute (2007): Epigenetic to low-grade tourmaline in the Gdoumont metaconglomerates (Belgium): A sensitive probe of its chemical environment of formation. Lithos, vol. 95, 165-176.

Van Hinsberg, V. J., D. J. Henry, H. R. Marschall (2011): Tourmaline: An ideal indicator of its host environment. The Canadian Mineralogist, vol. 49, 1-16.

PHOSPHATES FROM RARE-ELEMENT PEGMATITES OF THE EAST SAYAN BELT, EASTERN SIBERIA, RUSSIA

V. Makagon
Vinogradov Institute of Geochemistry, SB RAS, Irkutsk, Russia vmak@igc.irk.ru

The East Sayan belt includes several rare-element pegmatite fields of both spodumene and petalite subformations (Zagorsky *et al.,* 2003) or subclasses. In the southeast part of the belt, in the Urik-Iya graben, are the Urikskoye, Goltsovoye, Belskoye, Belorechenskoye, Belotagninskoye and Malorechenskoye spodumene pegmatite fields. The Vishnyakovskoye and Alexandrovskoye petalite pegmatite fields lie in the northwest part of the belt in the Elash graben. These grabens are composed of Paleoproterozoic metavolcanic and metasedimentary rocks and orthoamphibolites. Spodumene pegmatites are generally not differentiated and are largely composed of blocky albite-quartz-spodumene-microcline and fine-grained microcline-spodumene-quartz-albite masses on which muscovite-albite-quartz and quartz-albite aggregates subsequently crystallize. These pegmatites are rarely zoned. One vein in the Urikskoye field (Makagon, 2009) contains montebrasite-amblygonite in the central quartz-microcline-spodumene zone with accessory columbite-(Mn), tantalite-(Mn), elbaite, and pollucite. Additionally, the Museum vein, which hosts complex pegmatites showing clear zoning, occurs in the Belotagninskoye field (Makagon, 2009). The inward zonation begins with an albite zone (1) along the footwall and further inward is a spodumene-microcline zone (2) with albite and pink muscovite-quartz aggregates. Accessory minerals include amblygonite-montebrasite, beryl, apatite and tantalite. Pollucite is rare and cassiterite occurs in albite pegmatite with greenish muscovite and sicklerite. The central zone (3) contains quartz-spodumene blocky pegmatite with pollucite and beryl. The quartz-muscovite aggregate zone (4) with pink muscovite, blue and green tourmaline, albite, beryl, amblygonite-montebrasite and tantalite crystals is located in the hanging wall of the vein.

The Vishnyakovskoye field includes complex (Ta-Cs-Li) pegmatites (Makagon, 2011). The largest single bodies are characterized by asymmetrical zonation. The upper endocontact displays small muscovite-quartz or albite-muscovite-quartz rim with cassiterite and apatite. The adjacent intermediate blocky zone is composed of alkali feldspar blocks, cryptocrystalline quartz-albite ("porcelain") aggregates with rare unaltered petalite blocks and isolated quartz blocks, montebrasite-amblygonite, quartz-spodumene aggregates and coarse-crystalline eucryptite. The central zone is composed of medium- to coarse-grained albite and clevelandite with muscovite-quartz nests. Also present accessory tantalite-(Mn), wodginite and microlite. In central zone quartz core and large potash feldspar and montebrasite-amblygonite blocks, accessory wodginite, tantalite-(Mn) and microlite, are present. The footwall zone of the veins is composed of fine-grained albite. Pegmatites of the Alexandrovskoye field (Makagon, 2011) contain blocks of amblygonite-montebrasite in central zones of quartz-lepidolite and quartz-albite-lepidolite aggregates with white beryl, rose tourmaline, tantalite, microlite, topaz and in the outer part of the quartz core.

Phosphates are present in rare-element pegmatites (London, 2008). Montebrasite-amblygonite is common in pegmatites of the belt with Li mineralization. It occurs as white crystals in undifferentiated fine-grained spodumene-quartz-albite and in blocky albite-spodumene-quartz-microcline pegmatites of the spodumene subclass. In the central portions of the zoned veins of the Urikskoye field, large grayish blocks of these phosphates are present. The Museum vein contains numerous gray crystals of montebrasite-amblygonite in the spodumene-microcline zone with pink muscovite, quartz and tantalite. The large pegmatite vein of the Belorechenskoye field contains montebrasite-amblygonite only in the upper portion of the vein. These phosphates occur most commonly in petalite pegmatites as blocks along and near the quartz core boundary, sometimes in the central blocky microcline or orthoclase zones. In some cases, the montebrasite-amblygonite from both spodumene and petalite pegmatites is altered and replaced by apatite. This replacement is observed in pegmatites of the Museum vein, where secondary brownish or gray apatite is associated with muscovite in altered zones of montebrasite-amblygonite. In petalite pegmatites, this mineral alters to pure red or gray apatite. Sicklerite and ferrisicklerite occur in spodumene and petalite

pegmatites exclusively, with greenish muscovite, quartz, and sometimes albite. Lithiophilite-triphylite is very rare in spodumene pegmatites and is widespread in petalite pegmatites of the Vishnyakovskoye field. It commonly forms rose or red aggregates associated with microcline or orthoclase blocks. Primary apatite is observed both in spodumene and in petalite pegmatites, but the latter contains larger aggregates or single crystals of this mineral of dark blue, blue or bluish color, whereas secondary apatite is gray, red or brownish.

	1	2	3	4	5	6	7	8	9	10	11
SiO_2	-	15.33	11.90	-	7.03	3.55	-	-	-	-	-
Al_2O_3	33.81	12.02	9.33	34.20	13.95	4.96	33.84	<0.04	<0.04	<0.04	<0.04
Fe_2O_3	0.34	0.21	0.23	0.39	0.12	0.15	0.28	<0.1	0.36	0.18	<0.1
FeO	-	-	-	-	-	-	-	0.54	-	-	3.37
MnO	<0.03	0.03	0.06	<0.03	0.04	0.11	<0.03	<0.03	0.03	3.12	42.26
MgO	0.13	0.32	0.26	0.17	0.15	0.17	0.13	0.13	0.13	0.17	0.18
CaO	0.44	37.69	42.08	0.68	42.50	50.00	1.04	56.08	55.33	52.00	0.68
Na_2O	0.05	0.06	0.08	<0.02	0.21	0.05	<0.02	0.05	0.07	0.07	0.14
K_2O	0.06	3.38	2.71	0.06	0.92	1.45	0.04	0.03	0.04	0.07	0.07
Li_2O	9.80	0.02	0.01	9.73	0.28	0.005	9.64	0.008	0.01	0.01	8.86
P_2O_5	48.65	27.30	30.30	47.82	31.09	37.38	48.60	40.91	41.20	42.11	44.43
H_2O	4.17	2.25	1.56	4.86	2.45	0.47	5.86	<0.1	0.84	0.50	<0.1
F	4.56	2.30	2.50	3.55	2.35	3.10	1.40	3.54	3.54	3.26	0.10
-O=F	1.92	0.97	1.05	1.49	0.99	1.31	0.59	1.49	1.49	1.37	0.04
Total	100.09	99.94	99.95	99.96	100.10	100.09	100.24	99.79	100.36	100.12	100.05

Table 1. Composition of phosphates and secondary aggregates from pegmatites of the East Sayan belt

The "Museum" vein: 1 – montebrasite-amblygonite, 2 and 3 – inner (2) and outer (3) zones of its alteration (apatite + muscovite); 4 - montebrasite-amblygonite, 5 and 6 – inner (5) and outer (6) zones of its alteration. Vein of the Vishnyakovskoye field: 7 – montebrasite-amblygonite, 8 and 9 – secondary red (8) and gray (9) apatite, 10 – primary apatite; 11 – lithiophilite. Analyst Pogudina G.A.

Montebrasite-amblygonite $LiAl(PO_4)(OH,F)$ is distinguished by the F/OH ratio in the (OH, F) site. Chemical analyses show this atomic ratio ranges from 0.1 to 0.7, thus montebrasite is dominant. Alteration of these minerals in spodumene pegmatites leads to formation of apatite-(CaF) in association with muscovite (Table 1). In petalite pegmatites, apatite-(CaF) formed as a result of alteration, as opposed to that from pegmatites of the White Picacho District, where hydroxylapatite and carbonate-apatite are observed (London, Burt, 1982). The lithiophilite-triphylite series minerals often have compositions close to lithiophilite. In contrast to the secondary analogue, primary apatite is enriched in Mn. Thus, rare-element pegmatites of the East Sayan belt contain various primary phosphates. The presence of secondary apatite with F is in accordance with appearance of fluorite during the last stage of pegmatite formation.

Acknowledgement: the study was supported by SB RAS (IIP-123).

References

London, D., and D. M. Burt (1982): Alteration of spodumene, montebrasite and lithiophilite in pegmatites of White Picacho District, Arizona. The American Mineralogist, vol. 67, 97-113.

London, D. (2008): Pegmatites. Can. Mineralogist, vol. 10, Special Publication, 347 p.

Makagon, V. M. (2009): Geochemical and genetic differences of spodumene pegmatites in zonal veins of the East-Sayan belt. Estudos geologicos, vol. 19, #2, 203-206.

Makagon, V. M. (2011): Petalite rare-metal pegmatites of the East Sayan belt, Eastern Siberia, Russia: geological setting, mineralogy, geochemistry and genesis. Asociacion geologica Argentina, series D, Publicacion Especial, N 14, 135-137.

Zagorsky, V. Ye., V. M. Makagon, B. M. Shmakin (2003): Systematics of granitic pegmatites. Russian geology and geophysics, vol. 44, 422-435.

BISMUTOTANTALITE FROM PEGMATITES OF THE WESTERN BAIKAL REGION, EAST SIBERIA, RUSSIA

V. Makagon, O. Belozerova
Vinogradov Institute of Geochemistry, SB RAS, Irkutsk, Russia, vmak@igc.irk.ru

Rare-element mineralization was observed within the Olkhon Island region of Lake Baikal. The zoned Ilixin pegmatite vein, a steeply dipping lens-like body about 200 m long and 25 m wide, is hosted by the Early Paleozoic gabbro of the Buguldeyka massif. The bottom is composed of graphic microcline with thin biotite plates and rare garnet. The center of the vein is composed of microcline-plagioclase apographic pegmatite with minor biotite and muscovite plates as well as black tourmaline and garnet. Above the apographic pegmatite, at the top of the vein is blocky pegmatite composed of microcline, coarse-grained clevelandite, polychrome tourmaline, green and pink beryl, orange spessartine, and plates of lepidolite. Lepidolite-albite aggregate with elbaite, rose beryl and bismutotantalite was found in this zone. Crystals of bismutotantalite about 1 cm in size often occur with elbaite and lepidolite. Some bismutotantalite crystals exhibit compositional zoning and contain microinclusions of native bismuth, as was detected by electron microprobe analyses.

Table 1: Composition of bismutotantalite-bismutocolumbite (wt. %)

	1	2	3	4	5	6	7	7	8
Ta_2O_5	31.85	31.31	31.22	33.64	32.74	31.70	33.23	41.51	42.91
Nb_2O_5	13.76	12.55	12.45	10.97	10.36	9.92	8.98	4.42	3.74
SnO_2	0.16	0.08	0.20	0.01	0.23	0.13	0.01	0.19	0.20
Sb_2O_3	4.55	3.84	5.20	4.96	5.20	4.50	5.01	3.18	4.57
Bi_2O_3	49.39	51.58	50.91	50.92	49.71	53.18	51.51	50.60	48.58
Sum	99.72	99.36	99.97	100.50	98.24	99.43	98.74	99.89	100.00

The composition of bismutotantalite is given in Table 1. It ranges from $(Bi_{0.90}Sb_{0.18})_{1.08}(Ta_{0.82}Nb_{0.10})_{0.92}O_{3.92}$ to $(Bi_{0.87}Sb_{0.13})_{1.00}(Ta_{0.58}Nb_{0.42})_{1.00}O_{4.00}$, with the Ta/Nb ratio ranging from 1.4 to 8.2. Minerals with a high bismutocolumbite content are predominant. Bismutotantalite belongs to the stibiotantalite group (Voloshin, 1993). Sb content is low and varies only slightly as compared to data on the minerals from pegmatites of the Molo near Momeik, Nothern Shan State, Myanmar (Novak *et al.*, 2008). Studied crystals belong to the bismutotantalite-bismutocolumbite series. The latter was first discovered in pockets of miarolitic pegmatites from the Malkhan field in the Central Trans-Baikal region, Russia (Peretyazhko *et al.*, 1992), whereas bismutotantalite found in Olkhon region is the second find of this mineral in Russia.

The geochemical study of this pegmatite vein shows low Li, Rb, Cs, Ta, Nb and Bi near the bottom of the pegmatite (Table 2). These element concentrations are higher at the top of the vein where they are incorporated into rare-metal minerals. Ba and Sr concentrations are low in pegmatites at different levels of the vein. Lepidolite-albite intergrowths at the top of the pegmatite are distinguished by low SiO_2 (57.05 %) and relatively high Na (3.7 %), K (3.6 %) contents. The Li, Rb, Cs, Be, Sn, Ta, Nb, Bi, Sb, F and B abundances are very high. Thus, the Ta, Nb and Bi concentrations increase 30- to 200-fold compared to the blocky zone and Li, B and F are elevated. Available geochemical data show that exsolution of a volatile phase enriched in B and F and rare metals melt, from which lepidolite-albite integrowth with extremely high rare-metal concentrations was formed, took place during pegmatite vein formation. Part of the melt-fluid substance of this complex penetrated blocky pegmatite producing alteration.

Bismuth mineralization is observed in pegmatites of different formations. It is most common in rare-metal – rare-earth NYF pegmatites of the Kola Peninsula, Russia (Voloshin, Pahomovsky, 1986), and in miarolitic LCT pegmatites of the Malhan field, Trans-Baykal region, Russia, in which the complex Bi oxides bismutomicrolite-bismutobetafite, bismutotantalite and bismutocolumbite are widespread (Zagorsky, Peretyazhko, 1992).

In the latter, as in LCT pegmatites of Olkhon region, bismutotantalite-bismutocolumbite is most typical for pegmatite complexes with high B and F contents, whereas sulfides and simple oxides of Bi and native Bi often occur in rare-metal – rare-earth NYF pegmatites (Voloshin, Pakhomovsky, 1986).

Table 2: Contents of elements in pegmatite vein

	1	2	3	4	5	6
K	6.91	8.05	3.90	5.94	3.6	0.43
Na	1.52	1.21	2.50	1.96	3.7	3.58
F	80	120	130	310	2.5 %	60
B	<2	<2	110	200	8000	4.5
Li	10	30	59	130	9900	42
Rb	640	1100	700	4600	7205	28
Cs	13	12	28	610	3400	<2
Ba	30	35	35	31	23	30
Sr	100	50	65	27	34	74
Be	0.5	1.35	40	80	160	4.1
Pb	83	64	76	76	110	20
Sn	<0.8	<0.8	11	5.2	190	<0.8
Nb	6.5	-	73.7	61	2500	30.0
Ta	1.0	2.2	13.4	41	8000	2.6
Bi	1	1	3	500	1.5 %	-
Sb	-	-	-	-	500	-
Zr	30	33	30	20	120	60
Hf	0.3	0.7	0.3	5.0	30	2.6
K/Rb	108	73	56	13	5.0	154

Pegmatites: 1 – bottom of vein, 2 –central part, 3 – average data for pegmatites, 4 – top of vein, 5 – lepidolite-albite complex, 6 - contact zone of top of vein. Data are in ppm, besides K , Na and some other elements, pointed out in %.

Acknowledgements: this study was supported by RFBR (project 10-05-00964) and SB RAS (IIP 129).

References:

Novak, M., J. Sejkora, R. Skoda and V. Budina (2008): Bismutotantalite-stibiotantalite-stibiocolumbite assemblage from elbaite pegmatites at Molo near Momeik, Northern Shan State, Myanmar. N. Jb. Miner. Abh., vol. 185/1, 17-26.

Peretyazhko, I. S., V. Ye. Zagorsky, A. N. Sapozhnikov, Yu. D. Bobrov, A. D. Rakcheev (1992): Bismutocolumbite is new mineral from miarolitic pegmatites. Zapiski VMO, N 3, 130-134. (In Russian).

Voloshin, A. V. (1993): Ta-Nb oxides. Systematics, crystalochemistry and evolution of mineral formation in granitic pegmatites. Sankt-Peterburg, Nauka, 298 p. (In Russian).

Voloshin, A. V., Ya. A. Pakhomovsky (1986): Minerals and mineral evolution of mineral formation in amazonite pegmatites of Kola Peninsula, Leningrad, Nauka, 168 p. (In Russian).

Zagorsky, V. Ye., I. S. Peretyazhko (1992): Pegmatites with gems in the Central Trans-Baikal region, Novosibirsk, Nauka, 224 p. (In Russian).

GEOCHEMISTRY, MINERALOGY AND EVOLUTION OF MICA AND FELDSPAR FROM THE MOUNT MICA PEGMATITE, MAINE, USA

K. Marchal[1], W. Simmons[1], A. Falster[1], K. Webber[1], E. Roda-Robles[2], G. Freeman[3]

[1] Dept of Earth & Environmental Sci., University of New Orleans, New Orleans, LA 70149, kmarchal@uno.edu
[2] Dept. de Mineralogía y Petrología, Univ. del País Vasco UPV/EHU, P.O. Box. 644, E-48080 Bilbao, Spain
[3] Coromoto Minerals, 48 Lovejoy Road, Paris, ME 04271

Mt. Mica Pegmatite in Oxford Co., Maine, is part of the Oxford pegmatite field that formed during the Alleghenian Orogeny. Mt. Mica is classified as a lithium and boron rich LCT-type pegmatite and is being mined for gem tourmaline. Mt. Mica pegmatite is poorly zoned with a thin wall zone, an intermediate zone, and core. Miarolitic cavities, or "pockets," are abundant in the central region of the dike averaging one every 3 m. Mica minerals of assorted texture, composition, and structure occur in all of these zones. This study concerns compositional and chemical evolution of mica within the pegmatite.

Micas were sampled from the contact to the core of the pegmatite and range in size, from 2 mm flakes to crystals up to 5 cm in the intermediate zone. Micas from the core are large, euhedral crystals up to ~17 cm. Some mica adjacent and along the margins of pockets exhibit twinning. Crystals in close proximity or in direct contact with the pockets may have distinct lepidolite rims ranging in thickness from 0.5 to 1 cm in width.

Mica textures and compositions evolve throughout the Mt. Mica pegmatite zones with more Li-rich micas in and around the core. Al-rich micas from within the Mt. Mica pegmatite belong to the muscovite – lepidolite series with a compositional trend from dioctahedral muscovite [$K(Al_2\square)(Si_3Al)O_{10}(OH,F)_2$] to trioctahedral trilithionite [$K(Li_{1.5}Al_{1.5})(Si_3Al)O_{10}(F,OH)_2$]. The mechanisms for Li substitution into the octahedral sites of the mica structure are controlled by the vectors $Li_3Al_{-1}\square_{-2}$ ($\square$=vacancy), and Si_2LiAl_{-3}. According to Hawthorne and Černý (1982), the Li-Al mica series is not structurally or compositionally continuous, but has a gap midway between muscovite and polylithionite. Analyses that fall within this region represent "mixed forms", a physical mixture of muscovite and lepidolite. Based on the positive correlation between Li and F within micas, shown by Tischendorf *et al.* (1997), and DCP analysis of Li from selected samples, the equation: $Li_2O = 0.3935F^{1.326}$ was chosen as the best estimate of Li_2O for samples containing < 8 wt.% F. The equation $0.237F^{1.544}$ was used for > 8 wt.% F values to estimate Li_2O according to Tischendorf *et al.* (1997). Analyses show a clear compositional trend of Li substitution from muscovite to trilithionite. There is a cluster of analyses in the Li muscovite range, a gap between 0.9 – 1.4 Li *apfu* , and a nearly linear trend to just beyond end-member trilithionite (Fig. 1).

One sample with a lepidolite rim revealed a very interesting compositional layering that was discovered as a result of the inconsistencies of analyses performed parallel and perpendicular to cleavage. The sample mounted parallel to (001) shows Li-muscovite across the crystal with a lepidolite rim, whereas, the cross-section sample analyzed from core to rim (areas 1-7) shows a very heterogeneous distribution and a complete range of composition from Li-muscovite to lepidolite without a gap (Fig. 2). The absence of the gap implies that there is a linear trend in composition from Li-muscovite to lepidolite, which was not observed in any other core to rim analyses. To further investigate the inconsistent results, SEM X-ray maps from the cross-section and parallel to (001) sample were prepared. The cross-section maps reveal distinct compositional interlayering of muscovite and lepidolite at a scale of several microns (Fig. 3). Reanalysis of the sample on compositionally homogeneous domains indicate compositions of Li-muscovite and a range of lepidolite with a gap identical to the compositional trend previously described. Thus, the anomalous compositions were the result of analyzing areas of interlayered Li-muscovite and lepidolite. This phenomenon of fine-scale interlayering is only observed in crystals found adjacent to or in pockets, generally on crystals that show lepidolite rims. The compositional interlayering of muscovite and lepidolite is inferred to be the result of rapid crystallization of lepidolite and muscovite from diffusion controlled, boundary-layer crystallization. The interlayering is interpreted to be a product of the oscillatory availability of Li at the crystal liquid interface of the rapidly crystallizing mica.

The overall fractionation of micas in the intermediate zone is chemically homogeneous with

a slight spike in K/(Cs + Rb) around the garnet line. Crystals in close proximity or in direct contact with the pockets show no significant changes in composition across the crystal but abruptly change from dioctahedral Li muscovite to high-F lepidolite on the rim of the crystals. In addition, isolated pods of lepidolite occur intermittently within the core zone. Lepidolite from these pods is highly evolved, with elevated Si, Li, F, Rb, and Cs content. The most evolved mica occurs adjacent to a 2 m pollucite mass.

Feldspars from contact to core are dominantly sodic-rich plagioclase ($An_{1.8}$). K-feldspar is virtually absent except in the core zone where large masses of microcline, up to a meter in maximum dimension, are located in close proximity to pockets and rare pollucite masses. There is very little change in Ca composition of the albite from the wall zone inward. However, there is a slight increase in Ca immediately at the hanging wall contact and adjacent to the garnet line. The K/Rb (*apfu*) ratio of microcline ranges from about 40 to 70, which corresponds to values slightly higher than most complex rare element pegmatites. This, along with the overall mica composition in the Li-muscovite range, indicates that Mt. Mica is not overall highly evolved. However, the occurrence of such highly evolved species such as F-rich lepidolite, pollucite pods, elbaite tourmaline, Cs-rich beryl and spodumene in miarolitic cavities, suggests that the internal evolution mechanism was very effective, producing proportionally small volumes inside the pegmatite with very high enrichment in incompatible elements.

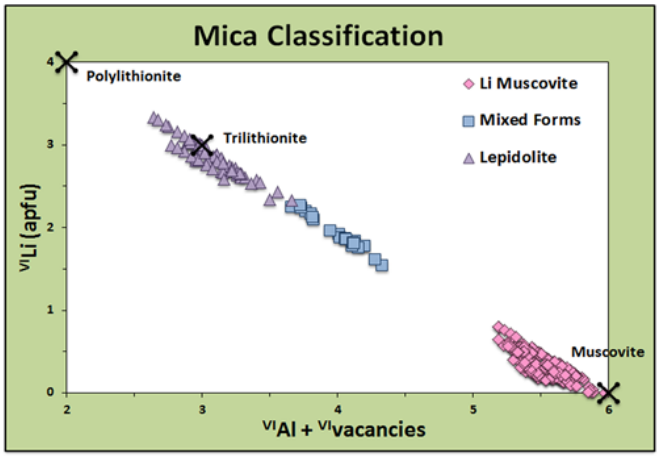

Fig. 1: Li-Al Mica classification showing a cluster of Li-muscovite, a miscibility gap, and linear trend beyond trilithionite

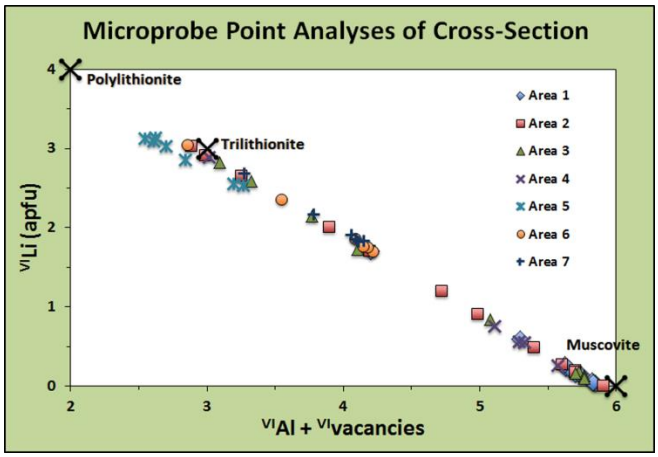

Fig. 2: Analyses of cross-section sample shows, from Li-muscovite to complete range of composition, without a gap to trilithionite

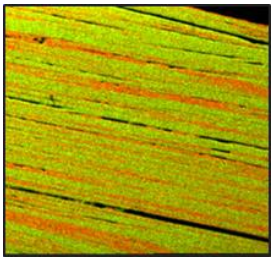

Fig. 3: X-ray map of lepidolite rimmed sample perpendicular to (001) cleavage. Si = red (lepidolite), Al = green (Li-muscovite)

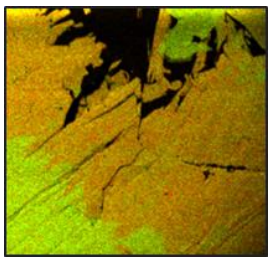

Fig. 4: X-ray map of lepidolite rimmed sample parallel to (001) cleavage. Si = red (lepidolite), Al = green (Li-muscovite)

References

Hawthorne, F.C., and P. Černý (1982): The Micas. MAC Short Course Handbook 8, 63-98.

Tischendorf, G., B. Gottesmann, H. Forster, and R. Trumbull (1997): On Li-bearing micas: estimating Li from electron microprobe analyses and an improved diagram for graphical representation. Mineralogical Magazine, vol. 61, 809-834.

THE SECULAR DISTRIBUTION OF GRANITIC PEGMATITES AND RARE-METAL PEGMATITES

A. McCauley[1], D. Bradley[2]
[1] University of Utah, Salt Lake City, Utah, USA; amccauley@egi.utah.edu
[2] USGS, Anchorage, Alaska, USA

A new global compilation has shown that common granitic pegmatites and rare metal pegmatites range in age from Mesoarchean to Neogene and have a semi-periodic age distribution. More than 250 pegmatite ages were included in our compilation, with a preponderance of North American, European and Australian data points. Common pegmatites show nine age maxima: ca. 2925, 2650, 1800, 1400, 1175, 1000, 525, 350, and 100 Ma (Fig. 1). A number of previous workers have catalogued the ages of pegmatites; most recently Tkachev (2011) documented a broadly similar age distribution. Our new compilation of U/Pb and $^{40}Ar/^{39}Ar$ ages differs in several respects from previous ones: (1) we include several recent high resolution U/Pb CA-TIMS ages (Bradley *et al.*, 2013); (2) we did not use Rb/Sr ages because they are likely to be compromised by open system behavior (Dicken, 2005); (3) we weighted each dated pegmatite equally in plotting the age distribution; and (4) for various undated pegmatites, we refrained from borrowing the age of a supposedly associated granite. Each age peak includes pegmatites from multiple continents, suggesting the ages have global significance and are not local artifacts. These peaks correspond broadly with those of orogenic granites (Condie and Aster, 2010), and with other proxy records of supercontinent assembly, including detrital zircon peaks in sedimentary rocks and river sand (Voice *et al.*, 2011), and declines in passive-margin abundance (Bradley, 2011). This compilation suggests peak times of pegmatite formation are generally offset a few tens of millions of years later than those of orogenic granites. This is in agreement with work in progress that places lithium-cesium-tantalum enriched (LCT) pegmatites in the second half of the Appalachian orogenic sequence (Bradley *et al.*, 2013).

Secular trends provide insight into the relationship between metallogenesis and evolving global tectonic, mantle, and geochemical phenomena, with implications for predicting deposit formation (Goldfarb *et al.*, 2010). LCT pegmatites occur in the rock record semi-periodically, with age populations centered around 2640, 1790, 960, 530, 375, and 275 Ma (Fig. 2). The ages of these rare-metal pegmatites correspond to the record of pegmatite formation in general, but economic lithium and tantalum ore deposits, having high grades and (or) tonnages, are concentrated in the Archean and Phanerozoic (Figs. 3 and 4). This bimodal distribution is particularly evident in the tantalum record, which is dominated by large Archean pegmatites like Wodgina and Pilgangoora of Western Australia and younger deposits like the Cambrian Kenticha pegmatite in Ethiopia (Fetherston, 2004). A similar pattern is observed in the orogenic gold record, which has been interpreted to reflect differences in preservation between Archean plume influenced tectonics, subsequent slab subduction and cordilleran orogeny (Goldfarb *et al.*, 2001). Niobium, yttrium, and fluorine enriched (NYF) pegmatites are notably concentrated during a Grenville-age peak at 1004 Ma (Fig. 5). NYF pegmatites have been associated with anorogenic granites formed in extensional settings (Martin and De Vito, 2005), so the long tenure and mantle heating of the supercontinent Nuna leading up to ca. 1 Ga (Bradley, 2011) may have fertilized the crust for NYF pegmatite formation.

References

Bradley, D.C. (2008): Passive margins through earth history. Earth-Science Reviews, vol. 91, 1–26.

Bradley, D.C. (2011): Secular trends in the geologic record and the supercontinent cycle. Earth-Science Reviews, vol. 108, 16-33.

Bradley, D.C., Buchwaldt, R., Shea, E., Bowring, S., O'Sullivan, P., Benowitz, J., McCauley, A., and Bradley, L. (2013): Geochronology and orogenic context of Northern Appalachian lithium-cesium-tantalum pegmatites. Geol. Soc. America, NE Section, Abstracts with Programs, v. 45, no. 1, in press.

Condie, K.C. and Aster, R.C. (2010): Episodic zircon age spectra of orogenic granitoids: the supercontinent connection and crustal growth. Precambrian Research, vol. 180, 227-236.

Dicken, A.P. (2005): Radiogenic isotope geology, 2nd edition. Cambridge University Press, 492 p.

Fetherston, J.M. (2004): Tantalum in Western Australia. Western Australia Geological Survey, Mineral Resources Bulletin 22, 162 p.

Goldfarb, R.J., Groves, D.I., Gardoll, S. (2001): Orogenic gold and geologic time: a global synthesis. Ore Geology Reviews, vol. 18, 1–75.

Goldfarb, R.J., Bradley, D.C., Leach, D.L. (2010): Secular variation in economic geology. Economic Geology, vol. 105, 459–465.

Martin, R.F. and De Vito, C. (2005): The patterns of enrichment in felsic pegmatites ultimately depend on tectonic setting. The Canadian Mineralogist, vol. 43, 2027-2048.

Tkachev, A.V. (2011): Evolution of metallogeny of granitic pegmatites associated with orogens throughout geological time: Geological Society, London, Special Publication 350, p. 7-23.

Voice, P.R., Kowalewski, M., and Eriksson, K.A. (2011): Quantifying the timing and rate of crustal evolution: global compilation of radiometrically dated detrital zircon grains. Journal of Geology, vol. 119, 109–126.

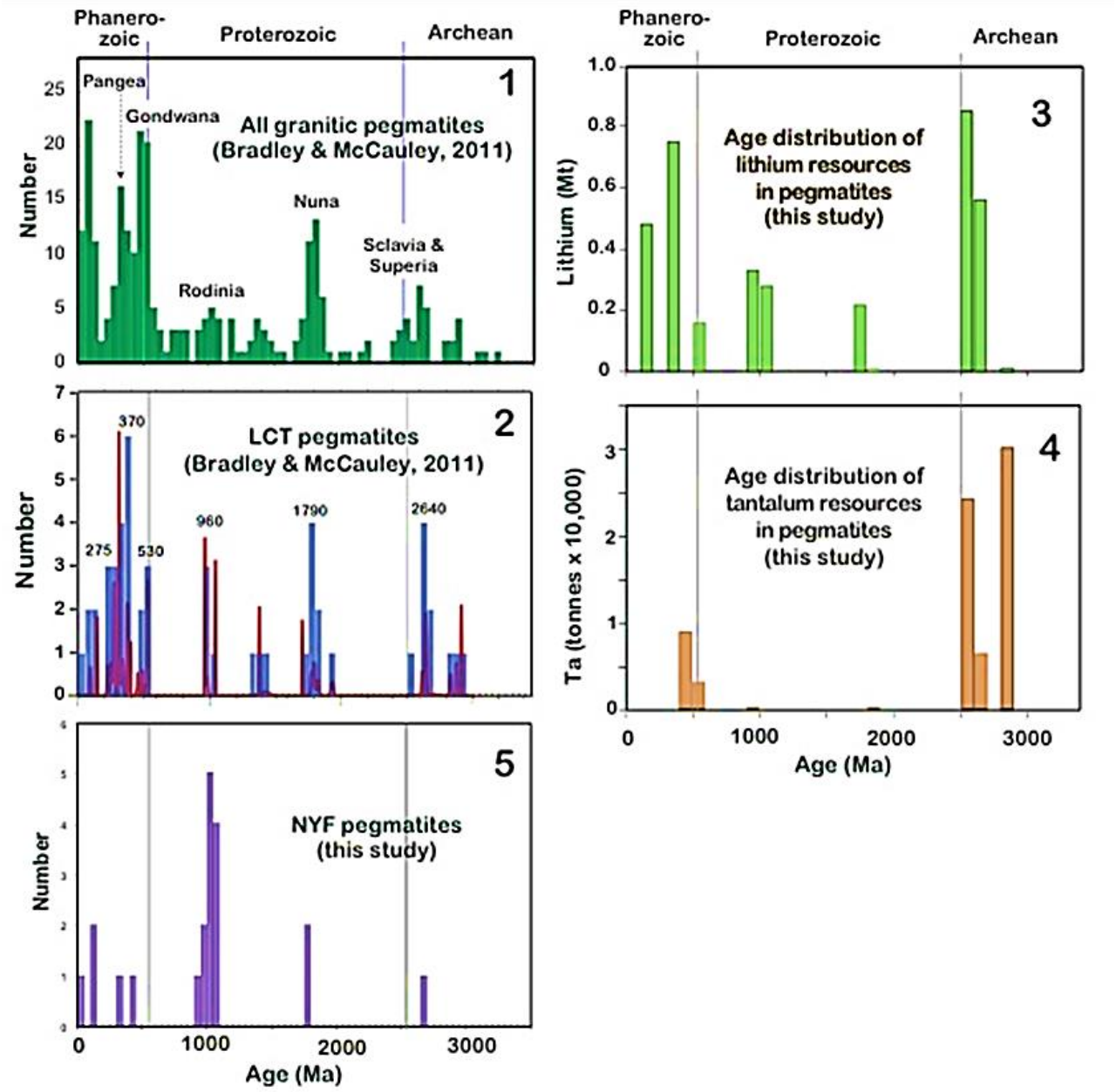

THE COMPOSITION OF GARNET AS INDICATOR OF RARE METAL (LI) MINERALIZATION IN GRANITIC PEGMATITES

L. Moretz[1], A. Heimann[1], J. Bitner[1], M. Wise[2], D. Rodrigues Soares[3], A. Mousinho Ferreira[3]
[1] Department of Geological Sciences, East Carolina University, 101 Graham Building, Greenville, NC 27858, heimanna@ecu.edu
[2] Department of Mineral Sciences, Smithsonian Institution, P.O. Box 37012, Washington, DC 20013-7012
[3] Instituto Federal de Educação, Ciência e Tecnologia da Paraíba (IFPB), R. Tranquilino Coelho Lemos 671, Campina Grande-Paraíba, 58100–000, Brazil

The chemical composition of garnet has been studied extensively in some mineral deposits, including metamorphosed massive sulfide deposits and kimberlites. Thus, the composition of this mineral is commonly used in the exploration for diamonds and metamorphosed Pb-Zn deposits. Evolved granitic pegmatites often contain economically important rare elements, including Li, Cs, Ta, Nb, Y, Be, and the rare earth elements. As a common accessory mineral in granitic pegmatites, the composition of spessartine-almandine solid solution garnet ($[Mn,Fe]_3Al_2Si_3O_{12}$) also has the potential to be used to identify pegmatites that contain rare metal mineralization. In this study, we present the major element chemical composition of garnet from Li-rich and Li-poor pegmatites, and those from LCT (lithium, cesium, tantalum), NYF (niobium, yttrium, fluorine), and muscovite type pegmatites (Černý and Ercit 2005). The pegmatites investigated include those from California (Cryogenie, Elizabeth R., Oceanview, Pala Chief), Maine (Emmons, Lord Hill, Mt. Mica), Maryland (Ben Murphy), North Carolina (Bon Ami, Hoot Owl, Ray, Sinkhole, and Sullins-Wiseman, Spruce Pine), New Mexico (San Miguel), New York (Batchellerville, Bayliss, Benson, and Greenfield), Pennsylvania (Avondale), Virginia (Rutherford #2), Brazil (Alto Mirador, Boqueirao, Capoeira, Carrascao, and Quintos of the Borborema Pegmatite Province, BPP), China (Guangdong), and Poland (Szklary).

In addition to the new data collected here, this study includes a compilation of garnet compositions in pegmatites published in the literature, including those from Brazil (Alto Mirador, Boqueirao, Capoeira, Escondido, Poaia, Quintos), Canada (Cat Lake - Winnipeg River pegmatite field), Czech Republic (Hina), Ireland (Aclare), Israel (Elat), Italy (Vinschgau Valley), Japan (Uzumine), Norway (Froland and Evje-Iveland), Switzerland (ZPU-Brissago), Thailand (Nong Sua), and the USA (including George Ashley Block, Himalaya, Little Three, Rutherford #2, Sebago, and Spruce Pine, among others).

The composition of garnet from the Li-rich, LCT Quintos pegmatite (BPP) exhibits the highest degree of pegmatite evolution of all the pegmatites analyzed in this study, as seen in a plot of wt.% FeO+MgO versus wt.% CaO+MnO (Fig. 1). Given in terms of mol % spessartine (Spss) and almandine (Alm) end members, these garnets have a compositional range of $Spss_{90\text{-}94}$ $Alm_{2\text{-}7}$. The least evolved of the pegmatites, based on the composition of garnet obtained in this study, is the Li-poor, NYF Batchellerville (NY) pegmatite, with a compositional range of $Spss_{2\text{-}3}Alm_{86.6\text{-}86.8}$. Garnet from the Li-rich, LCT Little Three Mine (CA) pegmatite (Morgan and London 1999) has a wide range of compositions reflecting a low-to-high degree of melt evolution, with the most Mn-rich garnet having an extreme composition of $Spess_{98}Alm_2$. In contrast, the Li-poor, LCT Nong Sua (Thailand) pegmatite (Linnen and Williams-Jones 1993) has the highest Fe content of the garnets analyzed in previous studies, and has a composition defined by $Spess_{<1}Alm_{37\text{-}63}$. This study shows that even though the compositional ranges of garnet within some individual pegmatites can be quite large and are useful indicators of pegmatite melt evolution, garnet in many individual pegmatites have restricted compositional ranges. Considering all the garnet compositions available, Li-poor, NYF pegmatites typically have garnet with the lowest Mn and highest Fe contents, whereas garnet in Li-rich, LCT pegmatites has the highest Mn and lowest Fe contents. This suggests that the major element composition of garnet can likely be used to distinguish pegmatites with Li mineralization from those with low Li contents. Trace element compositions of garnet will likely be proven to be good indicators of Li mineralization in granitic pegmatites.

References

Baldwin, J., von Knorring, O. (1983): Compositional range of Mn-garnet in zoned granitic pegmatites. Canadian Mineralogist, vol. 21, 683-688.

Černý, P., Ercit, T.S. (2005): The classification of granitic pegmatites revisited. Canadian Mineralogist, vol. 43, 2005-2026.

Morgan, G., London, D. (1999): Crystallization of the Little Three layered pegmatite aplite dike, Ramona District, California. Contributions to Mineralogy and Petrology, vol. 136, 310-330.

Linnen, R., Williams-Jones, A. (1993): Mineralogical constraints on magmatic and hydrothermal Sn-W-Ta-Nb mineralization at the Nong Sua aplite-pegmatite. European Journal of Mineralogy, vol. 5, 721-736.

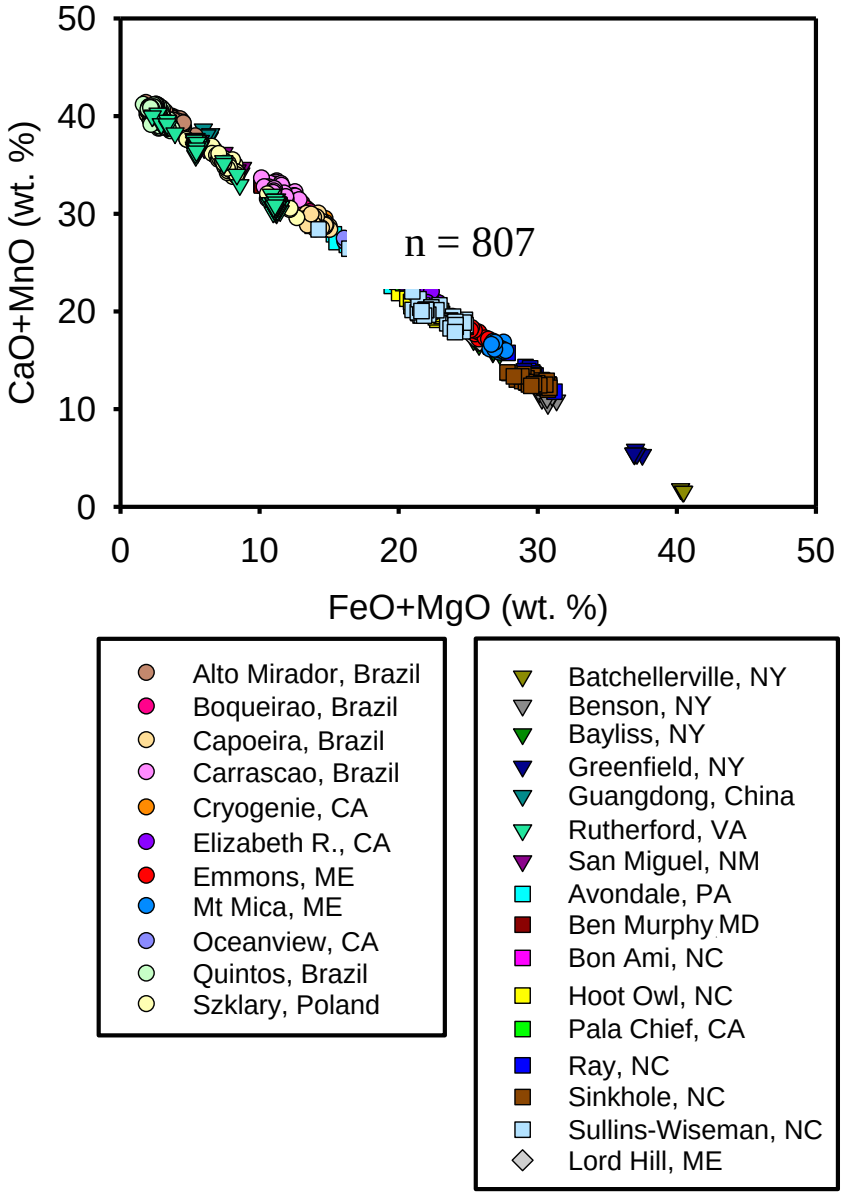

Fig. 1: Binary diagram in terms of FeO+MgO versus CaO+MnO (in wt. %) showing the composition of spessartine-almandine garnet in granitic pegmatites obtained in this study (After Baldwin and von Knorring 1983). Circles represent LCT pegmatites, triangles NYF pegmatites, squares Muscovite pegmatites, and diamonds pegmatites of uncertain type.

"AMAZONITE"-"CLEAVELANDITE" REPLACEMENT UNITS IN NYF-TYPE PEGMATITES – RESIDUAL FLUIDS OR IMMISCIBLE MELTS?

A. Müller[1,2], B. Snook[1,3], J. Spratt[2], B. Williamson[2,3], R. Seltmann[2]
[1] Geological Survey of Norway, Axel.Muller@ngu.no
[2] Natural History Museum of London
[3] Camborne School of Mines, University of Exeter

Occasionally, granitic pegmatites contain internal irregularly shaped bodies which are characterized by high concentrations of exotic minerals partially replacing minerals of the parent pegmatite; these are termed replacement units. Their distinct chemical compositions are often very different to those of their host pegmatite. In this study the structure, mineralogy and chemistry of "amazonite"-"cleavelandite" replacement units in NYF-type pegmatites from Evje–Iveland in southern Norway are characterized and discussed.

The Evje-Iveland pegmatites are rare-element REE pegmatites of the NYF-type class consisting of K-feldspar, plagioclase, quartz, biotite and muscovite, minor magnetite and garnet, with variable contents of a range of accessory rare-metal and REE minerals, among which are beryl, allanite, monazite, zircon, euxenite, aeschynite, and gadolinite. The pegmatites are zoned, consisting of a graphic wall zone, a megacrystic intermediate zone, and a core zone with crystal sizes of up to several meters. The emplacement age of the pegmatite melts is considered to be 910±14 Ma (Scherer *et al.* 2001).

Less than 10 % of the ca. 350 major (>5000 m^3) pegmatite bodies display small (2-50 m^3) but distinct replacement units containing "cleavelandite" (platy variety of albite), "amazonite" (green to bluish-green variety of K-feldspar), quartz, muscovite, topaz, beryl, spessartine and accessory fluorite, lepidolite, tourmaline (schorl), columbite, microlite group minerals, bismutite, zircon, and apatite. Topaz typically forms large white to pale yellow crystals which can be up to 60 kg in weight (Figure 1). The replacement units usually occur at the bottom of the core zone but can also extend into external parts of the pegmatite body. From textural relationships, replacement units are an intrinsic part of the pegmatite and developed during the late, probably final stage of pegmatite solidification.

From image analyses of three replacement units, their mineral composition is generally 46 vol.% quartz, 40 vol.% K-feldspar, 10 vol.% albite, 3 vol.% muscovite and 1 vol.% topaz which is different to the eutectic granitic composition of the host pegmatite. However, due to the complex intergrowth and replacement relationships of quartz and K-feldspar it is difficult to decide which of these minerals, or particular generations, are replacement rather residual from the pegmatite host.

There are distinct chemical differences between minerals which occur both outside and within the replacement units. Plagioclase of the intermediate and core zone has an oligoclase composition ($An_{12}Ab_{83}Or_5$) but the plagioclase of the replacement unit is almost pure albite ($An_0Ab_{98}Or_2$). The "amazonite" contains high Rb (~7500 ppm) and Cs (~1200 ppm), whereas the pink K-feldspar outside the replacement units has ~1400 ppm Rb and ~50 ppm Cs. Large, gas-rich two-phase fluid inclusions with negative quartz crystal shapes are very common in quartz of the replacement units but absent in those from the main zones of the pegmatites indicating formation of the replacement units from relatively H_2O-rich fluids. Quartz from the replacement units (RU) has lower average Ti (4.8±2.7 ppm) and higher Ge (8.2±2.1 ppm) compared to quartz of the intermediate pegmatite zone (iz) (Ti=27.3±3.4 ppm, Ge=1.8±0.5 ppm), whereas Al (Al_{ru}=46.6±20.0 ppm, Al_{iz}=49.2±24.4 ppm) and Li (Li_{ru}=8.4±2.9 ppm, Li_{iz}=9.2±2.0 ppm) are similar. The application of the Ti-in-quartz-geothermometer (Wark and Watson 2006) suggests an average crystallization temperature for the quartz in the intermediate and core zones of the pegmatites of 612±21°C whereas quartz of the RU crystallized at 479+38/-58°C. The low crystallization temperature of the replacement unit is consistent with enrichment of H_2O and F lowering the solidification temperature of the 'melts' which formed them, or that the replacement units form a liquid akin to a hydrothermal fluid.

In summary, the contacts of the replacement units represent a sharp chemical and thermal border separating a significantly fractionated, volatile-enriched silica melt characterized by high Rb, Cs, Ta, Mn and F, and low Fe, Ti, and REE from the parent peraluminous pegmatite-forming melt. Owing to the enrichment of H_2O and F, these residual melts interacted with and replaced crystallized parts of the pegmatite, a process that could be called "auto-metasomatism" of the pegmatite. These melts

probably do not resemble a normal silicate melt, but rather a transitional aqueous silicate fluid such as that found within fluid inclusions in pegmatites (e.g., London 1986, Thomas *et al.* 2006). However, the observations made so far do not fully explain why the chemical and thermal contrasts between the replacement units and the parent pegmatite are so sharp and strong and why only one or two small replacement units are commonly developed in the large Evje-Iveland pegmatites. It might be possible that the 'melt' which formed the replacement units separated at a relatively early stage of pegmatite evolution and became progressively enriched and concentrated in H_2O and F during crystallization.

Fig. 1: 60-kg topaz crystal (48 x 33 x 20 cm) from the "amazonite"-"cleavelandite" replacement unit of the Birkeland pegmatite near Evje, southern Norway. The photograph was taken by Mike Rumsey, mineralogical collections curator of the Natural History Museum of London. Courtesy of the Natural History Museum of London.

References

London, D. (1986): The magmatic–hydrothermal transition in the Tanco rare-element pegmatite: evidence fro fluid inclusions and phase equilibrium experiments. American Mineralogist, vol. 71, 376-395.

Scherer, E., Münker, C., Mezger, K. (2001): Calibration of the lutetium–hafnium clock. Science, vol. 293, 683-687.

Thomas, R., Webster, J.D., Rhede, D., Seifert, W., Rickers , K., Förster, H.-J., Heinrich, W., Davidson, P. (2006): The transition from peraluminous to peralkaline granitic melts: evidence from melt inclusions and accessory minerals. Lithos, vol. 91, 137-149.

Wark, D.A., Watson, E.B. (2006): TitaniQ: a titanium-in-quartz geothermometer. Contributions to Mineralogy and Petrology, vol. 152, 743–754.

FELDSPARS, MICAS AND COLUMBITE-TANTALITE MINERALS FROM THE ZONED GRANITIC LEPIDOLITE-SUBTYPE PEGMATITE AT NAMIVO, ALTO LIGONHA, MOZAMBIQUE

A. Neiva
Department of Earth Sciences and Geosciences Centre, University of Coimbra, 3000-272 Coimbra, Portugal, neiva@dct.uc.pt

The Namivo granitic lepidolite-subtype pegmatite is concentrically zoned. In K-feldspar, Rb and Cs contents increase and K/Rb and K/Cs ratios decrease from the pegmatite wall zone to the core, reflecting growth of K-feldspar from an increasing fractionated melt. The Ca and Sr contents and Sr/Ca ratio of albite decrease from the wall zone to the core, also supporting an increasing degree of melt fractionation. The two-feldspar geothermometry shows a decrease in temperature from 405ºC in the wall zone to 333-289ºC in the core at 3 kb.

Al-poorer micas (zinnwaldite, lepidolite and polylithionite) only occur in the outer intermediate zone. Al-richer micas (muscovite, lithian muscovite and "mixed form") occur in outer intermediate and inner intermediate zones and core and lepidolite in inner intermediate zone and core. The main substitution mechanism in trioctahedral micas is $3Li^{VI} \leftrightarrows Al^{VI} + 2\square^{VI}$ ($\square$ represents a vacancy) and in dioctahedral micas is $2Si + Li \leftrightarrows 3Al_{total}$. Some crystals are progressively zoned and the zoning patterns correspond to fractionation trends. Other crystals are reversely zoned, which may be explained by the hypothesis of oscillations in the compositions of the melt from which they grew, alternating between an Li-enriched boundary layer and a bulk melt that is less fractionated. But overgrowths and replacements also occur. In outer intermediate and inner intermediate zones and core, muscovite evolved to lithian muscovite and the latter to "mixed form", whereas "mixed form" evolved to lepidolite in inner intermediate zone and core, as shown by textural and chemical studies at the crystal scale. The Si and $Li_{calc.}$ contents increase from zinnwaldite to lepidolite and Fe-Mg containing polylithionite in the outer intermediate zone. The increase in Si, $Li_{calc.}$, F, Rb and Cs contents and the decrease in K/Rb ratio show a progressive evolution from muscovite to lithian muscovite and "mixed form" in the outer intermediate zone and from muscovite to lithian muscovite, "mixed form" and lepidolite in inner intermediate zone and core. Each Al-richer mica (muscovite, lithian muscovite and "mixed form") shows increase in Si, $Li_{calc.}$, F, Rb and Cs and decrease in K/Rb ratio from the pegmatite outer intermediate zone to inner intermediate zone and core. Lepidolite also shows a similar behavior from the inner intermediate zone to the core. The evolution of each of these micas is due to increasing melt fractionation.

Lepidolite and Fe-Mg containing polylithionite are the richest micas in Si, $Li_{calc.}$ and F and occur in the outer intermediate zone. They may be due to disequilibrium crystallization from an undercooled melt.

Most columbite-tantalite crystals are unzoned, but zoned crystals of columbite-(Mn) from the core show darker and lighter zones in BSE images. The lighter zone has higher Ta content, Ta/(Ta+Nb) and Mn/(Mn+Fe) ratios and a lower Nb content than the darker zone. The main trend starts from columbite-(Mn) of the outer intermediate zone towards more Mn-enriched and slightly Ta-enriched columbite-(Mn) from inner intermediate zone and core, which is similar to the trend of columbite-group minerals from the lepidolite-subtype complex granitic pegmatites. The extreme Fe-Mn fractionation before Ta enrichment in columbite-(Mn) may be due to an increase in the activity of fluorine derived from fractional crystallization, as muscovite, lithian muscovite and "mixed form" show a progressive increase in the F content from the outer intermediate zone to the core and lepidolite also shows it from the inner intermediate zone to the core. The increase in Ta content of columbite-(Mn) is also attributed to fractional crystallization.

Columbite-(Mn) very rich in Ta/(Ta+Nb), tantalite-(Fe) and tantalite-(Mn) only occur in the outer intermediate zone, associated with lepidolite and Fe-Mg containing polylithionite. They may be due to local depletion of Li and F in the melt that caused Ta precipitation.

THE PARAGENESIS OF FALSTERITE AND NIZAMOFFITE, TWO NEW ZINC-BEARING SECONDARY PHOSPHATES FROM THE PALERMO NO. 1 PEGMATITE, NORTH GROTON, NEW HAMPSHIRE

J. Nizamoff[1], A. Falster[2], W. Simmons[2], A. Kampf[3], R. Whitmore[4]
[1] Omya, Inc., 39 Main Street, Proctor, VT 05765; phosphate@gmail.com
[2] Dept. of Earth & Environmental Sci., University of New Orleans, New Orleans, LA 70148
[3] Mineral Sciences Dept., Natural History Museum of L. A. Co., 900 Exposition Blvd, Los Angeles, CA 90007
[4] 934 South Stark Highway, Weare, NH 03281

In 2003 a 1.5 m triphylite crystal with an unusual alteration assemblage was encountered in the core margin of the Palermo No. 1 pegmatite. The triphylite crystal is rimmed on one side by a 10-30 cm thick rind of siderite, fluorapatite and quartz. This carbonate-rich zone also contains minor amounts of sulfide minerals including pyrite, sphalerite, galena and chalcopyrite. A significant portion of the sulfides have been altered by aqueous solutions resulting in the formation of numerous secondary Zn- and Pb-bearing phosphate and carbonate species (Nizamoff *et al.* 2007).

Two new zinc-bearing secondary phosphates falsterite (Kampf *et al.* 2012) and nizamoffite (Kampf *et al.* 2013) were described from this assemblage.

Falsterite, $Ca_2MgMn^{2+}{}_2Fe^{2+}{}_2Fe^{3+}{}_2Zn_4(PO_4)_8(OH)_4(H_2O)_{14}$, is late-forming and minerals observed in direct association with falsterite include: messelite, mitridatite, phosphophyllite, quartz, schoonerite, siderite, smithsonite, and vivianite (Kampf *et al.* 2012). Nizamoffite, the Mn-analogue of hopeite $Mn^{2+}Zn_2(PO_4)_2(H_2O)_4$, is a relatively late-formed phase and occurs in direct association with childrenite-eosphorite, crandallite-goyazite, fairfieldite-messelite, falsterite, fluorapatite, frondelite-rockbridgeite, mitridatite, phosphophyllite, pyrite, quartz, siderite, schoonerite, sphalerite, and vivianite (Kampf *et al.* 2013).

In addition to falsterite and nizamoffite, a number of zinc- and lead-bearing secondary phosphates are also present in the assemblage. Parascholzite, $Ca_{0.92}(Zn_{1.80}Mn^{2+}{}_{0.17}Al_{0.02}Fe_{0.01})_{\Sigma=2.00}(P_{1.02}O_4)_2 \bullet 2\ H_2O$ occurs as colorless to white acicular or spear-shaped crystals associated with phosphophyllite, fluorapatite, vivianite, sphalerite, pyrite and quartz. A zinc bearing member of the jahnsite group, $(Ca_{0.95}Na_{0.05})_{\Sigma=1.00}(Mn^{2+}{}_{1.18}Mg_{0.35}Ca_{0.31}Zn_{0.18})_{\Sigma=2.02}(Fe^{3+}{}_{2.86}Mn^{3+}{}_{0.13}Al_{0.01})_{\Sigma=3.00}(P_{1.00}O_4)_4(OH)_3 \bullet 2\ H_2O$, is found as brownish-orange prismatic crystals in fissures with fluorapatite, phosphophyllite, sphalerite and quartz. Phosphophyllite, $(Zn_{1.83}Mn_{0.08}Mg_{0.03}Ca_{0.02}Al_{0.02}Na_{0.01})_{\Sigma=1.99}(Fe^{2+}{}_{0.66}Mn^{2+}{}_{0.34})_{\Sigma=1.00}(P_{1.00}O_4)_2 \bullet 4\ H_2O$, occurs as colorless, tapered prismatic crystals that may display twinning on {100}. Pyromorphite occurs in tiny (0.5 mm) globular masses on etched galena with falsterite (Nizamoff *et al.* 2007).

Rare, white botryoidal masses and coatings of smithsonite occur in Zn-bearing phosphate cavities with fluorapatite, quartz, altered sphalerite and falsterite. In polished sections a formation sequence of siderite to Mn-rich siderite/rhodochrosite? to smithsonite has been observed. The late increase in zinc content may be related to the alteration of primary sphalerite and subsequent formation of zinc-bearing secondary phosphates.

The combination of phosphate- and carbonate-bearing fluids reacting with locally abundant sulfides resulted in this unusual assemblage of rare secondary species for a granitic pegmatite.

References

Kampf, A.R., Mills, S.J., Simmons, W.B., Nizamoff, J.W. and Whitmore, R.W. (2012) Falsterite, $Ca_2MgMn^{2+}{}_2(Fe^{2+}{}_{0.5}Fe^{3+}{}_{0.5})_4Zn_4(PO_4)_8(OH)_4(H_2O)_{14}$, a new secondary phosphate mineral from the Palermo No. 1 pegmatite, North Groton, New Hampshire. American Mineralogist, 97, 496-502.

Kampf, A.R., Falster, A.U., Simmons, W.B. and Whitmore, R.W. (2013) Nizamoffite, $Mn^{2+}Zn_2(PO_4)_2(H_2O)_4$, the Mn analogue of hopeite from the Palermo No. 1 pegmatite, North Groton, New Hampshire. American Mineralogist, 98, *in press*.

Nizamoff, J.W., R.W. Whitmore, A.U. Falster, and W.B. Simmons (2007): Parascholzite, keckite, gormanite and other previously unreported secondary species and new data on kulanite and phosphophyllite from the Palermo #1 mine, North Groton, New Hampshire. Rocks and Minerals, V.82.

CONTAMINATION PROCESSES IN COMPLEX GRANITIC PEGMATITES

M. Novák
Department of Geological Sciences, Masaryk University, Brno, Czech Republic, mnovak@sci.muni.cz

Contamination of granitic pegmatites manifested by the presence of Ca,Mg,(Fe)-rich minerals such as clinopyroxenes (diopside to hedenbergite), amphiboles (tremolite, edenite, hastingsite), Mg-rich cordierite, phlogopite, scapolite, titanite, epidote, and/or calcite is quite a common process particularly in small, simply zoned to homogeneous and rather primitive pegmatites enclosed in compositionally contrasting rocks. Large, complex (Li-rich) granitic pegmatites typically exhibit much lower degree of contamination disregarding their host rocks. Contamination of (complex) granitic pegmatites (both melt and solid rock) may theoretically proceed in three stages (Novák 2007). In the *pre-emplacement stage* pegmatite melts are contaminated during their propagation from fertile granite to the sites of pegmatite solidification. *Post-emplacement stage* involves *in-situ* contamination of pegmatite melt from host rock. *Hydrothermal (subsolidus) stage* is characterized by alteration of a solid pegmatite by infiltrating (or diffused) fluids from host rocks after thermal and fluid re-equilibration of pegmatite and host rock.

Pre-emplacement contamination of melt is the most enigmatic contamination process and the only well-documented example was published only recently from the elbaite-subtype Bližná I pegmatite, Czech Republic (Novák *et al.* 2012). The pegmatite host-rock complex contains bodies of carbonatite-like marbles rich in REE, Sr and Ba, which pegmatite melt passed through. Fragments of this rock were consumed and completely dissolved in melt during their ascent to the site of emplacement (Fig. 1).

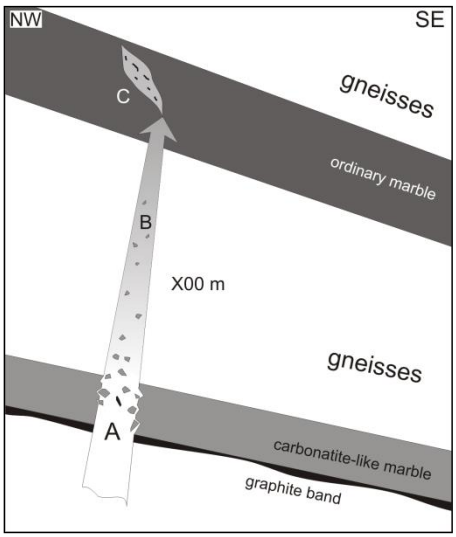

Fig. 1: Strongly schematized sketch showing pre-emplacement contamination of pegmatite melt of the Bližná I pegmatite by carbonatite-like marble. A – trapping of fragments of carbonatite-like marbles + very rare graphite fragments during forcible ascent of melt to the site of emplacement; B – dissolution of marble fragments and partial homogenization of the melt during the transport to the site of emplacement; C – crystallization of incompletely homogenized pegmatite melt. The sketch is not to scale (Novák *et al.* 2012).

Owing to rather short transport (likely hundreds of m), the melt was not completely homogenized, what can be seen from heterogeneous distribution of diopside-bearing nests (strongly digested fragments of carbonatite-like marbles with accessory bastnaesite-(Ce), parisite-(Ce), allanite-(Ce), titanite, and uvite) present within the dominant schorl-rich unit. Geochemical modeling provided further evidence for contamination of pegmatite melt by carbonatite-like marble (see Novák *et al.* 2012).

Post-emplacement contamination of melt is more abundant and it was manifested at several localities (e.g., Černý and Němec 1995, van Lichtervelde *et al.* 2006, Kuznetsova 2011, Novák *et al.* 2013). However, the option that elevated contents of unusual elements (mainly Ca, Mg, Fe and Ti) in some minerals canbe derived from pre-emplacement contamination was not previously discussed, so its influence cannot be entirely excluded in some cases. The first example, elbaite-subtype pegmatite from Vlastějovice, represents a pristine in-situ contamination; the pegmatite melt

passed from its parental granite only through Fe-skarn (Fig. 2), and Ca,Fe-contamination is manifested by the presence of primary danburite, fluorite, and magnetite, and high Ca,Fe-contents in tourmalines (Novák *et al.* 2013). The second example is the beryl-columbite subtype Věžná I pegmatite (Fig. 3) with rare pollucite, Li-micas and fluor-elbaite. The compositions of common phlogopite X_{Mg} = 0.72-0.75, cordierite X_{Mg} = 0.69-0.79, tourmaline X_{Mg} = 0.45-0.66 from border and wall zones, and reaction rims on contacts (anthophyllite, tremolite, actinolite, phlogopite) imply obvious *in-situ* Mg-contamination of pegmatite melt. Potential pre-emplacement contamination of the melt from host metapelitic complexes is hardly detectable due to very strong *in-situ* Mg-contamination. After crystallization of outer units the pegmatite was sealed to host rock and after exhaustion of Mg from melt during crystallization of phlogopite, cordierite and tourmaline the minerals from the most fractionated portions of pegmatite with pollucite + Li-micas + fluor-elbaite are typically Mg-free. Only very late Cs-rich polylithionite portions of zoned lepidolite crystals from veinlets cutting pollucite are Mg-enriched and confirm re-opening of the system to the host rock likely during magmatic-hydrothermal transition.

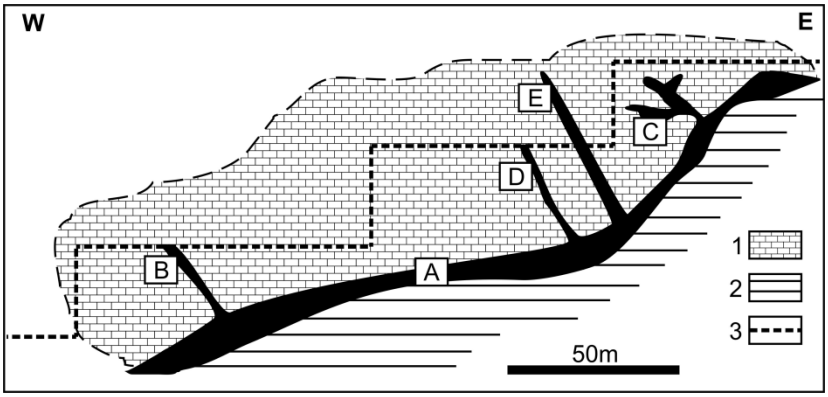

Fig. 2: Cross section through Fe-skarn (1), orthogneiss (2), Footwall granite-pegmatite (A) and related tourmaline-bearing pegmatites (B, C, D), E – elbaite pegmatite; (3) galleries of the quarry. (Breiter *et al.* 2010).

Post-emplacement contamination of solid pegmatite is abundant and rather easily detectable relative to the above processes; however, degree of total contamination of whole pegmatite body is usually low. Alteration of feldspars and mainly of primary Fe,Mn-phosphates is evidently subsolidus process with introduction of elements from host rocks (e.g., Galliski *et al.* 2012). Kerolitization of quartz (desilication) in the beryl-columbite subtype Věžná I pegmatite (Fig. 3) according to the reaction: 4 quartz + 3 $MgCl_2$ + 6 H_2O = kerolite + 6 HCl associated with albitization of oligoclase An_{15} (Dosbaba and Novák 2012) is a typical example of significant subsolidus contamination, where a quite high volume of quartz was replaced by kerolite, and bulk composition of pegmatite changed significantly.

In most zoned pegmatites, once outer zones crystallized, the pegmatite melt is sealed from external interaction, at least to the point of its thermal equilibration with wallrock (London 2008). Hence, the degree of contamination of large and more evolved complex pegmatites is typically very low. Only the elbaite-subtype Bližná I pegmatite with common diopside, Ca-rich tourmalines and REE-fluorocarbonates (Novák *et al.* 1999, 2012), scapolite-bearing spodumene pegmatites from Siberia (Kuznetsova 2011), both from metacarbonates-rich rock sequences, and elbaite-subtype pegmatite from Vlastějovice, Czech Republic cutting Fe-skarn (Novák *et al.* 2013) exhibit high degrees of contamination of complex pegmatites. However, all these pegmatites form relatively small bodies (up to several m thick) and host rocks have highly contrasting composition. Hence, combination of small volume of melt, its high reactivity and reactive host rocks (mainly metacarbonates) caused visible contamination with relative ease.

Input of elements during the individual stages of contamination includes mainly easily detectable elements strange for granitic pegmatites such as Ca and Mg, but also Ti, Fe, Ba, Sr, Cr, V and REE. External contamination is indicated via formation of new phases commonly absent in granitic pegmatites (e.g., clinopyroxenes, amphiboles, epidote, scapolite, calcite) or more frequently in exotic compositions of common pegmatite minerals (e.g.,

tourmalines, cordierite, garnets, beryl, micas, columbite-group minerals) and commonly also presence of reaction rims in the contact with host rock. In contrast, external contamination by the major pegmatite elements (Na, K, Al, Si) is hardly confirmable. Whether, it may change K/Na ratio or Al/Si ratio in pegmatite melt remains unclear. Nevertheless, evident Ca-contamination decreases ASI index of the melt as was manifested in the bulk compositions of contaminated spodumene pegmatites from the Solvelder River Basin, South Siberia (Kuznetsova 2011).

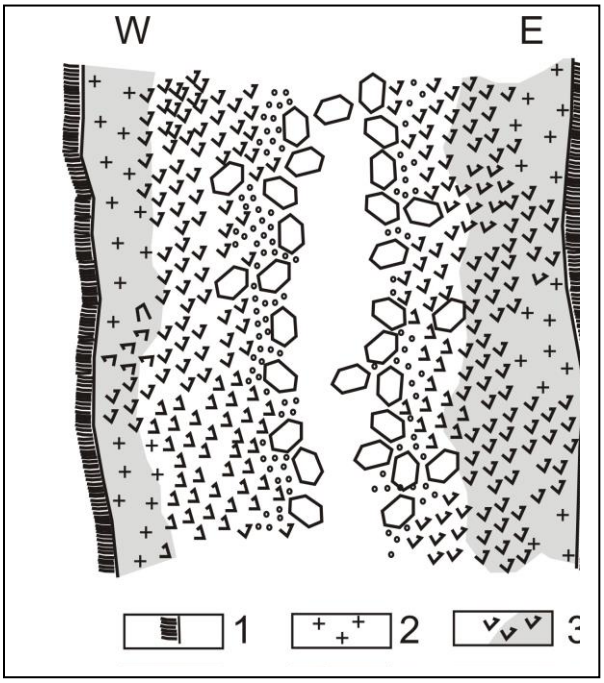

Fig. 3: Simplified cross-section through the Věžná I pegmatite, thickness of the dike - ~3 m. 1. – reaction rim (anthophyllite, phlogopite, tremolite-actinolite, talc) between pegmatite and serpentinized peridotite; 2 – granitic wall unit; 3 – intermediate graphic unit (shaded areas – kerolitization of quartz); 4 – albitization (albite unit); 5 – blocky feldspar, 6 – quartz core (Dosbaba and Novák 2012).

Owing to heterogeneous internal structure of most pegmatites, we can hardly study their bulk compositions and apply geochemical modeling to recognize or quantify degree of external contamination (Novák *et al.* 2012). Hence, we have to focus on chemical composition of individual minerals showing: (i) abundance in granitic pegmatites and in individual pegmatite zones, (ii) crystal structure available to incorporate variety of the elements indicating contamination such as Ca, Mg, Fe, Cr, and V at variable PT conditions, and if possible (iii) refractory behavior. Tourmaline and mica, and also garnet, cordierite, and beryl are suitable. In contrast, major pegmatite minerals (feldspars, quartz) have low ability to incorporate the contaminating elements, except for Ca, Sr and Ba in feldspars. However, their contents are controlled by rather low temperature of pegmatite crystallization and common subsolidus overprint in feldspars. A further problemis that no differences in the chemical composition of plagioclase from non-contaminated and contaminated tourmaline-bearing pegmatites cutting gneisses or Fe-skarn in Vlastějovice (Fig. 2) were observed (Novák *et al.* 2013).

The following factors control degree of contamination of pegmatite melts. (i) Contrasting chemical composition of host rocks (marbles, serpentinite, Fe- skarn) from both channelways and enclosing pegmatites *in-situ* after melt emplacement is perhaps the most important along with (ii) Solubility (reactivity) of the host rocks. Contaminations from rocks with similar chemical composition (e.g., orthogneiss, granulites) and/or from low-reactive rocks (e.g., quartzite) are hardly detectable. (iii) Reactivity of infiltrated fluids and their composition represents further essential factors, which operates mainly after emplacement of pegmatite melt (Dosbaba and Novák 2012). (iv) Volume of transported pegmatite melt is a substantial factor because larger volumes of melt have smaller mutual surface-area of the contact with host rocks. Nevertheless, a weak *in-situ* contamination may be recognizable along direct contact of large pegmatite bodies (e.g., Tanco, Manitoba; Selway *et al.* 2000, van Lichtervelde *et al.* 2006). (v) Degree of geochemical fractionation

of the individual pegmatite melts including amount of volatiles (H_2O, B, F and P) and δT between pegmatite melt and host rock are closely related factors. Emplacement of pegmatite melts into cold rocks causes undercooling and rapid crystallization; consequently, a short time for exchange of elements *in-situ* between melts and host rock (Novák *et al.* 2013). (vi) Length and velocity of transport of pegmatite melt through channelways is important factor but commonly unknown, as well as, (vii) Viscosity of pegmatite melt. Short transport and high velocity decrease reaction time for contamination, but even short transport of melt in decameters through chemically contrasting rock (Fig. 2) may produce *in-situ* contamination of pegmatite melt (Novák *et al.* 2013). This work was supported by the research project GAP210/10/0743.

References

Breiter, K., J. Cempírek, T. Kadlec, M. Novák, R. Škoda (2010): Granitic pegmatites and mineralogical museums in Czech Republic. Acta Mineralogica-Petrographica, Field Guide Series, vol. 6, 1-56.

Černý, P., D. Němec (1995): Pristine vs. contaminated trends in Nb,Ta-oxide minerals of the Jihlava pegmatite District, Czech Republic. Mineralogy and Petrology, vol. 55, 117-129.

Dosbaba, M., M. Novák (2012): Quartz replacement by kerolite in graphic quartz-feldspar intergrowths from the Věžná I pegmatite, Czech Republic; A complex desilicification process related to episyenitization. Canadian Mineralogist, Petr Černý Issue II, vol. 50, 1609-1620

Galliski, M.A., P. Černý, M.F. Márquez-Zavalía, R. Chapman (2012): An association of secondary Al–Li–Be–Ca–Sr phosphates in the San Elías pegmatite, San Luis, Argentina. Canadian Mineralogist, Petr Černý Issue I, vol. 50, 933-942.

Kuznetsova, L.G. (2011): Geochemical evolution and petrogenesis of rare-element pegmatites in the Solbelder River Basin (south Siberia, Russia). Associación Geológica Argentina, Serie D, vol. 14, 119-122.

London, D. (2008): Pegmatites. Canadian Mineralogist, Special Publication 10, 347 p.

Novák, M. (2007): Contamination in granitic pegmatites, examples from the Moldanubicum, Czech Republic. Granitic Pegmatites: The state of the art - International Symposium. Universidade do Porto – Faculdade de Ciências, Memórias, vol. 8, 9-12.

Novák, M., T. Kadlec, P. Gadas (2013): Geological position, mineral assemblages and contamination of granitic pegmatites in the Moldanubian Zone, Czech Republic; examples from the Vlastějovice region. Journal of Geosciences, vol. 58, submitted.

Novák, M., J.B. Selway, P. Černý, F.C. Hawthorne (1999): Tourmaline of the elbaite-dravite series from an elbaite-subtype pegmatite at Bližná, southern Bohemia, Czech Republic. European Journal of Mineralogy, vol. 11, 557-568.

Novák, M., R. Škoda, P. Gadas, L. Krmíček, P. Černý (2012): Contrasting origins of the mixed signature in granitic pegmatites; examples from the Moldanubian Zone, Czech Republic. Canadian Mineralogist, Petr Černý Issue I, vol. 50, 1077-1094.

Selway, J.B., P. Černý, F.C. Hawthorne, M. Novák (2000): The Tanco pegmatite at Bernic Lake, Manitoba. XIV. Internal tourmaline. Canadian Mineralogist, vol. 38, 1103-1117.

Van Lichtervelde, M., R.L. Linnen, S. Salvi, D. Beziat (2006): The role of metagabbro rafts on tantalum mineralization in the Tanco granitic pegmatite, Manitoba. Canadian Mineralogist, vol. 44, 625-644.

GORMANITE DISTRIBUTION AND EQUILIBRIUM CONDITIONS IN PEGMATITE FROM CORREGO FRIO FIELDS, GALILEIA, MINAS GERAIS, BRAZIL

F. Pires[1], H. Amorim [2], M. Fonseca [3],
[1] UERJ, Geology Dept., frmpires@yahoo.com
[2] UFRJ, Institute of Physics
[3] UFOP, CPRM.

The phosphate-rich Corrego Frio pegmatites at the Oriental Province of Minas Gerais, Galileia district are Li-poor and rich in brazilianite-herderite, in contrast with the Li-rich Sapucaia pegmatites, characterized by triphylite (Fig. 1). Joao Teodoro (JT) pegmatite (Corrego Frio) consists of gormanite ($Fe^{2+}{}_3Al_4(PO_4)_4(OH)_6.2H_2O$) recognized by optical, EMP and XRD analyses. It was formed during a low-T, late hydrothermal-pegmatite stage, together with barbosalite, scorzalite, strengite, vivianite, kingsmountite, heterosite, hureaulite and brazilianite. The pegmatites intrude both Proterozoic granite plutons and north-south trending, biotite-sillimanite-schists of the Archean Sao Tome formation. The JT pegmatite (15m thick), is subvertical, boudinaged and partly altered. Gormanite is a bluish green, triclinic phosphate mineral, occurring in pockets with partly kaolinized albite, barbosalite, scorzalite and brazilianite. Isolated pockets of strengite-vivianite-hureaulite, scorzalite-gormanite-variscite and gormanite-kingsmountite-barbosalite confirm the isolated pocket nature. Gormanite was previously described from a pegmatite at the type locality Big Fish River, Yukon, Canada, but also in the south of Karibib, Tsaobismund pegmatite, Namibia; at Newport, Sullivan Co. and at the Charles Davis pegmatite, Groton, Grafton Co., New Hampshire. The JT gormanite averages 35.61% P_2O_5, 23.06%Al_2O_3, 6.36%MgO, 21.69%FeO, 0.61%MnO (six UnB/EMP-analyses), occurring as blue needles perched on scorzalite, barbosalite and brazilianite. Small pockets of fine-grained gormanite-variscite-vivianite-barbosalite are abundant.. The graphical representation of the stability fields implies that gormanite is destabilized at any increase of μH^+ in favor of vivianite or kingsmountite. Significant increases in μH_2O result in augmenting the vivianite stability in any condition. It also shows the large barbosalite divariant field, coexisting with all phases. The univariant reactions plotting (Mg, Fe^{3+}, Fe^{2+}, Al^{3+}, Ca^{2+} and Mn^{2+} as they were not considered in stoichiometric balance) reveal a slight decrease in fO_2 and in phase stability. The result of scorzalite consumption is the allocation of Al^{3+} in gormanite and variscite. Apparently, barbosalite abundance is governed by scorzalite breakdown in a reaction to produce gormanite under increasing μH^+ condition: 3 Scorzalite + $20H^+$ = Barbosalite + Gormanite + $6H_2O$, or by the partial barbosalite breakdown: $2Fe^{2+}\ Fe^{3+}{}_2(PO_4)_2(OH)_2 + 4H_2O + 4Al^{3+} = Fe^{2+}{}_3\ Al_4(PO_4)_4(OH)_6.2H_2O + 2\ H^+ + 3Fe^{2+}$. Three univariant reactions can be plotted in space studying the stability of the Al-rich phases for JT pegmatite, showing that gormanite reacts under increasing μH^+ conditions, mostly to variscite.

Progemas and CNPq Grants supported this work.

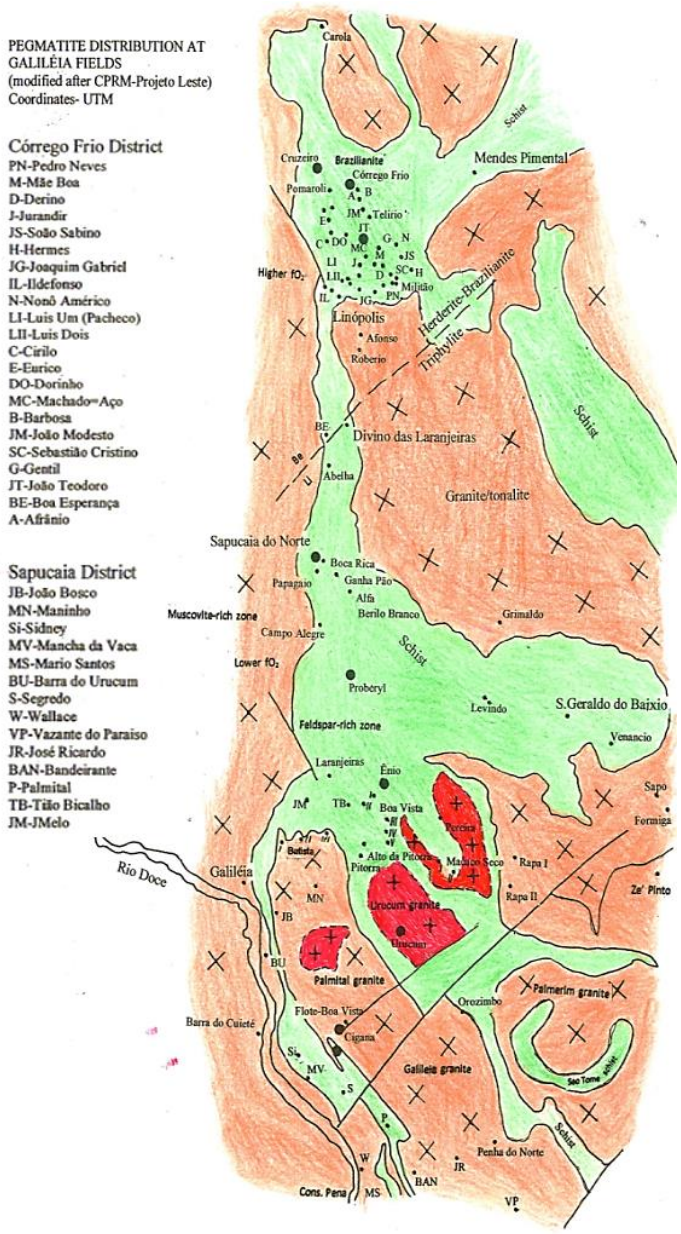
PEGMATITE DISTRIBUTION AT
GALILÉIA FIELDS
(modified after CPRM-Projeto Leste)
Coordinates- UTM
Córrego Frio District
PN-Pedro Neves
M-Mãe Boa
D-Derino
J-Jurandir
JS-João Sabino
H-Hermes
JG-Joaquim Gabriel
IL-Ildefonso
N-Nonô Américo
LI-Luis Um (Pacheco)
LII-Luis Dois
C-Cirilo
E-Eurico
DO-Dorinho
MC-Machado=Aço
B-Barbosa
JM-João Modesto
SC-Sebastião Cristino
G-Gentil
JT-João Teodoro
BE-Boa Esperança
A-Afrânio
Sapucaia District
JB-João Bosco
MN-Maninho
Si-Sidney
MV-Mancha da Vaca
MS-Mario Santos
BU-Barra do Urucum
S-Segredo
W-Wallace
VP-Vazante do Paraiso
JR-José Ricardo
BAN-Bandeirante
P-Palmital
TB-Tião Bicalho
JM-JMelo
Carola
Cruzeiro
Brazilianite
Córrego Frio
Pomarolí
Telirio
Mendes Pimental
Schist
Higher fO2
Herderite-Brazilianite
Triplolite
Militão
Linópolis
Afonso
Roberio
Divino das Laranjeiras
Abelha
Granite/tonalite
Sapucaia do Norte
Boca Rica
Papagaio
Ganha Pão
Alfa
Berilo Branco
Grimaldo
Muscovite-rich zone
Campo Alegre
Lower fO2
Proberyl
Levindo
S.Geraldo do Baixio
Feldspar-rich zone
Venancio
Laranjeiras
Ênio
Sapo
Boa Vista
Formiga
Rio Doce
Galiléia
Batista
Alto da Pitorra
Pitorra
Mabaco Seco
Rapa I
Rapa II
Ze' Pinto
Urucum granite
Palmital granite
Palmerim granite
Orozimbo
Barra do Cuieté
Flote-Boa Vista
Cigana
Galileia granite
São Tomé
Penha do Norte
Cons. Pena
VP

Fig.1

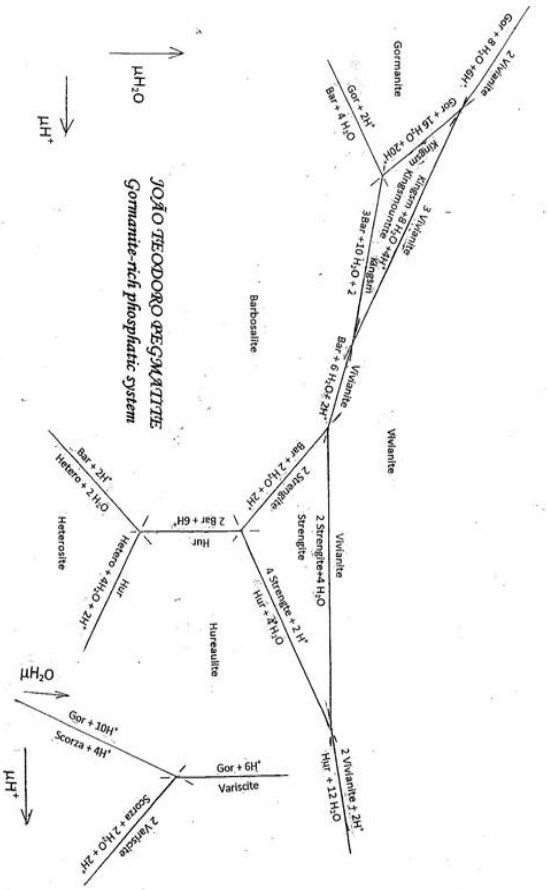
JOÃO TEODORO PEGMATITE
Gormanite-rich phosphatic system
Gormanite
Barbosalite
Hureaulite
Vivianite
Variscite
Scorza
Bar + 4 H2O
Gor + 2H+
Gor + 8 H2O +6H+
2 Vivianite
Gor + 18 H2O +20H+
Klingsten
Klingsten +Strengite
3 Vivianite
3Bar + 10 H2O + 2
Bar + 6 H2O+ 2H+
Bar + 2H+
Hetero + 2 H2O
2 Bar + 6H+
Hur
2 Strengite + 2 H2O
Hetero + 2H2O + 2H+
Hur + 2H2O
4 Strengite + 2 H+
2 Strengite + 2H+
2 Strengite
Gor + 10H+
Scorza + 4H+
Gor + 6H+
Hur + 12 H2O
2 Vivianite + 2H+
3 Variscite
Scorza + 2 H2O + 2H+

Fig. 2

CHRYSOBERYL AND ALEXANDRITE MINERALIZATION IN THE ORIENTAL PEGMATITE PROVINCE OF MINAS GERAIS, BRAZIL – DEPOSIT CONTROLS

F. Pires[1], M. Fonseca[2], R. Lima.[3]
[1] Uerj-Geology dept, frmpires@yahoo.com
[2] CPRM, 3.UFRJ

The area is worldwide known since the first half of the twenty century, by the presence of beautiful aquamarine, tourmaline and chrysoberyl gems and by muscovite deposits intensely mined since the 2nd World War. Chrysoberyl specimens as large as 22 x 15cm, a yellowish green gem weighing 43 ct from Aracuai, lies in the Britiish Museum; a 114 ct cushion shown at Smithsonian Institution; a 10 x 9mm dark yellow gem, in possession of Duke of Dree, now in Paris; a 400 ct, world's largest "cimophane" found at Aracuai (Calhau); a green-lettuce, 70 ct-gem after lapidated from Itambacuri; Mitra cat's-eye with 6250g and 20cm high; and a gem weighing 25.2kg from Socoto'-Jacunda' deposits in Bahia; are some gems found in the area. It was noticed that the chrysoberyl deposits are mostly in recent and ancient placers, which may correspond to, in some way, the proximity of source rock. The main deposits are distributed in the Oriental Pegmatite Province at Americaninhas, Santana river valley, where the gems and cat's-eye variety are exploited in "garimpos" and mines in Corrego do Gil, Barro Preto, Faisca and Cilindro and at Lambuza, Pavao and Crisolita region, all at Mucuri River headwaters (Fig. 1). Additional chrysoberyl occurrences in the OPP are Itambacuri, Corrego do Cascalho, Coimbras, Santa Cruz brook, nearby Catuji, and Corrego Comprido. Critical questions are: Do the chrysoberyl occurrences constitute a belt? What is the genetic and spatial relation between the chrysoberyl and regional/contact metamorphism? Some facts are unquestionable, such as the ubiquitous presence of K-feldspar, mainly orthoclase, biotite, topaz and beryl and almost complete absence of albite, tourmaline, Li- and phosphate-minerals. Muscovite may occur, but is not frequent, formed during late stages. Actually the Pavao-Americaninhas forms a discontinuous belt parallel to a high-grade metamorphic rock sequence where charnockites predominate. The belt may be connected north to Jequitinhonha (Tres Ilhas) and southward to Itambacuri, through a complex shear zone. Vereda (Cel. Murta) chrysoberyl occurrences, extending to Tres Ilhas, are the prolonging of Serafim Trancado (Minas Novas) deposits. Corrego do Fogo and Soturno are near Malacacheta and Minas Novas. An additional chrysoberyl belt may be defined by Itaguacu, Colatina, Santa Tereza, and Cachoeira do Itapemirim localities. Alexandrite deposits are confined to Hematita and Nova Era. A regional zoning is defined at the western boundary of the chrysoberyl belt, as a surface separating it from the tourmaline-Li-mineral zone, which follows northward to Itambe Li-bearing pegmatite fields. Chrysoberyl at Corrego do Faisca occurs as isolate and planar aggregates of crystals with quartz. Some single specimens (5 x 8cm) exhibit one portion of massive chrysoberyl partly engulfing fibrous chrysoberyl close to the "blackwall" contact zone (vein selvage) of the altered pegmatite, which is interpreted as sheared contacts with the enclosing charnockite. Similar feature also happens at the fibrous tourmaline from Barra do Cuiete, near Galileia. Minute beryl and topaz crystals also occur. Occasional beryl and phenakite association with chrysoberyl exists. The presence of andalusite and cordierite and the similar occurrences of Socoto'emerald deposit suggest metasomatic transformation under retrograde conditions. Pink and golden yellow hyaline quartz occurs in the belt. The equilibrium conditions of the system Be-Al-Si-O-H, studied in a μH^+-μH_2O diagram (Fig. 2), show that beryl breakdown results in chrysoberyl+quartz. Apparently, the Faisca and Gil deposits are of the schist-type, derived from the high-TP regional/contact metamorphism, similar to the Kerala deposits. The chrysoberyl bearing pegmatoids formed by residual melts of charnockitic liquids from partial melting of high-Al_2O_3 metamorphic rocks. Pervasive CO_2-rich fluids promoted the partial or total elimination of H_2O-fluids from the system. The existence of CO_2-rich fluid inclusions in the chrysoberyl is indicative of the system development. After chrysoberyl crystallization, pressure release and temperature fall, water-rich fluids predominate, yielding muscovite formation in different paragenesis, as multistage process operates. Andalusite and cordierite presence in the regional gneisses, pegmatoidal rocks and placer deposits, confirms the retrograde metamorphic process. The cordierite-granulite

occurrence at Jacinto-Jardinopolis belt, corroborates the metamorphic evolution. However the understanding of the geochemical behavior of beryllium is still poorly known (Beus, 1966).

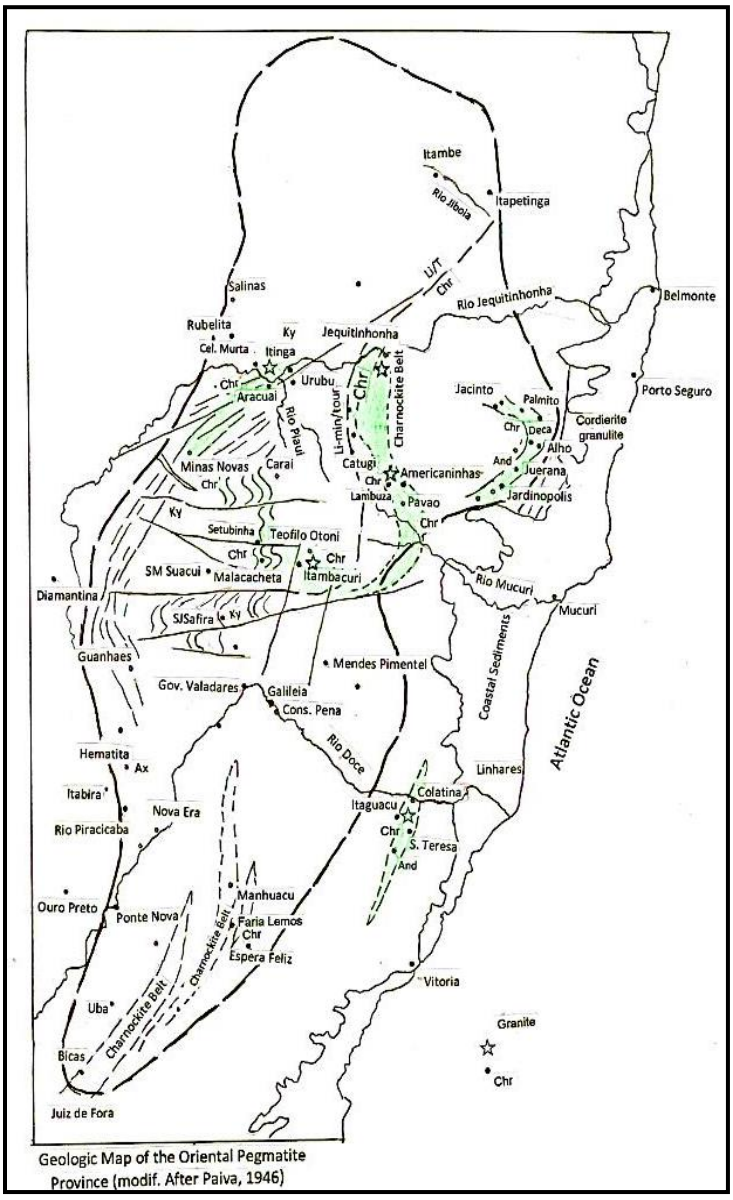

Geologic Map of the Oriental Pegmatite Province (modif. After Paiva, 1946)

Fig.1

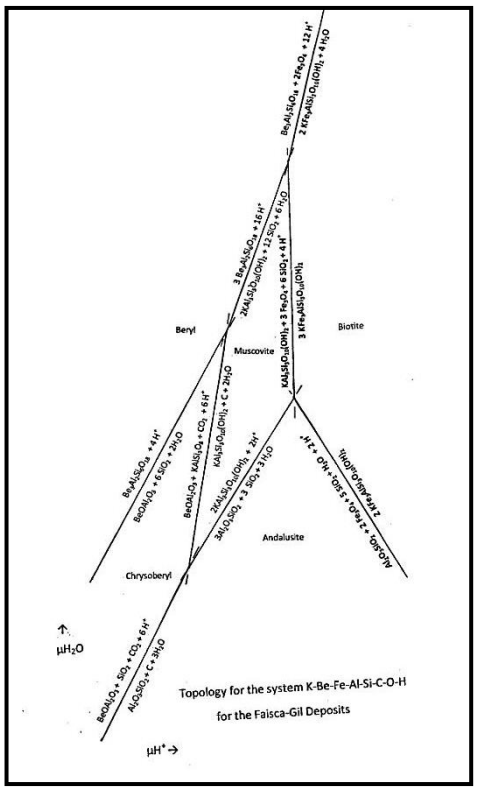

Fig.2

PHOSPHATE MINERALS FROM THE GALILEIA PEGMATITE FIELD, MINAS GERAIS, BRAZIL: EQUILIBRIUM CONDITIONS

F. Pires[1], N. Palermo[2], M. Fonseca [3] R. Lima[4]
[1] UERJ, Geology Dept., frmpires@yahoo.com
[2] State University of Rio de Janeiro
[3] UFOP/CPRM
[4] UFRJ

In the decades of 40s and 50s several new phosphate minerals have been discovered and described from the Galileia and Corrego Frio fields by investigators from USGS and DNPM (Pough & Henderson, 1945; Pecora & Fahey, 1948, 1949; Godoy, 1945; Lindberg and Pecora, 1953, 1955, 1958; Lindberg *et al.*, 1953; Lindberg and Murata, 1953; Lindberg, 1962) and recent findings as zanazziite (Leavens *et al.*, 1990); works on known species (Cassedanne & Cassedanne, 1978, 1981; Dunn *et al.*, 1979; Atencio *et al.*, 2004); Correia Neves *et al.*, 1980; Cassedanne & Guillemin, 1971; Cassedanne, 1983, 1989, 1999; Bilal *et al.*, 1998; Scholz *et al.*,2003). Among these phosphates we have, the phosphate minerals scorzalite, souzalite, barbosalite, brazilianite, faheyte, moraesite, tavorite, frondelite and Mn-lipscombite in addition to messelite, whiteite, childrenite-eosphorite, ludlamite, wolfeite, triphylite, bermanite, montebrasite, roscherite, cyrilovite, gordonite, heterosite, hureaulite, leucophosphite, lipscombite, metastrengite, strengite, variscite, vivianite, ferrisicklerite, gormanite, lazulite, lithiophylite, roeddingite, purpurite, herderite, saleeiite, augelite, arrojadite, berlinite, cacoxenite, dufrenite, lauite, phosphosiderite, lindbergite, besides several generations of apatite and the rose quartz (Cassedanne & Cassedanne, 1973, 1976, 1978, 1979, 1981; Cassedanne & Alves, 1990; Cassedanne & Baptista, 1999; Svizero, 1976; Dunn *et al.*, 1976; Wilson, 1999). Roscherite, zannazziite and greifensteinite found (Atencio *et al.*, 2005a; 2005b). study was refined (Tavora Filho, 1945), eosphorite zoning (White, 1990) and barbosalite twinning (Lindberg, 1969), complete reference list found in Pires, 2007. The distribution of the pegmatites may be visualized in the map, where a district zoning can be depicted: Brazilianite-Herderite at Corrego Frio and Li-rich phosphates at Sapucaia field. In addition, sabugalite, rutherfordine, autunite, siderite and sulfide minerals have been recognized. Pegmatites occur in two main types: 1. Intrusive in granite, tabular, subhorizontal, ”sheet-like”, partly zoned, with gigantic clear, well-formed quartz crystals in the core, surrounded by cleavelandite-muscovite. 2. Intrusive into regional biotite schist, sub-vertical, boudinaged with pinch-and-swell structure, “canoe-shaped”, discrete and obscure zoning without clear quartz. Type 2 in schist is regionally zoned consisting of Li-poor, Be-rich minerals and brazilianite-herderite association defined in the Corrego Frio field,whereas in the Sapucaia field pegmatites are Be-poor and Li-rich, characterized by relatively abundant triphylite, spodumene and rubellite. Both types contain phosphate minerals, but the type 2 contains more abundant phosphate minerals and a greater variety of species (Figs.1 and 2).

Granite and pegmatites from the Oriental Province experienced brittle deformation after ductile deformation, which increased inter-crystalline fluid percolation, where most of primary phosphate minerals were deposited. Pockets result from dissolution along the fissures and inter-crystalline spaces. According to this process, phosphate mineral crystallization proceeded as either isolated or semi-open systems. Small veins in fissured triphylite, found at Sapucaia, previously described (Lindberg & Pecora, 1955) show a particular zoning with hureaulite + vivianite in the selvages, barbosalite + tavorite in the intermediate zone and heterosite + ferrisicklerite in the core, allowing the construction of a μH^+-μH_2O diagram to explain the evolution. Understanding the phosphate behavior in the Galileia District μH^+-μH_2O diagrams must be constructed for the two field systems, Corrego Frio and Sapucaia. Most of the phosphate minerals previously identified by chemical, optical and XRD methods have been confirmed during a sabbatical stay at Universite de Liege. Work sponsored by CNPq and Progemas.

Reference

Pires,F.R.M., Fonseca, M.A. and Echternach, M., 2007. Mineralogical and Geochemical Zoning in the Pegmatites from the Oriental Province of Minas Gerais. 14 Sem. Geoquim./8 Cong. Geoq.,Univ.Aveiro.

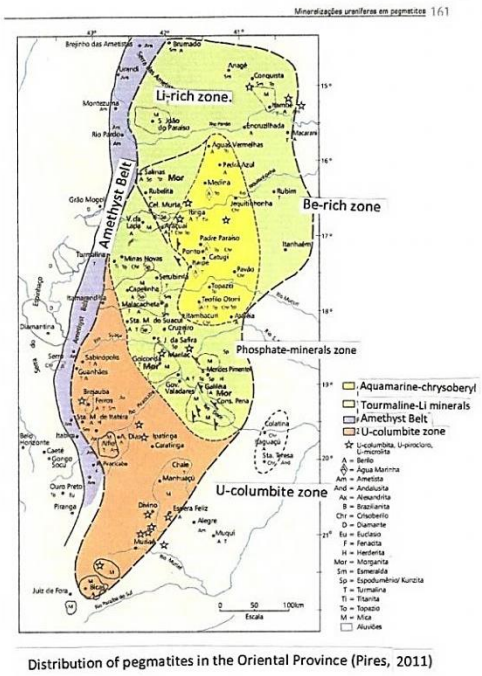

Distribution of pegmatites in the Oriental Province (Pires, 2011)

Fig. 1

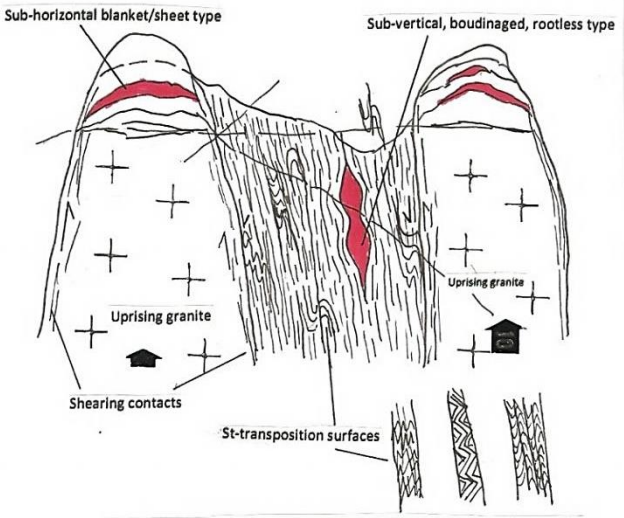

Emplacement of granite and pegmatites – Galileia District Sao Tome schist

Fig. 2

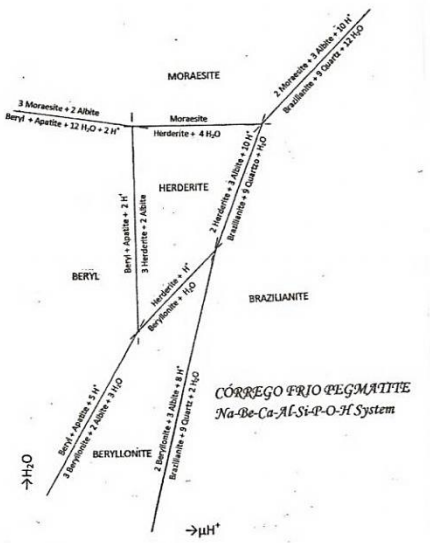

Fig. 3

Fig. 4

URANIUM IN PEGMATITES-BRAZILIAN CASE STUDY

F. Pires[1], S. Miano[2], R. Lima [3]
[1] Uerj-Geology Dept., frmpires@yahoo.com.br
[2] Eletronuclear
[3] UFRJ-Geology Departament

Pegmatites are both fascinating and frustrating due to the gem minerals they contain and mineral parageneses that could reveal their origins and, on the other hand, due to some important field aspects erased by total exploitation. Two important pegmatite provinces exist in Brazil, the Oriental Pegmatite in Minas Gerais and Bahia, and the Borborema, extended to Serido-Borborema, at Northeastern Brazil (Paiva, 1946; Scorza, 1944). Recent studies in both regions (Johnston, Jr., 1945; Rolff, 1946; Correia Neves,1986; Pires, 2007) improved their understanding. Comparison of levels of U and Th of Galileia and Urucum granite plutons with Nigerian volcanics, Niger ignimbrites at Younger granite Province (Bowden *et al.*, 1981), Pikes Peak batholith granite and intrusives of Varberg charnockite-granite associations suggest that Galileia granite is enriched in Th and with depletions of U relative to Th ; whereas the Urucum granite is enriched in U with similar levels of Th of Galileia (Fig. 1). The PPB and CGA associations are U-Th poor and meager Th-enrichment in PPB. Similarly the Nigerian volcanics lost considerable quantities of U in respect to Th. Galileia and Urucum granites do not host U-columbite pegmatites, in contrast to the granite at the southern region (Ipatinga, Divino and Uba). In fact, pegmatites hosted in the Urucum-type granite at Marilac and Golconda, contain U-columbite in pockets (Fig. 2). Transference of U, Th and other elements from granite to pegmatites depends on the process, such as fluid-rock interaction at the granite cupola, intrusion depth, fO_2, granite composition and the existence of eventual traps, or reducing conditions to retain uranium. Several tons of U-minerals have been extracted from pegmatites located at the southern portion of the Oriental Province, particularly in Uba, Divino, Ferros, Guanhaes, Ipatinga, Rio Pomba and Sabinopolis. The aeschinite, uranmicrolite and uranpyrochlore occur in muscovite-rich pockets at the southern zone of the Province. At Conquista-Itambe northern pegmatites there are several U-columbite concentrations. The center part of the Province is dominated by aquamarine, chrysoberyl and topaz in the pegmatites, with no Li-minerals; in contrast to the surrounding zone, where Li-minerals, tourmaline and morganite are relatively abundant. Phosphate minerals are abundant at the southern zone, where several primary and supergene species (scorzalite, brazilianite, herderite, gormanite-souzalite, barbosalite) have been described, together with gigantic, well formed, clear quartz and muscovite in large plates (Pecora *et al.*, 1949). Autunite and uraninite occur sporadically. Pegmatites intrude several types of granite and Sao Tome schists. At the western zone, within Espinhaco quartzites and itabirites, amethyst deposits are discontinuously distributed. Uranium is concentrated in samarskite from Uba and Divino in the range 14-19% U_3O_8 in contrast with polycrase from Rio Pomba (4-10% U_3O_8) and from Urubu (9-10% U_3O_8). U-columbite from Minerpeg ranges from 8% to 11% U_3O_8. In diagrams UO_2-TiO_2-Y_2O_3+ThO_2 the bimodal distribution between pegmatites from Rio Pomba and Divino can be observed (Fig. 3). Apparently, columbite, magnetite and uraninite occurrence in pegmatites is constrained by temperature, oxygen fugacity (fO_2) and molar fraction of Fe. Columbite crystallizes under low fO_2, being magnetite absent. High fO_2 favors hematite+uraninite deposition above the magnetite-fayalite curve.

References

Bowden, P., Bennett, J., N. Kinnaird, J., A. Whitley, J., E. Abaa, S., I. Hadzigeorgiou-Stavrakis, P., K. (1981): Uranium in the Niger-Nigeria Younger granite Province. Mineralogical Magazine, vol. 44, 379-389.

Correia Neves, J., M. Soares, A., C.P. Marciano, V., R. P. R. O. (1986): A provincia pegmatitica oriental do Brasil a luz dos conhecimentos atuais. Revista Brasileira de Geociencias, vol. 16, 106-118.

Johnston, Jr.,(1945): Os pegmatitos Berilo-tantaliferos da Paraiba e Rio Grande do Norte, no Nordeste do Brasil. Departamento Nacional da Produção Mineral/ Divisão de Fomento da Produção Mineral, bol. 72, 11-83.

Paiva, G., (1946): Provincias pegmatíticas do Brasil. Departamento Nacional da Produção Mineral/ Divisão de Fomento da Produção Mineral, bol.78, 13-22.

Pecora, W., T. Klepper, M., R. Larrabee, D., M. Barbosa, A., L.M. Frayha, R., (1949): Mica Deposits in Minas Gerais. US Geological Survay, bull. 964-A, 205-305.

Pires, F., R. M. (2011): Mineralizações em Pegmatitos. Uranio no Brasil, Geologia, Ocorrências e Gênese, Cap. 6, 159-180.

Rolff, P., A. M. A. (1946): Minerais dos pegmatitos da Borborema. Departamento Nacional da Produção Mineral/ Divisão de Fomento da Produção Mineral, bol.78, 23-75.

Scorza, E., P. (1944): Provincia pegmatítica da Borborema, Divisão de Geologia e Mineralogia/ Departamento Nacional da Produção Mineral, bol.112, 03-29.

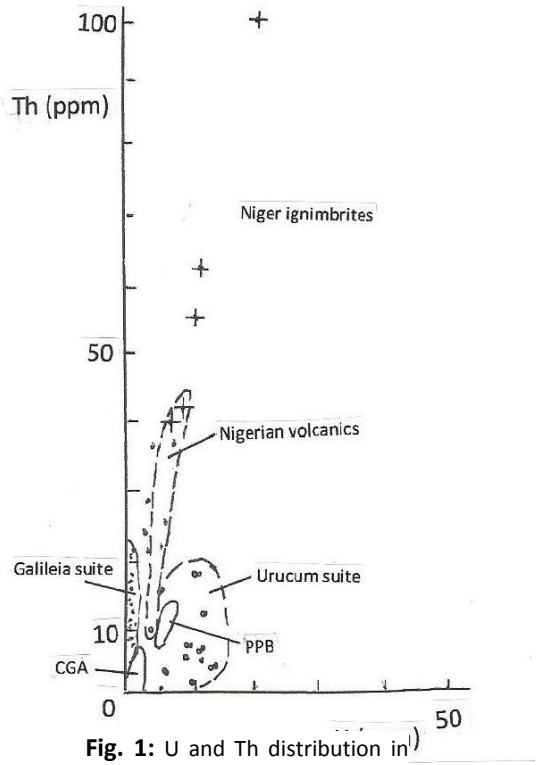

Fig. 1: U and Th distribution in Urucum and Galileia granite suites in comparison with Niger ignibrites (+), Nigerian volcanics, CGA and PPB=Pike's Peak batholith. CGA = Varberg charnockite-granite association-Sweden.

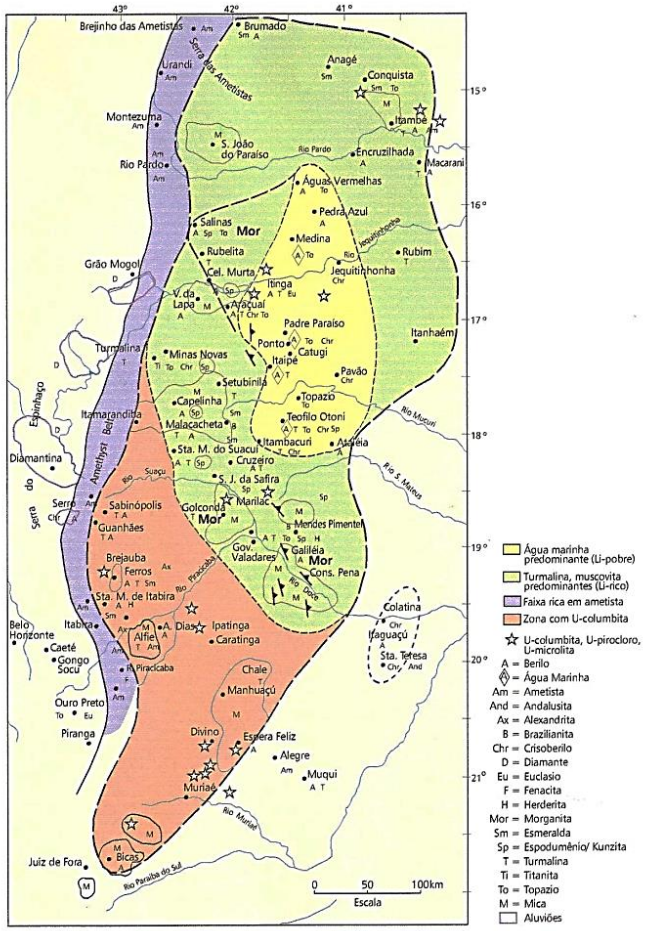

Fig. 2: Distribution of pegmatites in the Oriental Province (Pires,2011).

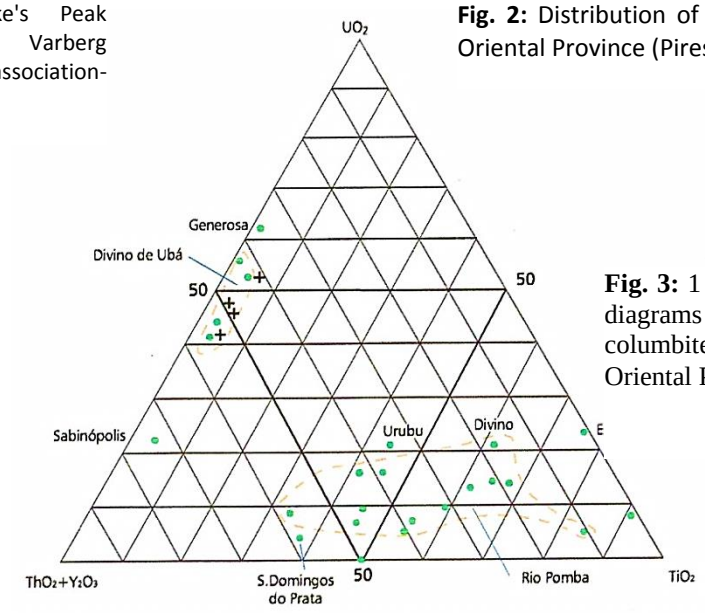

Fig. 3: 1 UO_2-ThO_2+Y_2O_3-TiO_2 diagrams to represent urano-columbite in pegmatites of Oriental Province.

ZONING IN THE URUBU PEGMATITE, ARACUAI DISTRICT, BRAZIL – LI-RICH PARAGENESES

F. Pires[1] J. Sa[2], R .Lima [3]
[1] Rio de Janeiro State University, frmpires@yahoo.com
[2] Federal University of Para
[3] Federal university of Rio de Janeiro

The Urubu pegmatite, located at the northern part of the Oriental Pegmatite Province, Minas Gerais, Brazil contains an unusual association of Li-minerals (amblygonite, lepidolite, petalite, spodumene, triphylite,), in association with pollucite, thoreaulite, cassiterite, tourmaline in a large variety of composition and colors (rubellite, elbaite, achroite, schorl), rare beryl, morganite and aquamarine, beautiful blue topaz, and sulfides such as arsenopyrite, pyrite and sphalerite. Pegmatites are intruding Sao Tome biotite-muscovite schist with including cordierite, andalusite, garnet, kyanite and sillimanite. The schist is part of the Aracuai Belt and encloses several meta-basaltic amphibolite, tourmalinite, graphitic phyllites, metacherts and meta-ultramafic bodies, suggesting they represent a highly metamorphosed greenstone in the kyanite zone, that underwent K-metasomatism. Granites form inselbergs and sugar loafs and are composed of microcline, quartz, oligoclase, biotite, muscovite, apatite, and hornblende. The samples display clear signs of fissuring and cataclasis. The Li-, Cs-, Be and Rb-contents are one to three orders of magnitude higher than in normal granites. Several famous pegmatite bodies occur in the Aracuai District, known as Urubu, Maxixe, Generosa, Limoeiro, Genipapo, Tesouras, Lavra Velha, Cachoeira, Meio, Lavra da Ilha, Mulundu, Morro Redondo, Lufa and Carlau. They are part of about 120 pegmatite bodies mined by CBL, Arqueana, Cesbra, Produco/Orquima and garimpeiros sprawling in the junctions of the Piaui, Aracuai and Jequitinhonha rivers. Cretaceous, unconsolidated, eolian sandstones cover ancient rocks forming buttes and mesas (Sa', 1977; Cassedanne & Cassedanne, 1981.) The Urubu pegmatite is particularly interesting due to its internal zoning, abundant minerals and gems, and production of Li-minerals. Zoning is defined by little crystals of black tourmaline along the contact with schist, followed by a wall zone with muscovite+quartz (M+Q+), muscovite (M) in large flakes, microcline (Kf) with albite (Ab) increasing toward the core, and abundant lepidolite+cleavelandite (L), local amblygonite (Am), petalite (Pet), triphylite (T) and spodumene (Spod) followed by quartz ± morganite (Q)core. Ignoring some more mobile elements such as Na+, Li+ and even Mn^{2+}, Fe^{2+} and Al^{3+} with respect to the less mobile PO_4^{3-} and regarding SiO_2 as relatively mobile, it possible to construct $\mu H+$-μSiO_2 diagrams. Aluminum dissolves in a number of complexes as a function of pH. The discussion on the magmatic origin of the pegmatites, assuming their derivation from Li-rich granitic magmas along a "crystallization path" is challenged by the proposal that they could be generated directly by anatexis of Li-rich sediments under high-T metamorphism. Tourmalinite lenses are distributed along the biotite schist, and pegmatites and S-type granites follow the same trend, which argues against the opinion that only evaporite beds could furnish the elements needed to form pegmatites (Steward, 1978; O'Connor *et al.*, 1991). In conclusion, the μH+-μSiO2 diagrams are useful to study and exhibit phase stabilities, respecting Morey-Schreinemakers Rules and the magmatic-sedimentary pegmatite derivation is still debatable.

References

Cassedanne, J. Cassedanne, J. (1981): The Urubu Pegmatite and vicinity. Min. Record, vol. 12, 73-77

Sa', J., H. S. (1991): Pegmatitos de Itinga-Aracuai (Medio Jequitinhonha),Minas Gerais. Doc. Thesis os São Paulo University, 103pg.

O'Connor, P., J. O. Gallagher, V., Kennan, P., S (1991): Genesis of lithium pegmatites, SE Ireland. Source, Transport and Deposition of Metals. Pagel & Leroy (eds), Balkema Rotterdam, 779-783.

Steward, D., B. (1978): Petrogenesis of lithium-rich pegmatites. Am. Miner, vol. 63, 970-980.

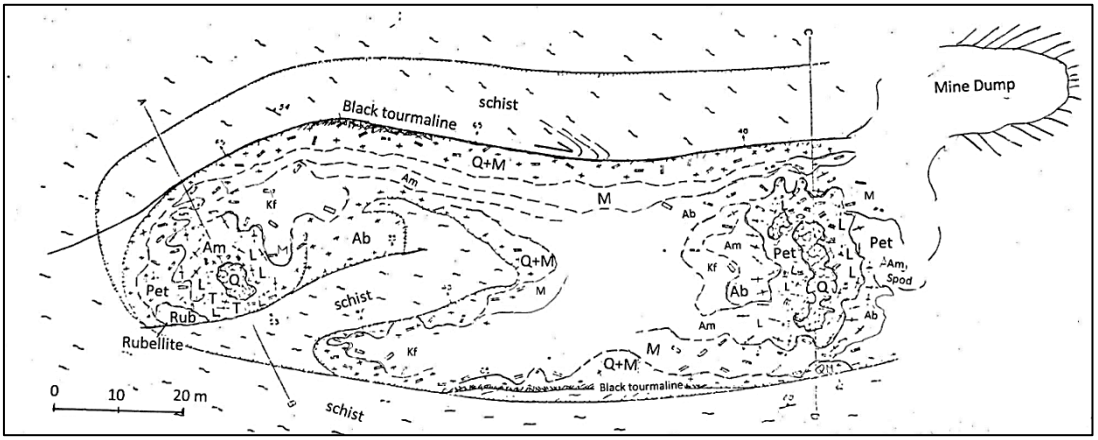

Fig. 1: Geologic Map of the Urubu Pegmatite (modified after Sa', 1977; Cassedani, 1981)- Q= Quartz, Q+M= Quartz + Muscovite, Am= Amblygonite, Pet= Petalite, Ab= Albite, M= Muscovite, L= Lepidolite, T= Tourmaline, Kf= Microcline and Spod=Spodumene

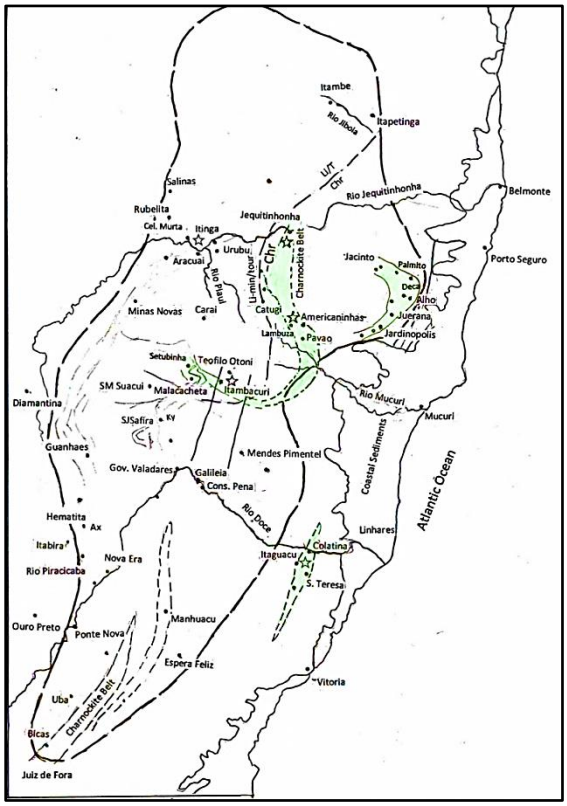

Fig. 2: Isobaric, isothermal, qualitative diagram for the Urubu Pegmatite

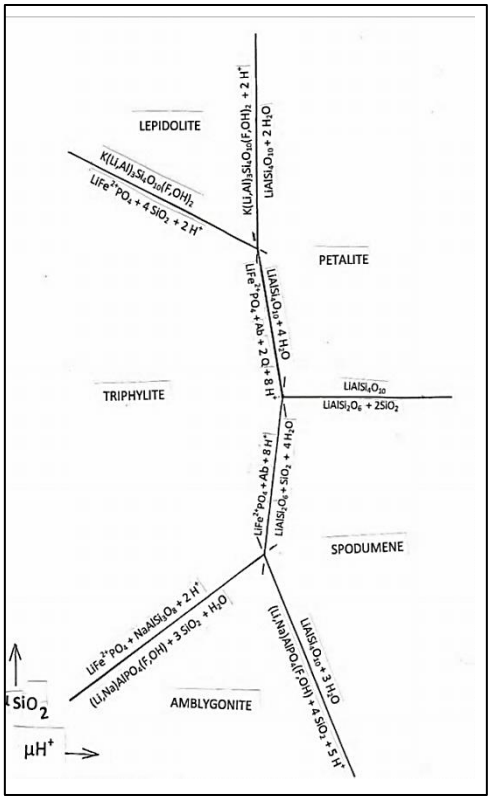

Fig. 3: Geologic Map of the Oriental Pegmatite Province (modif. after Paiva, 1946)

MINERAL EQUILIBRIA IN THE VOLTA GRANDE TA-NB-SN-LI PEGMATITE, SAO JOAO DEL REI DISTRICT, MINAS GERAIS, BRAZIL

F. Pires[1], D. Aranha [2], S. Miano [3], C. Assumpção [4], L.Silva[5]
[1] Uerj, Geology Dept., frmpires@yahoo.com
[2] Jaguar Mineração
[3] Eletronuclear
[4] Companhia Industrial Fluminense
[5] Instituto Estadual do Ambiente/RJ

Volta Grande (VG) pegmatite field is at the westernmost portion of the Precambrian Santa Rita granite pluton suite. The granite suite, intrusive in Archean Barbacena greenstone belt, is the source for the pegmatite fields and the associated Ta-Nb-Sn-Li mineralizations (Pires & Girodo, 2007). A muscovite-out surface surrounds the granite in its outer contacts, and beyond that, mineralization appears. Close to the granite, lithium enrichment occurs in the far distal zone (Fig. 1). Volta Grande (VG) pegmatite fields are composed of several tabular, sub-horizontal, stacked pegmatites. The VG pegmatite is the westernmost, followed by Urubu, Fumal, Tanque and Palmital pegmatites toward the Santa Rita Granite at the eastern portion. Zoning in the VG is defined in the several bodies, described by "F" and "E" body (lepidolite-microlite), "B" and "A" (zinnwaldite-spodumene-tantalite), "C", "C-south" and "Minas-Brasil" (zinnwaldite-Nb-tantalite-beryl) (Fig.2). Tantalite decreases toward Urubu, and beryl increases toward Fumal. In the "A" and "B" orebodies some tantalite crystals are mantled by microlite and cassiterite is mostly confined to muscovite-rich pockets are apparently not controlled by the zoning. Albite, blocky microcline, spodumene, zinnwaldite, gray bull quartz is present in the "A", the main orebody. Holmquistite, zinnwaldite, epidote concentrate at the exomorphic zone resulting from the reaction between Li-rich fluids and host amphibolite. The wall zone is followed by microcline-rich zone with metric and round inclusions of albite surrounded by perthitic alkali feldspar. Perthite exsolution in pegmatites begins after the formation of the alkali feldspars, around 600^{o}C, and continued down to 400 ^{o}C, because the energy barrier prevents farther diffusion. It means that feldspars are subjected to external pressure, and the strain activates Na+ resulting in exsolution continuing under still lower temperatures until unmixing is complete. Tourmaline-holmquistite-zinnwaldite-actinolite form sporadic pockets in the transition between bodies "A" and "E-F". Sub-vertical, narrow pegmatite stringers connect the sub-horizontal pegmatite bodies. At the pegmatite core, metric, sub-vertical, kinked spodumene crystals occur. Thirteen key reactions within the pegmatite, under the μSiO2-μH+ (chemical potential isobaric diagram) allowed one to study the stability and evolution of the VG pegmatite (Fig.3). It may be observed that muscovite is the dominant phase in the acid portion and lepidolite in the less acid side. At the exomorphic contact wall zone, the hornblende is destabilized in favor of holmquistite associated with zinnwaldite, forming also epidote and sporadic fluorite. Round xenoliths of amphibolite within pegmatite exhibit the same relationship of the wall zone (except for the presence of tourmaline) according to the reactions (Fig. 3). Holmquistite also appears as fibrous habit. It is concluded that the VG pegmatite displays distinct zoning and isolate muscovite-cassiterite and tourmaline-rich pockets, which may be represented by chemical potential diagrams.

References

Pires, F., R. M. Girodo, A., C. (2007): Mibra Mine, The Volta Grande Pegmatite, Nazareno, Minas Gerais, Brazil: Mining and Metallurgical Performance. Tantallum International Conference, bull. 131, 01-04.

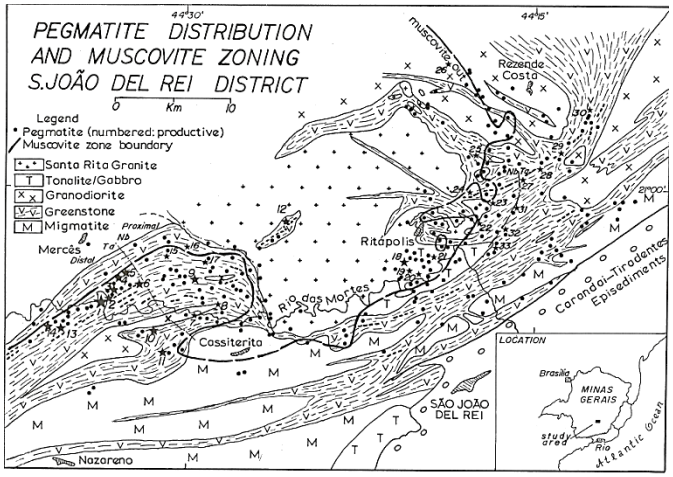

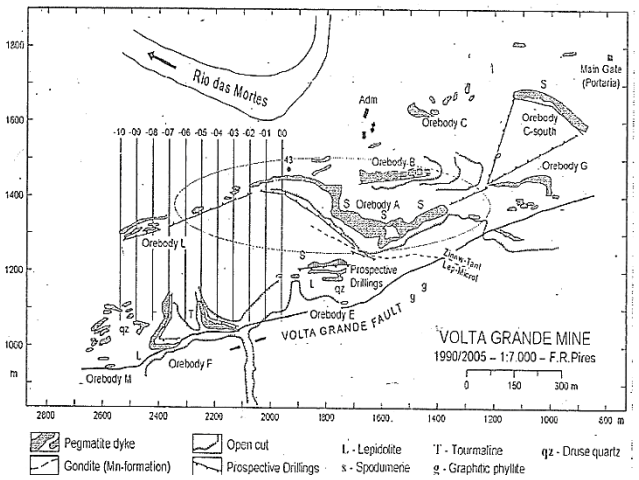

Fig. 2: Zoning in the Volta Grande Pegmatite Mimbra Mine, Nazareno, MG, Brazil.

Fig. 1: Geologic map of Sao Joao del-Rei Pegmatite district.

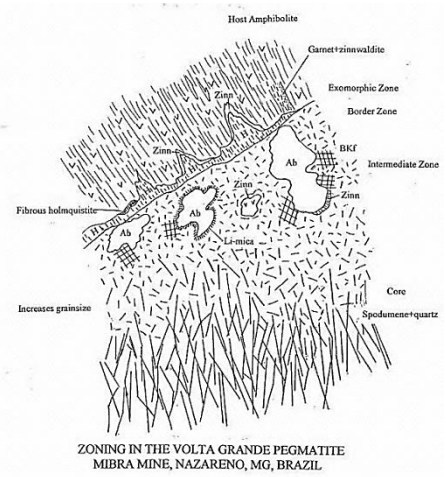

Fig. 3: Geologic map of Volta Grande Mine.

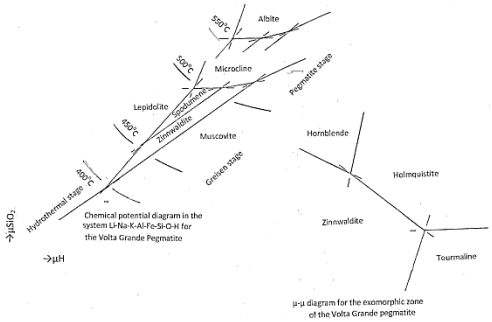

Fig. 4: chemical potential diagram for Volta Grande Pegmatites.

IRON-BEARING BERYL FROM GRANITIC PEGMATITES; EMPA, LA-ICP-MS, MÖSSBAUER SPECTROSCOPY AND POWDER XRD STUDY

J. Přikryl[1], M. Novák[1], J. Filip[2], P. Gadas[1], M. Galiová Vašinová[3]
[1] Department of Geological Sciences, Masaryk University, Brno, Czech Republic, janprikryl87@gmail.com
[2] Regional Centre of Advanced Technologies and Materials, Palacký University, Olomouc, Czech Republic
[3] Department of Chemistry, Masaryk University, Brno, Czech Republic

Chemical composition of beryl, general formula ^{CH}(Na,Cs,Rb,K,H2O,He,Ar) $^{T(2)}$(Be,Li,□)$_3$ ^{O}(Al,Fe^{3+},Sc,Cr,V,Fe^{2+},Mg,Mn^{2+})$_2$ $^{T(1)}$[Si$_6$O$_{18}$] (Černý 2002), from granitic pegmatites was presented in numerous papers. However, most previous research was focused chiefly on Fe-poor beryl, and its Cs,Na-enriched varieties (e.g., Černý 2002 and references therein); whereas, Fe,Mg-enriched beryl was studied rather extensively (e.g., Aurisicchio *et al.* 1998, Novák and Filip 2010 and references therein). We studied 6 samples (homogeneous to highly heterogeneous, fig. 1) of blue, bluish green, and green beryl from various granitic pegmatites to establish:

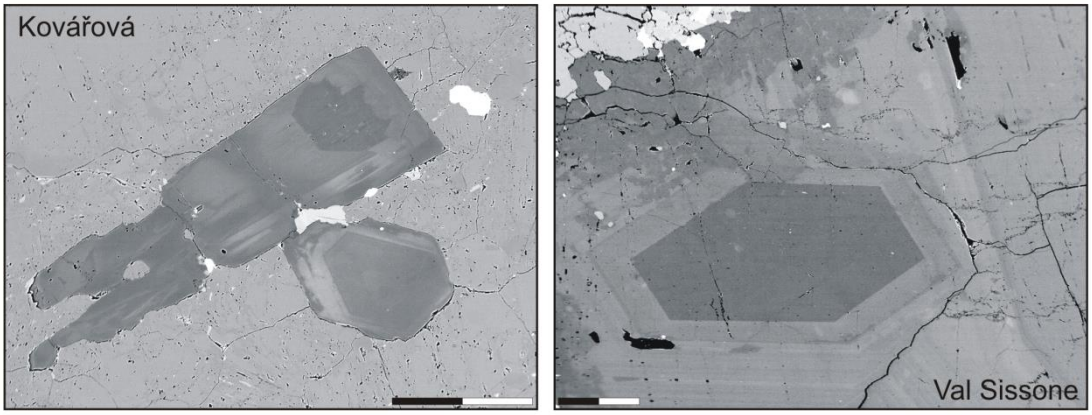

Fig. 1: BSE images of heterogeneous beryl in K-feldspar from LCT (left) and NYF pegmatite (right). Scale bar 0.2 mm.

(i) concentration of major and minor elements (EMPA), (ii) concentrations and structural position of Fe^{2+} and Fe^{3+} in beryl (Mössbauer spectroscopy), (iii) concentrations of selected trace elements (LA-ICP-MS), and to disclose: (iv) differences in chemical compositions of beryl between the pegmatites of LCT and NYF affinity, and (v) substitution mechanisms.

All beryl samples examined are enriched in Fe relative to common beryl in ordinary granitic pegmatites, with ∑Mg+Fe ranging from 0.194 to 0.427 *apfu* (Table 1). High to low Mg/Fe ratios = 0.59-2.96 (Table 1) could indicate: low degree of fractionation in a primitive pegmatite (Beryller, the Alps, Austria), contamination of the LCT pegmatites from host amphibolites (Boněnov, western Bohemia and Kovářová, western Moravia, Czech Republic), and specific composition of pegmatite melt (Kožichovice, Třebíč Pluton, Czech Republic; Novák *et al.* 2012). Beryl samples with low Mg/Fe from granitic pegmatites at Quadeville, Ontario, Canada and Val Sissone, the Alps, Italy represent pegmatites with evident NYF affinity.

All beryl samples have similar contents of Fe^{3+} ~ 25% located exclusively in the *O*-site (Table 1). They differ in the presence of Fe^{2+} in the *T2*-site, which is typical for green beryl. Blue and bluish green beryl shows no ^{T2}Fe^{2+}. Hence, influence of the iron-oxidation state and structural position of Fe on the color is evident. No relations of Fe^{2+}/Fe^{3+} to the pegmatite family (NYF/LCT) were revealed.

Nevertheless, Fe^{2+} evidently predominates over Fe^{3+} in beryl from all granitic pegmatites examined. Concentrations of selected trace elements are highly variable (Table 1) and using them as discriminators of LCT and NYF affinity is very limited except for Sc (NYF) and low Mg/Fe. Samples of beryl with lower Mg/Fe are rather Mn-enriched (Table 1). Use of the Cs and Li concentrations as indicators of the LCT affinity is also rather impracticable.

Locality/family	^{CH}Na apfu	^{CH}Cs ppm	^{T2}Li ppm	^{O}Sc ppm	^{O}Mn ppm	^{O}Mg apfu	$^{O}Fe^{2+}_{tot}$ apfu	Mg/Fe	$^{O,CH}Fe^{2+}$ mol. %	$^{T2}Fe^{2+}$ mol.%	$^{O}Fe^{3+}$ mol.%
Beryller primitive	0.343	2067	249	30	121	0.280	0.132	2.12	n.d.	n.d.	n.d.
Kovářová LCT	0.111	6659	267	5	117	0.092	0.102	0.90	60.5	14.5	25.0
Boněnov LCT	0.314	1098	160	297	150	0.284	0.143	1.99	75.9	0.00	24.1
Quadeville NYF	0.199	728	849	245	879	0.104	0.177	0.59	76.4	0.00	23.6
Val Sissone NYF	0.140	1947	120	2800	314	0.086	0.126	0.68	n.d.	n.d.	n.d.
Kožichovice NYF	0.241	18300	37	1388	134	0.311	0.105	2.96	80.0	10.0	10.0

Table 1. Chemical composition of beryl (from combination of EMPA, LA-ICP-MS and Mössbauer spectroscopy); ppm and *apfu* are shown as average values; the Kožichovice data are adopted from Novák and Filip (2010).

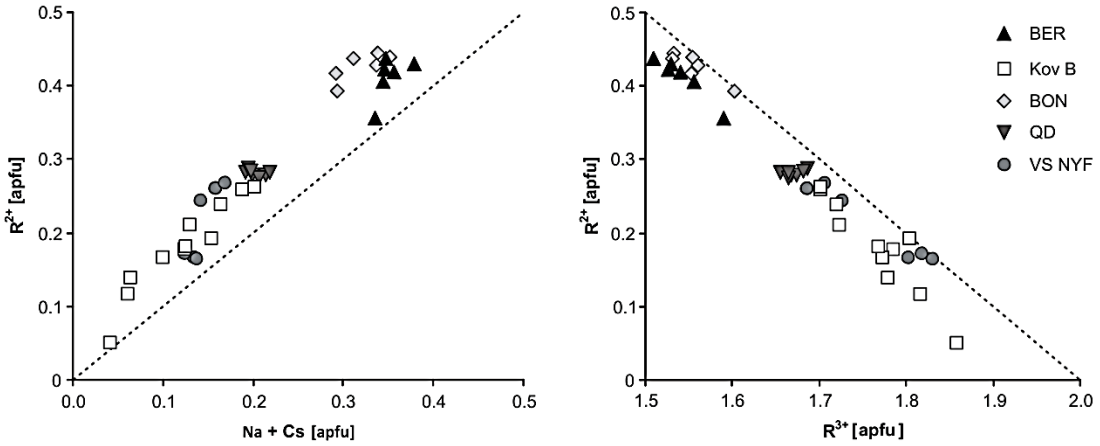

Fig. **Fig. 2:** Plots of R^{2+} versus Na+Cs and R^{2+} versus R^{3+} for beryl from granitic pegmatites. VS NYF – Val Sissone, BON – Boněnov, BER – Beryller, QD – Quadeville, Kov B – Kovářová.

The observed positive graph correlation of R^{2+} versus ∑Na+Cs along with negative correlation in R^{2+} versus R^{3+} (Fig. 2), where □ = vacancy in CH site; $R^{+} = Na^{+} > Cs^{+} > K^{+}, Rb^{+}$; $R^{2+} = Mg^{2+} \sim Fe^{2+} > Mn^{2+}$; $R^{3+} = Al^{3+} > Fe^{3+} > Sc^{3+}$, are both close to ratio 1. This suggest the substitution $^{CH}\square + {}^{O}R^{3+} \leftrightarrow {}^{CH}R^{+} + {}^{O}R^{2+}$ is dominant in all studied beryl samples and thus they belong to octahedral beryl (*o*-beryl). Also the cell dimensions (*c*/*a* = 0.991-0.996) correspond to an *o*-beryl. This research was funded by the research project GAP210/10/0743 granted to MN, JF and PG.

References:

Aurisicchio, C., G. Fooravanti, O. Grubessi, P. Zanazzi (1988): Reappraisal of the crystal chemistry of beryl. American Mineralogist, vol. 73, 826-837.

Černý, P. (2002): Mineralogy of Beryllium in Granitic Pegmatites. *In*: Beryllium - Mineralogy, Petrology and Geochemistry (Grew, E.S. editor). Reviews in Mineralogy and Geochemistry, vol. 50, 405-444.

Novák, M., J. Filip (2010): Unusual (Na, Mg)-enriched beryl and its breakdown products (beryl II, bazzite, bavenite) from euxenite-type NYF pegmatite related to the orogenic ultrapotassic Třebíč Pluton Czech Republic. Canadian Mineralogist, vol. 48, 615-628.

Novák, M., R. Škoda, P. Gadas, L. Krmíček, P. Černý (2012): Contrasting origins of the mixed signature in granitic pegmatites; examples from the Moldanubian Zone, Czech Republic. Canadian Mineralogist, vol. 50, 1077–1094.

TEXTURAL AND MINERALOGICAL FEATURES OF THE LI-F-SN-BEARING PEGMATITIC ROCKS FROM CASTILLEJO DE DOS CASAS (SALAMANCA, SPAIN): PRELIMINARY RESULTS

E. Roda-Robles, A. Pesquera, P. Gil-Crespo, I. Garate-Olabe, U. Ostaikoetxea-García
Dpto. Mineralogía & Petrología, UPV/EHU, Bilbao, Spain, encar.roda@ehu.es

Introduction

Li-rich pegmatites are widespread minor lithologies within the Central-Iberian-Zone (CIZ), in both Spain and Portugal. Some of them, including the Fregeneda-Almendra, Pinilla de Fermoselle and Cañada bodies, have been widely studied (e. g., Roda *et al.*, 2004; Roda *et al.*, 2006, Vieira *et al.*, 2011). Other Li-bearing mineralizations, as the Li-F-Sn-bearing pegmatitic rocks from Castillejo de Dos Casas (Salamanca, Spain), are less known. Textural and mineralogical descriptions of these rocks were reported by Martín-Izard *et al.* (1992), and Gallego-Garrido (1992). However, a detailed study on field and petrographic relations, whole-rock and mineral chemistry would be necessary to better understand the characteristics, genesis and significance of these deposits. On the other hand, the geological complexity of the CIZ, including a number of granitic bodies with different ages and signatures, makes it difficult to establish the affiliation of the Variscan Li-mineralizations relative to different potential parental granites. The present study describes a set of Li-bearing rocks from Castillejo de Dos Casas, which apparently relate to the Fuentes de Oñoro granite. Our work on these rocks integrates petrographic, mineralogical and chemical data in order to contribute to the knowledge of processes related to the petrogenesis of pegmatitic rocks.

Geological Setting

The Castillejo de Dos Casas area is located in the Central-Iberian-Zone (CIZ), where Variscan granitic rocks, intruding into metasedimentary materials of the Schist Metagraywacke Complex (SMC), are common. These granites may be classified according to their relationship to the Variscan deformation into pre- to syntectonic; and late- to post-tectonic granitoids. Granitic rocks occurring in the proximity of the Castillejo pegmatites form part of the Villar de Ciervo-Guarda batholith, close to the Fuentes de Oñoro sector. This batholith is an allochthonous calcalkaline granite, belonging to the second group, with an age close to 284 ± 8 m.a. (Rb-Sr method, García-Garzón & Locutura, 1981). The batholith is heterogeneous, with different facies that include granodiorites, porphyritic granites, monzonitic granites, fine-grained granites, aplitic-pegmatitic leucogranites and some apophysis of muscovite ± tourmaline-bearing leucogranites (Corretgé & López Plaza, 1977). Subsolidus alteration processes are locally important in the batholith, including muscovitization, albitization and silicification (Corretgé & López Plaza, 1977; Gallego-Garrido, 1992).

Pegmatite Description

The Castillejo de Dos Casas pegmatites occur in the upper part of one leucogranitic apophysis, the hanging wall being in direct contact to the metasediments of the SMC. The hosting granitic rocks are described as aplitic-pegmatitic, two-mica leucogranites, with quartz, albite, K-feldspar and micas as main minerals, and apatite, tourmaline, topaz, lepidolite, montebrasite and cassiterite as accessories (Corretgé & López-Plaza, 1977; Gallego Garrido, 1992). The pegmatitic bodies are heterogeneous and include four main mineral associations: (1) fine- to medium sized pegmatitic facies, with plagioclase, quartz, muscovite, lepidolite, topaz and montebrasite; (2) fine-grained matrix with quartz, plagioclase and Li-mica, where coarser crystals of K-feldspar grow perpendicularly to the contacts; (3) fine- to medium-sized layered facies, with lepidolite-rich bands alternating rhythmically with feldspars-rich ones; and, (4) medium- to coarse-sized facies with quartz + cassiterite ± Nb-Ta-oxides. Evidence of sub-solidus albitization processes, such as "chess-board" albite patches inside K-feldspar crystals and sacharoidal interstitial albite grains, are abundant in all the units of the pegmatite.

Mineral Chemistry And Discussion

Besides quartz, feldspars and muscovite, main minerals in the Castillejo pegmatites include lepidolite, topaz, montebrasite, cassiterite and manganocolumbite. More than 100 microprobe analyses were performed on these phases. Composition of plagioclase is extremely Ca-poor, with values of 0.00 wt. % for some of the crystals, specially the sacharoidal grains and the albite patches inside the K-feldspar crystals. The highest An contents found in the Castillejo samples belong to individual albite crystals of the layered

association, with values always ≤ 0.75 wt. % CaO. The micas are F-rich, with values ranging from 2.15 to 10.55 wt. %. The amount of Li was estimated using the equation $Li = 0.3112*F^{1.3414}$ (Roda-Robles *et al.* 2006). Accordingly, micas from the Castillejo de Dos Casas pegmatites belong to the muscovite-polylithionite series, some of them showing extremely high F (over 10 wt. %) and Si (over 59 wt. % SiO_2) contents. Montebrasite is common as well, with variable F concentrations, ranging between 0.65 and 3.85 wt. %. Analyses made across some montebrasite crystals show an irregular increase in F toward the border of the grains. In the case of the oxides, composition is markedly irregular inside the crystals. Under the microscope, cassiterite exhibits alternating dark reddish-brownish and clearer beige bands. The darkest layers are richer in Nb and Ta (up to 2.00 wt. % Nb_2O_5 and 1.7 wt. % Ta_2O_5), whereas in the clearer zones, the concentration of any element but Sn is below 1.00 wt. % oxide. In the samples studied up to now, all the Nb-Ta-oxides crystals occur as inclusions of very fine grains inside the coarse cassiterite. Cassiterite composition is quite heterogeneous in the Nb/Ta proportion, with values of Nb_2O_5 between 22.54 and 54.65 wt. %, and Ta_2O_5 values ranging from 22.87 to 60.89 wt. %. Analyses made across individual grains do not show a analogous chemical variation between the core and the rims of the crystals. The Fe and Mn contents are much more homogeneous, with MnO values in the range 12.67-19.49 wt. %; and FeO values always lower, between 0.41 and 6.17 wt.%. The highest values of Nb and Fe belong to the samples from association (4), where the F contents in micas and montebrasite are the lowest.

The mineralogy of the Castillejo de Dos Casas pegmatitic bodies corresponds to the rare element class, complex type, lepidolite subtype, of the LCT family, in the classification of Cerny & Ercit (2005). According to the chemical composition of the constituent mineral phases, this is a highly evolved body, probably crystallized from the most fractionated portions of melts related to the hosting leucogranites, which are significantly evolved as well. In order to confirm this hypothesis, it would be necessary to develop a model involving the rocks from the proximal Fuentes de Oñoro granite and Villar de Ciervo-Guarda batholith, the hosting leucogranitic apophyses and the pegmatitic rocks themselves. If the genetic link among these lithologies is confirmed, this would be in agreement with the lastest studies in the Fregeneda-Almendra field (Vieira, 2011), where quite similar Li-rich bodies were dated, giving ages that suggest they would be linked to late to post-tectonic granites, as the Villar de Ciervo-Guarda batholith is. This genetic link implies that most of the Li-bearing mineralizations occurring in the CIZ, associated with the Variscan orogeny, are related to the late- to post-tectonic allochthonous granitic rocks, probably via fractional crystallization processes.

Acknowledgements

This study has been carried out with the support of the Spanish MICINN (project nº CGL2012-31356).

References:

Cerny, P. & Ercit, T. S. (2005): The classification of granitic pegmatites revisited. *Canadian* Mineralogist, 43, 2005-2026.

Corretgé, L. G. & López-Plaza, M. (1977): Geología del area granítica y metamórfica al Oeste de Ciudad Rodrigo (Salamanca); II, Las rocas graníticas. Studia Geologica, vol. XII, 47-73.

Gallego Garrido, M. (1992): Las mineralizaciones de Li asociadas a magmatismo ácido en Extremadura y su encuadre en la Zona Centro-Ibérica. Tesis Doctoral. Universidad Complutense de Madrid), 323.

García Garzón, J. & Locutura, J. (1981): Datación por el método de Rb-Sr de los granitos de Lumbrales-Sobradillo y Villar de Ciervos-Puerto Seguro. Boletin Geol. y Minero, vol. 92, 68-72.

Martín-Izard, A., Reguilón, R. & Palero, F. (1992): Las mineralizaciones litiníferas del oeste de Salamanca y Zamora. Estudios Geológicos, vol. 48, 9-13.

Roda, E., Pesquera, A., Fontan, F. & Keller, P. (2004). Phosphate mineral associations in the Canada pegmatite (Salamanca, Spain): Paragenetic relationships, chemical compositions, and implications for pegmatite evolution. American Mineralogist, vol. 89, 110-125.

Roda-Robles, E., Pesquera, A., Gil-Crespo, P. P., Torres-Ruiz, J. & De Parseval, P. (2006): Mineralogy and geochemistry of micas from the Pinilla de Fermoselle pegmatite (Zamora, Spain). European Journal of Mineralogy, vol. 18, 369-377.

Vieira, R., Roda-Robles, E., Pesquera, A. & Lima, A. (2011): Chemical variation and significance of micas from the Fregeneda-Almendra pegmatitic field (Central-Iberian Zone, Spain and Portugal). American Mineralogist, vol. 96, 637-645.

PEGMATITES FROM THE IBERIAN MASSIF AND THE CENTRAL MAINE BELT: DIFFERENTIATION OF GRANITIC MELTS VERSUS ANATEXIS?

E. Roda-Robles[1], W. Simmons[2], A. Pesquera[1], K. Webber[2], A. Falster[2]
[1] Dpto. Mineralogía & Petrología, UPV/EHU, BIlbao, Spain, encar.roda@ehu.es
[2] Earth and Environmental Sciences, University of New Orleans, USA

Pegmatites are common in the Central Iberian Zone (CIZ) (Spain and Portugal) and in the Central Maine Belt (CMB) (USA). Many of them are barren bodies, however, rare-element-bearing pegmatites are also widespread in both regions. The development of these pegmatites seems to be related to the Variscan-Acadian/Alleghenian orogenies that took place primarily in the late Devonian and Carboniferous (between 370 and 290 million years ago), by the convergence and collision of two major continents: Laurasia and Gondwana. The CIZ and CMB belong to two of the three most important Paleozoic belts: the Variscan to the northeast and the Appalachians to the southwest respectively (Martinez-Catalán *et al.*, 2008). Despite important similarities regarding the geological setting of pegmatites along both the western and eastern continental margins of the Atlantic Ocean, significant differences exist.

In the CIZ, Variscan granitic rocks typically intrude a Schist Metagraywacke Complex (SMC). These granites are classified according to their relationship to Variscan deformation into: (1) pre- to syntectonic bodies; and (2) late- to post-tectonic granitoids. Pegmatites in the CIZ occur both inside or close to some of these granitic bodies. Major minerals of the rare-element pegmatites include quartz, feldspars, muscovite, lepidolite, spodumene, petalite, amblygonite-montebrasite, cassiterite and Nb-Ta-oxides and accessory Fe-Mn phosphates. Most pegmatites are thin (up to 15 m thickness), discordant dike-like bodies a few tens of meters to ~ 1.5 km in length. Internal concentric zonation is rare; and no blocky K-feldspar or quartz-core units are observed. Numerous dikes exhibit fine- to medium-grained layering, parallel to the contacts with the country-rock. Textures, such as wedge-shaped crystals and inward coarsening indicate that crystallization initiated at the contacts and proceeded inward. However, inward chemical fractionation is not commonly observed. Thus, Li±F-bearing minerals may appear at any place across the whole dike. In contrast, along some of the longest dikes, it is possible to observe fractionation, with a gradual increase in the Li, F, Rb and Cs contents along these pegmatites. Many of these dikes are discordant with SMC metasediments, intruding into late fractures commonly producing intense tourmalinization of the hosting schist. In rare cases, Li-rich dikes occur within granitic rocks with a sharp contact between both lithologies.

In the western portion of the CIZ, mainly in Portugal, another style of pegmatite is also relatively widespread. They are barren or, less commonly, enriched in Be, P ± B and have much coarser grain size and well-developed internal zonation, with prominent quartz-cores and blocky K-feldspar intermediate zones. Other major minerals include plagioclase, muscovite, biotite, beryl, Fe-Mn phosphates and black tourmaline. These dikes (e.g. Puentemocha, Nossa Sra de la Asunçao, Venturinha and Mangualde pegmatites) are usually hosted by syn- to late-tectonic leucogranites with gradational granite-pegmatite contacts. It is noteworthy that pockets bigger than a few centimeters have not been reported in any of these two "styles" of pegmatites from the CIZ.

The CMB, in the northern Appalachians, is a prominent NE-SW trending unit that is composed of a Lower Paleozoic sedimentary sequence that was intruded by Devonian to Permian igneous rocks (Solar & Brown, 2001). In this belt the metamorphic facies change from greenschist in the northern to upper amphibolite facies (and migmatite) in the southern portion (Solar *et al.*, 1998). Rare-element-bearing pegmatites are relatively common in the CMB, mainly in the southern area in the Oxford pegmatite field (Wise & Brown, 2010). Some of the best-studied pegmatites in this field occur inside or at the limits of the Sebago Migmatitic Domain (SMD). This domain surrounds the re-defined Sebago batholith (<400km^2), and consists of stromatic migmatites and diatexites, permeated by smaller bodies of more geochemically heterogeneous granite (Solar & Tomascak, 2009). Overall, pegmatite bodies in the SMD are concordant with the planar fabric of the host rocks, although some display irregular and locally discordant contacts. Migmatites and amphibolites are common host lithologies. Generally pegmatites show internal mineralogical and textural zonation. The outermost wall-zone is typically <1m thick,

with a homogeneous granitic, gneissic or fine-grained pegmatitic texture. Feldspars, quartz, biotite, muscovite, garnet ± schorl are the most common minerals in this zone (e. g. Berry-Havey, Mount Mica, Mount Marie, Mount Apatite). In other cases, comb, tapered, schorl crystals of up to 50 cm in length grow directly from the contact with the country rock in the hanging wall, inside a homogeneous matrix (e.g. Emmons). The wall-zone is gradational into the intermediate zone of graphically intergrown feldspar and quartz, with accessory garnet, biotite, muscovite and black tourmaline. The intermediate zone may be thick (> 5 m) mainly under the cores, on the lower side of the bodies. The core-zone consists of meter-sized masses of blocky quartz and K-feldspar with more evolved, finer-grained irregular pods of albite, muscovite, lepidolite, Li-tourmaline, Li-Al and Fe-Mn-phosphates, Sn, Nb and Ta oxides, beryl and Cs-beryl, spodumene, petalite and pollucite. Within the core-zone pods, pockets are relatively common. The pockets contain gemmy Li-rich tourmaline associated with quartz, lepidolite, albite, cassiterite and clay minerals. Another remarkable feature in the internal structure of CMB pegmatites is the occurrence of a garnet layer under the core, which helps the miners to determine the limits of the core and pockets, as pockets never occur below this layer. Prismatic schorl crystals intergrown or close to the garnet indicate the sense of upward crystal growth. Overall, the composition of these bodies is not significantly enriched in rare-elements, as these are concentrated only in the innermost parts of the bodies and constitute a low percentage of the volume of the pegmatite. As in the case of the pegmatites from the CIZ, textural and mineralogical criteria indicate that pegmatites in the CMB crystallized from the borders inward. In contrast, CMB fractionation processes were highly effective. The chemistry of the primary minerals changes progressively and dramatically from the border to the core zone, with an increase in the Li/(Fe+Mg) ratio in tourmaline, a decrease in the K/Rb for micas and K-feldspar and of Fe/(Fe+Mn) in phosphates, an increase in Li and F in mica and of Cs in beryl. Also, a general increase in the proportion of Li-, F- and/or Cs-bearing minerals, parallel to a decrease in Fe-Mn-Mg-bearing phases is observed.

During the last two decades, two main hypotheses have been proposed to explain the origin of the proto-pegmatitic melts. The most widely accepted theory by pegmatologists is that the pegmatite-forming melts are derived via fractional crystallization of a granitic pluton (Cameron *et al.*, 1949; Jahns, 1953; Jahns and Burnham, 1969; Černý, 1991). The idea that rare element pegmatites can form by direct anatexis has also been suggested. Simmons *et al.* (1995, 1996) and Simmons & Webber (2008) proposed that low-degree partial melts formed from migmatites surrounding plutons in orogenic environments could have the same composition as late-stage melts produced by fractional crystallization. Certain facts support the anatectic theory: (1) the difficulty to relate the highly evolved composition of many pegmatites to the chemistry of the possible parental plutonic source, which is much more primitive (Stewart, 1978; Norton & Redden, 1990); and, (2) the occurrence of many pegmatitic bodies, isolated from any possible plutonic source (Simmons *et al.*, 1995). In contrast, those in favor of the magmatic differentiation theory put forward the strong correlation in the enrichment trends for trace elements between the pegmatites and the granitic source when this is exposed. Moreover, they argue that it is difficult to extract small amounts of melt from the melting zones, and they also highlight the chemical differences between highly evolved pegmatites and the melts originated by partial melting (leucosomes in migmatites).

In the case of the Li-rich pegmatites from the CIZ most of the facts seem to agree with a magmatogenic theory: the bulk chemical composition of these pegmatites is very different from the composition of their country rocks or from the composition of melts that could be formed by the partial melting of those rocks. Moreover, in the Pinilla de Fermoselle pegmatite it is possible to observe a complete evolution from granitic to highly evolved pegmatitic facies (Roda-Robles *et al.* 2012), and at the Fregeneda-Almendra field a model using Rayleigh fractionation equations indicates that it is possible to attain the composition of the most evolved pegmatites starting from the composition of some of the granites in the region (Vieira, 2011).

In the case of the pegmatites from the CMB the bulk chemical composition of pegmatites is not far from the composition of leucogranites, of some aplitic bodies in the region, or even of the leucosomes of the surrounding migmatites. Therefore, it seems possible to start from any of these sources to derive the composition of the most

evolved pegmatites, provided that the melt subsequently follows a highly effective fractionation process. It is difficult to determine, given our present state of knowledge, if the origin of this starting pegmatitic melt was a granitic melt or a product of anatexis. Differences among pegmatites from the CIZ and from the CMB are evident. But it is unknown if these differences are the result of the melt being derived from a granitic source or via anatexis. However, what is clear is that, as there are granites and granites, there are pegmatites and pegmatites.

Acknowledgements

This study has been carried out with the support of the Spanish MICINN (project nº CGL2012-31356)

References

Cameron, E. N., Jahns, R. H., Mcnair, A. H. & Page, I. R. (1949): Internal structure of granitic pegmatites. Econ. Geol., 2.

Černý, P. (1991): Rare-element granitic pegmatites. Part II. Regional to global environments and petrogenesis. Geosci. Can., 18: 68–81.

Jahns, R. H. (1953): The genesis of pegmatites. I. Occurrence and origin of giant crystals. American Mineralogist, 38, 563-598.

Jahns, R. H. & Burnham, C. W. (1969): Experimental studies of pegmatite genesis: I. A model for the derivation and crystallization of granitic pegmatites. Econ. Geol., 64: 843–864. Martínez

Catalán, J. R.; Aller, J.; Alonso, J.L.; Bastida, F (2008): The Iberian Variscan Orogen. In: Una aproximación al patrimonio geológico español de relevancia internacional, (IGME), IGME, Spain, 15-30.

Norton, J. J.; Redden, J. A. (1990): Relation of zoned pegmatites to other pegmatites, granite, and metamorphic rocks in the southern Black Hills, South Dakota. American Mineralogist, 75, 631-655.

Roda-Robles, E.; Pesquera,A.; Gil, P., Torres-Ruiz, J. (2012): From granites to highly evolved pegmatites: a case study of the Pinilla de Fermoselle granite-pegmatite system (Zamora, Spain). Lithos, 153, 192-207

Simmons, Wm. B.; Webber K. L. (2008): Pegmatite genesis: state of the art. European Journal of Mineralogy, 20, 421-438.

Simmons, W.B.; Foord, E.E.; Falster, A. U. (1996): Anatectic origin of granitic pegmatites, Western Maine, USA. Geol. Assoc. Can. - Mineral. Assoc. Can. Program Abstr. A87.

Simmons, W. B.; Foord, E. E.; Falster, A. U.; King, V. T. (1995): Evidence for an anatectic origin of granitic pegmatites Western Maine, USA. Geol. Soc. Amer. Abstract Programs, 27, 411.

Solar, G. S.; Brown, M. (2001): Petrogenesis of migmatites in Maine, USA: possible source of peraluminous leucogranite plutons.

Solar, G. S.; Pressley, R. A.; Brown, M.; Tucker, R. D. (1998): Granite ascent in convergent orogenic belts: testing a model. Geoogy, 26, 711-714.

Solar, G. S.& Tomascak, P. B. (2009): The Sebago pluton and the Sebago Migmatite Domain, Southern Maine: results from new studies. 2009 Annual Meeting of Northeastern Section, Geol. Soc. America, Field Trip 2, 1-24.

Stewart, D. B. (1978): Petrogenesis of Li-rich pegmatites. American Mineralogist, 63, 970-980.

Vieira, R. (2011): Aplitopegmatitos com Elementos Raros da Região entre Almendra (Vila Nova de Foz-Côa) e Souto (Penedono). Génese e Caracterização Tecnológica. Ph. D: Thesis, University of Porto, Portugal.

Wise, M. A.; Brown, C. D. (2010): Mineral chemistry, petrology and geochemistry of the Sebago granite-pegmatite system, southern Maine, USA. Journal of Geosciences, 55, 3-26.

FE-MN-(MG) DISTRIBUTION IN PRIMARY PHOSPHATES AND SILICATES FROM THE BERYL-PHOSPHATE SUBTYPE PALERMO NO.1 PEGMATITE (NEW HAMPSHIRE, USA)

E. Roda-Robles[1], J. Nizamoff[2], W. Simmons[2], A. Falster[1]
[1] Dpto. Mineralogía & Petrología, UPV/EHU, BIlbao, Spain, encar.roda@ehu.es
[2] Dept. of Earth and Environmental Sciences, University of New Orleans, USA

Introduction

The Palermo No. 1 pegmatite, renowned for its complex secondary phosphate paragenesis, is located in the Grafton pegmatite field of New Hampshire, where pegmatites generally display low to medium degrees of geochemical and mineralogical evolution (barren, beryl, beryl-phosphate and beryl-columbite-phosphate subtypes) (Nizamoff & Whitmore, 2012). The Palermo No.1 body belongs to the beryl-phosphate subtype and, despite the numerous secondary phosphates occurring there (over ninety species), the primary association of both phosphates and silicates is relatively simple. Chemical composition of phosphates in pegmatites typically reflects the fractionation attained by the hosting pegmatite, with lower Fe/(Fe+Mn) ratios as differentiation degree increases. However, the occurrence of mafic silicates with primary phosphates may strongly influence this ratio (London 2008; Roda-Robles *et al.*, 2012). In this work we study the distribution of Fe-Mn-(Mg) among the primary phosphates, graftonite, triphylite and sarcopside; and the silicates tourmaline and garnet; and discuss the possible influence that the crystallization of some of these phases could have on the composition of the other mafic minerals.

Geology and Pegmatite Description

The Grafton pegmatitic field is located within the Acadian orogenic belt of the New England Appalachians. Pegmatites in this field are hosted by sillimanite-muscovite grade metamorphic rocks of the upper unit (Kearsarge) of the Devonian Littleton Formation, composed of alternating beds of mica-quartzite and mica-quartz-sillimanite schists. These materials underwent three metamorphic and/or deformative events during the Acadian orogeny (Spear *et al.* 2002): 1) metamorphism (M1) producing a staurolite-andalusite/kyanite assemblage with associated folding (D1); 2) minor deformation (D2) producing mild folding; and, 3) high grade metamorphism (M2) to a sillimanite-muscovite assemblage, accompanied by a more intense deformation (D3). The emplacement of the Palermo pegmatites was most likely post-Acadian orogeny (Nizamoff & Whitmore, 2012).

The Palermo No. 1 pegmatite is a large, "turnip-shaped" body, more or less concordant with the upper unit of the Littleton Formation. It shows a well-developed internal zonation, with five different zones (Nizamoff & Whitmore, 2012): border zone, wall zone, intermediate zone, core margin and core zone. The border zone, in sharp contact with the hosting schists, is discontinuous and usually < 10 cm. Main minerals include fine-grained quartz, muscovite, plagioclase and minor biotite. In the wall zone (0.2-5m) medium to coarse plagioclase, quartz and muscovite are the main minerals, with minor biotite and schorl. The wall zone surrounds the intermediate zone, with a very irregular thickness (3-25 m). Generally, coarse quartz, plagioclase and K-feldspar are the main mineral phases, with minor book muscovite and some beryl crystals. The core margin (< 10 m thick) is markedly heterogranular. In general, main minerals in the core margin are the same as in the intermediate zone. However, locally albite var. cleavelandite is the dominant phase. Moreover, this zone hosts the majority of accessory and rare minerals in the pegmatite, including large beryl crystals and giant masses of triphylite (some over 3 m Ø) close to the quartz core. Almandine and tourmaline are extremely rare in the core margin, where they occur together with more than one hundred phases. The core zone (> 30 m thick), in the central portion of the pegmatite, is mainly composed of large monomineralic masses of blocky quartz and K-feldspar. Late-stage, low temperature hydrothermal quartz veins emanate from the core and partially cross-cut the pegmatite.

Petrography And Chemistry of the Fe-Mn-(Mg) Minerals

Triphylite is the most abundant primary phosphate in the pegmatite. It commonly exhibits fine lamellae of sarcopside (TS association). Periodically triphylite occurs intergrown with graftonite, in an assemblage of graftonite containing coarse lamellae of triphylite (GTS association). Most lamellae are platy and form a single set that shows a quite uniform optical orientation, enclosed in monocrystalline graftonite, giving rise to a laminated parallel intergrowth. The triphylite lamellae may then host lamellae of sarcopside. In

general, nodules with the GTS association occur in the most external areas of the core margin, whereas those containing just triphylite and sarcopside (TS association) occur closer to the core zone. All phosphates from the two associations belong to Fe-rich end-members. In the GTS association values for the Fe/(Fe+Mn) ratio are in the range 0.57 to 0.73 for graftonite, 0.74 to 0.89 for triphylite, and 0.81 to 0.88 for sarcopside. In the TS association these values are generally lower, 0.77 to 0.80 for triphylite and 0.77 to 0.78 for sarcopside. Differences in the Mg content for the two associations are also evident. In the GTS, the Fe/(Fe+Mg) ratio for graftonite, triphylite and sarcopside are in the ranges 0.93-0.97; 0.79-0.92 and 0.89-0.95 respectively; whereas in the TS association this ratio is 0.95-0.97 for triphylite and is 0.98 for sarcopside.

In the core margin, tourmaline and garnet are accessory phases, appearing as very fine- to fine-subhedral crystals, often very close to the phosphate nodules (<1 cm). Microscopically, tourmaline crystals show concentric chromatic zoning, with brownish and orange colors, commonly darker at the rims, and a strong pleochroism. All analyzed crystals are alkali tourmalines, with schorl as the main component. In general, tourmaline crystals are slightly heterogeneous in composition, with Mg contents decreasing toward the rims. The negative correlation between Fe and Mg indicates that chemical variations observed in tourmaline from the Palermo No.1 pegmatite follow mainly the dravite-schorl exchange-vector $Mg_{-1}Fe_1$. In addition, the alkali-deficiency mechanism $Al(X)(R^{2+}Na)_{-1}$, where (X) represents the vacancies at the X site, probably also influenced the chemical variability in tourmaline. The composition of garnet is also heterogeneous. In all cases it is dominantly almandine with a high spessartine component. Compositions of garnet are in the range $Alm_{57.4}Sps_{42.2}Prp_{0.4}$ and $Alm_{66.9}Sps_{30.4}Prp_{2.7}$. Mn content typically increases toward the rims of the crystals, with a corresponding decrease in the Fe and Mg contents.

Discussion

A fractionation of Fe-Mn-(Mg) during pegmatitic crystallization seems evident in both phosphates and silicates. The decrease in the Fe/(Fe+Mn) ratio in phosphates, simultaneous with an increase in the Fe/(Fe+Mg) proportion from the GTS to the TS associations suggest a fractionation inward in the pegmatite. In the case of the silicates, this fractionation may be observed inside individual crystals, the Fe/(Fe+Mg) value increasing in tourmaline and garnet from the core to the rim of the crystals, whereas in garnet the Fe/(Fe+Mn) ratio decreases in the same sense. In relation to the distribution of Fe, Mn and Mg among coexisting primary phosphate phases, in all cases, graftonite shows a strong preference for Mn, whereas both triphylite and sarcopside are Fe-rich. Mg is clearly partitioned preferentially into triphylite, with graftonite being the Mg-poorest of the three phosphates. Regarding the silicates, as it is commonly observed, the Fe/(Fe+Mn) is considerably lower for garnet than for the coexisting tourmaline. This is due to the preference for Mn for garnet whereas Fe is more compatible in tourmaline (London, 2008). The concentration of Fe and Mn in pegmatite-forming melts is usually low. The crystallization of tourmaline and/or garnet in outer zones of pegmatites would deplete the melt in those elements, preventing the crystallization of important volumes of Fe-Mn phosphates at later stages.In the Palermo No. 1 pegmatite, tourmaline and garnet occur only as minor minerals. Thus, Fe and Mn are available for later crystallization of volumetrically important phosphates inside this body. As observed in other pegmatites, Fe-Mn-rich phosphates started crystallizing at intermediate degrees of differentiation. Consequently, Fe and Mn are sequestered by phosphates, controlling the Fe/(Fe+Mn) in the melt and preventing crystallization of garnet. Thus, Fe/(Fe+Mn) and Fe/(Fe+Mg) ratios in primary phosphates reflect the original ratio in the melt and its evolution during inward fractionation; these values reflect a rather primitive character for the Palermo No. 1 pegmatite.

References

London, D. (2008): Pegmatites. Can. Mineral. Sp. Publ., 10, 347 pp.

Nizamoff, J. W., Whitmore, R. W. (2012): The Palermo pegmatites, North Groton, NH: Trip B-3 in Thompson, P. J. and Thompson, T.B., eds., Guidebook , 104th ann. NEIGC, NewburyNH, 165-182.

Roda-Robles, E., Galliski, M., Roquet, M.B., Hatert, F., de Parseval, P. (2012): Phosphate mineral associations in the Cema pegmatite (San Luis province, Argentina): paragenesis, chemistry and significance in the pegmatite evolution. Can. Min., 50, 913-931.

Spear, F. S., Kohn, M. J., Cheney, J. T., Florence, F. (2002): Metamorphic, thermal, and tectonic evolution of Central New England, Journal of Petrology, 43, 2097-2120

TRACE ELEMENT CONTENT IN PRIMARY FE-MN PHOSPHATES FROM THE TRIPHYLITE-LITHIOPHILITE, GRAFTONITE-BEUSITE AND TRIPLITE-ZWIESELITE SERIES: DETERMINATION BY LA-ICP-MS METHODS AND PRELIMINARY INTERPRETATION

E. Roda[1], A. Pesquera[1], S. García de Madinabeitia[2], J.I. Gil Ibarguchi[1], J. Nizamoff[3], W. Simmons[3], A. Falster[3], M. A. Galliski[4]

[1] Dpto. Mineralogía & Petrología, UPV/EHU, BIlbao, Spain, encar.roda@ehu.es
[2] SGIker-Geochronology, UPV/EHU, Spain
[3] Dept. of Earth and Environmental Sciences, University of New Orleans, USA
[4] IANIGLA-CCT Mendoza, CONICET, Mendoza, Argentina

Phosphates of Fe-Mn are common accessory mineral phases in some granites and in many pegmatites, and they become important constituents in the beryl-columbite-phosphate pegmatite subtype of Černý & Ercit (2005), and in some hydrothermal quartz-rich dykes (e. g. Garate-Olabe *et al.*, 2012). The chemical composition of phosphates has been used to establish the degree of evolution of the pegmatites in which they occur, just as the composition of some silicates (micas, K-feldspar, tourmaline, garnet and beryl) and of oxides (columbite-group minerals) is used to indicate evolution. Indeed, a decrease of the Fe/(Fe+Mn) value in phosphates is associated with increasing evolution of pegmatites (Ginsburg 1960; Fransolet *et al.* 1986; Keller *et al.* 1994; Roda *et al.* 2005; Roda-Robles *et al.* 2010). However, this ratio may be influenced by the presence of other Fe-(Mg-Mn)-rich minerals, such as tourmaline, biotite and/or garnet (Roda-Robles *et al.* 2012), and, therefore, this criteria must be followed with caution. A more complete chemical characterization of the Fe-Mn phosphates, including trace elements, could help to better understand the petrogenetic role of phosphates during the evolution of pegmatites. With this purpose, samples belonging to the triplite-zwieselite $(Mn^{2+},Fe^{2+},Mg,Ca)_2(PO_4)(F,OH)$, triphylite-lithiophilite $Li(Fe^{2+},Mn^{2+})PO_4$ and graftonite-beusite $(Ca,Fe^{2+},Mn^{2+})_3(PO_4)_2$ primary phosphate series were analyzed by microprobe and LA-ICP-MS methods at the Université Paul Sabatier (Toulouse, France) and at the SGIker-Geochronology Laboratory of the Universidad del País Vasco UPV/EHU (Bilbao, Spain) respectively. For each series the widest possible Fe-Mn compositional range was covered. Overall, more than 700 microprobe analyses and close to 400 LA-ICP-MS analyses were made on eight samples of the triplite-zwesielite series, six samples of the triphylite-lithiophilite series, and five samples of the graftonite-beusite series from pegmatites and hydrothermal quartz dykes in Europe (Hagendorf Sud, Cañada, Folgosinho and Nossa Senhora de la Assunçao), Argentina (Cema, El Criollo and El Gigante), Canada (Swanson), and the United States (Tourmaline Queen, Beryl, Storm Mountain, Palermo n.1, Keystone and Emmons).

The results obtained show important differences for the studied series of primary Fe-Mn phosphates. Members of the triphylite-lithiophilite series contain extremely low amounts of all the analyzed elements, except for Zn (570-8990 ppm). Members of the triplite-zwieselite series, in contrast, are enriched in Nb (78-537 ppm) and Zn (437-4093 ppm), with a broader range for ΣHREE (0-124 ppm), Ta (4-176 ppm), Y (0-280 ppm), Zr (6-233 ppm), and U (7-50 ppm). Samples of the graftonite-beusite series are the richest in REE, with ΣHREE up to 300 ppm and of ΣLREE up to 345 ppm. Other trace elements, such as Zn (1508-4238 ppm), Sr (3-91 ppm) and Y (0-509 ppm) occur also in significant amounts in the graftonite-beusite. The variations in the trace element contents observed among the different phosphate series are most probably controlled by the crystal structure more than by the bulk composition. For example, triphylite and graftonite coexisting in the Palermo n.1 pegmatite show clearly different trace element contents. Nevertheless, the broad range in the content of some trace elements for the same series could be attributed to the different geological settings. The plot of the different trace elements contents versus the Fe/(Fe+Mn) ratio shows a complex correlation, which would indicate either that this ratio does not reflect the differentiation degree of the hosting rock, or that the trace element concentrations in phosphates do not account (or not solely) for the evolution degree attained by these phosphates-bearing pegmatites. Further investigation must be done to determine (i) the factors controlling the variability in the content in trace elements for the different primary phosphate series, (ii) the distribution coefficients between phosphates and silicates such as biotite, tourmaline and garnet, and (iii) the influence of the bulk

composition and geological setting on the geochemistry of the primary Fe-Mn phosphates.

References

Černý, P. & Ercit, T. S. (2005): The classification of granitic pegmatites revisited. Canadian Mineralogist, vol. 43, pp 2005-2026.

Fransolet, A. M., Keller, P. & Fontan, F. (1986): The phosphate mineral associations of the Tsaobismund pegmatite, Namibia. Contributions to Mineralogy and Petrology, vol. 92, pp 502-517.

Garate-Olabe, I., Roda-Robles, E., Gil-Crespo, P.P., Pesquera-Pérez, A., Vieira, R., Lima, A. (2012): Estudio textural y mineralógico del dique de cuarzo con fosfatos de Folgosinho (Guarda, Portugal). Macla, vol. 16, pp 220-221.

Ginsburg, A. I. (1960): Specific geochemical features of the pegmatitic process. 21st Intern. Geol. Congress Session Norden Rept. Part 17, 111-121.Keller 1994;

Keller, P., Fontan, F. & Fransolet, A. M. (1994): Intercrystalline cation partitioning between minerals of the triplite-zwieselite-magniotriplite and the triphylite-lithiophilite series in granitic pegmatites. Contributions to Mineralogy and Petrology, 118, 239-248.

Roda, E., Pesquera, A, Gil-Crespo, P.P., Torres-Ruiz, J. & Fontan, F. (2005): Origin and internal evolution of the Li-F-Be-B-P-bearing Pinilla de Fermoselle pegmatite (Central Iberian Zone, Zamora, Spain). American Mineralogist, 90,1887-1899.

Roda-Robles, E., Vieira, R., Pesquera, A., & Lima, A. (2010): Chemical variations and significance of phosphates from the Fregeneda-Almendra pegmatite field, Central Iberian Zone (Spain and Portugal). Mineralogy and Petrology 100, 23-34.

Roda-Robles, E., Galliski, M.A., Roquet, M. B., Hatert, F., de Parseval, P. (2012): Phosphate nodules containing two distinct assemblages in the Cema granitic pegmatite, San Luis province, Argentina: paragenesis, composition and significance in the pegmatite evolution. Canadian Mineralogist, vol. 50, pp 913-931.

NEW INSIGHTS INTO THE PETROGENESIS OF THE BERRY-HAVEY PEGMATITE FROM TOURMALINE PETROGRAPHY AND CHEMISTRY

E. Roda-Robles[1], W. Simmons[2], A. Pesquera[1], P. Gil-Crespo[1], J. Nizamoff[2], J. Torres-Ruiz[3]
[1] Dpto. Mineralogía y Petrología, UPV/EHU, Bilbao, Spain, encar.roda@ehu.es
[2] Earth and Environmental Sciences, University of New Orleans, USA
[3] Dpto. Mineralogía y Petrología, Universidad de Granada, Spain

Introduction

The Berry-Havey pegmatite (Androscoggin County, Maine, USA), is a highly evolved pegmatite enriched in Li, F, B, Be and P. It belongs to the Oxford pegmatite field, at the northeast limit of the Sebago Migmatite Domain (SMD), where metapelitic migmatite and diatexite are the main lithologies, locally with pegmatitic and aplitic units (Solar & Tomascak, 2009). The SMD belongs to the Central Maine Belt (CMB), a prominent NE-SW trending unit where a Lower Paleozoic sedimentary succession was intruded by Devonian to Permian igneous rocks (Solar & Brown, 2001). In the CMB the metamorphic facies change from greenschist in the north to upper amphibolite facies (and migmatite) to the south (Guidotti, 1989). Pegmatites from the Oxford field show different degrees of evolution, some of them being highly evolved, with a well developed internal zonation. A representative example of this group is the rare-element Berry-Havey pegmatite, which contains four different zones. Analyses of tourmaline, which is present in all zones, reveal important chemical and textural variations that reflect the internal evolution of the crystalizing pegmatitic melt. In this study we offer new data on the petrographic characteristics and composition of tourmaline in the different zones of the Berry-Havey pegmatite, to better understand its origin and evolution.

General Geology of the Pegmatitic Body

With the present exposure of the Berry-Havey pegmatite it is difficult to accurately determine the shape and internal structure of this pegmatite. To the southwest of the quarry, the pegmatite is conformable to the host rock ($\beta \sim 40^{o}$ SSE), whereas in the northern part the body is more horizontal. The country rock is mainly a biotite-amphibole-rich schist, although migmates occur in places. The pegmatite shows a well-developed internal structure, with four different zones: wall zone, intermediate zone, core margin and core zone. These zones are subparallel, with quite irregular limits among them, mainly for the core margin-core zone transition. From the contact with the host rock to the core of the pegmatite, the following sequence is observed (Roda-Robles *et al.*, 2011): (1) Wall zone (WZ), is the most homogeneous facies in the pegmatite, commonly with a granitic character and very fine to medium sized crystals. Main minerals are quartz, K-feldspar, plagioclase, biotite and muscovite, with tourmaline and garnet as common minor phases. (2) Intermediate zone (IZ) volumetrically is the most important, mainly in the lower portion of the dyke, with more than the 85 % belonging to graphic intergrowths of quartz-K-feldspar (IZ-I). Other minor minerals are biotite, garnet and black tourmaline. In the lower part of the IZ, locally the texture and mineralogy change to coarse quartz, K-feldspar and black prismatic tourmaline (IZ-II). (3) Core margin (CM), volumetrically quite important, this unit hosts the different pods that constitute the core of the pegmatite. Main minerals are albite (cleavelandite), quartz and tourmaline. Moreover, garnet commonly occurs as medium sized reddish-brownish crystals concentrated in a layer just below the core pods. (4) Core zone (CZ) is not a continuous unit, but several pods of different sizes (2 to ~10m Ø) hosted by the CM, commonly isolated but also frequently interconnected. Inside the pods occasionally meter sized pockets occur. Main minerals in the pods are blocky quartz and K-feldspar, fine-grained lepidolite, book muscovite balls often rimmed by lepidolite, albite (cleavelandite), greenish and pinkish tourmaline, whitish to pinkish beryl and amblygonite-montebrasite- or Fe-Mn-phosphates-bearing sub-rounded nodules. Inside the pockets main minerals include smoky quartz, cleavelandite, lepidolite, gemmy tourmaline and clay minerals.

Textural Characteristics of Tourmaline

Tourmaline is present in all the zones of the pegmatite. In the WZ tourmaline is scarce, occurring as very fine- to fine-grained, an- to subhedral, black crystals. In backscattered electron (BSE) images, tourmaline from the WZ may be completely homogeneous, or it may present with marked heterogeneity, with successive finger shaped overgrowths, developing and pointing toward the inner parts of the pegmatite.

In the IZ-I, tourmaline appears as black, sub- to anhedral, fine-grained crystals, occasionally as pseudographic intergrowths with quartz; whereas in the IZ-II tourmaline crystals are black prisms < 6 x 40 cm. In BSE images, tourmaline from the IZ is mostly homogeneous; although some crystals may be discontinuously rimmed by concentric portions of a different color.

In the CM, tourmaline forms a layer under the CZ bodies, where many crystals exhibit a tapered black prism (~ 0.5 m in length, < ~ 15 cm in Ø) growing perpendicular to the pegmatite contacts. The thick ends of most crystals are crowned by black ± green/bluish tourmaline, intergrown with quartz ± albite (cleavelandite), giving a pseudographic texture. Less commonly, tourmaline crystals are broken, giving rise to a "puzzle" structure inside a matrix of quartz and albite. The transition from black to colored tourmaline is apparently sharp in hand samples. However, BSE images reveal that this transition is not always so sharp. Close to the greenish areas the color is changing, with an irregular limit between the black and green areas. The greenish parts of the crystals are markedly heterogeneous, showing patchy zoning or cellular textures in the inner zones of the crystals, which are overgrown by darker rims.

In the CZ, tourmaline occurs with different colors and textures. Greenish, fine–to–medium–grained tourmaline prisms are associated with medium–to–coarse book crystals of muscovite. Small pinkish tourmaline crystals have been observed inside the fine-grained lepidolite masses. Prismatic crystals of bluish, pink or watermelon tourmaline, up to 15 cm in length, also occur in this zone. Moreover, radial prisms, up to 20 cm in length, of multicolored tourmaline embedded in feldspars and quartz are also abundant. The pockets hosted by the pods of the CZ may contain gem–quality tourmaline prisms (< 10 cm length). This tourmaline is usually greenish and rarely occurs as watermelon or pinkish crystals.

Tourmaline Chemistry

Most of the tourmalines are alkali tourmalines, although important contents of vacancies are present in many cases. Tourmalines from the WZ, IZ-I and IZ-II, as well as the black tourmalines from the CM and some colored ones, belong to the alkali subgroup 1 of the (Na+K)-R^{2+} species (Henry *et al.*, 2011). The rest of the colored tourmaline crystals from the CM and all the tourmalines from the CZ belong to the alkali subgroup 2 of the (Na+K)-Li species. Based on the W-site occupancy, the tourmalines analyzed from the WZ, IZ, and most of the black tourmaline crystals from the CM can be considered as hydroxy-tourmalines. However, some black crystals and most of the greenish and bluish ones may be classified as fluor-tourmalines. More than a half of the analyses of tourmaline from the CZ are F-rich, whereas the rest are hydroxy-tourmalines. There is a gradual decrease from the WZ to the CZ in the Fe+Mg and Ca values, parallel to a general increase in Al, Li and F. Behavior of Na and Mn is more complex, with an increase until the beginning of the crystallization of the CZ, and a later decrease for the Li-richest crystals. The chemical composition of tourmaline evolved through the following sequence from the WZ to the pockets inside the CZ: (1) tourmaline from the WZ may be classified as Fe-rich dravite, with a high foitite component. (2) in the IZ, schorl is the dominant tourmaline component, also with a high foitite content; (3) in the CM tourmaline composition changes in a broad range. Elbaite content increases from the black to the greenish and bluish crystals, and composition changes in this zone from foitite-rich schorl to schorl-rich elbaite, with an important rossmanite content; (4) in the CZ all the tourmalines are elbaites with high rossmanite content. In addition, some gemmy elbaite crystals from the pockets show a significant olenite component.

Discussion

Textural and chemical variations observed in tourmaline, from the WZ to the CZ, suggest an inward crystal fractionation model. The gradual increase in Li given in tourmaline across the pegmatite is more consistent with progressive Rayleigh fractionation than a zone-refining process, as Li appears to have been progressively enriched in the residual melt. Asymmetry in the mineral distribution inside the pegmatite is evident, with the garnet and the tapered tourmaline layers of the CM occurring only under the rare-element enriched zone. There is also an important asymmetry between the proportions of the zones over and under the CZ, with a clearly bigger volume for the IZ in the lower part. These asymmetries indicate that the crystallization from the footwall and from the hanging-wall proceeded in a different way. On the one hand, differences in the volume indicate that the rate of crystallization from the footwall was higher.

This could be related to the ascent of bubles and volatites by gravity (Nabelek *et al.*, 2010), which would lower the solidus in the upper part, therefore preventing its crystallization. At the same time, slowly diffusing components such as Mg and Fe would be enriched in the bottom crystallization front of quartz and feldspars (as proposed by Webber *et al.*, 1997, for the origin of the line rock), which could lead to the saturation of garnet and tourmaline to generate the layers under the CZ. Textures inside the pegmatite such as the quartz-K-feldspar and quartz-tourmaline graphic intergrowths, and the comb tourmaline crystals, suggest that crystallization proceeded under disequilibrium conditions from an undercooled melt (London, 2008). Crystallization of the tourmaline layer in the CM ends with the breaking of some of the tourmaline crystals, mainly belonging to the crowns around the tapered prisms. The occurrence of an important volume of tourmaline in this layer would imply a significant depletion of B in the melt during its crystallization. Some authors (e.g., Holtz *et al.*, 1993) claim that the presence of B_2O_3 enhances the solubility of water in the melt. Accordingly, the formation of the tourmaline layer most probably lowered dramatically the solubility of water in the remaining melt, which could lead to exsolution of a water-rich fluid and the formation of pockets. Assuming a closed system, we speculate that the breaking of some of the last formed tourmaline crystals could be related to a sudden increase in the fluids pressure provoked by the exsolution processes. At this point, the concentration of Fe was low enough and Li was high enough to allow the crystallization of the first colored tourmalines, still in the CM, followed by the crystallization of the CZ, where all the tourmaline corresponds to elbaite, with variable amounts of F, Li, Al, Mn and vacancies.

Acknowledgements

This study has been carried out with the support of the Spanish CICYT (project no. CLG2009-12677) and MICINN (project nº CGL2012-31356).

References:

Guidotti, C.V. (1989): Metamorphism in Maine: an overview. In R.D. Tucker, and R.G. Marvinney, Eds. Studies in Maine Geology. 3, p. 1-19. Maine Geological Survey.

Henry, D.J., Novak, M., Hawthorne, F.C., Ertl, A., Dutrow, B.L., Uher, P. & Pezzotta, F. (2011): Nomenclature of the tourmaline-supergroup minerals. American Mineralogist, vol. 96, 895-913.

Holtz, F., Dingwell, D.B. & Behrens, H. (1993): Effects of F, B2O3 and P2O5 on the solubility of water in haplogranite melts compared to natural silicate melts. Contributions to Mineralogy and Petrology, vol. 113, 492-501.

London, D. (2008): Pegmatites. The Canadian Mineralogist, Special Publication nº 10, 347.

Nabelek, P.I., Whittington, A.G. & Sirbescu, M.-L.C. (2010): The role of H2O in rapid emplacement and crystallization of granite pegmatites: resolving the paradox of large crystals in highly undercooled melts. Contributions to Mineralogy and Petrology, vol. 160, 313-325.

Roda-Robles, E., Simmons, W., Nizamoff, J., Pesquera, A., Gil-Crespo, P.P. & Torres-Ruiz, J. (2011): Chemical variation in tourmaline from the Berry-Havey Pegmatite (Maine, USA), and implications for pegmatitic evolution. Asociación Geológica Argentina, Serie D, Publicación Especial, 14.

Solar, G.S. & Brown, M. (2001): Petrogenesis of Migmatites in Maine, USA: Possible Source of Peraluminous Leucogranite in Plutons? Journal of Petrology, vol. 42, 789-823.

Solar, G.S. & Tomascak, P.B. (2009): The Sebago Pluton and the Sebago Migmatite Domain, southern Maine; results from new studies. 2009 Annual Meeting of Northeastern Section, Geol Soc Amer, Field Trip 2, 1-24.

Webber, K. L.; Falster, A. U.; Simmons, Wm. B.; Foord, E. E. (1997): The Role of Diffusion-Controlled Oscillatory Nucleation in the Formation of Line Rock in Pegmatite-Aplite Dikes. Journal of Petrology, Vol. 38, No. 12, 1777-1791.

LEAD-RICH GREEN ORTHOCLASE FROM BROKEN HILL PEGMATITES

L. Sánchez-Muñoz1, I. Sobrados2, J. Sanz2, G. Van Tendeloo3, A. Cremades4, Xiaoxing Ke3, F. Zúñiga5, M. Rodriguez1, A. del Campo1, Z. Gan6

[1] Institute for Ceramics and Glasses (CSIC), Kelsen 5, E-28049 Madrid, Spain, lsm@icv.csic.es
[2] Instituto de Ciencia de Materiales de Madrid (CSIC), Campus de Cantoblanco, E-28049 Madrid, Spain
[3] EMAT, University of Antwerp, Groenenborgerlaan 171, B-2020 Antwerp, Belgium
[4] Dpt. Física de Materiales, Fac. Ciencias Físicas, Universidad Complutense de Madrid, E-28040, Spain
[5] Dpto. de Física de la Materia Condensada, Fac. Ciencia y Tecnología, Univ. País Vasco, 48080 Bilbao, Spain
[6] NHMFL, Tallahassee, Florida State Univerisity, 32306 Florida, USA

Alkali feldspar-quartz pegmatites occurring in the Broken Hill Pb-Zn-Ag deposit (New South Wales, Australia) contain green amazonitic lead-rich orthoclase (amazonite) and galena as common minerals phases (Čech *et al.* 1971, Plimer 1976, Stevenson and Martin 1986, Murakami *et al.* 2000). Amazonite specimens have been studied by polarized light optical microscopy (PLOM), powder and single-crystal X-ray diffraction (XRD), X-ray fluorescence (XRF), confocal Raman microscopy (CRM), cathodoluminescence imaging (CL) scanning electron microscopy (SEM), high resolution transmission electron microscopy (TEM), high resolution magic angle spinning multi-nuclear magnetic resonance spectroscopy (NMR), including ^{29}Si, ^{27}Al, ^{23}Na and ^{207}Pb spectra at 9.4 as well as ^{27}Al, ^{39}K, ^{23}Na and ^{207}Pb spectra at 19.6 T. Amazonite with deep green color occurs, in specimens which are uniform without exsolution microtextures at the optical scale, have monoclinic average symmetry and space group, *C*2/m with a = 8.569 (2), b = 12.988 (1), c = 7.206 (1) Å, β = 116.03 (1) (R = 0.056), from single-crystal XRD, TEM images with the typical tweed contrast and diffuse streaks, and homogeneous CL-SEM contrast using the blue and infrared light emissions, and the highest quantity of $PbAl_2Si_2O_8$ from XRF data circa 3 % mol. The NMR spectra suggest that partial Si/Al order in framework sites is correlated with partial order for the alkali atoms in the cavity sites, implying a medium-range structure with molecular-like Al-O-X^+ arrangements, in a triclinic-like structure at the local scale. The ^{207}Pb spectra in orthoclase and galena are different, and the orthoclase spectra are consistent with Pb atoms in the cavity sites of the feldspars structure. When some anorthite-rich exsolution takes place, orthoclase to microcline recrystallization units propagate in the typical orthogonal configuration from interfaces and stress centers at the macroscopic scale as seen by PLOM, forming crossovers involving positive and negative interference effects which were clearly recorded by CMR images as well as large scale microcline twins. CL-SEM images shows that Pb atoms are not concentrated into the plagioclase exsolutions. The development of macroperthitic textures and later sericitic alteration (from retrogressive metamorphism) seen in other specimens is not related to extended microcline formation. It is suggested that the modulated structure of orthoclase is partly stabilized by Pb atoms which act as chemical hinderers, similar to its occurrence with P atoms in the framework sites (Sánchez-Muñoz *et al.* 2012). Orthoclase is also preserved due to low content of water catalyst during both, the magmatic stage during pegmatite crystallization from melt at peak granulite metamorphism and also during the subsolidus stage on cooling.

References

Čech, F., Mísrař, Z., Povondra, P. (1971): A green lead-containing orthoclase. Tschermaks Min. Petr. Mitt., vol. 15, 213-231.

Murakami, H., Takashima, I., Nishida, N., Shimoda, S., Matsubara, S. (2000) Solubility and behavior of lead in green orthoclase (amazonite) from Broken Hill, New South Wales, Australia. J. Min. Petr. Econ. Geol. vol. 95, 71-84.

Plimer, I.R. (1976): A plumbean feldspar pegmatite associated with the Broken Hill orebodies, Australia. Neues Jahrb. Mineral. Monatsh. vol. 6, 272-288.

Sánchez-Muñoz, L., García-Guinea, J., Zagorsky, V.Ye., Juwono, T., Modreski, P.J., Cremades, A., Van Tendeloo, G., De Moura, O.J.M. (2012) The evolution of twin patterns in perthitic K-feldspar from granitic pegmatites. Canadian Mineralogist, vol. 50, 989-1024.

Stevenson, R.K. Martin, R.F. (1986): Implications of the presence of amazonite in the Broken Hill and Geco metamorphosed sulfide deposits. Canadian Mineralogist, vol. 24, 729-745.

TWIN AND PERTHITIC PATTERNS OF K-RICH FELDSPARS OF PEGMATITES FROM DIFFERENT GEOLOGICAL ENVIRONMENTS

L. Sánchez-Muñoz[1], P. Modreski[2], V. Zagorsky[3], B. Frost[4], O. De Moura[5]
[1] Institute for Ceramics and Glasses (CSIC), Kelsen 5, E-28049 Madrid, Spain, lsm@icv.csic.es
[2] U.S. Geological Survey, Federal Center Denver, Colorado, U.S.A
[3] Vinogradov Institute of Geochemistry, Siberian Branch of Russian Academy of Science, Irkutsk, Russia
[4] Deparment of Geology and Geophysics, University of Wyoming, U.S.A
[5] Joaquim Neves Ferreira 238, 35030-391 Governador Valadares, Brazil

Granitic pegmatite provinces comprised of large and numerous pegmatites are singular geological regions because their origin can be framed in most cases in the context of thickened continental crust (Tkachev 2011) during orogenic collisions in the aggregation stage of supercontinents (syn-collisional pegmatites), immediately after post-orogenic extension (post-collisional pegmatites), and sometimes even during their final breakup (an-orogenic pegmatites). Syn-collisional pegmatites have a typical LCT geochemistry and are associated with S-type peraluminous granites, post-collisional pegmatites are rare-element and/or rare-earth elements-rich rocks, whereas anorogenic pegmatites shows a distinctive NYF signature and are frequently associated with A-type granitoids, as inherited features from the source lithologies of original melts (Černý 1991, Martin & De Vito 2005). However, the coupling between tectonic setting and geochemistry can be problematic and it is not always evident, particularly when there is not obvious spatial connections with granite plutons (i.e. derived from small-scale anatectic melts), in poorly differentiated pegmatites without a clear chemical signature, and also when "hybrid" geochemistry exists. Hence, it is not always possible to discriminate tectonic settings by geochemical criteria only. Note that when studying the geochemical enrichment, the source dependence could apparently predominate over tectonic control, particularly if this is the only basis of information.

In this work, it is shown that twin and perthitic patterns of K-rich feldspars from granitic pegmatites can be used as an additional criterion to recognize geotectonic settings. Twin patterns are formed during the subsolidus stage from the order-disorder transformation of an orthoclase precursor (which is derived from a previously formed sanidine ancestor as the magmatic phase), and also from the microcline to microcline recrystallizations related to changes in the orientations of the twin variants without modifications in the local order of low microcline (Sánchez-Muñoz et al, 2012). When these mineral structures are considered as complex systems, with certain adaptation capability to the geological environments related to the cooling rate and directed tectonic stresses and involving self-organization capacity (Sánchez-Muñoz et al, 2008), twin patterns can be useful for geotectonic setting recognition.

Twin and perthitic patterns have been studied in (001) sections by a combination of polarized light optical microscopy (with the help of a red plate) and a confocal Raman microscopy-based imaging system. This experimental procedure allows distinguishing the distribution of the alkali feldspar phases, the order-disorder states and the structural strains in the K-feldspars through the patterns. Samples were obtained from selected outcrops from twenty-nine granitic pegmatite districts around the world of Phanerozoic, Proterozoic and Archean ages. Miarolitic pegmatites were not studied because in most cases the feldspar features are mostly controlled by interactions with residual aqueous fluids. The twin patterns can be described by three twin-generations (I-, II-, and III-tg) in which different developments imply particular and distinguishable evolutionary trends, toward single-twin orientation (low) microcline perthite as the ending stage. The evolutionary trends can be correlated with the characteristic geotectonic setting in which the K-feldspars were formed and resided on cooling. The studied an-orogenic pegmatites have orthoclase-microcline mixtures, or microcline twin patterns formed mainly by the I-tg, in some cases with exceptional self-organized perthitic patterns as in the Laramie Mt. hypersolvus pegmatites (WY, USA) where manifold "complex" periodic patterns emerge. The twin patterns of microcline from syn-collisional subsolvus pegmatites consist of the II- and III-tg. The considered post-collisional subsolvus pegmatites can have microcline mostly formed by a single-twin orientation as a distinctive character, which has not been seen in the other two cases.

In addition, twin patterns can be used to distinguish different pegmatite generations in polychronous pegmatite provinces. In the Eastern Brazilian Province, twin patterns are different for the

syn- and post-collisional pegmatites related in the two cases to the Panafrican Orogeny, which coexist side by side in the same province. In the Olary and Broken Hill districts in Curnamona Province (East Australia) syn- and post-orogenic pegmatites also coexist geographically. In this case, the K-feldspars and their twin patterns formed in the Mesoproterozoic Olarian Orogeny (~1.6 Ga) are reasonably well preserved despite the sericitic and deformational overprinting related to the Paleozoic Delamerian Orogeny (~500 Ma).

The development of the K-feldspar transformations and recrystallizations can be affected by chemical hinderers, particularly phosphorous which can stabilize the modulated structure of partially ordered orthoclase in both syn-collisional and post-collisional environments. It also depends on the availability of water as a kinetic agent, and mesoperthite orthoclase can predominate in pegmatites intruded and/or formed within granulite facies of metamorphism. Taking into account these considerations and limitations, twin and perthitic patterns are seen here as precious non-equilibrium mineralogical information helpful to identify the geotectonic settings of granite pegmatites during the subsolidus stage.

References:

Černý, P. (1991): Fertile granites of Precambrian rare-element pegmatite fields: is geochemistry controlled by tectonic setting or source lithologies. Precambrian Research, 51, 429-468

Martin, R.F., De Vito, C. (2005). The patterns of enrichment in felsic pegmatites ultimately depend on tectonic setting. Canadian Mineralogist, 43, 2027-2048.

Sánchez-Muñoz, L., García-Guinea, J., Zagorsky, V.Ye., Juwono, T., Modreski, P.J., Cremades, A., Van Tendeloo, G., De Moura, O.J.M. (2012) The evolution of twin patterns in perthitic K-feldspar from granitic pegmatites. Canadian Mineralogist, vol. 50, 989-1024.

Sánchez-Muñoz L., García-Guinea, J., Beny, J.M., Rouer, O. Campos, R., Sanz, J., De Moura O.J.M. (2008): Mineral self-organization during the orthoclase-microcline transformation in a granite pegmatite. European Journal of Mineralogy, vol. 20, 439-446.

Tkachev, A.V. (2011): Evolution and metallogeny of granitic pegmatites associated with orogens throughout geological time. Geological Society, London, Special Publications, 350, 7-23.

CHEMICAL VARIATION OF LI TOURMALINE FROM NAGATARE PEGMATITE, FUKUOKA PREFECTURE, JAPAN

Y. Shirose, S. Uehara
Department of Earth and Planetary Sciences, Faculty of Sciences, Kyushu University, Fukuoka 812-8581, Japan,
shirose@kyudai.jp

Tourmaline is an accessory mineral that occurs commonly in igneous and metamorphic rocks. The general formula of tourmaline is $XY_3Z_6(BO_3)_3T_6O_{18}V_3W$ (X = Na, Ca, K, vacancy; Y = Fe^{2+}, Mg, Mn^{2+}, Al, Li, Fe^{3+}, Cr; Z = Al, Fe^{3+}, Mg, Cr; T = Si, Al, B; B = B; V = OH, O; W = OH, F, O) (Henry *et al.*, 2011). Chemical variation of tourmaline in a Li pegmatite shows increasing (Li + Al) and decreasing Fe from the country rock to the core of the pegmatite, reflecting the chemical development of melts (Jolliff *et al.*, 1986). Later the chemical trends of tourmaline in some pegmatite subtypes were reported (e.g., Novák and Povondra, 1995; Selway et al, 1999; Tindle et al, 2002; Tindle et al, 2005). Nagatare pegmatite, Fukuoka Prefecture, Japan, is a complex-type, granitic pegmatite and is a classic mineral locality in Japan. Many rare element minerals (lepidolite, elbaite, petalite, pollucite, tantalite etc.) were reported (e.g., Shibata, 1934), but these mineralogical descriptions are insufficient. The chemical compositions of the tourmaline have not been determined in detail, and no XRD results were reported. In this study, tourmaline specimens from the Nagatare pegmatite were classified into 5 types, type-A (black), type-B (indigo), type-C (light blue-pink), type-D (pink) and type-E (pink-light blue), on the basis of localities, associated minerals, color, and texture. Type-A was collected at Li-poor pegmatite intruding metamorphic rocks, and other types were obtained from the Li ore deposit of the old Nagatare mine. Type-C shows color zoning composed of a light blue core and a pink rim. In contrast, type-E has a pink core and a light blue rim. A total of 29 samples were analyzed by EPMA and XRD.

Substitution of (Li + Al) for Fe at the Y site was significant, showing result of melt fractionation (Fig. 1a). The minor cations at the Y site, such as Mg, Mn, Zn and Ti, were also characteristic in each type. The X-site in type-B was Na dominant, and Na decreases with increasing (Li + Al) in type-C, D and E (Fig. 1b). The contents of F were well correlated with X-site charge except for type-A. The mineral species of the tourmaline are composed of schorl (type-A, B), fluor-schorl (type-B), elbaite (type-B, C, D, E), fluor-elbaite (type-B, C, D, E) and rossmanite (type-D, E). The unit-cell parameters were in the range between rossmanite, elbaite and schorl.

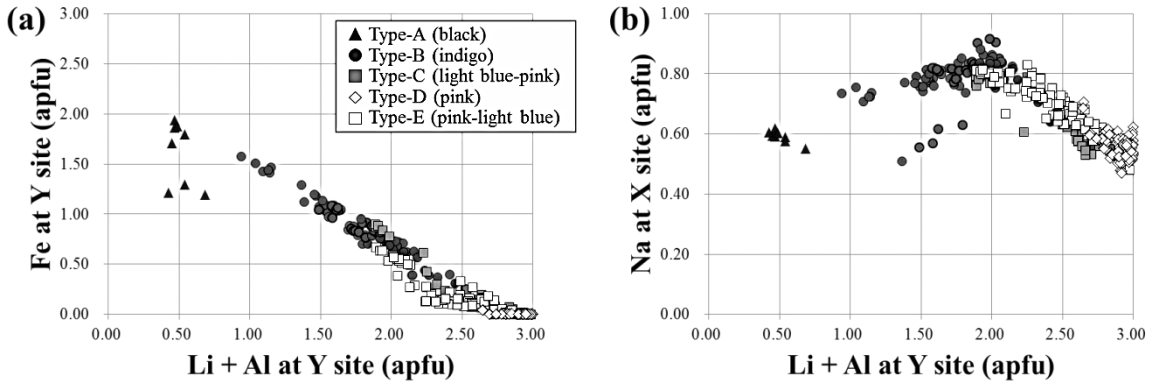

Fig. 1: Chemical variations of tourmaline from Nagatare. (a) Substitution of (Li + Al) for Fe at the Y site. Li = 3 - Y-site cation sum. (b) Relationship between Na at the X site and (Li + Al) at the Y site.

Compared to other LCT pegmatites, the chemical trend of tourmaline from the Nagatare pegmatite was similar in major chemical components, but different in minor elements such as Zn and Mn. Though these elements are generally trace except some localities, the intermediate fractionated tourmaline (type-B) had both Zn (0.00-0.20 *apfu*) and Mn (0.11-0.38 *apfu*) (Fig. 2). It indicates that the pegmatite forming melt contained less Fe, and more Zn and Mn than other localities. In type-E, the

rim had greater Fe and Mn contents than the core, and it differs from the trends of the melt development. Vacancy, Al and OH rich Li tourmaline (type-D and the pink part of type-E) were selectively replaced by muscovite. These features indicate that several stages of alterations occurred in the late stage of the pegmatite forming process.

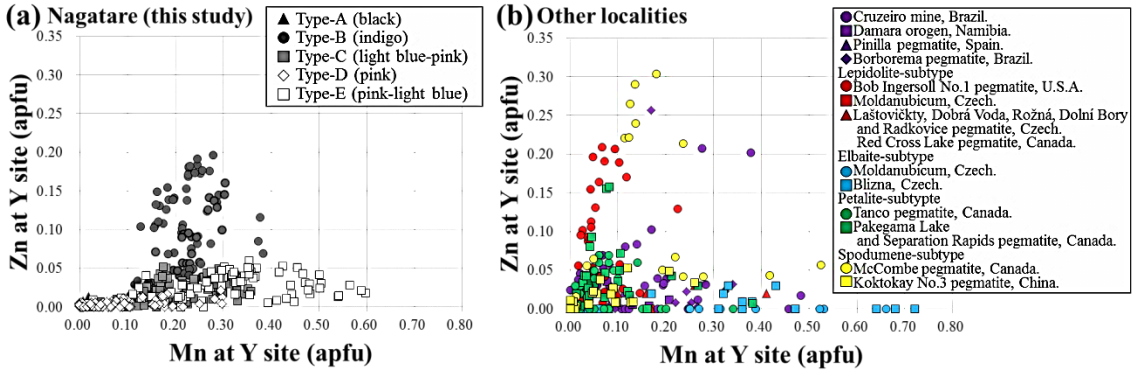

Fig. 2: Zn and Mn contents at the Y site of tourmaline from (a) Nagatare pegmatite and (b) other localities. References are as follows: Federico *et al.* 1998 (purple circle). Keller *et al.* 1999 (purple square). Roda *et al.* 2004 (purple triangle). Soares *et al.* 2008 (purple diamond). Jolliff *et al.* 1986 (red circle). Novák and Povondra 1995 (red square). Selway *et al.* 1999 (red triangle). Novák and Povondra 1995 (blue circle). Novák 1999 (blue square). Selway *et al.* 2000 (green circle). Tindle *et al.* 2002 (green square). Tindle *et al.* 2005 (yellow circle). Zhang *et al.* 2008 (yellow square).

References:

Federico, M., Andreozzi, G.B., Lucchesi, S., Graziani, G. and César-Mendes, J. (1998): Compositional variation of tourmaline in the granitic pegmatite dykes of the Cruzeiro mine, Minas Gerais, Brazil. Canadian Mineralogist, vol. 36, 415-431.

Henry, D.J., Novák, M., Hawthorne, F.C., Ertl, A., Dutrow, B.L., Uher, P. and Pezzotta, F. (2011): Nomenclature of the tourmaline-supergroup minerals. American Mineralogist, vol. 96, 895-913.

Jolliff, B.L., Papike, J.J and Shearer, C.K. (1986): Tourmaline as a recorder of pegmatite evolution: Bob Ingersoll pegmatite, Black Hills, South Dakota. American Mineralogist, vol. 71, 472-500.

Keller, P., Roda-Robles, E., Pesquera Pérez, A. and Fontan, F. (1999): Chemistry, paragenesis and significance of tourmaline in pegmatites of the Southern Tin Belt, central Namibia. Chemical Geology, vol. 158, 203-225.

Novák, M. and Povondra, P. (1995): Elbaite pegmatites in the Moldanubicum: a new subtype of the rare-element class. Mineralogy and Petrology, vol. 55, 159-176.

Novák, M., Selway, J.B., Černý, P., Hawthorne, F.C. and Ottolini, L. (1999): Tourmaline of the elbaite-dravite series from an elbaite-subtype pegmatite at Bližná, southern Bohemia, Czech Republic. European Journal of Mineralogy, vol. 11, 557-568.

Roda, E., Pesquera, A., Gil, P.P., Torres, J. and Fontan, F. (2004): Tourmaline from the rare-element Pinilla pegmatite, (Central Iberian Zone, Zamora, Spain): chemical variation and implications for pegmatitic evolution. Mineralogy and Petrology, vol. 81, 249-263.

Selway, J.B., Černý, P. and Hawthorne, F.C. (2000): The Tanco pegmatite at Bernic Lake, Manitoba. XIV. Internal tourmaline. Canadian Mineralogist, vol. 38, 877-891.

Selway, J.B., Novák, M., Černý, P. and Hawthorne, F.C. (1999): Compositional evolution of tourmaline in lepidolite-subtype pegmatites. European Journal of Mineralogy, vol. 11, 569-584.

Shibata, H. (1934): Lithium pegmatite from Nagatare, Imajuku Village, Itoshima Country, Fukuoka Prefecture. Journal of the Geological Society of Japan, vol. 41, 582-603 (in Japanese).

Soares, D.R., Beurlen, H., Barreto, S.B., Da Silva, R.R. and Ferreira, A.C.M. (2008): Compositional variation of tourmaline-group minerals in the Borborema pegmatite province, northern Brazil. Canadian Mineralogist, vol. 46, 1097-1116.

Tindle, A.G., Breaks, F.W. and Selway, J.B. (2002): Tourmaline in petalite-subtype granitic pegmatites: evidence of fractionation and contamination from the Pakeagama Lake and Separation Lake areas of northwestern Ontario, Canada. Canadian Mineralogist, vol. 40, 753-788.

Tindle, A. G., Selway, J.B. and Breaks, F.W. (2005): Liddicoatite and associated species from the McCombe spodumene-subtype rare-element granitic pegmatite, northwestern Ontario, Canada. Canadian Mineralogist, vol. 43, 769-793.

Zhang, A.C., Wang, R.C., Jiang, S.Y., Hu, H. and Zhang, H. (2008): Chemical and textual features of tourmaline from the spodumene-subtype Koktokay No.3 pegmatite, Altai, northwestern China: a record of magmatic to hydrothermal evolution. Canadian Mineralogist, vol. 46, 41-58.

MOUNT MICA PEGMATITE, MAINE, USA

W. Simmons[1], A. Falster[1], K. Webber[1], E. Roda-Robles[2]
[1]Dept of Earth & Environmental Sci., University of New Orleans, New Orleans, LA 70149, wsimmons@uno.edu
[2]Dept. de Mineralogía y Petrología, Univ. del País Vasco UPV/EHU, P.O. Box. 644, E-48080 Bilbao, Spain

Mount Mica pegmatite is the site of the first find of tourmaline in North America and is famous for gem tourmaline production for nearly 200 years. The dike ranges in thickness from 1 to 8 meters and dips 20° to the SE. A new phase of mining activity by Coromoto Minerals began in 2003 and now continues down dip underground for over 100 meters to a depth of about 30 meters. Hundreds of pockets ranging in size from a few cm^3 to one in excess of 500 m^3 have been found. Several dozens of the larger pockets have produced thousands of carats of gem quality tourmaline and some morganite. Pocket density averages about one every 3 meters with larger pockets having greater spacing and small ones having less, making this one of the most pocket-rich pegmatites in North America. In addition to the gem material, thousands of high-quality mineral specimens including tourmaline, beryl, apatite, lepidolite, rose and smoky quartz, hydroxylherderite, cassiterite, pollucite, and kosnarite have been recovered.

Contact relationships examined by Clark *et al.* (this issue) reveal only minor loss of components to the country rock. The correspondence of the Fe/(Fe+Mg) ratio between tourmaline, garnet and biotite confirms the minor exchange between the pegmatite and country rock. Leucosomes in the surrounding migmatite appear to be continuous with no distinct contact with the pegmatite, suggesting that the pegmatite was in thermal and chemical equilibrium with the leucosomes.

The wall zone and intermediate zone of Mt. Mica are unusual as they are essentially devoid of K-feldspar. These outer zones of the pegmatite consist of quartz, muscovite, nearly end-member albite and schorl. Muscovite is the dominant K-bearing species in the outer portion of the pegmatite. K-feldspar only appears as large masses in the core zone of the pegmatite adjacent to pockets, where it serves as a pocket indicator in some cases.

The principal mica in the wall zone and intermediate zone is muscovite which is rather homogeneous with Li content ranging only up to about 0.9 *apfu* toward the interior. Lepidolite only occurs in the core zone in pods up to several meters in size near pockets. Muscovite crystal size increases, in some cases dramatically, adjacent to and in pockets. Additionally, crystals extending into pockets are commonly rimmed with lepidolite. The compositional change from muscovite to lepidolite is abrupt without intermediate compositions. The lepidolite compositions range from "mixed" to just beyond trilithionite (Marchal *et al.*, this issue). Intimate muscovite–lepidolite intergrowths occur on a several micron scale where muscovite extends into pockets, suggesting conditions of rapid crystal growth in the pocket environment.

Columbite group minerals show only minor to moderate enrichment in Mn and Ta, reaching only columbite-(Mn). In fact, Mt. Mica seems rather depleted in Ta relative to other B-rich LCT pegmatites. The presence of masses of Mn and Fe carbonates in the core zone indicates an important role of CO_2 in the late stages of the consolidation of the pegmatite (Johnson *et al.*, this issue). Compositionally these are just barely Mn-dominant, whereas carbonates from the more evolved Bennett and Emmons pegmatites are essentially rhodochrosite. The enrichment of Rb and Cs in most of the pegmatite is also moderate. The muscovite K/Rb ratio averages about 30 and the K-spar K/Rb ratio is about 55. These values indicate that overall Mt. Mica is only moderately evolved compared with other B-rich LCT pegmatites which have values below 5 (Marchal *et al.*, this issue). Only in the core zone in and around pockets does K-feldspar show low K/Rb ratios near 7, similar to more evolved pegmatites. The lower K/Rb values in and around pockets and the presence of the evolved mineral species elbaite, lepidolite, and pollucite in the core zone demonstrate that Mt. Mica's internal evolution mechanism was very effective, producing proportionally small volumes inside the pegmatite with very high enrichment in incompatible elements.

The bulk chemical composition of Mt. Mica was calculated using a novel approach of combining detailed mapping of the mined portion of the pegmatite by Gary Freeman with whole rock analyses of 45 equally spaced drill cores from hanging wall to foot wall contact. Samples of equal mass were pulverized, homogenized and analyzed by fusion ICP. The volumes of pegmatite mined, open space of the pockets and the volume of lepidolite and K-feldspar masses adjacent to pockets

using the digitized map, thickness estimates, and modal analysis of lepidolite from lepidolite masses was calculated. The appropriate percentage of lepidolite was added to the powder of the 45 cores to provide the correct Li content of whole-rock bulk chemistry for the Mt. Mica pegmatite (for details see Boudreaux *et al.*, this issue). Water content was calculated in similar fashion using the calculated volume of open space (pocket volumes), assuming that the pockets were filled with H_2O. This water content was added to water determined by LOI (above 500°C) to estimate the total H_2O content of 1.2 wt.% of the pegmatite melt. The resulting whole rock bulk composition of Mt. Mica pegmatite is shown in Table 1.

Garnet-biotite thermometry from sample pairs in the country rock at the contact yield a temperature range of 650-690°C (Clark *et al.*, this issue). Considering the textural evidence of the gradational contact of the leucosomes and the pegmatite, we infer that the pegmatitic melt was at the same temperature. This temperature is consistent with the P-T conditions inferred for rocks of the Sebago Migmatite Terraine from an assemblage of sillimanite, quartz, muscovite, biotite and alkali feldspar (650°C and 3 kb) by Guidry *et al.*, (this issue).

Plots of the chemistry of the bulk pegmatite 45-core composite with leucosomes from the migmatitic country rock are strikingly similar in REE content and spider diagrams of rock vs. average crust also show very similar patters (Figs. 1 & 2). In conclusion, in contrast to suggestions of previous authors that this pegmatite must be derived by fractional crystallization from the Sebago Granite pluton (or any other pluton), we believe the evidence presented here is quite suggestive that the Mt. Mica pegmatitic melt could be derived directly from partial melting of the metapelitic rocks of the Sebago Migmatitic terraine. Batches of melt flow and accumulated to larger volumes that subsequently form the pegmatite.

Table 1 Bulk Composition Mt. Mica

oxide	wt. %	element	ppm
SiO_2	72.08	Sr	44
TiO_2	0.067	Ba	35
Al_2O_3	17.33	Nb	23.5
FeOt	1.21	Ta	6.3
MnO	0.039	Zr	17
MgO	0.15	Hf	1
CaO	0.48	Sn	84
Na_2O	5.35	Cs	99.9
K_2O	2.08	Rb	636
P_2O_5	0.20	B*	287
Li_2O*	0.24		
H_2O (pocket)	0.22		
LOI	0.94		
F^{α}	0.25		
subtotal		100.64 wt.%	
- O Ξ F		0.11 wt.%	
TOTAL		**100.53 wt.%**	

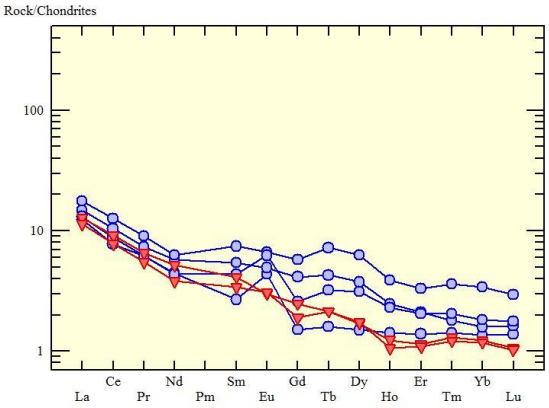

Fig. 1: Whole-rock chondrite normalized REE plot of Mt Mica Pegmatite (red) vs. SMD Leucosomes (blue),

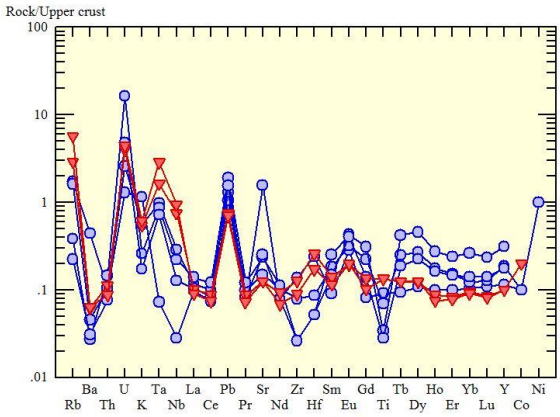

Fig. 2: Whole-rock spider diagram of Mt. Mica pegmatite (red) and SMD leucosomes (blue) vs. upper crust.

TOWARDS EXPLORATION TOOLS FOR HIGH PURITY QUARTZ IN THE BAMBLE-EVJE PEGMATITE BELT, SOUTH NORWAY

B. Snook[1,2], A. Müller[2,3], B. Williamson [1,3] F. Wall[1,3]
[1] Camborne School of Mines – University of Exeter, Penryn, Cornwall TR10 9EZ, UK bs225@exeter.ac.uk
[2] Norges Geologiske Undersokelse (NGU), Postboks 6315 Sluppen, 7491 Trondheim, Norway
[3] The Natural History Museum, Cromwell Road, London, SW7 5BD, UK

High Purity Quartz (HPQ); quartz containing less than 50 ppm trace elements (Harben, 2002), is of increasing economic significance due to its necessity in certain high-tech components (computer chip and semiconductor manufacture) and in green technologies (silicon wafer production for photo-volatic cells) (Glover *et al.*, 2012). Current HPQ deposits (typically hydrothermal veins and leuco-granites) are rare and volumetrically small. Unless significant new deposits are found, increasing demand for HPQ will raise its price, elevating the strategic nature of this limited commodity. The large volumes and simple mineralogy of pegmatites and the often high chemical purity of their constituents (Glover *et al.*, 2012) make them an attractive target for HPQ. Trace element, cathodoluminescence (CL) and O-isotope data will be presented from PhD studies being carried out on quartz from the Evje-Iveland pegmatite field of the Bamble-Evje pegmatite belt, southern Norway. The area was targeted due to its well constrained geological setting and previously identified potential for HPQ (e.g. Larsen *et al.*, 2000); indeed, there are HPQ pegmatites elsewhere in Norway e.g. Drag. The overall aim of the investigation is to develop exploration tools for HPQ by determining the genetic history of the pegmatites and mode of HPQ formation.

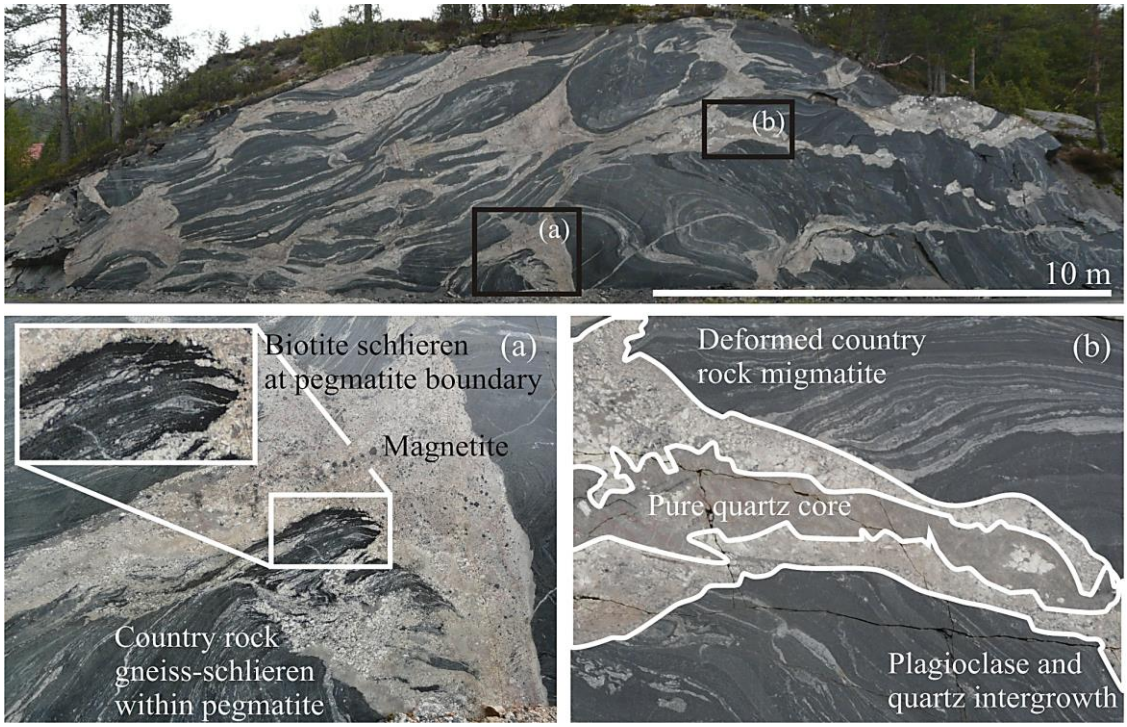

Fig. 1: Partial melting of host meta-gabbros directly contributing to pegmatite meltsThe Evje-Iveland field consists of around 350 major pegmatite

The Evje-Iveland field consists of around 350 major pegmatite occurrences emplaced within migmatitic amphibolites and metagabbros; around 260 of the pegmatites have been mined historically for feldspar. The study is focussed on the profiling of 7 pegmatites and their host rocks, obtaining whole-rock geochemical compositions from relatively fine grained border facies and country rocks and assessing pegmatite mineral compositions. Each pegmatite shows distinctive zonation, with quartz/feldspar intergrowths at the margins, a massive quartz core and a variety of accessory (including REE-bearing) phases. The pegmatites are classified as Niobium-Yttrium-(Fluorine)-type, rare-

element, REE pegmatites (Černý and Ercit, 2005). The proximal Høvringsvatnet granite was previously suggested to have supplied late-stage, highly fractionated melts to form the pegmatites (Bjørlykke, 1937). However, a distinctly different trace element signature and a difference in U/Pb age of approximately 70 Ma exist between the granite and the pegmatites. Additionally, there is no relationship between trace element content, degree of pegmatite fractionation or pegmatite position relative to the granite. Field studies indicate that the Iveland pegmatite formed by 'in situ' partial melting of host meta-gabbros (Fig. 1). This has been corroborated by geochemical modelling using trace elements (mainly REE). However, field evidence and modelling of other pegmatites suggest they originated from more distal sources of basement rock. Quartz was imaged using CL in a scanning electron microscope (SEM), and then analysed by laser ablation inductively coupled plasma mass spectrometry (LA-ICP-MS). For pegmatite quartz, no relationship could be found between its trace element content and the degree of fractionation in each pegmatite body. After field evidence, and from the trace element compositions of the pegmatites and the U/Pb age of the granites, it is deemed highly unlikely that the pegmatites formed by fractional crystallisation of melts represented by the Høvringsvatnet granite; anatexis of country rock is suggested as an alternative.

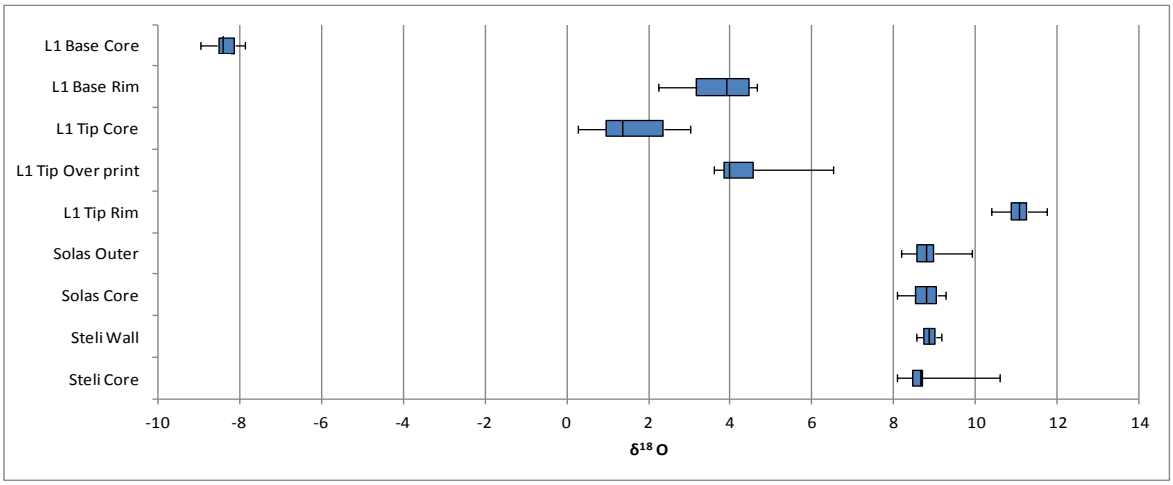

Fig 2: O-isotope values of quartz from the L1, Solås and Steli pegmatites. Hydrothermal quartz (L1) $\delta^{18}O$ values have a huge range, from -9 ‰ to 11 ‰; typically 0 – 5 ‰. Magmatic quartz (Solås and Steli) $\delta^{18}O$ values are much more consistent; typically 8-9%.

Certain pegmatites (the Landsverk region) contain brecciated feldspar and replacement quartz, interpreted to be of 'hydrothermal' origin. From LA-ICP-MS data, hydrothermal quartz, compared with magmatic quartz, shows a reduced total trace element content, with relatively elevated levels of Al and Li, low Ge and no detectable Ti, indicating relatively low temperature formation. Different quartz domains (from SEM-CL imaging) show distinct $\delta^{18}O$ values (Fig. 2); late-stage, low-trace element zones show values consistent with meteorically derived fluids. In situ LA-ICP-MS chemistry and fluid inclusion studies will provide further information about the composition of the fluids which have replaced the magmatic quartz with high purity meteoric/hydrothermal quartz. This beneficiation process is a potential mechanism for the generation of economically significant HPQ deposits.

References:

Bjørlykke H. (1937). The granite pegmatites of Southern Norway. Journal of the Mineralogical Society of America, vol. 22, 241-255.

Černý P. & Ercit, T.S. (2005). The classification of granitic pegmatites revisited. Canadian Mineralogist, vol. 43, 2005-2026.

Glover, A.S, Rogers, W.Z. and Barton, J.E. (2012). Granitic Pegmatites: Storehouses of Industrial Minerals. Elements, vol. 8, 269-273.

Harben, P.W. (2002). The industrial minerals handybook – a guide to markets, specifications and prices. 4th edition, Industrial Mineral Information, Worcester Park, United Kingdom, pp. 412.

Larsen, R.B., Polvè, M. & Juve, G. 2000. Granite pegmatite quartz from Evje-Iveland: trace element chemistry and implications for the formation of high-purity quartz. NGU-Bull, vol. 436, 57-65.

MINERALOGY MEETS MINERAL ECONOMICS: HOW DOES PEGMATOLOGY INTERFACE WITH THE MINERAL INDUSTRY, SOCIETY AND MARKET FORCES

M. Sweetapple
CSIRO Earth Sciences and Resource Engineering, PO Box 1130, Bentley, W.A., Australia

Granitic pegmatites are well known as current or potential sources of a wide range of rare metals. Some of these metals have recently come to prominence as critical elements, as designated by bodies such as the U.S. Department of Energy and the British Geological Survey. These critical elements are specific metals or minerals perceived to be of economic importance and are subject to a supply risk. Thus it is straightforward to relate the importance of granitic pegmatites to questions of supply of certain strategic elements. However, a further question raised by these concerns, is how do we as scientists bring our detailed and extensive knowledge of the field of granitic pegmatites to the needs and concerns of commercial entities, and decision makers formulating policies in governments and elsewhere.

Firstly, it is instructive to consider the supply chain within which minerals are brought from their natural forms to an end product (Fig. 1).

The application of 'pegmatology' to geoscience based targeting, exploration and resource development is typically self-evident, but frequently the application of mineralogical and geochemical knowledge to the mineral processing stage is often overlooked. Invariably, the commodities recovered from granitic pegmatites require considerable investment at later stages of project development, after the traditional application of geoscientific knowledge. Such later stages typically include capital-intensive, specialized mechanical and/or chemical processes of ore beneficiation. Thus the value of mineral projects involving the mining of pegmatites (and consequently the operating companies) is realized at the later stages of project development, as opposed to 'simple' commodities such as lode gold. A convenient way of classifying different commodities in economic terms is as either 'concave' or 'convex' minerals in terms of the realization of value over the stages of project development (Trench and Packey, 2012) (Fig. 2).

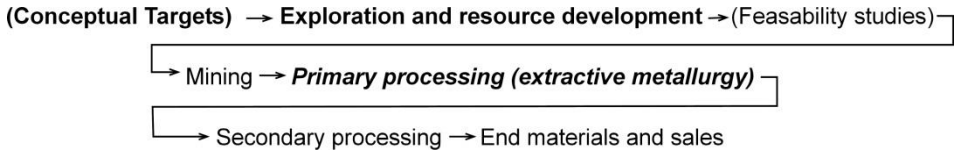

Fig. 1: Schematic supply chain for an operating metalliferous mine, with the stages of most significant or potential contribution from geoscience indicated in bold type.

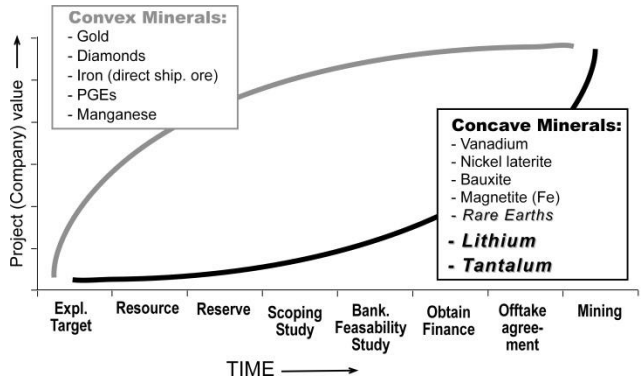

Fig. 2: Simplified schematic diagram classifying commodities on the basis of the realization of project value versus progressive stages of project development from early exploration through to mining (Adapted from Trench and Packey, 2012).

Specific examples of how the knowledge base of 'pegmatology' have, and can, be applied to mineral processing and economics, are provided here for lithium and tantalum. These are the two most important commodities derived from exploitation of granitic pegmatites. Both of these are prime examples of concave commodities where value is mostly added later in the project life, including the development of specialized metallurgical processing pathways, where characterization of the physical and chemical properties of mineralogy is essential.

At face value, it would seem that evaporation from brine and salar deposits is a more efficient and cost effective source of lithium than pegmatite mining. Although brine deposits constitute the bulk of world Li production, 'hard rock' mining of pegmatites currently contributes ~26% of global lithium production (Pistilli, 2012), almost entirely from spodumene. However, granitic pegmatites provide a geographic diversity of sources with a consequent reduction of supply risk, coupled with higher Li contents (Kesler *et al.*, 2012). Furthermore, it has been recently demonstrated that lithium carbonate product from spodumene may have significantly less contaminants, especially Mg, but also Na, K, Ca and Fe (Galaxy Resources, 2012). Reduced trace element contents in turn facilitate significantly improved Li_2CO_3 based battery performance. Thus the minor element contents of spodumene and accompanying gangue minerals are very consequential. Cost of mineral recovery is important, but product suitability, and therefore saleability, is more so.

In the case of tantalum, the relationship of mineral chemistry to processing is a key issue. In terms of mineralogy, minerals of simple compositions are easier to process than complex species, e.g. a columbite-tantalite based ore is preferable to than a pyrochlore/microlite dominated ore. In general, more complex ore minerals are typically harder to 'crack' via hydrometallurgy, and may generate more complex waste products, particularly if significant U and Th are present. Correspondingly, the lack of deleterious elements in an ore mineral product is of considerable importance. In the case of Ta ores, maximum levels in saleable concentrates of varying specifications range from 6-25% SnO_2, 0.02-0.25% As, 0.2% Sb, 0.1-1% ThO_2+U_3O_8, and 5% S (data summarized from Global Advanced Metals, 2010).

A related application of Ta-Nb mineral chemistry, in terms of both mineral economics and social impact, is the fingerprinting of African conflict Ta ores down to deposit scale, by a combination of both bulk and single mineral analysis techniques. These techniques include SEM-MLA analysis of concentrates, LA-ICP-MS analysis and U-Pb dating by TIMS of columbite-tantalite (e.g. Melcher *et al.*, 2008). The application of such fingerprinting to the origin of Ta-Nb concentrates is potentially of immense importance, as geopolitical and human rights concerns are ongoing in relation to 'conflict minerals' including 'coltan' from the Congo and neighbouring countries.

Thus, the provision of detailed mineral chemistry of economic mineral species, together with the knowledge of the distribution of these minerals across different 'zones' or units contributes to mining, metallurgical testwork, plant design, and recovery of these minerals. Given the 'concave' nature of the specific commodities associated with granitic pegmatites, the contribution of pegmatology to the supply chain of rare metals is not just limited to geoscience based targeting and exploration, but provides a critical contribution to mineral processing, marketing and supply, and an ultimate impact on society.

References

Galaxy Resources Ltd. (2012): Galaxy improves product quality at Jiangsu. ASX announcement/media release, 15th August 2012, 6 pp.

Global Advanced Metals Ltd. (2010): Typical product specifications. http://www.globaladvancedmetals.com/our-products/tantalum-concentrate/typical-product-specifications-.aspx, retrieved 22/1/2013.

Kesler, S.E., Gruber, P.W., Medina, P.A., Keoleian, G.A., Everson, M.P., Wallington, T.J. (2012): Global lithium resources: Relative importance of pegmatite, brine, and other deposits. Ore Geology Reviews vol. 48, 55-69

Melcher, F., Sitnikova, M.A., Graupner, T., Martin, N., Oberthür, T., Henjes-Kunst, F., Gäbler, E., Gerdes, A., Brätz, H., Davis, D.W., Dewaele. S. (2008): Fingerprinting of conflict minerals: columbite-tantalite ('coltan') ores. SGA News No. 23. 1, 7-14.

Pistilli, M. (2012): Lithium Deposit Types: Brine, Pegmatite and Sedimentary. Lithium Investing News, http://lithiuminvestingnews.com/6529/lithium-deposits-brine-pegmatite-sedimentary/, retrieved 21/1/2013.

Trench, A., Packey, D. (2012): Australia's Next Top Mining Shares – Understanding Risk and Value in Minerals Equities. Major Street Press. 336 pp.

INTERNAL EVOLUTION OF AN ADIRONDACK PEGMATITE DIKE, NEW YORK

P. Tomascak, S. Pratt, C. Spath III,
Department of Earth Sciences, SUNY Oswego, Oswego, NY

Trace element concentrations of samples of feldspar and quartz from mineralogically distinct zones of an undeformed granitic pegmatite at Day, NY, in the southern Adirondack highlands, have been measured to assess models of internal evolution. The overall aim of the study is to use trace elements in these minerals to better understand processes of internal evolution in relatively simple granitic pegmatites, those which lack mineralization of, for example, Li, Cs, Nb-Ta, REE. The samples from the Day (also known as "Overlook") pegmatite were removed from a roughly circular, c. 10 m diameter, cross-section of the lenticular dike, the outcrop of which extends for tens of meters. The quarried section exposes a rose quartz core rimmed with blocky (20-50 cm diameter) albitic feldspar, with sharp contacts with an exterior zone (quartz + plagioclase + K-feldspar) dominated by coarse graphic granite (mainly smoky quartz intergrown with albitic plagioclase). Tourmaline (schorl) is locally present in the blocky zone and biotite is locally abundant in the graphic zone. Hand-picked grains of quartz and feldspar were analyzed in the Interdisciplinary Elemental Measurement Facility at SUNY Oswego using solution ICP-MS (Bruker 820MS). Feldspar samples were examined by SEM-EDS to evaluate the nature of major element homogeneity and exsolution. Leachable elements in quartz were examined separately and appear to rule out control of the mineral's elemental budget by fluid inclusions.

There is no systematic difference between concentrations and ratios of alkalis (Rb, Cs), alkaline earths (Sr, Ba), or U/Pb between plagioclase samples from the graphic zone and those from the blocky zone. Plagioclase samples from the two zones have identical REE pattern shapes, with significant LREE enrichment and sharp positive Eu anomalies. Quartz samples from the graphic and core zones show small differences in average trace element contents, with core quartz generally having higher Rb/Sr (2x), lower Sr/Ba (<2x) and U/Pb (10x). Whereas alkali and alkaline earth concentrations of graphic zone quartz are uniformly higher than in core quartz, Li concentrations are uniform throughout (c. 3-6 ppm). Quartz REE abundances are too low to determine complete distributions, but core quartz appears poorer in LREE than quartz in the graphic zone. Compared to the Li-mineralized Tin Mountain pegmatite (Black Hills, SD), the Day quartz is c. 10x poorer in Li, but elemental ratios are similar for Rb/Sr and Rb/Cs. The observations of insignificant variation in chemistry of feldspar and of slightly greater trace element enrichment in quartz from the graphic (exterior) zone than in the core are contrary to a model in which rare elements are progressively enriched following early crystallization of feldspar-rich assemblages.

INCLUSIONS AND INTERGROWTHS IN MONAZITE-(CE) AND XENOTIME-(Y): THERMAL BEHAVIOR AND RELATION TO CRYSTAL-CHEMICAL PROPERTIES

N. Tomašić[1], V. Bermanec[1], R. Škoda[2], M. Šoufek[3], A. Čobić[1]

[1] University of Zagreb, Faculty of Science, Institute of Mineralogy and Petrology, Horvatovac 95, HR-10000 Zagreb, Croatia, ntomasic@geol.pmf.hr

[2] Faculty of Science, Institute of Geological Science, Masaryk University, Kotlařska 2, 61137 Brno, Czech Republic

[3] Croatian Natural History Museum, Demetrova 1, HR-10000 Zagreb, Croatia

Inclusions and intergrowths in monazite and xenotime have proven to be of a great importance when mineral formation, metamictization induced by actinide content, and different metasomatic and metamorphic events are considered.

Three monazite and a one xenotime samples were investigated for inclusions and intergrowths therein. Two of the monazite samples come from the Garta and Eptevann granite pegmatites in Aust-Agder province and the xenotime sample from the Eikeråsen (Eretveit) pegmatite (Norway). The third monazite sample was collected from the carbonatite dykes of Eureka Farm, Namibia.

Chemical analyses (EMPA), X-ray powder diffraction (XRD), scanning electron microscope (SEM) employing backscatter electron (BSE) and energy dispersion (EDS) detector for crystal-chemical characterization of the host and inclusion/intergrowth minerals. To estimate thermal behavior of the host minerals and their inclusions at 1 atm, the minerals were heated (annealed) at 200, 500, 800 and 1000°C for 24 hours and examined by XRD afterwards.

The EMPA gave monazite-(Ce) composition for all monazite samples, with Ce_2O_3 ranging from 22.69 to 34.53%, ThO_2 ranging from 9.18 to 9.92% and UO_2 ranging from 0.47 to 0.53%. An exception is monazite-(Ce) from Eureka Farm, being considerably depleted in ThO_2 and UO_2 (0.6 and 0.03%, respectively). The xenotime-(Y) sample contains 0.75% ThO_2 and 1.15% UO_2.

BSE images of the pegmatite monazite samples revealed several types of inclusions such as altered monazite areas, an anhedral $ThSiO_4$ phase and apatite inclusions (Figure 1). In many cases, $ThSiO_4$ inclusions are surrounded by altered monazite with increased Y_2O_3 and UO_2 content and slightly decreased SiO_2 relative to unaltered monazite. Xenotime-(Y) also contains $ThSiO_4$ inclusions, which are sometimes intergrown with uraninite. Zircon, mica and quartz are intergrown with xenotime. These obviously indicate a complex evolution of inclusion formation that would fit well into the proposed dissolution-reprecipitation model described for the inclusions in monazite and xenotime of the granite pegmatites in the Hidra anorthosite massif (Hetherington & Harlov, 2008). In monazite-(Ce) from the carbonatite dykes mainly cheralite inclusions occur. Sparse ThO_2 euhedral inclusions also occur.

Annealing experiments for all monazite and xenotime samples induced a slight decrease of unit cell volume ranging 0.66-0.76% (Figure 2). Measurements of crystallite size and strain for monazite from Eptevann and from Eureka Farm showed an increase of crystallite size and decrease of the strain with temperature increments. The crystallite size of unheated carbonatitic monazite is by an order of magnitude larger compared to the pegmatitic monazite. This can be attributed to very low actinide content in the sample from carbonatite, causing less intensive structure disturbances. The diffraction peak *200* was also used as a diagnostic feature of crystal structure adjustments during the annealing process. Full with at half (FWHM) and intensity of the maxima were determined by using pseudo-Voight function to fit the peak. Generally, for all the minerals the values decrease with increasing temperatures (Figure 2), while the intensity increases. An exception is xenotime-(Y) in which a phase with monazite-structure type crystallizes above 800°C, most probably huttonite. Inclusions of $ThSiO_4$ in the unheated monazite and xenotime are most likely thorite, which is frequently metamictized (Seydoux-Guillaume *et al.*, 2007). During annealing they recrystallize and occur as a discrete phase in xenotime. However, in the case of monazite, two scenarios are possible: either crystallization of huttonite and co-existence (overgrowth?)(Harlov *et al.*, 2005) with monazite, that is disguised in powder diffraction patterns by peak overlapping of the two phases with the same structure type, or thermally induced incorporation of $ThSiO_4$ into monazite. Previous experimental data showed preferable incorporation of $ThSiO_4$ component into monazite relative to xenotime at the same temperature range but significantly higher pressures (Seydoux-Guillaume *et al.*, 2002).

Since the fate of the observed inclusions upon thermal treatment cannot be unambiguously concluded solely using diffraction techniques, the annealed samples must be examined using electron microscopy.

References:

Harlov, D., With, R., H. –J. Föster (2005): Growth of huttonite ($ThSiO_4$) on monazite-(Ce) from 300-900 °C and 200-1000 MPa. Geophysical Reasearch Abstracts, Vol. 7,07171-07173.

Hetherington, C. J., D. E. Harlow (2008): Metasomatic thorite and uraninite inclusions in xenotime and monazite from granitic pegmatites, Hidra anorthosite massif, southwestern Norway: Mechanics and fluid chemistry. American Mineralogist, vol. 93, 806-820.

Seydoux-Guillaume, A., R. Wirth, W. Heinrich, J. Montel (2002): Experimental determination of thorium partititoning between monazite and xenotime using analytical electron microscopy and X-ray diffraction Rietveld analysis. European Journal of Mineralogy, vol. 14, 869-878.

Seydoux-Guillaume, A., R. Wirth, J. Ingrin (2007): Contrasting response of $ThSiO_4$ and monazite of natural irradiation. European Journal of Mineralogy, vol. 19, 7-14.

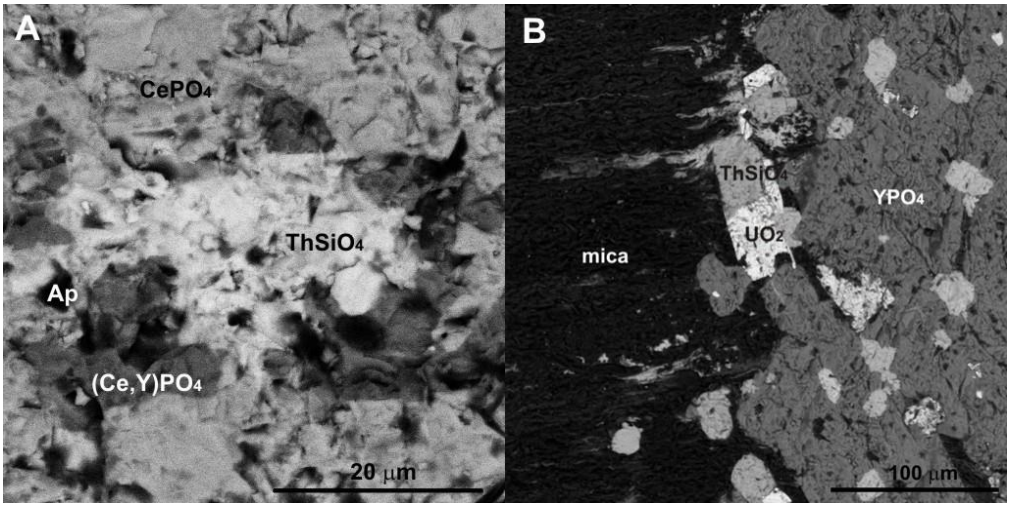

Fig. 1: BSE images of the monazite-(Ce) from Garta (A) and xenotime-(Y) from Eikeråsen (B) with mineral inclusions identified.

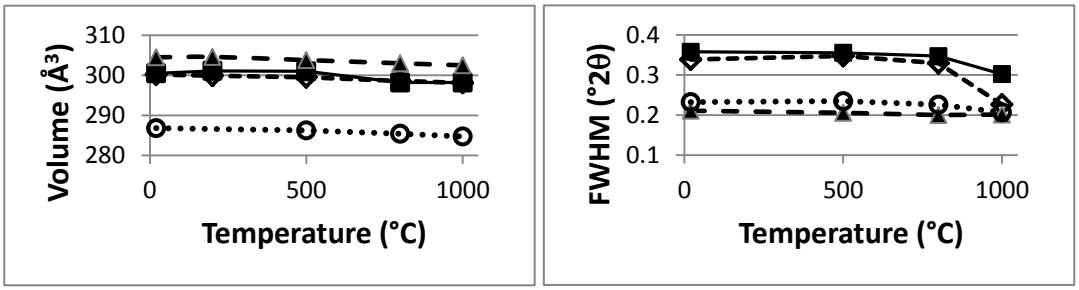

Fig. 2: Change of unit cell volume (left) and FWHM (right) with temperature (monazite: ◇ - Eptevann, ■ - Garta, , ▲ - Eureka Farm; xenotime: ○).

NAMIBITE AND HECHTSBERGITE FROM THE NAGATARE MINE, FUKUOKA PREFECTURE, JAPAN

S. Uehara, Y. Shirose
Department of Earth and Planetary Sciences, Faculty of Sciences, Kyushu University, Fukuoka 812-8581, Japan, uehara@geo.kyushu-u.ac.jp

The first mineralogical report of the Nagatare pegmatite was made by Ko in 1933. The following year, the pegmatite was designated a national monument and was named the "Nagatare Pegmatite Dyke with Lepidolite". A part of the pegmatite is lithium-rich and was mined for lithium ore during World War II. Excavated lithium ore, mainly composed of lepidolite and elbaite was stockpiled after mining, although there is at present little remaining lithium ore. Mineralogical studies of the pegmatite were made by Shibata (1934) and Okamoto (1944). After these investigations and before 1970 several descriptive mineralogical studies were made, however, modern systematic and detailed investigations of characteristic minerals in the Nagatare Li-pegmatite are missing. Therefore we have been reinvestigating lepidolite, tourmaline (Shirose and Uehara, 2012), and other rare minerals from the deposit. In the present study so called "bismuth ocher" was examined.

Namibite is a rare dark-green Cu-Bi-V-species, originally described from Khorixas, Namibia and was assumed to be an oxide mineral with the formula $CuBi_2VO_6$ (von Knorring and Sahama, 1981). Mrázek *et al.* (1994) redefined namibite as a vanadate with the formula $Cu^{2+}(BiO)_2V^{5+}O_4(OH)$. Namibite has been described from 12 localities worldwide (Dunning and Cooper, 1998). The crystal structure of namibite was determined by single crystal X-ray diffraction data to exhibit triclinic symmetry (Kolitsch and Giester, 2000). Hechtsbergite is a rare mineral with the formula $Bi_2O(VO_4)(OH)$. It was originally described from the Hechtsberg quarry at Hausach, in Black Forest, Germany (Krause *et al.*, 1997), where it is associated with chrysocolla, bismutite, beyerite, namibite, mixite, and eulytite in minute cavities in gneiss. After the original description, hechtsbergite has been described from three other localities, Brejaúba, Minas Gerais, Brazil (Burns *et al.*, 2000), the Clara Mine, Black Forest, Germany (Kolitsch *et al.*, 2004), and Smrkovec, western Bohemia, Czech Republic (Sejkora *et al.*, 2004). The Nagatare hechtsbergite is the 5th recognized occurrence in the world.

The old Nagatare lithium mine is located at Nagatare, Fukuoka City, Fukuoka Prefecture, Japan (Lat. 34°35´N, Long. 1.30°17´E). The ore body is a granitic pegmatite containing lepidolite, elbaite and petalite. The Cretaceous Sawara granite and the Itoshima granodiorite are found in the Nagatare area. Many pegmatite dikes of 1 to 200 m in width cross-cut the Itoshima granodiorite (Karakida *et al.*, 1994). The Nagatare lithium pegmatite contains minor amounts of "bismuth ocher" in lepidolite-albite-quartz pegmatite. Minerals in the ocher were identified by X-ray powder diffraction and electron-microprobe analyses. Namibite, hechtsbergite, clinobisvanite, waylandite, eulytite, beyerite, and bismutite were found in the mineral collection of one of the authors (S.U.) and were collected mainly in the late 1960s and 1970s; in the Yohachiro Okamoto Mineral Collection housed at Kyushu University, Hakozaki, Fukuoka (Okamoto, 1944); and in specimens obtained in our field survey of the pegmatite since 2008.

Dark green namibite occurs in crusts of 0.1 mm in thickness associated with yellow clinobisvanite SEM observation indicates that crusts of Bi-minerals are mainly found along grain boundaries and on cleavage faces of lepidolite. The crusts are composed of fine-grained namibite intergrown with fine-grained clinobisvanite and waylandite. Euhedral, rhombohedral crystals of waylandite are also found in clinobisvanite and fine cookeite veins. On the two samples studied, these Bi-mineral aggregates are mostly associated with cookeite. The spherical namibite is made up of radiating aggregates of tabular or fibrous crystals of 10 to 20 μm in length. Hechtsbergite is found in fine-grained yellow crusts or aggregates of euhedral crystals. The crystals are also found in cookeite and range in size from 10 to 50 μm. Eulytite is also found with cookeite in this specimen. Quantitative chemical analyses of namibite and hechtsbergite were carried out using a JEOL JXA8530F electron-probe microanalyzer. The ZAF method was used for data correction. The water content was calculated according to stoichiometry. The empirical formula of namibite, calculated on the basis of O = 6.5 per formula unit in the anhydrous part, is $Cu_{0.98}Bi_{1.92}Al_{0.04}O_2$ $(V_{0.96}Si_{0.07}P_{0.02})O_4(OH)$, and is in good agreement with previously published namibite analyses (von Knorring and Sahama, 1981; Mrázek

et al., 1994). The empirical formula of hechtsbergite, calculated on the basis of O = 5.5 per formula unit in the anhydrous part, is $Bi_{1.94}Al_{0.01}O(V_{1.00}Si_{0.04})O_4(OH)$, which is also in good agreement with the original hechtsbergite data (Krause *et al.*, 1997). The Nagatare clinobisvanite has an end member composition.

X-ray powder diffraction (XRD) data were collected on crystal fragments using a Rigaku RINT RAPIDII curved imaging plate microdiffractometer. The original powder pattern of namibite had been indexed with a monoclinic unit cell. However, the crystal structure determination (Kolitsch and Giester, 2000) showed that the true symmetry is in fact triclinic. The unit-cell parameters from the original description were recalculated. The calculated unit-cell parameters for the present specimen, a = 6.216(4), b = 7.384(6), c = 7.467(6) Å, V = 308.1(3) Å^3, α = 90.19(8), β = 108.65(7), γ = 107.36(8)°,are slightly smaller than those of the original material from Namibia, a = 6.222(6), b = 7.401(9), c = 7.486(9) Å, α = 89.96(12), β = 108.94(10), γ = 107.38(11)°, V = 309.4(4) Å^3, whereas these values agree well with those of the Iron Monarch namibite, which has an ideal composition within detection limits of energy-dispersive spectroscopic chemical analyses (Kolitsch and Giester, 2000). The calculated unit-cell parameters for the present hechtsbergite specimen are a = 6.954(5), b = 7.539(8), c = 10.87(9) Å, β = 106.87(5) °, V = 545.4(6) Å^3. These values are in good agreement with those of the type specimen, a = 6.971(1), b = 7.535(1), c = 10.881(1) Å, β = 107.00(1) °, V = 546.6 Å^3.

The Nagatare Bi-minerals namibite, hechtsbergite, eulytite and waylandite, are closely associated with cookeite. This type of occurrence of namibite and hechtsbergite has not been reported in previous studies (e. g. von Knorring and Sahama, 1981; Krause *et al.*, 1997). Native bismuth in albite and quartz, bismuthinite in montebrasite, bismutotantalite and bismuthian microlite in lepidolite-quartz-albite-elbaite pegmatite were also identified in our study. All of these bismuth minerals are scarcely found, but they are characteristic components of the later hydrothermal stage in this highly evolved Li pegmatite.

References

Burns, P.C., Roberts, A.C., Stirling, J.A.R., Criddle, A.J. and Feinglos, M.N. (2000) Dukeite, $Bi^{3+}{}_{24}Cr^{6+}{}_{8}O_{57}(OH)_6(H_2O)_3$, a new mineral from Brejaúba, Minas Gerais, Brazil: Description and crystal structure. American Mineralogist, 85, 1822–1827.

Dunning, G.E. and Cooper, J.F.Jr. (1998) Namibite: a summary of world occurrences. Mineralogical Record, 29, 163–166.

Karakida, Y., Tomita, S., Shimoyama, S. and Chijiwa. K (1994) Geology of Fukuoka district. With Geological Sheet Map at 1 : 50,000. Geological Survey of Japan, pp192. (in Japanese with English abstract 7p).

Knorring, O. von and Sahama, T.G. (1981) Namibite, a new copper-bismuth-vanadium mineral from Namibia. Schweizerische Mineralogische und Petrographische Mitteilungen, 61, 7-12.

Ko, S. (1933) A pegmatite dyke, lepidolite and ceylonite from Nagatare, Fukuoka Prefecture, Japan. Warerano Koubutu (Present "Journal of Geoscience"), 2, 1-3 (In Japanese).

Kolitsch, U. and Giester, G. (2000) The crystal structure of namibite, $Cu(BiO)_2VO_4(OH)$, and revision of its symmetry. American Mineralogist, 85, 1298–1301.

Kolitsch, U., Blaß, U.G., Graf, H.-W. and Gröbner, J. (2004): Neufunde aus der Grube Clara im mittleren Schwarzwald. Lapis, 29, 18-23 (in German).

Krause, W., Bernhardt H.-J., Blaß, G., Effenberger, H. and Graf H.-W. (1997) Hechtsbergite, $Bi_2O(OH)(VO_4)$, a new mineral from the Black Forest, Germany. Neues Jahrbuch für Mineralogie Monatshefte, 271–287.

Mrázek, Z., Veselovský, F., Moravcováušek, J., Moravcová, H. & Ondruš, P. (1994) Redefinition of namibite, $Cu(BiO)_2VO_4OH$. Neues Jahrbuch für Mineralogie Monatshefte, 481-488.

Okamoto, Y. (1944) Minerals of Fukuoka Prefecture. pp.208, Present "Masutomi Museum of Geoscience", Kyoto, Japan (In Japanese).

Sejkora, J; Cejka, J; Hlousek, J, Novák, M. and Srein, V. (2004) Phosphowalpurgite, the (PO4)-dominant analogue of walpurgite, from Smrkovec, Slavkovsk Les Mountains, Czech Republic. Canadian Mineralogist, 42, 963-972.

Shibata, H. (1934) A lithium pegmatite from Nagatare, Imajyuku, Itoshima, Fukuoka Prefecture, Japan. Journal of the Geological Society of Japan, 41, 582-603 (In Japanese).

Shirose, Y. and Uehara, S. (2012) Chemical compositions of Li-tourmaline and mica from Nagatare, Fukuoka Prefecture, Japan. Abstract of the Annual Meeting of Japan Association of Mineralogical Siences. 38 (In Japanese).

A SINGLE-CRYSTAL NEUTRONS DIFFRACTION STUDY OF BRAZILIANITE, $NaAl_3(PO_4)_2(OH)_4$

P. Vignola[1], G. Gatta[1], M. Meven[2,3]

[1] Dipartimento di Scienze della Terra, Universita' di Milano, Via Botticelli 23, I-20133 Milano, Italy

[2] Institut für Kristallographie, RWTH Aachen, Jägerstrasse 17-19, 52056 Aachen, Germany

[3] Jülich Centre for Neutron Science – Outstation at FRM II, Lichtenbergstrasse 1, 85747 Garching, Germany

Brazilianite, ideally $NaAl_3(PO_4)_2(OH)_4$, typically forms equant to elongated monoclinic crystals with yellow to yellowish-green color. In Brazil many gem quality locations for brazilianite are known along the Rio Doce valley mainly in Minas Gerais. Brazilianite occurs as single-crystals or groups up to 20 cm growing in large pockets in the platy albite (cleavelandite) unit of zoned and complex granitic pegmatites. In granitic pegmatites brazilianite is considered a common product of alteration of montebrasite-amblygonite under Na-metasomatic conditions (Simmons *et al.* 2003). Thus far, only a few studies have been devoted to the crystal chemistry of brazilianite (Frondel and Lindberg 1948). Its crystal structure was solved by Gatehouse and Miskin (1974), on the basis of single-crystal X-ray diffraction data, in the space group $P2_1/n$, with a~11.23, b~10.14, c~7.10, and β~97.4° (Z = 4). Its structure consists of chains of edge-sharing Al-octahedra linked by P-tetrahedra forming a three-dimensional network, with Na atoms located in cavities parallel to [100]. In the structure model of Gatehouse and Miskin (1974), there are two different configurations of the Al-octahedra: *trans*-$AlO_4(OH)_2$ and *trans*-$AlO_3(OH)_3$.

The crystal structure of brazilianite has been reinvestigated by means of single-crystal X-ray and neutron diffraction. A prismatic, elongated, single-crystal of pale yellow, gem-quality brazilianite, up to18 mm in length and 5 mm in diameter, coming from the Telírio pegmatite, Linópolis, Divino das Laranjeiras district (Minas Gerais, Brazil), was used for diffraction experiments and chemical analysis. The brazilianite crystal was taken from a specimen constituted by 4 gem-quality crystals of brazilianite up to 20 mm perched on platy albite (sample of 3x3x2 cm of cleavelandite) and closely associated to zanazziite crystals up to 3 mm. The WDS electron-microprobe analysis shows that our sample of brazilianite from the Telírio claim is homogeneous and approaches an almost ideal composition with the following empirical formula: $(Na_{0.955}Mg_{0.003}Ca_{0.002}Sr_{0.002}K_{0.001})_{\sum 0.963}(Al_{3.007}Fe^{3+}_{0.002})_{\sum 3.009}(PO_4)_2(OH)_4$. The single-crystal X-ray and neutron structure refinement of this study confirm the general structure model of brazilianite described by Gatehouse and Miskin (1974). The building-block units of the brazilianite structure consist of chains of edge sharing *trans*-$AlO_4(OH)_2$ [*i.e.* around Al(2)] and *trans*-$AlO_3(OH)_3$ [*i.e.* about Al(1) and Al(3)] octahedra. The two chains are connected, via corner-sharing, by P-tetrahedra to form a three-dimensional framework, with Na atoms located in distorted cavities running along [100]. The Na-polyhedron, here described with a coordination number of 9 (with $Na\text{-}O_{max}$ ~ 3.11 Å), is strongly distorted. Gatehouse and Miskin (1974) suggested that the distortion of the Na-polyhedron might be due to the H sites in the [100]-cavity: the effect of mutual repulsion forces the Na site to one side of the cavity, leading to a stronger Na-O interaction with oxygen sites on one side of the cavity than on the other. This can now be confirmed by our neutron structure refinement, as Na – H(4) distance is ~3.06 Å, Na – H(3) is ~3.16 Å and Na – H(2) is ~3.21 Å, and H(4), H(3) and H(2) lie on the same side of the cavity. Both the X-ray and neutron structure refinements show that the Al-octahedra appear to be significantly distorted, with $\Delta[Al(1)\text{-}O]_{max}$ ~ 0.32 Å, $\Delta[Al(2)\text{-}O]_{max}$ ~ 0.31 Å, and $\Delta[Al(3)\text{-}O]_{max}$ ~ 0.17 Å (*i.e.* the difference between the longest and the shortest Al-O distances, based on the X-ray structure refinement). The longest Al-O bond distances are those with the bridging oxygen shared between two Al-octahedra and one P-tetrahedron. The shortest Al-O bond distances are those with oxygen of OH-groups. P-tetrahedra appear to be less distorted, as $\Delta[P(1)\text{-}O]_{max}$ ~ 0.044 Å and $\Delta[P(2)\text{-}O]_{max}$ ~ 0.036 Å (*i.e.* the difference between the longest and the shortest P-O distances, based on the X-ray structure refinement). The neutron structure refinement of this study provides an unambiguous location of the H-sites, allowing the description of the H-bonding scheme in brazilianite structure. Five independent H sites have been located, here labelled as H(1), H(2a), H(2b), H(3) and H(4). The configuration of the OH groups (*i.e.* O(1)–H(1), O(2)–H(2a), O(2)–H(2b), O(3)–H(3), O(4)–H(4)), along with the hydrogen bonding scheme, are now well defined (Fig. 1). O(1), O(2), O(3) and O(4) act as *donors*, whereas O(2), O(4), O(9) and O(12) as *acceptors*.

Symmetry-related O(2) act both as *donor* and as for "riding motion" (Busing and Levy 1964), range between ~0.992 and ~1.010 Å, the O···O distances between ~2.67 and ~2.93 Å, and the O–H···O angles between ~151 and ~174° (Table 5). The H(2a) and H(2b) are only ~1.37 Å apart. The neutron structure refinement was conducted without any restrain on the site occupancy factor (*s.o.f.*) of H(2a) and H(2b), leading to *s.o.f.* (H2a) = 0.546(6) and *s.o.f.* (H2b) = 0.446(6), respectively. We can thus consider a general *s.o.f.* of 50% of both H(2a) and H(2b), and so the two H-sites are mutually exclusive. Additional test refinements have been *acceptor* of H-bond. The O-H distances corrected performed in order to check if this H-site split reflects a lower symmetry than $P2_1/n$, but unsuccessfully. The key to understanding the split in two mutually exclusive H(2a) and H(2b) sites is in the H-bonding scheme of the structure. In fact, if only one "virtual" H(2) site occurs, located between H(2a) and H(2b), it should have an H-bond configuration energetically not favourable with O(2)-H(2)·O(9) ~ 113° and O(2)-H(2)···O(2) ~ 127°, whereas O(2)-H(2a)···O(9) ~ 151° and O(2)-H(2b)···O(2) ~171°.

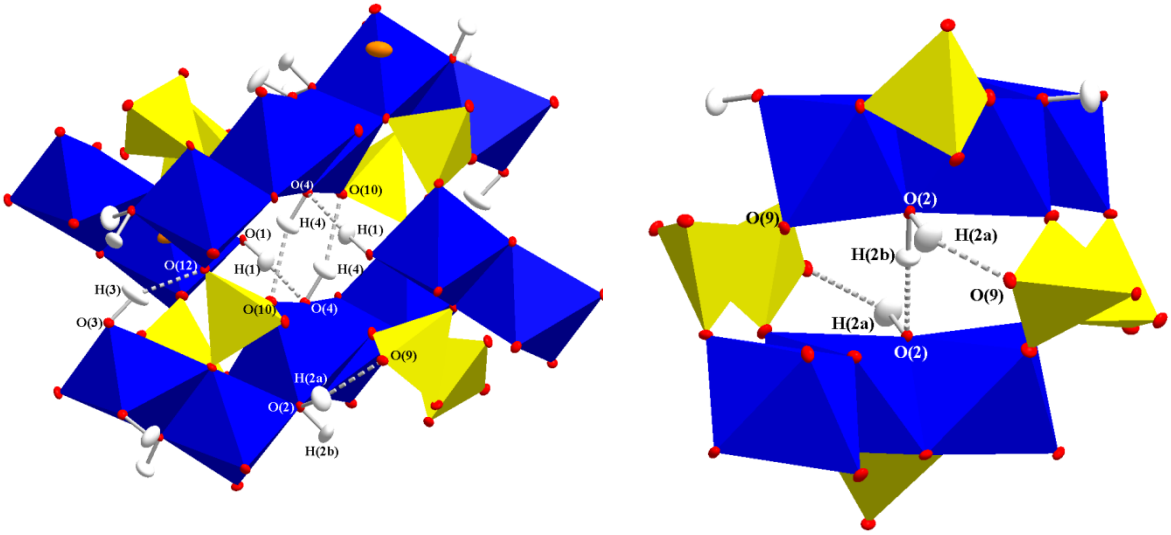

Fig. 1: Hydrogen site locations and, H-bonding scheme in the structure of brazilianite based on the neutron structure refinement of this study. The sites H2a and H2b are mutually exclusive. Thermal ellipsoid probability factor: 60%.

References*:*

Busing W.R., Levy H.A. (1964): The effect of thermal motion on the estimation of bond lengths from diffraction measurements. Acta Crystallographica, 17, 142-146.

Frondel, C., Lindberg, M.L. (1948) Second occurrence of brazilianite. American Mineralogist, 33, 135–141.

Gatehouse, B.M., Miskin, B.K. (1974): The crystal structure of brazilianite, $NaAl_3(PO_4)_2(OH)_4$. Acta Crystallographica, 30, 1311–1317.

Simmons, W.B., Webber, K.L., Falster, A.U. & Nizamoff J.W. (2003) Pegmatology: pegmatite mineralogy, petrology & petrogenesis. Rubellite Press, New Orleans.

HYDROXYL GROUPS AND H_2O MOLECULES IN PHOSPHATES: A NEUTRON DIFFRACTION STUDY OF EOSPHORITE, $MnAlPO_4(OH)_2 \cdot H_2O$

P. Vignola[1], G. Gatta[1], G. Nénert[2]
[1] Dipartimento di Scienze della Terra, Universita' degli Studi di Milano, Via Botticelli 23, I-20133 Milano, Italy
[2] Institut Laue-Langevin, BP 156, 38042 Grenoble Cedex 9, France

Minerals belonging to the eosphorite [$MnAl(PO_4)(OH)_2 \cdot H_2O$] - childrenite [$FeAl(PO_4)(OH)_2 \cdot H_2O$] series are widespread secondary phosphates occurring in medium to strongly evolved rare-element granitic pegmatites, ranging from the beryl to the petalite subtype in the classification of Černý and Ercit (2005). Eosphorite is a low-temperature metasomatic mineral in Lithium-Cesium-Tantalum (LCT) granitic pegmatites that frequently crystallizes in open cavities occurring in platy albite (cleavelandite) units of zoned pegmatitic dikes (Simmons *et al.* 2003). Eosphorite constitutes one of the low temperature products of alteration of primary phosphates, mainly lithiophilite or triplite. The unit-cell constants and the possible space groups of childrenite (*Bbam* or *Bba*2) were first reported by Barnes (1949). The crystal structure of childrenite was later solved by Giuseppetti and Tadini (1984) by means of X-ray single-crystal diffraction. The authors refined the crystal structure in the acentric space group *Bba*2, with a = 10.395(1), b = 13.394(1), and c = 6.918(1) Å (Z = 8). The crystal-structure of eosphorite was first solved by Hanson (1960) in the centric *Bbam* space group, with a = 10.52, b = 13.60, and c = 6.97 Å (Z = 8) using a sample from Newry, Maine and later reinvestigated by Hoyos *et al.* (1993) using a sample from Taquaral, Brazil, by means of X-ray single-crystal diffraction, in the *Cmca* space group, with a = 6.928(1), b = 10.445(1), and c = 13.501(2) Å [eosphorite composition: $(Mn_{0.76}Fe_{0.24})Al(PO_4)(OH)_2 \cdot H_2O$]. The crystal structure of both eosphorite and childrenite consists of chains parallel to the *a*-axis (in the *Cmca* space group) constituted by (Mn,Fe)-distorted octahedra, sharing opposite O-O edges, and chains of Al-octahedra. The two types of chains are connected, via corner-sharing, to form a set of (100) sheets held together by [PO_4] tetrahedra (and hydrogen bonds) to form a three-dimensional network.

The crystal structure of eosphorite has been reinvestigated by means of single-crystal neutron diffraction. A gemmy single-crystal of eosphorite up to 14 mm in length and 5 mm in diameter from a granitic pegmatite outcropping in the area of Chamachhu (Changmachhu), Skardu district, Baltistan, Pakistan, was used for the diffraction experiment and for the chemical analysis. The specimens from Chamachhu show eosphorite crystals perched on white platy albite (cleavelandite) or directly on pollucite or topaz crystals up to 20-30 cm contained in large miarolitic cavities. The mineralogical association of these pegmatites is fairly evolved and consists of muscovite, lepidolite, spessartine, gem elbaite, gem topaz, beryl (gem aquamarine and morganite), pollucite, tantalite-(Mn), fluorapatite, eosphorite, and väyrynenite. The WDS electron-microprobe analysis shows that our sample of eosphorite is homogeneous and approaches an almost ideal composition with the following empirical formula: $(Mn^{2+}_{0.95}Fe^{2+}_{0.02}Al_{0.10})_{\Sigma 1.07}\ AlPO_4(OH_{1.93}F_{0.07})_2 \cdot H_2O$. Our single-crystal neutron structure refinement, based on diffraction data collected at 20 K, provides a general structural model in agreement with the one reported by Hoyos *et al.* (1993). The building block units of the eosphorite structure consists of chains of (Mn,Fe)-octahedra (sharing opposite O-O edges) running along the *a*-axis, and chains of Al-octahedra. The two types of chains are connected, via corner-sharing, to form a set of (100) sheets held together by P-tetrahedra (and hydrogen bonds) to form a three-dimensional framework. Distorted channels, confined by 6-membered ring of polyhedra, run along [100]. The (Mn,Fe)-octahedron is significantly distorted, with $\Delta(O\text{-}O)_{max}$ ~ 0.81 Å, as the O-O distance of the shared edge is significantly shorter than the non-shared ones. We cannot exclude that this effect is due to the cation-cation repulsion, as $M\text{-}M$ ~ 3.46 Å. The Al-octahedron and the P-tetrahedron appear to be less distorted, with $\Delta(O\text{-}O)_{max}$ ~ 0.15 Å and $\Delta(O\text{-}O)_{max}$ ~ 0.03 Å. The low-T structure refinement does not show any evidence of (Mn, Fe)-octahedral ordering, which should lead to a lowering of the symmetry. In addition, the principal root-mean-square components of the atomic displacement parameters do not show any pronounced displacement about the equilibrium position, compared with those of the other atomic sites, suggesting the absence of a local split. The Fe-content deduced on the basis of the structure refinement is 0.165 *a.p.f.u.* where the chemical

analysis shows a Fe-content of about 0.025 *a.p.f.u*. This difference can be ascribed to a multi-element population at the *M* site, in which Mn, Fe and Al might coexist. In fact, the EPMA-WDS data show an excess of Al, as often reported in other eosphorite analyses (*e.g.* samples from Black Mountain and Buckfield, Maine; Hurlbut 1950). The neutron structure refinement of this study allowed an unambiguous location of the H-sites along with the description of the H-bonding scheme in eosphorite structure. We can now describe the structure as made by (Mn, Fe) $O_4(OH, H_2O)_2$ and $AlO_2(OH)_2$ $(OH, H_2O)_2$ octahedra (Figure 1). The *O3* site is the OH^- group (*i.e. O3-H3*) oxygen, whereas *O4* is the oxygen of OH^- group (*i.e. O4-H1*) and H_2O molecules (*i.e. H2-O4-H1*). In particular, H_2O molecules have site occupancy of 50%, so that the two H_2O molecules generated by the mirror plane are mutually exclusive. In other words, the two equivalent *O4* sites generated by the mirror plane are respectively the oxygen of one OH group and one H_2O molecule, with a local breaking of the symmetry. Among the three independent Al-O bond distances of the $AlO_2(OH)_2(OH,H_2O)_2$ octahedron, the Al-OH bond distance (*i.e.* Al-O3) is the shortest and the Al-(OH,H_2O) distance (*i.e.* Al-O4) the longest. In the (Mn, Fe)$O_4(OH,H_2O)_2$ polyhedron, the *M*-$(OH,H_2O)_2$ bond distance (*i.e. M-O4*) is the longest. The geometry of the H_2O molecule and the OH group, along with the hydrogen bonding scheme in eosphorite, are now well defined. The *O4-H1* and *O4-H2* distances, corrected for "riding motion", are ~1.003 and ~1.071 Å, respectively, and two strong energetically favorable hydrogen bonds occur: *O4···O5* = 2.711(1) Å, *H1···O5* = 1.757(1) Å and *O4-H1···O5* = 161.9(1)°; *O4···O4* = 2.504(1) Å, *H2···O4* = 1.454(1) Å and *O4-H1···O4* = 170.9(1)° (Fig. 1). In other words, symmetry-related *O4* act as *donor* and as *acceptor* of the H-bond. The *H1-O4-H2* angle approaches the ideal value (*i.e.* 107.2(1). The OH-group shows: *O3-H3* distance, corrected for "riding motion", of ~ 0.995 Å, *O3···O1* = 2.836(1) Å, *H3···O1* = 1.930(1) Å and *O3-H3···O1* = 154.0(1)°. The *O1* site (*i.e.* the *acceptor* of the H bond of the *O3-H3* group) is *under-bonded*, as it is shared by two (Mn, Fe)- octahedra and one P-tetrahedron (Fig. 1). The anisotropic structure refinement shows that the principal root-mean-square components of the atomic displacements parameters of the *H3* site (belonging to the OH group) are larger in magnitude than those of the *H1* and *H2* sites.

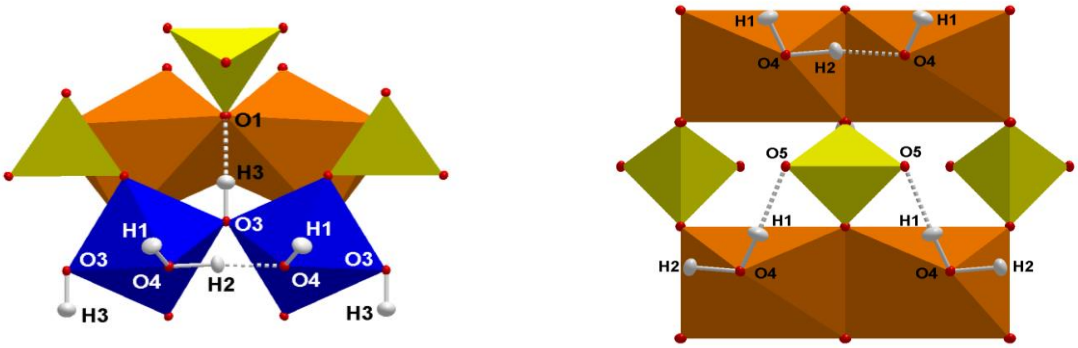

Fig. 1: Hydrogen location, configuration of OH groups and H_2O molecules, along with the H-bond scheme, in the structure of eosphorite. The occupancy factor of the H2 site is 50%.

References:

Barnes, W.H. (1949) The unit cell and space group of childrenite. American Mineralogist, 34, 12-18.

Černý, P. and Ercit, S. (2005): The classification of granitic pegmatites revisited. Canadian Mineralogist, 43, 2005-2026.

Giuseppetti, G., and Tadini, C. (1986) The crystal structure of childrenite from Tavistock (SW England), $Ch_{89}E0_{11}$ term of childrenite-eosphorite series. Neues Jahrbuch für Mineralogie Monatshefte, 263-271.

Hanson, A.W. (1960) The crystal ctructure of eosphorite. Acta Crystallographica, 13, 384-387.

Hoyos, M.A., Calderon, T., Vergara, I., and Garcia-Solé, J. (1993) New structure and spectroscopic data for eosphorite. Mineralogical Magazine, 57, 329-336.

Hurlbut, C. (1950) Childrenite-eosphorite series. American Mineralogist, 35, 793–805.

Simmons, W., Webber, K.L., Falster, A.U., and Nizamoff, J.W. (2003) Pegmatology – Pegmatite Mineralogy, Petrology and Petrogenesis. Rubellite Press, New Orleans, LA, 176pp.

KARENWEBBERITE, NA(FE^{2+},MN^{2+})PO_4, A NEW PHOSPHATE MINERAL SPECIES FROM THE MALPENSATA PEGMATITE, LECCO PROVINCE, ITALY

P. Vignola[1], F. Hatert[2], A-M Fransolet[2], O. Medenbach[3], V. Diella[1], S. Andò[4]

[1] CNR-Istituto per la dinamica dei processi ambientali, via Mario Bianco 9, 20131 Milano, Italy
[2] Laboratoire de Minéralogie, Dépt. de Géologie, Université de Liège, Bâtiment B18, Sart Tilman, B-4000 Liège, Belgium
[3] Institut für Geol., Mineral. une Geop., Ruhr-Universität Bochum, Universitätsstrasse 150, D-44780 Bochum, Germany
[4] Dipt. di Scienze Geologiche e Geotecnologie, Univ. di Milano-Bicocca- piazzale della Scienza 4, 20126Milano, Italy

The triphylite group is constituted by several Fe-Mn-bearing phosphates which are widespread in medium to highly evolved LCT granitic pegmatites, ranging from the beryl-columbite-phosphate subtype to the spodumene subtype, according to the classification of Černý and Ercit (2005). This group contains primary and weakly oxidized phosphates, for example: minerals of the triphylite – lithiophilite solid solution series [Li(Fe^{2+},Mn)PO_4 – Li(Mn,Fe^{2+})PO_4] and natrophilite [Na(Mn,Fe^{2+})PO_4], but the oxidation also frequently produces more oxidized phosphates such as ferrisicklerite-sicklerite [$\square_{1-x}Li_x(Fe^{3+},Mn^{2+})PO_4$ – $\square_{1-x}Li_x(Mn^{2+},Fe^{3+})PO_4$] or heterosite-purpurite [$\square(Fe^{3+},Mn^{3+})PO_4$ – $\square(Mn^{3+},Fe^{3+})PO_4$]. Triphylite hosted by Triassic pegmatites embedded into the crystalline basement of the central Southern Alps had been recently described at Brissago (Switzerland) and Piona (Italy) (Vignola *et al.* 2008a, Vignola *et al.* 2010, Vignola *et al.* 2011a). Here we report the description of a new Na-bearing mineral species belonging to the triphylite group (Table 1), karenwebberite, Na(Fe^{2+},Mn^{2+})PO_4 (IMA 2011-015, Vignola *et al.* 2011b; Vignola et al, 2013).

The mineral was found by one of the authors (P.V.) at the Malpensata granitic pegmatite, Colico commune, Lecco province, north Italy. The Malpensata dike, mined for ceramic feldspar and mica during 1943-1946, is located on the east side of the Piona peninsula, 1.2 km north of the Olgiasca village and 200 m south of the Piona Abbey, at an elevation of 110 m above sea level (46°, 07', 20'' N; 9°, 10', 33''E). The Malpensata dyke belongs to the Piona pegmatite swarm which is embedded into the high-grade metapelites (sillimanite-, biotite-bearing mica schists and gneisses) of the Dervio-Olgiasca Zone which constitute the crystalline basement of the Central Southern Alps (Bertotti *et al.* 1999). The dike is constituted by plagioclase ($An_{0.08}$) and quartz, with muscovite, schorl, and almandine-rich garnet as common accessories, and belongs to the beryl-columbite-phosphate sub-type of LCT granitic pegmatites referred to the classification of Černý and Ercit (2005). Karenwebberite rarely occurs in the central portion (the most evolved one) of the blocky plagioclase unit as thin lamellae embedded in graftonite constituting elliptical nodules up to 1 cm diameter. These nodules were found in close association with cassiterite, hafnian zircon, tapiolite-(Fe), oxycalciomicrolite, ferrowyllieite and other evolved phosphates (Vignola *et al.* 2008b, Vignola *et al.* 2010). Karenwebberite, Na(Fe^{2+},Mn^{2+})PO_4, belongs to the triphylite group and correspond to the Fe-equivalent of natrophillite or to the Na-equivalent of triphylite. It forms late stage magmatic exsolution lamellae up to 100μm thick, hosted in graftonite and associated with Na-bearing ferrisicklerite and with a heterosite-like phase. Lamellae are pale green, with very pale grayish-green streak. The luster is greasy to vitreous, and lamellae are translucent (pale green) to opaque (dark green). Optically, the mineral is anisotropic, biaxial (+), $\alpha = 1.701(2)$, $\beta = 1.708(2)$, $\gamma = 1.717(2)$ (for $\lambda = 589$ nm), $2V_{meas.} = 87(4)°$, $2V_{calc.} = 41°$, with Z parallel to the *b* axis. Pleochroism is medium with X = dark grey, Y = brown, and Z = yellow. The mineral is brittle with a Mohs hardness of 4.5; in thin section it displays a perfect cleavage along {001} with an irregular fracture. Karenwebberite is non-fluorescent either under short-wave or long-wave ultraviolet light, and its calculated density is 3.65 g/cm^3. The mean chemical composition, determined by the electron-microprobe from 16 point analyses (wt. %), is: P_2O_5 41.12, $Fe_2O_3^*$ 7.00, FeO^* 25.82, MgO 0.23, ZnO 0.11, MnO 9.31, CaO 0.10, Na_2O 14.66, total 98.41 (*: calculated values). The empirical formula, calculated on the basis of 1 P atom per formula unit from, is $(Na_{0.817}Ca_{0.003}\square_{0.180})_{\Sigma 1.000}$ $(Fe^{2+}_{0.622}Mn^{2+}_{0.228}Fe^{3+}_{0.151}Mg_{0.010}Zn_{0.002})_{\Sigma 1.013}PO_4$. Karenwebberite is orthorhombic, space group P*bnm*, $a = 4.882(1)$Å, $b = 10.387(2)$Å, $c = 6.091(1)$ Å, V = 308.9(1)$Å^3$, and Z = 4. The mineral, which shows the olivine structure, is characterized by two octahedral sites: M1 which is occupied by Na, and M2 which is occupied by Fe and Mn. The eight strongest lines in the X-ray powder pattern are [*d* in

Å (intensities estimated visually) (*hkl*)]: 5.16 (strong) (020), 4.44 (very strong) (110), 3.93 (very strong) (021), 3.56 (very strong) (120), 3.04 (strong) (002), 2.817 (very strong) (130), 2.559 (very strong) (131), and 1.657 (strong) (061). The mineral has been approved by the Commission on New Minerals and Mineral Names of the International Mineralogical Association under number IMA 2011-015 (Vignola *et al.*, 2011), and is named in honour of Dr. Karen Louise Webber, Assistant Professor Research at the Mineralogy, Petrology and Pegmatology Research Group, Department of Earth and Environmental Sciences, University of New Orleans, Louisiana, U.S.A.

Table 1. Comparison of the physical properties for phosphates of the triphylite group (Vignola et al 2013)

Mineral	Triphylite	Lithiophilite	Natrophilite	Karenwebberite
Ideal formula	$Li(Fe^{2+},Mn)PO_4$	$Li(Mn,Fe^{2+})PO_4$	$Na(Mn,Fe^{2+})PO_4$	$Na(Fe^{2+},Mn)PO_4$
Space group	*Pbnm*	*Pbnm*	*Pbnm*	*Pbnm*
a (Å)	4.6904(6)	4.7383(1)	4.987(2)	4.882(1)
b (Å)	10.2855(9)	10.429(1)	10.523(5)	10.387(2)
c (Å)	5.9871(4)	6.0923(4)	6.312(3)	6.091(1)
Z	4	4	4	4
Strong X-ray	5.175 (34)	5.236 (28)	5.24 (30)	5.16 (25)
lines	4.277 (76)	4.313 (56)	4.50 (60)	4.44 (48)
	-	-	4.05 (60)	-
	3.923 (26)	-	3.90 (30)	3.93 (37)
	-	-	3.66 (50)	3.79 (8)
	3.487 (70)	3.516 (71)	3.61 (10)	3.56 (86)
	3.008 (100)	3.051 (89)	3.15 (50)	3.04 (52)
	-		2.863 (80)	-
	2.781 (34)	-	-	2.817 (57)
	-	-	2.702 (20)	-
	-	-	2.604 (100)	-
	2.525 (81)	2.548 (100)	2.583 (100)	2.559 (100)
	-	2.492 (28)	2.487 (30)	-
Cleavage	{001} perfect, {010} imperfect	{001} perfect, {010} good	{001} good, {010} indistinct, {120} interrupted	{001} perfect
Density	3.54(4)	3.47(3)	3.41; 3.47 (calc.)	3.65 (calc.)
Optical sign	B(+)	B(+)	B(+)	B(+)
2V (°)	0-55	48-70	75(5)	87(4)
α	1.675-1.694	1.663-1.696	1.671(3)	1.701(2)
β	1.684-1.695	1.667-1.700	1.674(3)	1.708(2)
γ	1.685-1.700	1.674-1.702	1.684(3)	1.717(2)
Hardness	4-5	4-5	4.5-5	4.5(5)
Colour	Bluish grey to greenish grey	Yellowish brown, honey-yellow, grey	Deep wine-yellow	Pale green; brownish when oxidized

References:

Bertotti G., Seward D., Wijbrans J., ter Voorde M. and Hurford A.J. (1999) Crustal thermal regime prior to, during, and after rifting: A geochronological and modeling study of the Mesozoic South Alpine rifted margin. Tectonics, 18/2, 185-200.

Černý, P.and Ercit S. (2005) The classification of granitic pegmatites revisited. Canadian Mineralogist, 43, 2005-2026.

Vignola, P., Diella, V., Oppizzi, P., Tiepolo, M., and Weiss, S. (2008a) Phosphate assemblages from the Brissago granitic pegmatite, western Southern Alps, Switzerland. Canadian Mineralogist, 46, 635-650.

Vignola, P., Guastoni, A., and Diella, V. (2008b) Nb Ta Sn oxides association from the Malpensata granitic pegmatite, central Southern Apls (Lecco province, Italy): magmatic differentiation, crystallization mechanism and geochemical inference. Geophysical Research Abstracts, EGU2008-A-03866.

Vignola, P., Hatert, F., Fransolet, A.M., and Diella, V. (2010) The Na-rich phosphate minerals from

Malpensata granitic pegmatite, Piona, Lecco province, Italy. Acta Mineralogica Petrographica, abstract series, 6, 609.

Vignola, P., Fransolet, A.M., Diella, V., and Ferrari, E.S. (2011a) Complex mechanisms of alteration in a graftonite + sarcopside + triphylite association from the Luna pegmatite, Piona, Lecco province, Italy. Canadian Mineralogist, 49, 765-776.

Vignola, P., Hatert, F., Fransolet, A.-M., Medenbach, O., Diella, V, and Ando', S. (2011b) Karenwebberite, IMA 2011-015. CNMNC Newsletter No. 10, October 2011, page 2551; Mineralogical Magazine, 75, 2549-2561.

Vignola, P., Hatert, F., Fransolet, A.-M., Medenbach, O., Diella, V, and Ando', S. (2013)

Karenwebberite, $Na(Fe^{2+},Mn^{2+})PO_4$, a new member of the triphylite group from the Malpensata pegmatite, Lecco Province, Italy. American Mineralogist, 98, 767-772.

CRYSTAL-CHEMISTRY OF A NEAR END-MEMBER TRIPLITE, $Mn^{2+}_2(PO_4)F$, FROM CODERA VALLEY (SONDRIO PROVINCE, CENTRAL ALPS, ITALY)

P. Vignola[1], G. Gatta[2], F. Hatert[3], A. Guastoni[4], D. Bersani[5]

[1] CNR, Istituto per la dinamica dei processi ambientali, via Mario Bianco 9, 20131 Milano, Italy
[2] Dipartimento di Scienze della Terra, Università degli Studi di Milano, via Botticelli 23,20133 Milano, Italy
[3] Laboratoire de Minéralogie, Dépt de Géologie, Université de Liège, Bâtiment B18,Sart Tilman, B-4000 Liège, Belgium.
[4] Dipartimento di Mineralogia e Petrologia, Università di Padova, Corso Garibaldi 3735137 Padova, Italy
[5] Dipartimento di Fisica, Università di Parma, Viale G.P. Usberti 7/a, 43124 Parma, Italy

Phosphate minerals of the solid solution series triplite-zwieselite-magnotriplite, respectively $Mn^{2+}_2(PO_4)F$, $Fe^{2+}_2(PO_4)F$ and $(Mg,Fe^{2+},Mn^{2+},Ca)_2(PO)_4F$, are primary phosphates commonly found in complex granitic pegmatites. These phosphates usually occur in fluorine-rich Lithium-Cesium-Tantalum (LCT)-type dikes, even as gigantic masses up to 4 meters in diameter (Simmons *et al.* 2003). Triplite was discovered more than two centuries ago by Vauquelin (1802) at Limoges, Chanteloube, Haute-Vienne, France and described as "phosphate natif de fer mélangé de manganèse". Some years later, Hausmann (1813) named "triplite" this new phosphate mineral. In the following two centuries, occurrences of phosphate minerals belonging to the triplite-zwieselite-magnotriplite and triplite-triploidite solid solutions were described in a significantly high number of granitic pegmatites (among the most famous: Stoneham and Auburn, Maine; Branchville, Connecticut; 7U7 Ranch and Mt Loma, Arizona; Mica Lode and School Section, Colorado; San Luis and Salado, Argentina; Varuträsk, Sweden; Zwiesel and Hagendorf, Germany; Fregeneda and Cañada, Spain; Mangualde, Portugal; Alto do Ligonha, Mozambique; Tsaobismund and Okatjimukuju, Namibia; Olary Block, South Australia). Chemical analyses of triplite summarized in the paper of Heinrich (1951), along with those reported by other authors, show rather variable Mn:Fe:Mg ratios with different compositions belonging to the solid solution triplite-zwieselite-magnotriplite. Particularly interesting is the F/OH-substitution, which appears to have a rather continuous variation in the solid-solution triplite-triploidite (Figure 1).

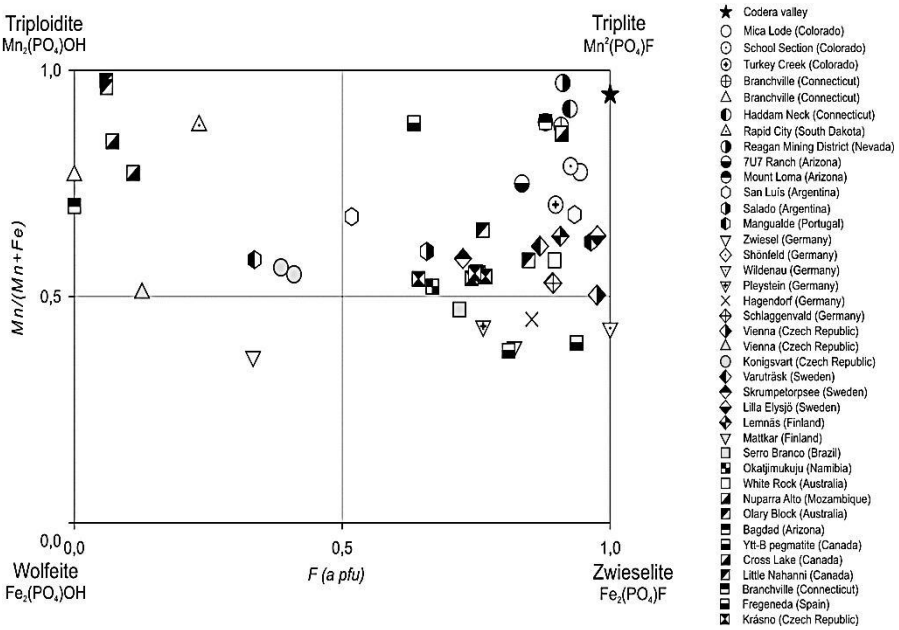

Fig. 1: Diagram F versus Mn/(Mn+Fe) representing the chemical compositions of triplite, triploidite, wolfeite and zwieselite found in the literature and based on our experimental findings.

The crystal structure of this primary phosphate was first solved by Waldrop (1969) on a sample from Mica Lode, Freemont County, Colorado. The chemical composition of such a sample was previously reported by Heinrich (1951): $(Mn_{0.95},Fe_{0.27},Mg_{0.69},Ca_{0.08})_{\Sigma 1.99}(PO_4)(F_{0.91},OH_{0.03})_{\Sigma 0.94}$

The crystal structure of triplite was refined by Waldrop in the space group *I*2/*a* with the following unit-cell constants: *a*=12.065(1), *b*=6.454(1), *c*=9.937(1) Å and β=107.093(6) °. The structure is composed by isolated PO_4 tetrahedra joined on the vertices to distorted MO_4F_2 octahedra. The octahedra M(1) and M(2) are linked into chains by shared edges. The chains of M(1) octahedra are parallel to [010], those of M(2) parallel to [100]. According to the structure model of Waldrop (1969), fluorine is distributed between two mutually exclusive sites, with partial site occupancy, only ~0.62 Å apart. Waldrop (1969) reported that, in the sample from Mica Lode, Mn and Fe appear to be disordered in the two octahedral sites.

During a field survey in Codera valley (Novate Mezzola, Sondrio province, northern Italy), one of the authors (A.G.) found some masses of triplite up to 5 mm, hosted in a granitic pegmatite dike, and in close association with fluorapatite, Mn-rich elbaite and Mn-oxides. In thin section, triplite occurs in rounded masses deeply fractured; fractures are sharp and filled by Mn oxides. Under polarized light, the mineral is colorless, pleochroism is absent, and no evidence of alteration was detected. Triplite from Codera valley is biaxial (+) with a very high relief and anomalous interference colors up to first-order red. Tiny grains of fluorapatite occur inside the triplite masses, mainly located along fractures. Phosphate masses, hosted by feldspar, are rimmed by poly-granular quartz and albite lamellae. Electron-microprobe chemical analyses in wavelength dispersive mode revealed a composition very close to the end-member, and with the following empirical formula $(Mn^{2+}_{1.75}Fe^{2+}_{0.10}Ca_{0.10}Mg_{0.01})_{\Sigma 1.96}(PO_4)F_{1.00}$. The almost total absence of OH^- is confirmed by Raman spectroscopy. The presence of a very small Raman band ascribable to the OH^- stretching modes, at 3498 cm^{-1}, is visible only when using the 473.1 nm laser line (the most sensitive one to OH^- groups). This weak OH band is also visible at 3485 cm^{-1} on the infrared spectrum of triplite from Codera. The single-crystal structure refinement confirms the general model previously described by Waldrop (1969) for a natural triplite and by Rea & Kostiner (1972) for a synthetic $Mn_2(PO_4)F$ compound. The main difference with the structure model reported by Waldrop (1969) concerns the F site. Our data led to one independent F site with full site occupancy, whereas Waldrop (1969) reported two mutually exclusive F sites with partial site occupancy, being only ~0.62 Å apart, with unusually high anisotropic displacement parameters if compared to the other O sites. In her comparative study of the crystal structure of triplite and triploidite (i.e. $(Mn,Fe)_2PO_4(OH)$), Waldrop (1970) considered the analogy of the split of the F site in two subsites in triplite (mutually exclusive) and that of the OH^- sites in triploidite. However, in the latter, the split leads to an ordered distribution with distinct OH^- sites with full occupancy and a doubling of the cell volume (*a* = 12.366, *b* = 13.276, *c* = 9.943 Å, β = 108.23°, space group $P2_1/a$). Such a configuration appears to be ascribable to the proton-metal repulsion. Despite Waldrop (1970) not considering the possibility of a solid solution along the triplite-triploidite join, as the different F/OH environments make the structure non-isotypic, the chemical composition of triplites and triploidites reported in the literature appear to show a potential F/OH substitution. Likely, the structure of triplite can preserve its metrics and symmetry (i.e. *a* = 12.109 , *b* = 6.516 , *c* = 10.117 Å, β = 106.16°, space group *I*2/*a*) even with a modest F/OH substitution. Such a behaviour was observed in several F/OH-bearing minerals, in which the end-members of the solid solution have different symmetry [e.g. topaz: $Al_2SiO_4(F,OH)_2$]. The chemical analysis of the sample of triplite used by Waldrop (1969) was performed by Henrich (1951), and appeared to contain only a modest amount of hydroxyl [i.e. $(Mn_{0.95},Fe_{0.27},Mg_{0.69},Ca_{0.08})_{\Sigma 1.99}(PO_4)(F_{0.91},OH_{0.03})_{\Sigma 0.94}$]. In their structure refinement of the synthetic $Mn_2F(PO_4)$ compound, Rea and Kostiner (1972) found only one F site, according to our experimental findings.

References:

Hausmann, J.F.L. (1813) Handbuch der Mineralogie. 1st edition, 3 volumes, Göttingen, 3, 1079.

Heinrich, E.W. (1951) Mineralogy of triplite. American Mineralogist, 36, 256-271.

Rea, J.R. and Kostiner, E. (1972) The crystal structure of manganese fluorophosphates, $Mn_2(PO_4)F$. Acta Crystallographica, B28, 2525-2529.

Simmons, W.B., Webber, K.L., Falster, A.U. & Nizamoff J.W. (2003) Pegmatology: pegmatite mineralogy, petrology & petrogenesis. Rubellite Press, New Orleans.

Vauquelin, L.N. (1802) Phosphate natif de fer melangé de manganèse. Journal des Mines, 11, 295.

Waldrop, L. (1969) The crystal structure of triplite, $(Mn,Fe)_2FPO_4$. Zeitschrift für Kristallographie, 130, 1-14.

Waldrop, L. (1970) The crystal structure of triploidite and its relation to the structures of other minerals of the triplite-triploidite group. Zeitschrift für Kristallographie, 131, 1-20.

HISTORY OF MOUNT MICA

K. Webber[1], W. Simmons[1], A. Falster[1], R. Sprague[2], G. Freeman[3], F. Perham[4]
[1]Dept of Earth & Environmental Sci., University of New Orleans, New Orleans, LA 70148, kwebber@uno.edu
[2]10 Yates Street, Mechanic Falls, ME 04256
[2]Coromoto Minerals, 48 Lovejoy Road, Paris, ME 04271
[4] 1 Dunham Road, West Paris, ME 04289

Maine's many pegmatite quarries have long been important as commercial sources of industrial minerals, gemstock, and specimens of interest to scientists and collectors. None is more famous than Mount Mica, America's first gem pegmatite (Hamlin, 1895) located just east of Paris, Maine. The discovery of gem quality elbaite tourmaline at Mount Mica dates to 1820 when Elijah L. Hamlin and Ezekiel Holmes discovered a gemmy green crystal at the base of an uprooted tree near an outcropping ledge (Hamlin, 1873, 1895; Francis, 1985; Perham, 1987; King, 2000).

After the specimen was identified as tourmaline, many more crystals were recovered from the ledge by Hamlin and Holmes as well as others in the community. Two years after the initial discovery, Elijah's younger brothers, Cyrus and Hannibal, undertook a more thorough exploration of the ledge by drilling and blasting. They exposed a pocket filled with red and green tourmaline crystals up to 8 cm in length (Hamlin, 1873). Small-scale exploration continued on the ledge by a number of different people, including Samuel R. Carter who mined unsuccessfully in 1864. Two years later, O. M. Bowker, owner of the farm on which the Mount Mica pegmatite was located, discovered a large tourmaline pocket. Bowker's find encouraged Augustus Hamlin and his father, Elijah, to begin work at Mount Mica that continued from 1868 until 1890. Numerous fine specimens of tourmaline and other pegmatite minerals were discovered. In 1871 Hamlin blasted open a large pocket and discovered several large achroite crystals, including one that was more than 11 cm in length (Hamlin, 1895).

Many additional pockets discovered shortly after this find produced fine gem material, including beautiful multicolored crystals with a dark blue base, followed by a pink zone that grades into colorless, with a grass-green termination. In 1881 the Mount Mica Tin and Mica Company was formed with Augustus Hamlin and Samuel Carter as president and superintendent, respectively. They operated Mount Mica until 1890 (Hamlin, 1895).

In 1882 some of the best crystals from the Hamlin and Carter collections were publicly displayed for the first time at a special exhibition at the Academy Hall in Paris Hill, ME. In 1886 Hamlin and Carter opened Mount Mica's largest pocket at that time. It produced many tourmaline crystals in a cookeite and lepidolite matrix. The most valuable specimen was a spectacular green tourmaline crystal 24 cm long and 5 cm wide that was recovered in four pieces. At the time it was valued at $1,000. A faceted portion of this crystal provided the 34.2-carat center stone for the famous Hamlin Necklace (Perham, 1987) which was later donated to Harvard University.

From 1890 until 1913, Loren B. Merrill and L. Kimball Stone had the mining rights to Mount Mica. In 1891 they opened a pocket with exceptional blue tourmalines (Hamlin, 1895). According to Hamlin's records, by May 1895, Merrill and Stone had opened fifty-nine pockets and had extensive mine workings (Figs. 1-4). In 1899 they uncovered a pocket that yielded a 411-carat, flawless blue-green tourmaline nodule that was part of a crystal more than 20 cm long. A second 584-carat gem nodule found in a later pocket was sold to Harvard Professor Charles Palache and is now in the Harvard Mineralogical Museum collection (Francis, 1985). In 1904 Merrill and Stone opened yet another very large pocket that produced more than 34 kilograms of tourmaline crystals, including achroite nodules and a single polychrome tourmaline crystal that weighed more than 13 kilograms and was 35 cm tall and over 15 cm wide This remarkable crystal was sold and disappeared until rediscovered in a home on Beacon Hill in Boston by Benjamin Shaub in 1961(Perham, 1987). It is now in the Harvard collection.

Tourmaline mining in Maine began to decline after about 1910, in part because of competition from important new discoveries of high-quality tourmaline in San Diego County, California, and in part because of the collapse of the Chinese tourmaline market. After about 1920, tourmaline production was sporadic at best. Mount Mica was purchased by Howard Irish in 1926 but remained inactive until he began mining feldspar in the late 1940s. Consequently, Mount Mica was not included in the World War II era study of pegmatites by the

U.S. Geological Survey, and a description of this historic pegmatite is conspicuously missing from Pegmatite Investigations 1942-45 New England (Cameron *et al*., 1954).

Frank Perham leased Mount Mica in 1964 and mined in the old Merrill and Stone tourmaline diggings. He produced some bicolored tourmaline, including a crystal that cut a 25-carat flawless green stone and a gem nodule that produced a 59.59-carat flawless blue-green stone.

Mount Mica was purchased by Plumbago Mining Corporation in 1973, with the operation headed by Frank Perham. Later, Rene Dagenais ran the operation, and in 1974 he discovered the 4 x 5.5 x 16-meter "Dagenais" pocket that required two months to excavate (Francis, 1985) but unfortunately was devoid of gem material. In 1989 Plumbago and private investors reopened Mount Mica as the Mount Mica Land Company, with Phil McCrillis as the operator. Although tourmaline was sporadically produced, the results were not economically viable, and mining ceased in 1997.

Coromoto Minerals, LLC acquired the Mount Mica property in 2003. Coromoto's plan to systematically mine the entire pegmatite has proven to be highly successful. Mount Mica continues to be a prolific pocket producer (Fig. 5). Pockets occur along the core zone, and some large pockets are associated with local bulges in the pegmatite. However, it should be noted that the mining history at Mount Mica has shown little or no relationship between pocket dimensions and the size or quality of tourmaline found. Some of the largest pockets found (the 1905 2.4 x 1.5 x 1 m. pocket and the 1907 2 x 6 x 3.7 m. pocket) were void of tourmaline. In addition to gem tourmaline, Mount Mica has also produced pockets with a number of other minerals including beryl, apatite, lepidolite, rose and smoky quartz, hydroxylherderite, and pollucite.

References

Cameron, E. N., R. H. Jahns, A. H. McNair, L. R. Page, G. W. Stewart and V. E. Shainin, 1954. Pegmatite Investigation, 1942-1945, New England. U.S.G.S. Prof Paper 255.

Francis, C. A. (1985). Maine tourmaline. Min Rec 16, 365-388

Hamlin A.C. (1873) *The Tourmaline*. James R. Osgood & Co., Boston, MA, 107 pp., republished in 2004 by Rubellite Press, New Orleans, LA.

Hamlin A.C. (1895) *The History of Mount Mica of Maine, U. S. A. and its Wonderful Deposits of Matchless Tourmalines*. Publ. by A.C. Hamlin, 72 pp. plus color plates, republished in 2004 by Rubellite Press, New Orleans, LA.

King V.T., Ed. (2000) *Mineralogy of Maine, Vol. 2: Mining History, Gems, and Geology*. Maine Geological Survey, Augusta, ME, 524 pp.

Perham, J. C. (1987) *Maine's Treasure Chest: Gems and Minerals of Oxford County*, second edition: Quicksilver Publications, West Paris, 267 p.

Fig. 1: Postcard of Mt. Mica ca. 1900.

Fig. 2: Tourmaline Crystal from Hamlin (1873)

Fig. 3: Sticks marking tourmaline pockets ca. 1900

Fig. 4: Merrill Pocket 1907.

Fig. 5: Coromoto Minerals Pocket 2012.

THE DISCRIMINATION OF LCT AND NYF GRANITIC PEGMATITES USING MINERAL CHEMISTRY: A PILOT STUDY

M. Wise
Department of Mineral Sciences, National Museum of Natural History, Smithsonian Institution, Washington, DC, USA; wisem@si.edu

The currently accepted classification scheme for granitic pegmatites is largely modeled on the depth-zone classification of granitic rocks and utilizes depth of emplacement, metamorphic grade, mineralogy and minor to trace element chemistry as the basis for differentiating pegmatites of different categories (Černý and Ercit, 2005). The LCT and NYF designation of granite-pegmatite systems, originally proposed by Černý (1991), was intended to relate granitic pegmatites of similar geochemical affinities to specific types of granites that ultimately generate them. Inherent in the LCT-NYF categorization is an underlying petrogenetic aspect which attempts to associate granite-pegmatite systems to tectonic settings. In general, it is believed that LCT granite-pegmatite systems are related to S-type granites found in orogenic settings, whereas NYF granite-pegmatite systems are derived from late- to post-tectonic to anorogenic A-type granites. As attractive as this simplistic view appears, the simple fact is that all too frequently the tectonic setting of the parent granite (if at all identified) is not always known. Astute observations of the accessory mineralogy of the pegmatites can provide some insight into the LCT or NYF geochemical nature of the granite-pegmatite system (e.g., amazonitic microcline as characteristic of NYF pegmatites), but there are also examples where the situation is ambiguous (e.g., aquamarine occurring in both LCT & NYF pegmatites). In an attempt to better understand the relationship between granite type, tectonic setting and pegmatite genesis, this study examines the use of mineral chemistry in discriminating between pegmatites of LCT and NYF affiliation. The proposed discrimination scheme is applied only to pegmatites of the rare-element and miarolitic classes and is based on the major, minor and trace element chemistry of K-feldspar, biotite, topaz and beryl.

Reasonably good discrimination between LCT and NYF affiliated pegmatites can be obtained using the Ga concentrations of K-feldspar. Gallium contents in K-feldspars from NYF pegmatites commonly fall between 20 and 100 ppm. By comparison, K-feldspar from LCT pegmatites, typically contain Ga contents between 10 and 40 ppm with only the most evolved pegmatites (e.g., Tanco) having as much as 100 ppm. A plot of K/Rb versus Ga has proven to be useful in distinguishing K-feldspar between LCT and NYF pegmatites despite showing considerable scatter in the overall data. Plotted in the ternary diagram Al_2O_3-MgO-total FeO, biotite from NYF pegmatites appear to separate into two distinct groups from the LCT pegmatites. Biotite from the NYF groups have been identified as those that are related to A-type granites (designated here as NYF-A) and a second group apparently affiliated with I-type granites (NYF-I). Although biotite from both NYF and LCT pegmatites may have similar Fe concentrations, biotite from LCT pegmatites generally have higher Al and Mg contents than the NYF-I and NYF-A group, respectively. The distinction between topaz from LCT and NYF pegmatites corresponds closely to differences in their F content and the *b* unit-cell dimension. The relationship between Na and Al in beryl provides the best discrimination for NYF and LCT pegmatites. Although beryl from both geochemical families may show similar ranges in Al concentrations, NYF beryl generally have lower concentrations of Na compared to LCT beryls. In consideration of the four minerals examined in this pilot study, it is suggested that the chemical composition of major and/or accessory minerals have great potential for clarifying the petrogenetic classification of granitic pegmatites.

References:

Černý, P. (1991): Fertile granites of Precambrian rare-element pegmatite fields: is geochemistry controlled by tectonic setting or source lithologies? Precambrian Research, vol. 51, 429-468.

Černý, P., Ercit, T.S. (2005): The classification of granitic pegmatites revisited. Canadian Mineralogist, vol. 43, 2005-2026.

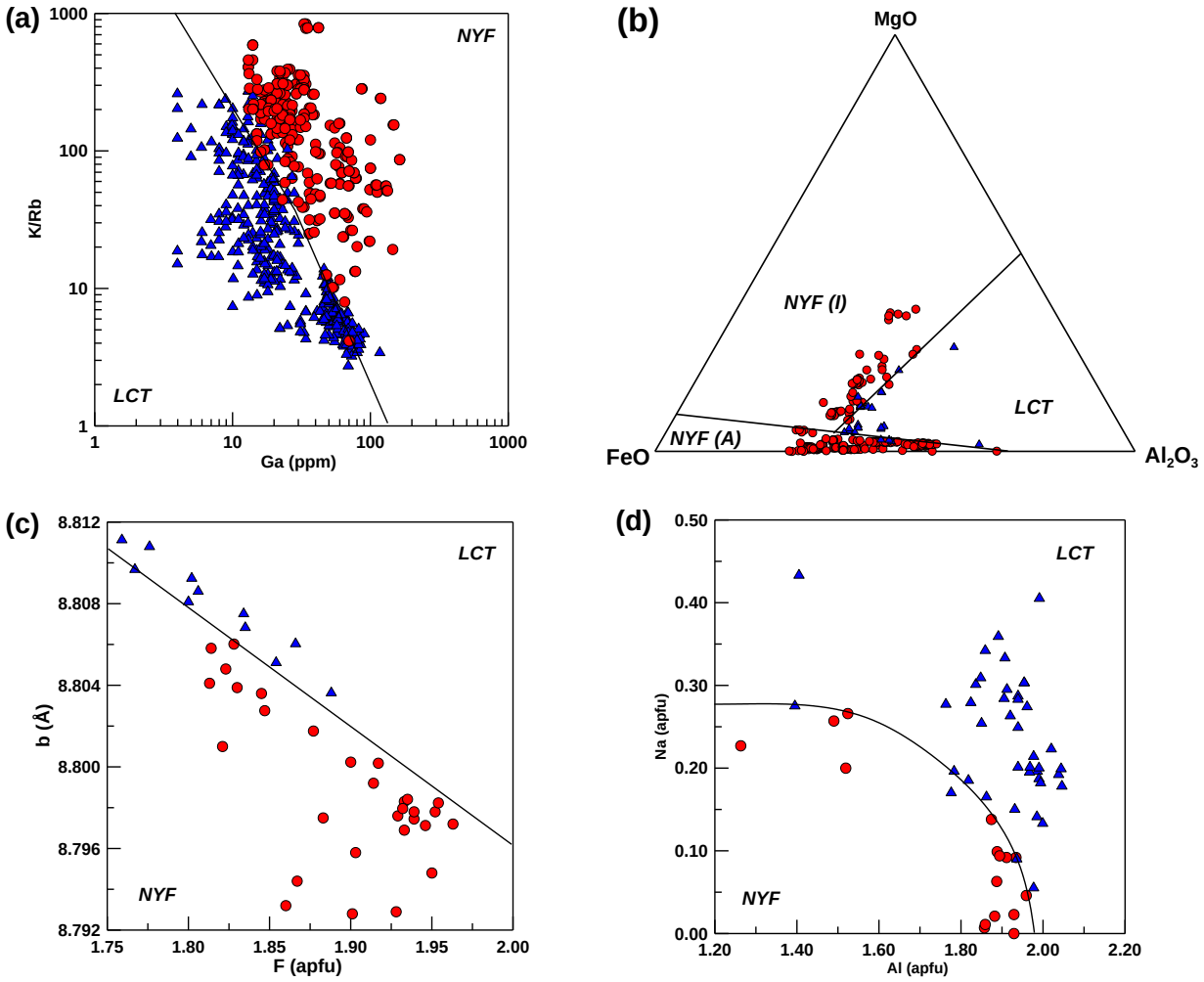

Fig. 1: Discrimination diagrams for LCT and NYF-family granitic pegmatites. (a) K/Rb-Ga plot for K-feldspar, (b) Al_2O_3-MgO-FeO ternary diagram for biotite, (c) F vs. *b* unit cell parameter plot for topaz, (d) Al-Na plot for beryl.

THE COMPOSITION OF GAHNITE AS INDICATOR OF RARE METAL (LI) MINERALIZATION IN GRANITIC PEGMATITES

J. Yonts[1], A. Heimann[1], J. Bitner[1], M. Wise[2], D. Soares[3], A. Ferreira[3]

[1] Department of Geological Sciences, East Carolina University, 101 Graham Building, Greenville, NC 27858, yontsj12@students.ecu.edu

[2] Department of Mineral Sciences, Smithsonian Institution, P.O. Box 37012, Washington, DC 20013-7012

[3] Instituto Federal de Educação, Ciência e Tecnologia da Paraíba (IFPB), Tranquilino Coelho Lemos 671, Campina Grande-Paraíba, 58100–000, Brazil

Gahnite (ZnAl2O4), the zinc end-member of the spinel series [(Zn,Fe,Mg)Al2O4], is commonly found as an accessory mineral in aluminous metasedimentary rocks, metabauxites, skarns, marbles, metamorphosed sulfide deposits, quartz veins, granites, and granitic pegmatites (Spry and Scott 1986, Heimann *et al.* 2005). The chemical composition of gahnite has been extensively investigated in massive sulfide deposits and its major element composition is used as an indicator of mineralization (e.g., Spry and Scott 1986). In spite of this, gahnite compositions in granitic pegmatites are very scarce. Batchelor and Kinnaird (1984) suggested that the composition of gahnite in granitic pegmatites could present information about the degree of evolution and/or fractionation of these rocks. The degree of evolution of the pegmatite can be inferred by the magnitude of the Zn/Fe ratio in gahnite, which increases with the degree of evolution (Batchelor and Kinnaird 1984; Soares *et al.* 2007). Here, we present the results of a study aimed at determining if the composition of gahnite can be used to distinguish Li-rich from Li-poor pegmatites, as well as LCT (lithium, cesium, tantalum) from NYF (niobium, yttrium, fluorine) pegmatites (e.g., Černý and Ercit 2005). The major element compositions of gahnite in granitic pegmatites from Maine (Greenlaw, Pulsifer and Lord Hill pegmatites), Maryland (Ben Murphy Mica Mine), North Carolina (Siskoe Ridge pegmatite), Borborema Pegmatite Province, Brazil (BPP; Alto Mirador, Capoeira 2, Boqueirao, Carrascao, and Quintos pegmatites), Eastern Brazil Pegmatite Province, Poland (Strzegom-Sobótka pegmatite), and Argentina (La Magdalena, Sin Nombre, Nancy, La Ona, Blanco Dora, and Juan Roman pegmatites) were investigated. Gahnite compositions from these study sites, expressed and plotted in a ternary diagram in terms of mol % hercynite (Hc), gahnite (Ghn), and spinel (Spl) end members (Fig. 1), fall within the igneous pegmatite field (Batchelor and Kinnaird 1984; Spry *et al.* 1986; Heimann *et al.* 2005). The range of these compositions can be defined by: Hc0.0-27.0Ghn72.1-98.5Spl0.0-4.7. Gahnite compositions in the Strzegom-Sobótka NYF pegmatite provide evidence for the lowest degree of evolution of all the LCT and NYF pegmatites studied, whereas those from the BPP LCT pegmatites indicate the highest degree of evolution among all the pegmatites. The compositions of gahnite from Argentina pegmatites reflect moderate evolution and plot between the Poland and Brazil pegmatites (Fig. 1). Based on the composition of gahnite, some Argentina pegmatites (i.e., La Magdalena, Juan Roman) are the least evolved of the studied LCT pegmatites. They include Li-rich and Li-poor pegmatites, and the Li-rich have higher Zn content than the Li-poor pegmatites. Gahnite in the La Ona pegmatite from Argentina displays the highest degree of evolution among the Argentina pegmatites. Gahnite from the NYF-type Strzegom-Sobótka pegmatite has the highest Fe and lowest Zn content of all the studied LCT and NYF pegmatites, and its composition is described as Hc18.9-25.5Ghn74.0-81.5Spl0.1-0.6. On the other hand, gahnite from the LCT pegmatites has the highest Zn content (Hc0.0-20.2 Ghn78.8-98.5Spl0.0-4.7) of all pegmatites, with those from Carrascao and Capoeira 2 (BPP) reflecting the highest degree of evolution. The highest Zn content in gahnite is characteristic of more fractionated magmas (Batchelor and Kinnaird 1984) and is associated with LCT-type and Li-rich pegmatites. A plot of mol (Fe+Mg)/Al vs. mol (Zn+Mn)/Al additionally proves that gahnite from NYF-type pegmatites exhibits the lowest degree of fractionation, while gahnite from the LCT-type pegmatites shows the highest degree of fractionation. The data obtained in this study and those derived from limited previous studies indicate that Li-rich pegmatites have gahnite with elevated Zn content, whereas Li-poor pegmatites have gahnite with comparatively lower Zn content. Our results show that gahnite compositions can be used to differentiate Li-rich from Li-poor pegmatites and NYF from LCT pegmatites.

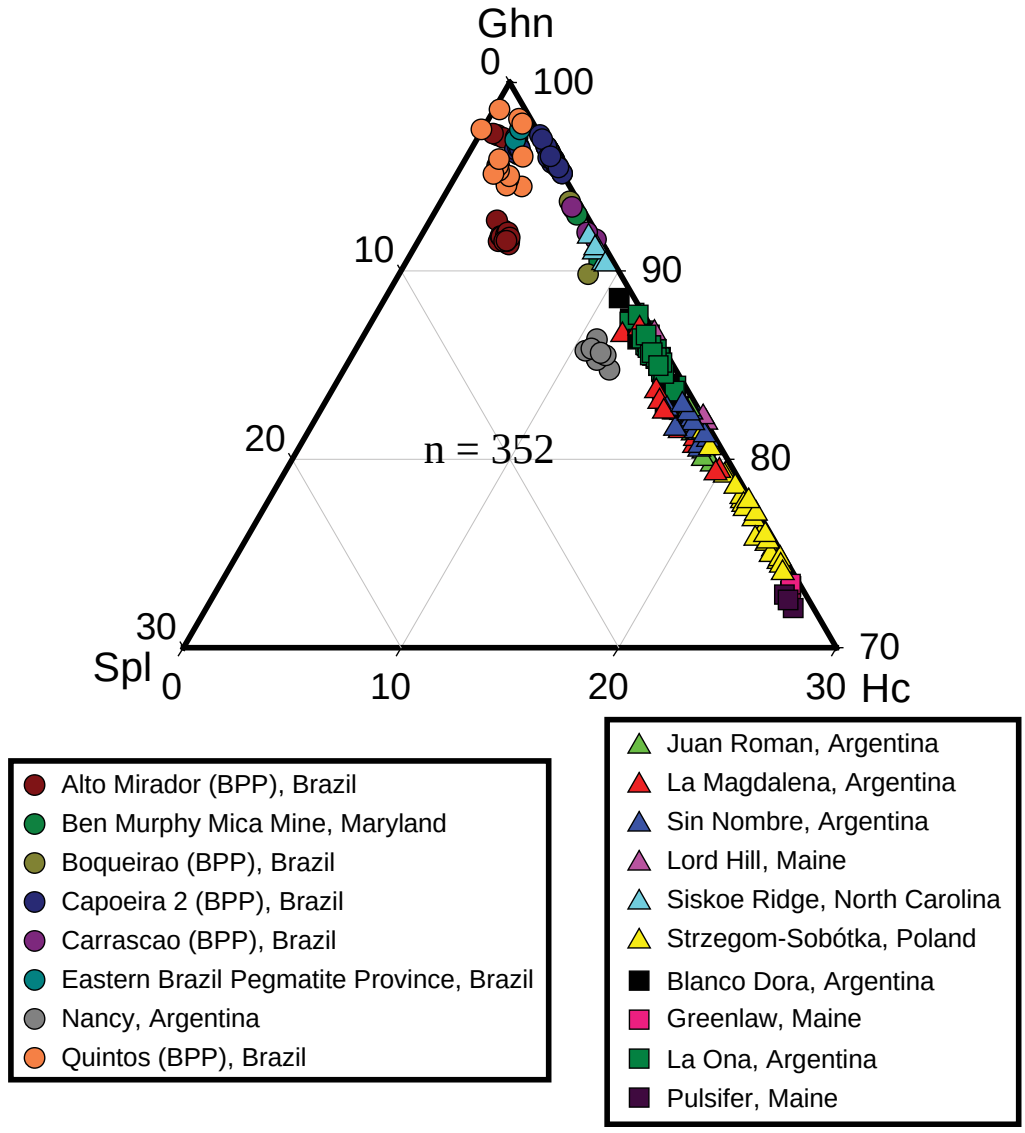

Fig. 1: Ternary diagram showing the composition of zincian spinel (in mol %) in granitic pegmatites in terms of the gahnite (Ghn), hercynite (Hc), and spinel (Spl) end members (After Batchelor and Kinnaird 1984). Only the top 30% of the diagram is shown (Ghn end member). Circles represent Li-rich pegmatites, triangles Li-poor pegmatites, and squares pegmatites of unknown Li content.

References:

Batchelor, R., Kinnaird, J. (1984): Gahnite compositions compared. Mineralogical Magazine, vol. 48, 425-429.

Černý, P., Ercit, T.S. (2005): The classification of granitic pegmatites revisited. Canadian Mineralogist, vol. 43, 2005-2026.

Heimann, A., Spry, P., Teale, G. (2005): Zincian spinel associated with metamorphosed Proterozoic base-metal sulfide occurrences, Colorado: A re-evaluation of gahnite composition as a guide in exploration. Canadian Mineralogist, vol. 43, 601-622.

Soares, D., Beurlen, H., Ferreira, A., Da Silva, M. (2007): Chemical composition of gahnite and degree of pegmatitic fractionation in the Borborema Pegmatitic Province, northeastern Brazil. Anais Academia Brasileira de Ciências, vol. 79, 395-404.

Spry, P., Scott, S. (1986): The stability of zincian spinels in sulfide systems and their potential as exploration guides for metamorphosed massive sulfide deposits. Economic Geology, vol. 81, 1446-1463.

MIAROLITIC FACIES OF RARE-METAL – MUSCOVITE PEGMATITES, AZAD KASHMIR, PAKISTAN

V. Zagorsky
Vinogradov Institute of Geochemistry, SB RAS, Irkutsk, Russia, victzag@igc.irk.ru

Following most popular classifications, e.g. by Ginzburg and Rodionov (1960), Černý (1982) and Černý and Ercit (2005), pocket-bearing pegmatites are referred to as an independent class (or formation) of pegmatites, called miarolitic pegmatites. It is worth noting that the word combination "*miarolitic rare-metal pegmatite*" is referred to in many publications. In above-mentioned popular classifications, this expression seems ambiguous and unacceptable. However, it is consistent with observations of pegmatites in nature. Many true rare-metal pegmatites, such as the Kulam, Stuart, Pala Chief and other gem deposits, are miarolitic as well. This contradiction is eliminated in the pegmatite classification system developed by Zagorsky *et al.* (1999_1; 2003), in which the concept of *miarolitic facies* is inherent to varying degree in the majority of pegmatitic formations. The degree of miarolitic cavity development decreases gradually from low-pressure pegmatites to high-pressure ones, with complete absence in most abyssal pegmatites. Thus, the term "*miarolitic"* should be used as an additional modifyer to describe any pocket-bearing pegmatites. For example, this paper reports a typical occurrence of *miarolitic rare-metal – muscovite pegmatites.*

Geological setting. The occurrence of gem-bearing miarolitic pegmatites studied is located 80-100 km south of gem-rich Gilgit area, in the northwestern Himalayas on the right bank of the Nilum River, along the present boundary between northeastern Pakistan and Indian Kashmir. Pegmatite-bearing territory is located within the Himalayan crystalline zone, which also includes the Nanga Parbat gneiss massif that hosts most of Gilgit miarolitic pegmatites. This zone is bounded by the Main Mantle Thrust on the north (the Indus suture zone) and by the Sub-Himalayan Thrust zone to the south [Kazmi, 1989]. Pegmatite-host rocks of the Azad Kashmir area belong to the Salhala Series of Precambrian age, subdivided into the Sharda Formation and Migmatite Complex. The Migmatite Complex is thrusted over the Sharda Formation from the north along the Nilum River. The pegmatites are found within the Migmatite Complex only. It is composed of garnet-biotite, sillimanite-garnet-biotite schists and gneisses, granite gneisses and the so–called "sheet granites". The sheet granites are interlayered with the schists. The pegmatites form clusters of veins and lenses that are conformable or transverse to the host rocks. The largest bodies are up to 100 m long and 3-4 m thick. Initially, beginning in 1984, pegmatites were explored for large-flaky muscovite and hand-sorted beryl. Later, miarolitic cavities with colored tourmaline and morganite were found. Large quartz crystals and a brown-yellowish gem-quality garnet ("kashmir garnet") were found in one of the lens-like pegmatite bodies in 1994. The age of pegmatites is proposed to be Alpine (Zagorsky, 1993).

Inner structure and composition of pocket-bearing pegmatites. Particularly interesting are pegmatite bodies with commercial muscovite, beryl, and gems, e.g. Donga-Nar-1 and Bhukri Pari-2. The *Donga-Nar-1*, the best known gem-bearing pegmatite, was formerly mined for muscovite. This vein-like body with broadly variable thickness strikes over 90 m northeast and dips northwest. It cuts the highly metamorphosed schists and sheet granites of the Migmatite Complex. Its thickness is seldom more than 3 m. The body has an indistinct internal zonal structure. The southwestern termination is partly covered by a glacier. The pegmatite contains narrow (5-10 cm) fine- to medium-grained endocontact rims of quartz-muscovite (locally with oligoclase). Toward the center of the body is fine- to medium-grained quartz-oligoclase pegmatite that contains large nodules of gray K-feldspar (up to 10-15 cm), flaky muscovite (5-7 cm) and crystals of black tourmaline.

The intermediate productive part of the pegmatite has more complex zonation. Here, the endocontact rims are locally absent, and the unequigranular zone of muscovite-albite/oligoclase +/- quartz composition, is present along the contact with country rocks. There are also sporadic inclusions of K-feldspar, increasing in size and proportion toward the center. This zone, especially in the hanging wall of the body, contains abundant large crystals of light-brown muscovite (mica books). Along with black schorl, green tourmaline appears in this zone in close proximity to the next interior zone. The large quantities of quartz and blue beryl increase toward the center, and mica develops a distinctive

silver-like hue. Such "silver mica" frequently contains abundant inclusions of needle-like crystals of green tourmaline.

The 1-1.2 m thick central zone consists of blocky K-feldspar, hosting individual nodules of quartz and quartz-oligoclase pegmatite with schorl. Its boundaries with the previous zone are indistinct and winding. This zone is unique as it contains "silver mica", green tourmaline and blue beryl. However, the most distinctive feature is the presence of gem-bearing miarolitic cavities with verdelite and multi-colored tourmaline. Rubellite and colorless and light-rose beryl are not very abundant in pockets. Cut material is represented by verdelite and, to a lesser extent, morganite. The nodules of albite-lepidolite units, locally with colorless or light-rose semi-transparent beryl, occur on the walls of miarolitic cavities around them. Blue-green amazonite is also characteristic of the central zone.

There is no zoning near where the pegmatite body wedges out on its northeastern flank. There, the pegmatite is completely composed of fine- to medium-grained quartz-oligoclase rock with abundant large crystals of schorl and sporadically distributed K-feldspar.

Bhukri Pari-2 is a small lens-like pegmatite occurring at the contact of schists and amphibolites. At a distance of 0.5 meters from the contact with pegmatite, the amphibolites are strongly replaced with protolithionite-zinnwaldite. The 1.5 meter thick unequigranular zone of quartz-K-feldspar-albite/oligoclase with muscovite books up to 20 cm thick is present in hanging wall of the pegmatite. Schorl and blue beryl are also present. Below this zone is a zone of blocky K-feldspar with quartz nodules. Amazonite occurs along with predominant grey K-feldspar. The central quartz core contains pockets up to 0.5 m in diameter. The cavities are filled with white clay containing gem verdelite and morganite. The crystals of green and rose tourmaline sometimes have blue rims. The cavities below the quartz core are surrounded by fine-grained quartz-lepidolite aggregates. The structure of the lower part of the pegmatite is similar to that of the hanging wall.

Mineralogy. K-feldspars from pocket-bearing bodies comprise microclines (Δt_1=041-078; $\sum t_1$ = 0.88-0.96) or a mixture of monoclinic and triclinic phases. They are enriched in Li, Rb and Cs four to six times as compared to K-feldspar from cavity-devoid pegmatites that produce only muscovite and/or beryl. The highest contents of rare alkalis are typical of amazonite: up to 100 ppm Li, 4000 ppm Rb, and 2400 ppm Cs. The Ba and Sr abundances in the samples from unproductive flanks of bodies are 6 to 25 times higher relative to K-feldspars from the pocket-bearing zones. The albite content in K-feldspars is 12-25 %. Micas are presented by muscovite (including "silver-mica") and trilithionite varieties. The latter contains up to 0.57 % Rb and 0.71 % Cs. Garnet from pocket-bearing zones is spessartine with 15 % of almandine and 6 % of pyrope molecule. White and rose morganite contain 820-860 ppm Cs, and 0.85-1.15 % Na_2O (Zagorsky *et al.*, 1999_2).

Acknowledgements: the author is very grateful to the United Nation's Programme of Development and the "AKMIDC" Company (Pakistan) for a much appreciated possibility to visit pegmatites of Azad Kashmir, and to reviewers for improvement of English.

References

Černý P. (1982): Anatomy and classification of granitic pegmatites. *In* Granitic Pegmatites in Science and Industry (P. Cerny ed.). Mineral Assoc. Can., Short-Course Handbook **8**, 405-461.

Černý P., T. S. Ercit (2005): The classification of granitic pegmatites revisited. Canadian Mineralogist, vol. 43, 2005-2026.

Ginzburg A. I., G. G. Rodionov (1960): On depths of formation of granitic pegmatites. Geologiya rudnykh mestorozhdeniy, V. 2, N 1, 45-54. (in Russ.).

Kazmi A.N. (1989): A brief overview of the geologyand metallogenic provinces of Pakistan. In Emeralds of Pakistan (geology, gemology, genesis). Karachi: Elite Publishes Limited, 1-12.

Zagorsky V.Ye. (1993): Pegmatites of Azad Kashmir. Mission Report, UN project PAK/86/019. N.Y.: United Nations, 28p.

Zagorsky V. Ye., V. M. Makagon, B. M. Shmakin (1999_1): The systematics of granitic pegmatites. Canadian Mineralogist, vol. 37, 3, 800-802.

Zagorsky V. Ye., V. M. Makagon, B. M. Shmakin (2003): The systematics of granitic pegmatites. Russian Geology and Geophysics, vol. 44, 5, 422-435.

Zagorsky V. Ye., I. S. Peretyazhko, B. M. Shmakin (1999_2): Granitic pegmatites, V.3. Miarolitic pegmatites. Novosibirsk, Nauka, Siberian Enterprise RAS, 385 p. (in Russ.).

ON THE PROBLEM OF GRANITE-PEGMATITE RELATIONSHIPS: TYPES OF GRANITE-PEGMATITE SYSTEMS

V. Zagorsky, V. Makagon
Vinogradov Institute of Geochemistry, SB RAS, Irkutsk, Russia, victzag@igc.irk.ru

Granite-pegmatite systems are viewed as segments or volumes of the earth crust where the evolution of felsic melts can cause the formation of granitic pegmatites with both spatiallly associated and (para)genetically related granites, pegmatites, syngranitic and synpegmatitic metasomatites. As pegmatites are derived by diverse geological and P-T-conditions (Zagorsky *et al.*, 2003; Cerny and Ercit, 2005), the granite-pegmatite relations differ widely as well.

The magmatic nature of most granitic pegmatites is not contested. Formation of pegmatite melts is commonly thought to be the result of fractional crystallization of granitic magma (Fersman, 1940; Jahns and Burnham, 1969; Jahns 1982; London, 2008). The mode of extreme concentration and transport of abundant rare elements into localized chambers during the formation of large-scale and unique pegmatite deposits is not clear, largely due to diversity and vagueness of granite-pegmatite relationships. In some pegmatite fields containing enormous pegmatitic masses, granites are absent, or are not contemporaneous with pegmatite formation. The problem of determining the parental granite becomes more complex when pegmatite fields are more sizable and older in age. In practice, this problem is often determined on the basis of spatial proximity of pegmatites to one or the other granitic massif. But this approach often leads to erroneous inferences if geochronological data for granites and pegmatites, or both, are absent. Based on available geological, geochemical and geochronological data, four possible types of granite-pegmatite systems, which differ in spatial-time and genetic granite-pegmatite relationships, are recognized (Zagorsky, 2009).

Type I. Geochronological data available for some pegmatite fields indicate a considerable time gap between formation of assumed parental granites and spatially associated pegmatites. This is especially typical for large fields of rare-metal pegmatites and, to a smaller extent, pegmatites with rare-metal – rare-earth affiliation. In some regions the time gap ranges from tens to hundreds of millions of years. Within the East-Sayan pegmatite belt, rare-metal pegmatites of the Gol'tsovoye (1.69Ga) and Vishnyakovskoye (1.49Ga) deposits are significantly younger than the assumed parental granites of the Sayan complex (1.86 Ga) (Makagon and Zagorsky, 2011). In this region, there are no granites that are closer in age to the pegmatites. A larger time gap is established for alkali granites and spatially closely related rare-metal – rare-earth amazonite pegmatites within the Keivy structure, Kola Peninsula. The age of alkali granites is 2.67 Ga, and that of pegmatites is 1.67-1.7 Ga (Vetrin, Rodionov, 2009). In such cases, *independent pegmatite impulse* within the history of magmatism of pegmatite-bearing geological structures must be implied.

Type II implies a paragenetic relationship between pegmatites and granites, with their sequential intrusion from one or several chambers within a single magmatic column. The Zavitaya multi-stage granite-pegmatite system, with available U-Pb-age data for all main types of magmatic rocks, may serve as typical example. Three types of granite within pegmatite field, with distinctly different ages, are related to the *Kukulbey* magmatic complex (J_3-K_1). They include: 1) porphyritic biotite granites (169.0±3.0 Ma); 2) two-mica granites-leucogranites (147.5±3.1 Ma); 3) subalkaline garnet-bearing muscovite leucogranites (140.0±3.0 Ma). In turn, four types of pegmatites are recognized in the Zavitaya field: 1) granite–pegmatites; 2) inequigranular to blocky quartz–two-feldspar pegmatites; 3) porphyry-like quartz–albite pegmatites; 4) banded quartz–spodumene–albite aplite–pegmatites. Barren pegmatites of types 1 and 2 are in close proximity to small bodies of muscovite leucogranites, and have the same age (139.6±3.1 Ma), whereas quartz–spodumene–albite pegmatites are essentially younger (129.6±2.7 Ma). The time of the Zavitaya multi-stage granite–pegmatite system formation coincides with the stage in the geodynamic regime of change in the region. The age of granitic and barren pegmatitic members of the system corresponds to the cessation of collision, whereas the formation of spodumene-rich pegmatites is related to the onset of rifting (Zagorsky, 2011).

Type III. A close spatial and genetic relationship of pegmatites with one or the other granitic massif is distinctive feature of this type of granite-pegmatite system. One of the typical examples is the Durulguy zonal pegmatite field in Transbaikalia, Russia, where the genetic link between pegmatites and granites is confirmed by gradual transition between two-mica granites and granite-pegmatites, as well as between different types of pegmatites. The genetic relationship between granites and pegmatites in such granite-pegmatite systems, with the family relation terms are applied, is best described as "brothers-sisters", rather than "parents-children". In this case, it is believed that pegmatites are not derived by the intra-chamber differentiation within a granitic massif. Instead, the melts of pegmatite-bearing two-mica or muscovite granites and pegmatites, the products of felsic magma evolution in deep magmatic chambers, intrude jointly into the higher levels of the Earth's crust. One such geochronologically studied system of this type is the Malkhan granite-pegmatite system, where the age of granites and pegmatites lies completely within 123.8-127.6 Ma (Zagorsky and Peretyazhko, 2010).

Type IV represents a variant of the direct genetic relation of pegmatites and granites, with the formation of basically syngenetic schlieren pegmatites as derived from magma differentiation within parental granitic massifs, for instance, the Aya pegmatite field in the Western Baikal area.

It is evident that petrological models for different types of granite-pegmatite systems are highly divergent. We believe two main processes may be responsible for granitic magma differentiation and formation of pegmatitic melts: a) fractional crystallization; b) fluid-magma interaction under above-liquidus conditions within crustal magma chambers. In the series from type I to type IV of granite-pegmatite systems, the contribution of the first mode of felsic magma evolution increases, whereas the role of the second one, on the contrary, decreases.

Acknowledgements

We are grateful to reviewers for improvement of English. The study was supported by RFBR (projects 1005-00964-a, SS-6153.2012.5) and SB RAS (project IIP-123).

References:

Černý P., T. S. Ercit (2005): The classification of granitic pegmatites revisited. Canadian Mineralogist, vol. 43, 2005-2026.

Fersman A. E. (1940): Pegmatites. V. 1. Moscow-Leningrad: Izd-vo AN SSSR, 712 p. (in Russ.).

Jahns R.H. (1982): Internal evolution of pegmatite bodies. In Granitic Pegmatites in Science and Industry (P. Černý, ed.). Mineralogical Association of Canada, Short Course Handbook 8, 293-327.

Jahns R.H., C. W. Burnham (1969): Experimental study of pegmatite genesis. I. A model for the derivation and crystallization of granitic pegmatites. Economic Geology, vol. 64, 843-864.

London D. (2008): Pegmatites. Canadian Mineralogist, 10, Special Publication, 347 p.

Makagon V.M., V. Ye. Zagorsky (2011): The East Sayan rare-metal pegmatite belt as result of independent stage in the history of magmatism within East Sayan region. In Large igneous provinces of Asia: mantle plumes and metallogeny (Abstract volume). Irkutsk: Penrographica, 150-153.

Vetrin V. R., N. V. Rodionov (2009): Geology and geochronology Neoarchean anorogenic magmatism of the Keivy structure, Kola Peninsula. Petrology, vol.17, 6, 578-600.

Zagorsky V. Ye. (2009): On emplacement of compositionally heterogeneous pegmatite melts: petrogenetic implications // Estudos Geológicos, 2009, vol. 19(2), 365-369.

Zagorsky V. Ye. (2011): The Zavitaya lithium-rich granite-pegmatite system, Central Transbaikalia, Russia: geology, geochemistry, petrogenetic aspects. Asociación Geológica Argentina, Serie D: Publication Especial, 14, 229-232.

Zagorsky V. Ye., V. M. Makagon, B. M. Shmakin (2003): Systematics of granitic pegmatites. Russian geology and geophysics, vol.44, 5, 422-435.

Zagorsky V. Ye., I. S. Peretyazhko (2010): First 40Ar/39Ar age determinations on the Malkhan granite-pegmatite system: geodynamic implications // Doklady Earth Sciences, vol. 430, part 2, 172-174.